

**UNIVERSITY OF SOUTHAMPTON**

**FACULTY OF MEDICINE, HEALTH AND LIFE SCIENCES**

**School of Biological Sciences**

**Relapse in neuroinflammatory disease:  
studies into events at the blood-brain barrier**

**by**

**Ian Galea**

**Thesis for the degree of Doctor of Philosophy**

**July 2006**

ABSTRACT

FACULTY OF MEDICINE, HEALTH AND LIFE SCIENCES  
SCHOOL OF BIOLOGICAL SCIENCES

Doctor of Philosophy

RELAPSE IN NEUROINFLAMMATORY DISEASE:  
STUDIES INTO EVENTS AT THE BLOOD-BRAIN BARRIER

by Ian Galea

Neuroinflammatory diseases such as multiple sclerosis are characterized by exacerbations which result in considerable morbidity and health economic cost. There is evidence that systemic infections precipitate such exacerbations and contribute to neurodegeneration, the underlying substrate of progressive accumulation of disability. For this to happen, the peripheral immune system signals to the central nervous system (CNS) across the blood-brain barrier (BBB), resulting in the induction of inflammation within the brain. Such immune-to-brain signalling may occur via several routes; three such mechanisms were investigated.

First, prostaglandin E<sub>2</sub> (PGE<sub>2</sub>) is considered to be the inflammatory mediator responsible for various CNS responses to systemic inflammation such as fever and sickness behaviour. Whether it plays a role in the induction of cytokine expression within the brain was unknown. *De novo* cytokine transcription within the brain occurs during systemic inflammation and is thought to be one of the mechanisms underlying exacerbation of neuroinflammatory disease. It is shown that intraperitoneal administration of indomethacin, which inhibits PGE<sub>2</sub> synthesis, did not prevent the upregulation of TNF $\alpha$ , IL1 $\beta$  and IL6 mRNA which occurs in the brain during systemic endotoxin challenge in rats. This suggests that exacerbation of neuroinflammatory disease following a systemic infection occurs via a prostaglandin-independent pathway. Future research efforts are therefore needed to identify the humoral mediator(s) signalling CNS cytokine induction during systemic inflammation.

Second, cerebral CD163-positive macrophages and endothelial cells are the cellular constituents of the BBB which are activated during systemic inflammation. However their relative contribution to immune-to-brain signalling was not known. Therefore, cerebral CD163-positive macrophages were selectively depleted using an intracerebroventricular infusion of clodronate liposomes. This technique was optimized in order to preserve the peripheral immune system's response to systemic inflammatory challenge. It was observed that depletion of cerebral CD163-positive macrophages did not affect immune-to-brain signalling after a systemic endotoxin challenge as assessed by studying several events which are considered to reflect the brain's response to systemic inflammation: fever, *de novo* transcription of the cytokines TNF $\alpha$ , IL1 $\beta$  and IL6, IL1 $\beta$  protein expression and upregulation of microglial phosphorylated ERK 1/2. This shows that the role of cerebral CD163-positive macrophages in immune-to-brain signalling is not essential. Therefore the cerebral endothelium is mainly responsible for the inflammatory pathway across the BBB, and represents a potential therapeutic target.

Third, the role of CD8 T cells in neuroinflammatory disease is increasingly being recognized. In order to initiate inflammation, neuroantigen-specific CD8 T cells need to infiltrate the brain. Here, a novel route whereby CD8 T cells gain access to the CNS in an antigen-dependent manner is described. An *in vivo* model of antigen-specific CD8 T cell recruitment was developed by injecting cognate antigen in the striatum of CD8 TCR-transgenic mice using a minimally invasive technique. Upregulation of MHC Class I was observed on the luminal side of endothelial cells: it was temporally and spatially associated with the CD8 T cell infiltrate. Intravenous injection of blocking MHC I antibody resulted in a marked reduction in CNS-infiltrating CD8 T cells. This shows that luminal MHC Class I expression by cerebral endothelium directs antigen-specific CD8 T cell traffic into the brain *in vivo* and represents a novel therapeutic target in inflammatory neurological diseases.

# Contents

## Chapter 1

### Introduction

|                |   |           |
|----------------|---|-----------|
| <b>1</b>       | <b>Overview</b>   | <b>2</b>  |
| <b>1.1</b>     | <b>Relapse is a feature of various neuroinflammatory diseases</b>   | <b>2</b>  |
| <b>1.2</b>     | <b>Triggers of relapse</b>  | <b>3</b>  |
| <b>1.3</b>     | <b>The short and long term implications of relapse</b>              | <b>4</b>  |
| <b>1.3.1</b>   | <b>Short term morbidity</b>   | <b>4</b>  |
| <b>1.3.2</b>   | <b>Long-term effects: progression of underlying disease</b>         | <b>5</b>  |
| <b>1.4</b>     | <b>Systemic infection and neurodegeneration</b>                     | <b>6</b>  |
| <b>1.5</b>     | <b>The immune-brain interface</b>                                   | <b>6</b>  |
| <b>1.5.1</b>   | <b>Cerebral blood vessels</b>                                       | <b>7</b>  |
| <b>1.5.2</b>   | <b>The leptomeninges</b>  | <b>9</b>  |
| <b>1.5.3</b>   | <b>The circumventricular organs</b>                                 | <b>9</b>  |
| <b>1.5.4</b>   | <b>The choroid plexus</b>   | <b>9</b>  |
| <b>1.6</b>     | <b>Mechanisms of relapse in neuroinflammatory disease</b>           | <b>10</b> |
| <b>1.6.1</b>   | <b>Humoral route</b>  | <b>10</b> |
| <b>1.6.1.1</b> | <b>Humoral route: direct entry</b>                                  | <b>12</b> |
| <b>1.6.1.2</b> | <b>Humoral route: relay mechanism at the immune-brain interface</b> | <b>12</b> |
| <b>1.6.2</b>   | <b>Cellular influx into the central nervous system</b>              | <b>17</b> |
| <b>1.6.2.1</b> | <b>T cell stimulation</b>   | <b>18</b> |
| <b>1.6.2.2</b> | <b>Transendothelial migration of T cells</b>                        | <b>20</b> |
| <b>1.7</b>     | <b>Aims</b>   | <b>22</b> |

## Chapter 2

### Materials and methods

|            |  |           |
|------------|--|-----------|
| <b>2.1</b> | <b>Animals</b>                             | <b>25</b> |
| <b>2.2</b> | <b>Reagents for intracranial injection</b> | <b>27</b> |
| <b>2.3</b> | <b>Reagents for intravenous injection</b>  | <b>27</b> |
| <b>2.4</b> | <b>Multilamellar liposomes</b>             | <b>27</b> |

|                |  |           |
|----------------|--|-----------|
| <b>2.5</b>     | LPS injections   | <b>29</b> |
| <b>2.6</b>     | Immunization   | <b>30</b> |
| <b>2.7</b>     | Surgery  | <b>30</b> |
| <b>2.7.1</b>   | Telemetry capsule implantation                               | <b>30</b> |
| <b>2.7.2</b>   | Intracerebroventricular liposome infusion                    | <b>31</b> |
| <b>2.7.3</b>   | Intracranial injections                                      | <b>31</b> |
| <b>2.7.3.1</b> | Antigen injections   | <b>34</b> |
| <b>2.7.3.2</b> | Other injections   | <b>34</b> |
| <b>2.7.4</b>   | Optic nerve crush  | <b>34</b> |
| <b>2.7.5</b>   | Stab lesions   | <b>37</b> |
| <b>2.8</b>     | Telemetric measurement of core body temperature              | <b>37</b> |
| <b>2.8.1</b>   | Minimization of factors potentially affecting telemetry data | <b>37</b> |
| <b>2.8.2</b>   | Analysis of telemetry data                                   | <b>39</b> |
| <b>2.9</b>     | Cardiac puncture and serum processing                        | <b>39</b> |
| <b>2.10</b>    | Perfusion and tissue processing                              | <b>40</b> |
| <b>2.11</b>    | Immunohistochemistry   | <b>40</b> |
| <b>2.12</b>    | Enzyme-linked immunosorbent assay                            | <b>43</b> |
| <b>2.13</b>    | Semi-quantitative real time reverse transcriptase PCR        | <b>44</b> |
| <b>2.13.1</b>  | mRNA extraction  | <b>44</b> |
| <b>2.13.2</b>  | cDNA synthesis   | <b>44</b> |
| <b>2.13.3</b>  | RT-PCR   | <b>44</b> |
| <b>2.13.4</b>  | Standard curve   | <b>46</b> |
| <b>2.14</b>    | T cell culture   | <b>46</b> |
| <b>2.15</b>    | FACS   | <b>47</b> |
| <b>2.16</b>    | Quantification of cells                                      | <b>47</b> |
| <b>2.17</b>    | Statistics   | <b>49</b> |

**Chapter 3** **Inhibition of prostaglandin synthesis does not prevent *de novo* cytokine transcription in the brain parenchyma during systemic inflammation**

|              |   |           |
|--------------|---|-----------|
| <b>3.1</b>   | Introduction  | <b>51</b> |
| <b>3.2</b>   | Results   | <b>52</b> |
| <b>3.2.1</b> | <i>De novo</i> cytokine transcription within the brain after systemic LPS challenge | <b>52</b> |

|                  |  |           |
|------------------|--|-----------|
| <b>3.2.2</b>     | <i>De novo</i> cytokine transcription within the brain after systemic LPS challenge occurred despite indomethacin treatment  | <b>54</b> |
| <b>3.2.3</b>     | Indomethacin suppressed the febrile response to systemic LPS challenge   | <b>54</b> |
| <b>3.3</b>       | Discussion   | <b>54</b> |
| <b>3.4</b>       | Materials and methods  | <b>59</b> |
| <b>Chapter 4</b> | <b>Characterization and optimization of the clodronate liposome technique to deplete CD163-positive macrophages in rats</b>  |           |
| <b>4.1</b>       | Introduction   | <b>61</b> |
| <b>4.2</b>       | Results  | <b>62</b> |
| <b>4.2.1</b>     | ICV infusion of 50µl of clodronate liposomes completely depletes meningeal and perivascular macrophages but not CVO macrophages  | <b>62</b> |
| <b>4.2.2</b>     | Kupffer cell and splenic red pulp macrophage numbers recover ten days after ICV infusion of 50µl of clodronate liposomes   | <b>64</b> |
| <b>4.2.3</b>     | ICV infusion of 50µl of clodronate liposomes attenuates the circulating cytokine response to systemic endotoxin challenge  | <b>71</b> |
| <b>4.2.4</b>     | ICV infusion of clodronate liposomes affects the circulating cytokine response to systemic endotoxin challenge and depletes cerebral CD163-positive perivascular macrophages in a dose-dependent fashion | <b>71</b> |
| <b>4.2.5</b>     | ICV infusion of 50µl of clodronate liposomes results in their leakage to the periphery   | <b>73</b> |
| <b>4.2.6</b>     | Liposome leakage from brain to periphery is a protracted process   | <b>78</b> |
| <b>4.2.7</b>     | Optimization of the clodronate liposome technique  | <b>78</b> |
| <b>4.3</b>       | Discussion   | <b>79</b> |
| <b>4.4</b>       | Materials and methods  | <b>83</b> |
| <b>Chapter 5</b> | <b>Cerebral CD163-positive macrophages in immune-to-brain signalling</b>   |           |
| <b>5.1</b>       | Introduction   | <b>85</b> |
| <b>5.2</b>       | Results  | <b>87</b> |

|              |   |           |
|--------------|---|-----------|
| <b>5.2.1</b> | An intact cerebral CD163-positive macrophage population is not essential for the febrile response to systemic inflammation                          | <b>87</b> |
| <b>5.2.2</b> | Systemic endotoxin challenge induces gene transcription of the cytokines TNF $\alpha$ , IL1 $\beta$ and IL6 in the frontoparietal cortex            | <b>87</b> |
| <b>5.2.3</b> | Cerebral CD163-positive macrophage depletion does not affect <i>de novo</i> cytokine expression in the brain occurring during systemic inflammation | <b>89</b> |
| <b>5.2.4</b> | The contribution of cerebral endothelium to the cytokines assayed was insignificant   | <b>93</b> |
| <b>5.2.5</b> | CD163-positive macrophages are excluded at the blood-brain interface  | <b>96</b> |
| <b>5.3</b>   | Discussion  | <b>96</b> |
| <b>5.4</b>   | Materials and methods   | <b>99</b> |

**Chapter 6** **Mannose receptor expression specifically reveals murine cerebral perivascular macrophages**

|              |                                 |            |
|--------------|---------------------------------|------------|
| <b>6.1</b>   | Introduction                    | <b>105</b> |
| <b>6.2</b>   | Results                         | <b>106</b> |
| <b>6.2.1</b> | Control animals                 | <b>106</b> |
| <b>6.2.2</b> | Acute inflammatory model        | <b>110</b> |
| <b>6.2.3</b> | Excitotoxic model               | <b>110</b> |
| <b>6.2.4</b> | Wallerian degeneration model    | <b>112</b> |
| <b>6.2.5</b> | Chronic neurodegeneration model | <b>112</b> |
| <b>6.3</b>   | Discussion                      | <b>112</b> |
| <b>6.4</b>   | Materials and methods           | <b>116</b> |

**Chapter 7** **The role of cerebral endothelial cells and perivascular macrophages in antigen-specific CD8 T cell traffic into the brain**

|              |  |            |
|--------------|--|------------|
| <b>7.1</b>   | Introduction                                       | <b>122</b> |
| <b>7.2</b>   | Results  | <b>123</b> |
| <b>7.2.1</b> | Antigen-specific CD8 T cell traffic into the brain | <b>123</b> |
| <b>7.2.2</b> | The role of cerebral perivascular macrophages      | <b>127</b> |
| <b>7.2.3</b> | The role of cerebral endothelium                   | <b>130</b> |

|                  |                                 |            |
|------------------|---------------------------------|------------|
| 7.3              | Discussion                      | 137        |
| 7.4              | Materials and methods           | 141        |
| <b>Chapter 8</b> | <b>Summary &amp; Discussion</b> | <b>148</b> |
|                  | <b>References</b>               | <b>154</b> |

## Figures

### Chapter 1

|     |   |    |
|-----|---|----|
| 1.1 | The cerebral perivascular macrophage  | 8  |
| 1.2 | Exacerbation of central nervous system inflammation following a systemic infection: humoral and cellular routes | 11 |
| 1.3 | Temporospatial spread of immune activation from circumventricular organs to surrounding nuclei                  | 13 |
| 1.4 | The prostaglandin synthetic pathway   | 16 |

### Chapter 2

|     |   |    |
|-----|---|----|
| 2.1 | The CL4 transgenic mouse                                | 26 |
| 2.2 | Clodronate-loaded multilamellar liposomes               | 28 |
| 2.3 | Fourth ventricular infusion                             | 32 |
| 2.4 | Lateral ventricular infusion                            | 33 |
| 2.5 | Intrastriatal injection                                 | 35 |
| 2.6 | Intrahippocampal injection                              | 36 |
| 2.7 | Telemetric measurement of core body temperature of rats | 38 |
| 2.8 | CL4 CD8 T cells after culture protocol                  | 48 |

### Chapter 3

|     |  |    |
|-----|--|----|
| 3.1 | <i>De novo</i> cytokine transcription in the rat brain during systemic inflammation  | 53 |
| 3.2 | Indomethacin did not significantly affect cytokine mRNA upregulation in frontoparietal cortex after systemic endotoxin challenge | 55 |
| 3.3 | Indomethacin dosing regimen used resulted in sufficient bioavailability in the CNS   | 56 |

### Chapter 4

|     |   |    |
|-----|---|----|
| 4.1 | Complete depletion of perivascular macrophages in brain parenchyma after ICV infusion of 50 $\mu$ l clodronate liposomes in the | 63 |
|-----|---|----|

|               |   |           |
|---------------|---|-----------|
| 4th ventricle |   |           |
| <b>4.2</b>    | Complete depletion of meningeal macrophages after ICV infusion of 50µl clodronate liposomes in the 4th ventricle  | <b>63</b> |
| <b>4.3</b>    | No depletion of ED2-positive macrophages in the area postrema after infusion of 50µl clodronate liposomes in the 4th ventricle                          | <b>65</b> |
| <b>4.4</b>    | No depletion of ED2-positive macrophages in the subfornical organ after infusion of 50µl clodronate liposomes in the 4th ventricle                      | <b>66</b> |
| <b>4.5</b>    | No depletion of ED2-positive macrophages in the organum vasculosum laminae terminalis after infusion of 50µl clodronate liposomes in the 4th ventricle. | <b>67</b> |
| <b>4.6</b>    | No depletion of ED2-positive macrophages in the choroid plexus after infusion of 50µl clodronate liposomes in the 4th ventricle                         | <b>68</b> |
| <b>4.7</b>    | Kupffer cells in liver and red pulp macrophages in spleen on day 10 post ICV infusion of 50µl liposomes   | <b>69</b> |
| <b>4.8</b>    | Hepatic and splenic macrophages after ICV liposome infusion   | <b>70</b> |
| <b>4.9</b>    | ICV clodronate liposome infusion attenuated the circulating cytokine response to systemic endotoxin challenge in a dose-dependent manner                | <b>72</b> |
| <b>4.10</b>   | ICV clodronate liposome infusion depleted ED2-positive macrophages in a dose-dependent manner   | <b>74</b> |
| <b>4.11</b>   | Cervical lymph nodes on day 9 after infusion of 50µl DiI-labelled liposomes in the 4th ventricle  | <b>75</b> |
| <b>4.12</b>   | Liver on day 9 after infusion of 50µl DiI-labelled liposomes in the 4th ventricle   | <b>76</b> |
| <b>4.13</b>   | Spleen on day 9 after infusion of 50µl DiI-labelled liposomes in the 4th ventricle  | <b>77</b> |
| <b>4.14</b>   | The optimized technique did not affect the circulating cytokine response to systemic endotoxin challenge  | <b>80</b> |
| <b>4.15</b>   | Transepodial and transpial routes for ICV liposomes   | <b>82</b> |

## Chapter 5

|            |   |           |
|------------|---|-----------|
| <b>5.1</b> | An intact cerebral CD163-positive macrophage population is not essential for the febrile response to systemic inflammation                          | <b>88</b> |
| <b>5.2</b> | <i>De novo</i> cytokine transcription in the rat brain during systemic inflammation   | <b>90</b> |
| <b>5.3</b> | Liposome infusion does not affect <i>de novo</i> cytokine expression in the brain occurring during systemic inflammation.                           | <b>91</b> |
| <b>5.4</b> | Cerebral CD163-positive macrophage depletion does not affect <i>de novo</i> cytokine expression in the brain occurring during systemic inflammation | <b>92</b> |

|     |  |    |
|-----|--|----|
| 5.5 | IL1 $\beta$ protein in the right frontoparietal cortex | 94 |
| 5.6 | Phosphorylation of ERK1/2 in the model used            | 95 |

## Chapter 6

|     |  |     |
|-----|--|-----|
| 6.1 | Mannose receptor expression in naïve brain                               | 108 |
| 6.2 | Localization of the PVM in the perivascular space by confocal microscopy | 109 |
| 6.3 | Perivascular macrophages in different pathologies                        | 111 |
| 6.4 | Perivascular macrophages in chronic neurodegenerative disease            | 113 |

## Chapter 7

|      |   |     |
|------|---|-----|
| 7.1  | An antigen-specific model of CD8 T cell infiltration into the brain   | 125 |
| 7.2  | Antigen-specific CD8 T cell infiltration in non-transgenic mice   | 126 |
| 7.3  | Antigen-specific CD8 T cell infiltration into the brain: simultaneous HA & Cw3 injection                          | 128 |
| 7.4  | Non-antigen specific CD8 T cell infiltration into the brain   | 129 |
| 7.5  | Cerebral perivascular macrophage depletion did not affect antigen-specific CD8 T cell infiltration into the brain | 131 |
| 7.6  | Endothelial MHC Class I in antigen-specific CD8 T cell infiltration into the brain                                | 132 |
| 7.7  | Luminal endothelial MHC Class I upregulation  | 134 |
| 7.8  | Luminal endothelial MHC Class I plays a role in antigen-specific CD8 T cell traffic into the brain                | 135 |
| 7.9  | Brain-infiltrating CD8 T cells are not activated in the model of antigen-specific CD8 T cell traffic used         | 136 |
| 7.10 | MHC-dependent transendothelial CD8 T cell migration into the brain  | 138 |

## Tables

### Chapter 2

|            |   |           |
|------------|---|-----------|
| <b>2.1</b> | Antibodies used for immunohistochemistry and FACS                           | <b>42</b> |
| <b>2.2</b> | Quantitative real time polymerase chain reaction primer and probe sequences | <b>45</b> |

## Acknowledgements

I would like to thank the following people with whom I collaborated during the course of this work: Tracey A Newman, Leigh M Felton, Delphine Boche, Martine Bernardes-Silva, Penny A Forse, Sara Waters and Karin Palin (at the CNS Inflammation Group, University of Southampton); Roland S Liblau (at INSERM U563, Purpan University Hospital, Toulouse); Christine D Dijkstra, Nico van Rooijen and Babs O Fabriek (at the Department of Molecular Cell Biology, Free University, Amsterdam).

I would also like to extend my acknowledgements to the following people for their help with advice, discussions, reagents, and/or technical support: Sonia Quarantino, Martin J Glennie, Tim Elliott, Anthony P Williams, Colm Cunningham, Sandra J Campbell, Debbie Bucks, Emma L Rankine, Matt Cuttle, Anton Page and Roger Alston (at the University of Southampton); Jacques P Zappulla, Julie Cabarrocas and Eliane Piaggio (at INSERM U563, Purpan University Hospital, Toulouse); John W McCauley (at the Compton Laboratory, Institute for Animal Health, Newbury); Pedro R Lowenstein (at the Gene Therapeutics Research Institute, University of California, Los Angeles)

The work described here has been funded by the European Union (Grant QLG3-CT-2002-00612) and the Multiple Sclerosis Society (Grants 667/01 and 784/03).

Lastly I would like to thank Hugh Perry for his stirring supervision and my wife Marylyse for her unstinting support.

## Abbreviations

|        |   |
|--------|---|
| ACTH   | adrenocorticotrophic hormone  |
| AD     | Alzheimer's disease   |
| ANOVA  | analysis of variance  |
| APC    | antigen-presenting cell   |
| APP    | amyloid precursor protein   |
| AUC    | area under curve  |
| ATP    | adenosine triphosphate  |
| BBB    | blood-brain barrier   |
| CD     | cluster differentiation   |
| cDNA   | complementary deoxyribonucleic acid                                 |
| CFA    | complete Fruend's adjuvant  |
| CI     | confidence interval   |
| CL     | clone   |
| CNPase | 2'3'-cyclic-nucleotide 3'-phosphodiesterase                         |
| CNS    | central nervous system  |
| COX    | cyclooxygenase  |
| CpG    | unmethylated cytosine-guanine dinucleotide                          |
| CPM    | choroid plexus macrophage   |
| CR     | complement receptor   |
| CRD    | carbohydrate recognition domain                                     |
| CRH    | corticotrophin-releasing hormone                                    |
| CSF    | cerebrospinal fluid   |
| CSL    | carbohydrate-specific lectin  |
| CVO    | circumventricular organ   |
| DAB    | 3,3'-diaminobenzidine   |
| Dil    | 1,1'-dioctadecyl-3,3,3',3'-tetramethyl indocarbocyanine perchlorate |
| DMEM   | Dulbecco's modified Eagle's medium                                  |
| DNA    | deoxyribonucleic acid   |
| EAE    | experimental autoimmune encephalomyelitis                           |
| ED2    | antibody named after E Dopp, who developed it                       |

|                |   |
|----------------|---|
| EDTA           | ethylenediaminetetraacetic acid           |
| ELISA          | enzyme-like immunosorbent assay           |
| ERK1/2         | extracellular signal-regulated kinase 1/2 |
| ET             | endothelin                                |
| EU             | endotoxin units                           |
| FACS           | fluorescence-assisted cell sorting        |
| FcR            | Fc receptor                               |
| FCS            | foetal calf serum                         |
| FITC           | fluorescein isothiocyanate                |
| g              | grammes                                   |
| GAPDH          | glyceraldehyde-3-phosphate                |
| GFAP           | glial fibrillary acidic protein           |
| HA             | haemagglutinin                            |
| HLA            | human leucocyte antigen                   |
| HPA            | hypothalamo-pituitary-adrenocortical      |
| HPLC           | high performance liquid chromatography    |
| HTLV           | human T cell lymphotropic virus           |
| hrs            | hours                                     |
| ICAM           | intercellular adhesion molecule           |
| ICV            | intracerebroventricular                   |
| IFN            | interferon                                |
| Ig             | immunoglobulin                            |
| IHC            | immunohistochemistry                      |
| IL             | interleukin                               |
| IL1RA          | interleukin-1 receptor antagonist         |
| i.p.           | intraperitoneal                           |
| i.v.           | intravenous                               |
| K <sub>D</sub> | dissociation constant                     |
| KA             | kainic acid                               |
| kDa            | kilodaltons                               |
| kg             | kilogramme                                |
| LAL            | Limulus amoebocyte lysate assay           |
| LFA            | lymphocyte function associated antigen    |

|         |  |
|---------|--|
| LFB     | Luxol Fast Blue  |
| LPS     | lipopolysaccharide                                       |
| LTA     | lipoteichoic acid  |
| M       | molar  |
| MAP2    | microtubule-associated protein 2                         |
| MBP     | myelin basic protein                                     |
| mg      | milligrammes   |
| MHC     | major histocompatibility complex                         |
| min     | minutes  |
| ml      | millilitres  |
| mm      | millimetres  |
| MM      | meningeal macrophages                                    |
| MOG     | myelin oligodendrocyte glycoprotein                      |
| MOM     | mouse-on-mouse   |
| mPGES   | microsomal prostaglandin E <sub>2</sub> synthase         |
| MR      | magnetic resonance                                       |
| MR      | mannose receptor   |
| MRI     | magnetic resonance imaging                               |
| mRNA    | messenger ribonucleic acid                               |
| MS      | multiple sclerosis                                       |
| n       | number   |
| NBF     | neutral buffered formalin                                |
| nm      | nanometres   |
| NSAID   | non-steroidal anti-inflammatory drug                     |
| OD      | optical density  |
| ONC     | optic nerve crush  |
| ORO     | Oil Red O  |
| PAMP    | pathogen-associated molecular pattern                    |
| PBS     | phosphate-buffered saline                                |
| PC      | personal computer  |
| PCR     | polymerase chain reaction                                |
| pERK1/2 | phosphorylated extracellular signal-regulated kinase 1/2 |
| PFU     | plaque-forming units                                     |

|         |   |
|---------|---|
| PG      | prostaglandin   |
| p.i.    | post infusion <i>or</i> post injection                      |
| PLP     | proteolipid protein   |
| polyIC  | polyriboinosinic-polyribocytidylic acid                     |
| PPAR    | peroxisome proliferator-activated receptor                  |
| PVM     | perivascular macrophage                                     |
| rRNA    | ribosomal ribonucleic acid                                  |
| RT-PCR  | real-time (reverse transcriptase) polymerase chain reaction |
| SE      | standard error  |
| sec     | seconds   |
| TCR     | T cell receptor   |
| TGF     | transforming growth factor                                  |
| TNF     | tumour necrosis factor                                      |
| tPA     | tissue plasminogen activator                                |
| tRNA    | transfer ribonucleic acid                                   |
| VCAM    | vascular cell adhesion molecule                             |
| VLA     | very late antigen   |
| $\mu$ g | microgrammes  |
| $\mu$ l | microlitres   |
| $\mu$ m | micrometres   |

## Chapter 1

## Introduction

## **Introduction**

### **1      Overview**

Inflammation is a physiological process which evolved to help the body deal with injury and infection. It results in activation of cells in the tissue involved, a local increase in blood flow, and an influx of leucocytes which serve to eliminate the infectious agent and to clear compromised tissue. This occurs at the price of some local tissue damage, which is usually repairable, so the benefits of inflammation far outweigh its consequences. However, if inflammation is prolonged or occurs out of its physiological context, tissue damage is excessive, the consequences far outweigh the benefits and inflammation becomes pathological. This is accentuated in tissues which have a poor capacity for repair, such as the central nervous system (CNS).

Once inflammation is established within the central nervous system, it can manifest itself clinically in two ways. Firstly, it can result in acute clinical deficit as a result of abnormalities in electrical conduction, for example, slowing of conduction due to demyelination or conduction block mediated by inflammatory mediators such as nitric oxide<sup>1</sup>. This is potentially reversible if the inflammation subsides. Secondly, clinical deficit can arise from neuronal or axonal death (neurodegeneration), a largely irreversible event. Therefore the clinical picture in neuroinflammatory disease is characterized by exacerbations, which may remit, as well as by accumulation of permanent neurological deficit.

#### **1.1      Relapse is a feature of various neuroinflammatory diseases**

The archetypal neuroinflammatory disease is multiple sclerosis (MS). It is increasingly being recognized that a significant inflammatory component occurs in Alzheimer's disease (AD)<sup>2</sup>. Neurodegeneration is a core feature in both conditions. It is a hallmark in AD and preferentially affects the temporal lobes. Neurodegeneration in MS has only been recently appreciated, occurs early on during the disease and affects the CNS more globally compared to AD<sup>3</sup>. On a background of this ongoing neurodegeneration, both conditions are characterized by clinical exacerbations, "relapses" in MS and "delirium" in AD, which

remit to varying extents. The fluctuating nature of behavioural and psychiatric symptoms in AD is a common clinical observation which has been borne out clearly by natural history studies<sup>4</sup>. A relapsing-remitting course is characteristic of neuroinflammation and indeed, an inflammatory disease is the prime differential diagnosis when a patient presents with a relapsing-remitting neurological picture. Other less common neuroinflammatory diseases may also be characterized by relapses, such as acute disseminated encephalomyelitis<sup>5</sup>, primary CNS angiitis<sup>6</sup>, neuro-Behçet's disease<sup>7</sup> or neurological involvement in Sjogren's syndrome<sup>8</sup>.

## 1.2 Triggers of relapse

Relapses may be triggered by intrinsic or extrinsic factors. That intrinsic factors exist has been illustrated several times when animals with chronic relapsing forms of experimental autoimmune encephalomyelitis (EAE), a model of MS, were housed under sterile conditions: relapses still occurred<sup>9</sup>. Intrinsic factors have not been studied in detail but could include the following mechanisms. The first is "epitope spreading" which occurs when T cell responses during an autoimmune process are first detectable against one particular epitope but then occur against an increasing number of epitopes within the same molecule ("intramolecular spread") or within other molecules ("intermolecular spread")<sup>10,11</sup>. The second is a vicious cycle whereby CNS inflammation from a preceding relapse releases brain antigens for peripheral priming of a second relapse: there is evidence that a cryolesion increases the cerebral burden of disease in EAE six-fold but this is nearly halved by cervical lymphadenectomy<sup>12</sup>. The third is stochastic fluctuations in the immune response: this has been forecasted for T cell reactivity by a mathematical model<sup>13</sup>.

Extrinsic triggers are more appealing since they represent more amenable targets for therapeutic intervention. Serial magnetic resonance imaging (MRI) studies of brain and spinal cord in patients with early relapsing-remitting MS showed a strong association between brain and spinal cord activity<sup>14</sup>. That brain and spinal cord lesions occur concurrently implies a systemic trigger for disease activity. Although several possible extrinsic triggers have been investigated, the strongest association is with infections: approximately 1/3 of relapses in MS are associated with a systemic infection<sup>15-19</sup>. This is likely to be an underestimate because of the existence of inflammatory activity in clinically non-eloquent areas of the brain and the high frequency of asymptomatic infections, both of

which would have been missed by the studies. A causative role of systemic infections in relapse, as opposed to an association between the two, is impossible to prove in observational studies. However there are indicators favouring a causative role. The first is the temporal relationship. Median time between the onset of systemic infection and occurrence of MS exacerbation is 8 days<sup>17</sup>. The second is the fact that infection-related relapses lead to more sustained clinically detectable damage than other exacerbations<sup>15</sup>. The third is a growing body of evidence on the role of systemic inflammation in triggering relapses in EAE. This has been shown for pathogens prevalent in conventional animal facilities<sup>20</sup>, virus<sup>21</sup>, lipopolysaccharide (LPS)<sup>22</sup>, bacterial superantigen<sup>23</sup> and IL12<sup>24</sup>.

Delirium is a recognized manifestation of systemic infections in AD<sup>25</sup>. Since an episode of delirium increases the risk of developing dementia threefold<sup>26</sup>, it is possible that infections precipitate delirium in preclinical cases of AD. Again it is difficult to establish cause and effect in observational studies, but simulation in experimental models provides valuable information. In preclinical murine prion disease, systemic administration of endotoxin resulted in exaggeration of sickness behaviour compared to controls<sup>27</sup>.

### **1.3 The short and long term implications of relapse**

The investment into studying relapses has to be justified by an economic analysis of the consequences of relapse. In an American study, the average healthcare cost of an MS relapse in 2002 was calculated to be \$12,870, \$1,847 and \$243 for severe, moderate and mild cases respectively<sup>28</sup>. In another American study, the occurrence of delirium in patients with dementia was associated with substantial health care costs compared to a control group of patients with dementia alone<sup>29</sup>. These studies do not take into account the national economic losses occurring as a result of loss of productivity.

#### **1.3.1 Short term morbidity**

Relapses are accompanied by a wide variety of morbidities. The most obvious is the acute psychiatric or neurological deficit occurring at presentation. However there are several under-recognized consequences of relapses. For instance, it has been shown using a battery of neuropsychological tests that cognitive problems occur in patients during an MS relapse<sup>30</sup>. These symptoms would go undetected during a routine neurological evaluation

yet are likely to impact significantly on the patient's life. In addition exacerbations of symptoms increase the likelihood of depression; one of the mechanisms is a heightening of patients' levels of uncertainty about their illness<sup>31</sup>. There are also indirect morbidities arising out of the acute psychiatric or neurological deficits such as venous thromboembolism resulting from immobility, aspiration pneumonias as a consequence of swallowing difficulties, and head injuries or fractures after falls.

### **1.3.2 Long-term effects: progression of underlying disease**

Although the contribution of exacerbations to progression of underlying disease is intuitive, recent evidence shows that the relationship between these two factors is not straightforward. Natural history studies have shown that relapse frequency is associated with time to onset of disability but not progression once disability is established<sup>32</sup>. A similar result has been borne out by MRI studies examining the relationship between brain lesion load and cerebral atrophy. Accumulation of lesion load in the first 5 years of the disease, but not later, was correlated with subsequent brain atrophy over a 14 year follow-up period<sup>33</sup>. Anti-inflammatory treatment at different stages of the disease has yielded comparable results. Patients with early relapsing remitting and secondary progressive MS (mean disease duration of 2.7 and 11.2 years respectively) were leucodepleted with Campath-1H. This resulted in a profound reduction of relapses in both groups but progression of disability was only arrested in patients with early relapsing-remitting disease<sup>34</sup>. Less potent immunomodulatory agents such as interferons and glatiramer acetate reduce relapses with little effect on disability progression whatever the stage of the disease<sup>35</sup>.

It therefore seems that inflammation and neurodegeneration are coupled in the early phases of the disease. This inflammation underlies relapse generation and is accessible to manipulation by anti-inflammatory treatments. If sufficiently immunosuppressive, treatments at this stage are able to curtail both inflammation and neurodegeneration, as has been seen with Campath-1H<sup>34</sup> and natalizumab<sup>36</sup>. As the disease progresses, the clinical picture is dominated by a self-perpetuating neurodegenerative process which is independent of relapses and unresponsive to any immunosuppression. Despite the lack of association with clinically overt inflammation at this stage, it remains possible that this neurodegeneration is related to inflammation occurring behind the blood-brain barrier

(BBB), as has been demonstrated in a delayed-type hypersensitivity model<sup>37</sup>. Indeed positron emission tomography studies using radiolabelled PK11195, which binds to a benzodiazepine receptor expressed by activated microglia, have shown that cerebral atrophy is related to microglial activation within normal appearing white matter<sup>38</sup>.

In AD, episodes of delirium are significantly associated with a higher risk of developing dementia<sup>26</sup>, a decline in the performance of activities of daily living<sup>39</sup>, a shorter time to permanent institutionalization<sup>40</sup>, and increased mortality<sup>26</sup>. However such associations are not proof of causality.

#### **1.4 Systemic infection and neurodegeneration**

Systemic infection is the best known trigger of relapses, and the relationship between relapses and neurodegeneration has been discussed above. Little is known about the effect of systemic infections on ongoing neurodegeneration. There are no studies looking into this issue in MS. In AD, a pilot study revealed sustained cognitive decline for at least two months after the resolution of a systemic infection<sup>41</sup>. There is recent data from animal studies demonstrating biological plausibility of the hypothesis that systemic infections accelerate ongoing neurodegeneration. A significant increase in neuronal apoptosis was observed after systemic endotoxin challenge in a murine prion model of chronic neurodegeneration<sup>42</sup>. Similarly chronic LPS administration to presymptomatic SOD1<sup>G37R</sup> mice, which model motor neurone disease, exacerbated the degeneration of motor axons and shortened the life span of the mice<sup>43</sup>.

In summary, there is substantial evidence that systemic infections result in exacerbation of ongoing neuroinflammation and neurodegeneration, and this might be accompanied by a clinically overt event: relapse in MS and delirium in AD.

#### **1.5 The immune-brain interface**

Rational design of therapies aimed at reducing the impact of relapses in neuroinflammatory conditions necessitate a knowledge of the underlying mechanisms. Although the CNS was traditionally thought to be shielded by the BBB, it is now recognized that regulated contact

with the circulation occurs at four distinct anatomical areas, collectively referred to as the immune-brain interface:

- (1) cerebral blood vessels
- (2) the leptomeninges
- (3) the circumventricular organs
- (4) the choroid plexus

Since the genesis of relapses during systemic inflammation depends on cross-talk between the peripheral immune system and the brain, this has to occur across the immune-brain interface at these areas.

### **1.5.1 Cerebral blood vessels**

In terms of surface area, the BBB at cerebral blood vessels represents the largest contribution to the immune-brain interface. It serves to protect the brain from acute insults such as infections and metabolic disturbances, and therefore maintains the stable milieu required for efficient neural activity. Rather than representing an absolute barrier, it allows for the regulation of traffic of cells and molecules into and out of the brain. It is a complex structure composed of cerebral endothelium, endothelial and glial basement membranes, and astrocytic foot processes. Pericytes are mesenchyme-derived cells enclosed within the endothelial basal lamina. CD163-positive macrophages occupy the potential perivascular space between endothelial and glial basement membranes (**Figure 1.1**). Several features of cerebral endothelium contribute to barrier function: lack of endothelial fenestrations, the presence of continuous tight junctions, lower endocytotic/transcytotic capacity, efflux transport systems, and a combination of intracellular and extracellular enzymes with broad specificity<sup>44</sup>. CD163-positive perivascular macrophages are constitutively phagocytic and are effective scavengers of the perivascular space<sup>45</sup>. They have the capacity to detect potential microbial threats at the BBB by their surface expression of several pathogen-associated molecular pattern receptors such as DC-SIGN, the mannose receptor, CD14 and scavenger receptor A<sup>46</sup>. All cell types around the BBB (astrocytes, neurons, perivascular macrophages and pericytes) have been shown to contribute to the induction of barrier characteristics in cerebral endothelium<sup>44</sup>.

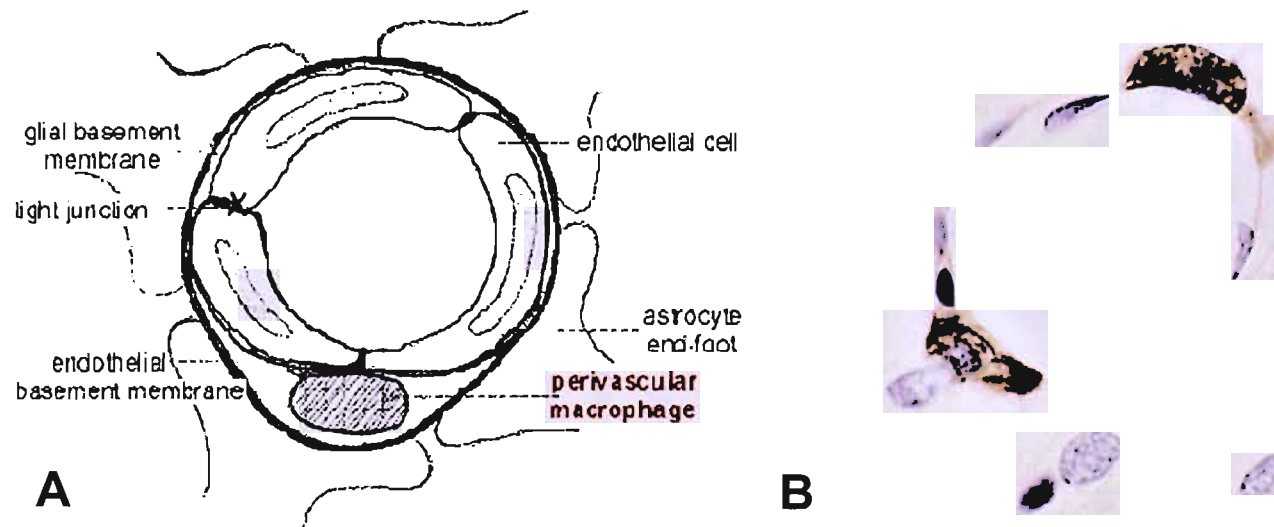


**Figure 1.1. The cerebral perivascular macrophage.** A is a cartoon illustrating the location of the cerebral perivascular macrophage between the glial and endothelial basement membranes at the blood-brain barrier. The photomicrograph in B shows two cerebral perivascular macrophages, stained brown after immunohistochemistry with ED2 antibody against CD163.

### **1.5.2 The leptomeninges**

The meninges, which cover the entire surface of the brain and spinal cord, are composed of the outer dural meninges and the inner leptomeninges, separated by the subarachnoid space. The dura mater is outside the BBB since the endothelium of the vessels supplying it lacks tight junctions. The leptomeninges is composed of the outer arachnoid layer and the inner pia mater. Cells in the outer layer of the arachnoid are joined by numerous desmosomes and tight junctions<sup>47</sup> and pial vessel endothelia have structural characteristics of BBB-containing vessels<sup>48</sup>. CD163-positive macrophages are present on the pial surface of the brain and represent an important component of its barrier function since their depletion results in a significantly worse outcome in experimental pneumococcal meningitis in rats<sup>49</sup>.

### **1.5.3 The circumventricular organs**

The circumventricular organs (CVOs) are well-defined areas of the CNS which lie outside the BBB. To compensate for this, tight junctions between the processes of tanycytes and astrocytes isolate the CVOs from brain parenchyma<sup>50</sup>. Similarly, specialized ependymal cells at the ventricular border of CVOs possess tight junctions<sup>50</sup>. The CVOs include the area postrema, the subfornical organ, the median eminence and the organum vasculosum laminae terminalis. Neurons in these areas are in direct contact with the external environment and relay information to neural structures within the BBB. Compared to brain parenchyma, CVOs have an enriched immune environment as shown by the expression of a variety of molecules involved in both innate and acquired immunity<sup>51</sup>.

### **1.5.4 The choroid plexus**

The choroid plexus is a vascular organ which ramifies throughout the ventricular system and is mainly responsible for cerebrospinal fluid (CSF) formation. It is a villous structure composed of blood vessels covered with cuboidal epithelium. Tight junctions are found between the epithelial rather than endothelial cells of the choroid plexus<sup>50</sup>, which therefore lies outside the BBB.

## 1.6 Mechanisms of relapse in neuroinflammatory disease

Relapse of neuroinflammatory disease during systemic inflammation implies an interaction across the immune-brain interface, which represents the brain's foremost contact with its external environment. Since systemic inflammation is accompanied by circulating inflammatory mediators and activated cells, relapse may thus occur as a consequence of humoral or cellular routes across the immune-brain interface (Figure 1.2).

### 1.6.1 Humoral route

During a systemic infection, a variety of inflammatory mediators are released into the circulation as part of a genetically programmed response to fight infection, clear cellular debris, repair tissue damage and restore homeostasis. Some of these molecules are derived from components of the infectious agent itself, like LPS, lipoteichoic acid (LTA), CpG and polyriboinosinic-polyribocytidylic acid (polyIC), collectively referred to as pathogen-associated molecular patterns (PAMP). Other molecules signify the host's response to infection and include cytokines, prostaglandins, acute-phase reactants, heat-shock proteins, hormones, enzymes, enzyme inhibitors, antibodies and complement proteins. Such circulating inflammatory mediators give rise to the myriad manifestations of infection, including localized inflammation, fever, sickness behaviour, systemic hypotension, and in extreme cases, multi-organ dysfunction.

Neuroinflammatory disease is driven by cytokines secreted by both glia and invading haematogenous macrophages. There is experimental evidence that further increases in CNS cytokine concentrations exacerbate the disease process in models of both MS<sup>52</sup> and AD<sup>53</sup>. Thus augmentation of central cytokines as a result of systemic infection may exacerbate neuroinflammatory disease. The molecular basis of this mechanism is the phenomenon of "priming"<sup>54</sup>. *In vitro* and *in vivo* studies have shown that macrophages exposed to a pro-inflammatory stimulus display a heightened response to a second inflammatory stimulus<sup>55,56</sup>. Thus macrophages may be "primed" or "conditioned" by an inflammatory environment to over-react to further stimulation. It is therefore not surprising that in 3 different models of chronic neurodegeneration (amyloid precursor protein transgenic mice, presenilin-1 transgenic mice and pre-clinical murine prion disease), there is an exaggerated central cytokine response to systemic endotoxin challenge<sup>27,57,58</sup>.

## 1.2. Exacerbation of CNS inflammation following a systemic infection

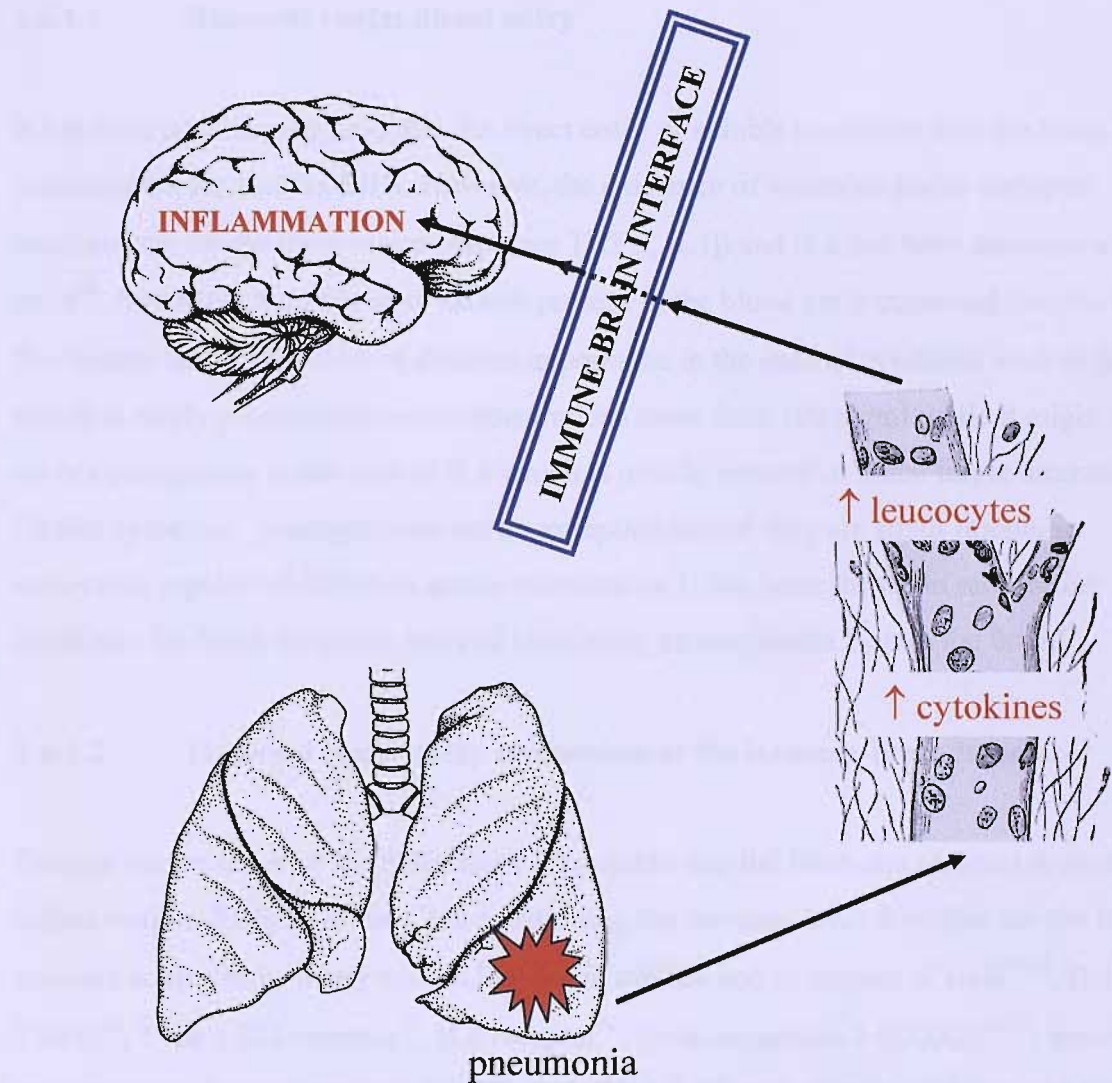


**Figure 1.2. Exacerbation of central nervous system inflammation following a systemic infection: humoral and cellular routes.**

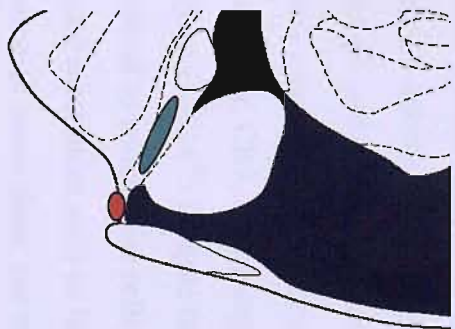
Similarly, in a rodent optic nerve crush model of MS, the innate inflammatory response along the visual pathways is exacerbated by a peripheral challenge of endotoxin: microglia are increased in number and transcribe higher levels of pro-inflammatory cytokines<sup>59</sup>.

### **1.6.1.1      Humoral route: direct entry**

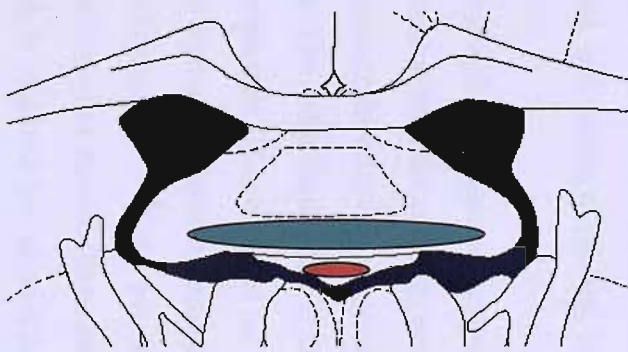
It has been traditionally held that the direct entry of soluble mediators into the brain is restricted because of the BBB. However, the existence of saturable active transport mechanisms for the three major cytokines TNF $\alpha$ , IL1 $\beta$  and IL6 has been demonstrated in mice<sup>60</sup>. Since less than 1% of cytokines present in the blood are transported into the brain, this system is thought to be of dubious importance in the case of cytokines such as IL1 $\beta$  which is rarely present in serum concentrations more than 100 pg/ml while it might be of more consequence in the case of IL6 which is usually present in much larger amounts<sup>61,62</sup>. Unlike cytokines, prostaglandins are an exception in that they are small lipophilic molecules capable of diffusion across membranes. It has been shown in rabbits that cytokines facilitate the direct entry of circulating prostaglandin E<sub>2</sub> into the brain<sup>63</sup>.

### **1.6.1.2      Humoral route: relay mechanism at the immune-brain interface**

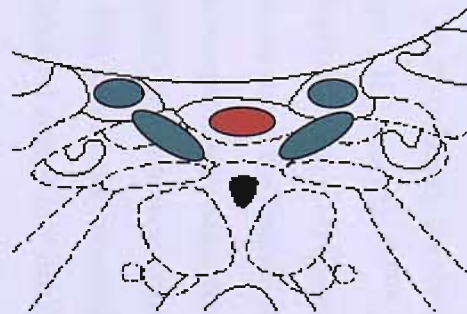
Despite the presence of the BBB, there is no doubt that the brain can respond to systemic inflammation. Regions in the CNS constituting the immune-brain interface are the first to respond as shown by many studies looking at mRNA and/or protein of I- $\kappa$ B<sup>64,65</sup>, IL1 $\beta$ <sup>66-68</sup>, TNF $\alpha$ <sup>69</sup>, Type 1 IL1 receptor<sup>70</sup>, IL6 receptor<sup>71</sup>, cyclooxygenase 2 (COX2)<sup>72-77</sup>, microsomal prostaglandin E<sub>2</sub> synthase (mPGES)<sup>72</sup>, and CD14<sup>78</sup>. There is strong evidence of a relay mechanism operating at three anatomical locations of the immune-brain interface: parenchymal blood vessels, meninges and CVOs. Four independent groups (led by M. Herkenham and C.B. Saper in the United States, S. Rivest in Canada and R. Dantzer in France) have produced evidence of a biphasic response after systemic immune activation. This is characterized by a rapid initial first phase of stimulation of brain structures lying immediately outside the BBB at these three sites (endothelium of parenchymal blood vessels, the meninges and CVOs), followed by a second delayed and prolonged phase of activation of structures within the BBB at these sites (parenchyma, outer cortex and peri-CVO nuclei respectively). As an example, **Figure 1.3** illustrates the temporospatial spread



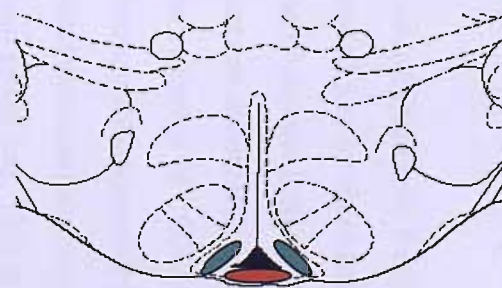
from organum vasculosum laminae terminalis to median preoptic nucleus



from subfornical organ to ventral hippocampal commissure



from area postrema to nuclei of solitary tract and gracile nuclei



from median eminence to arcuate nuclei

**Figure 1.3. Temporospatial spread of immune activation from circumventricular organs (red) to surrounding nuclei (blue)**

of immune activation from some CVOs to surrounding nuclei. This has been shown to be the case using different markers including c-fos mRNA<sup>79</sup>, I- $\kappa$ B mRNA<sup>64,65</sup>, IL1 $\beta$  mRNA<sup>67</sup>, IL1 $\beta$  protein<sup>80</sup> and TNF $\alpha$  mRNA<sup>69,81</sup>. The first phase usually occurs around 1-2 hours following the systemic immune stimulus and it then dies down to be followed by a second phase a few hours later. Differences between studies include level of activation, extent of spread, and timing of phases, but an essential feature is the biphasic nature of the response.

Such a biphasic response argues against a predominant role for direct entry of circulating humoral mediators and suggests the existence of a relay mechanism whereby cells at the immune-brain interface respond first and then relay the inflammatory message into the brain. The cells implicated in this mechanism are endothelial cells and CD163-positive macrophages. This is based on observational evidence of COX2 upregulation by both cell types during systemic inflammation using immunohistochemistry and *in situ* hybridization<sup>72,74,82,83</sup>. As yet, there are no interventional studies of the functional contribution of these cells to immune-to-brain signalling. This is essential information which is required for rational design of therapies aimed at manipulating immune-to-brain signalling.

Cerebral endothelial cells and CD163-positive perivascular macrophages are equipped to respond to circulating humoral mediators. On stimulation, cerebral endothelial cells transcribe mRNA for receptors such as Type 1 IL1 receptor<sup>70,84,85</sup>, TNF receptor<sup>86</sup>, IL6 receptor<sup>71</sup> and CD14<sup>78</sup>. Depending on activation status, CD163-positive macrophages also express a variety of receptors enabling them to sense the haemal milieu, including Type 1 IL1 receptor, CR3, FcR receptor, mannose receptor, scavenger receptor types I and II, DC-SIGN and CD14<sup>46</sup>. Despite the fact that CD163-positive macrophages are situated abluminal to endothelial cells at the BBB, they have been reported to take up intravenously injected substances such as fluorescently labelled acetyl-low density lipoprotein and horseradish peroxidase, but whether this occurs as a result of direct uptake by the macrophages or transendothelial transport is unclear<sup>87</sup>. Given that these macrophages express the Type I IL1 receptor<sup>83</sup> and are capable of secreting IL1 $\beta$ <sup>88</sup>, there is potential for amplification of endothelial signals at the immune-brain interface.

Because of the marked upregulation and colocalization of COX2 and mPGES in vascular cells at the immune-brain interface, the molecular identity of the secondary mediator

responsible for relaying the inflammatory message into the brain is thought to be prostaglandin E<sub>2</sub> (PGE<sub>2</sub>)<sup>72</sup>. Prostaglandin synthesis is a stepwise process (**Figure 1.4**) starting with mobilization of arachidonic acid from membrane phospholipids by phospholipase A<sub>2</sub>, followed by conversion to PGG<sub>2</sub> and then PGH<sub>2</sub> by COX, of which there are two types. COX1 is expressed constitutively and produces housekeeping PGs while COX2 is undetectable under basal conditions but is rapidly upregulated during inflammation<sup>89</sup>. PGH<sub>2</sub> may be converted to several PGs by various synthases: microsomal PGE<sub>2</sub> synthase (mPGES) is responsible for PGE<sub>2</sub> synthesis. PGE<sub>2</sub> is a small lipophilic molecule and is therefore an ideal candidate as a secondary messenger. Interestingly the basal (i.e. abluminal) to apical (i.e. luminal) ratio of PGE<sub>2</sub> release by cultured murine cerebral endothelial cells *in vitro* was 4:1<sup>90</sup> and PGE<sub>2</sub> immunoreactivity was observed on the parenchymal side of the cerebral endothelium in endotoxin-treated rats<sup>91</sup>, in support of a role as an inflammatory messenger.

PGE<sub>2</sub> has been shown to mediate several CNS responses to systemic inflammation:

1. **Fever**, by acting on EP3 receptors in the preoptic area, ventrolateral medulla and nucleus of the tractus solitarius<sup>92,93</sup>. Fibres from all three areas project to the parvocellular component of the paraventricular hypothalamic nucleus which is thought to constitute the main thermoregulatory centre<sup>61</sup>.
2. **Hyperalgesia**, by binding to EP1 receptors in the ventromedial hypothalamus and EP3 receptors in the preoptic area and diagonal band of Broca<sup>94</sup>.
3. **Hypothalamo-pituitary-adrenocortical axis (HPA) activation**, by agonizing EP1 and EP3 receptors on corticotrophin-releasing hormone (CRH) positive parvocellular neurones in the paraventricular hypothalamic nucleus<sup>95</sup>. These neurones project to the external layer of the median eminence where CRH is released to be carried by the hypophyseal portal system to the anterior pituitary resulting in adrenocorticotropic (ACTH) hormone secretion into the circulation. In turn, ACTH stimulates adrenocortical cells to synthesize and release corticosteroids.
4. **Sickness behaviour**. Inhibition of COX2 by NSAIDs has shown that PGs mediate the behavioural consequences of systemic IL1 $\beta$  challenge<sup>96</sup> and EAE<sup>97</sup> in mice. In addition, a

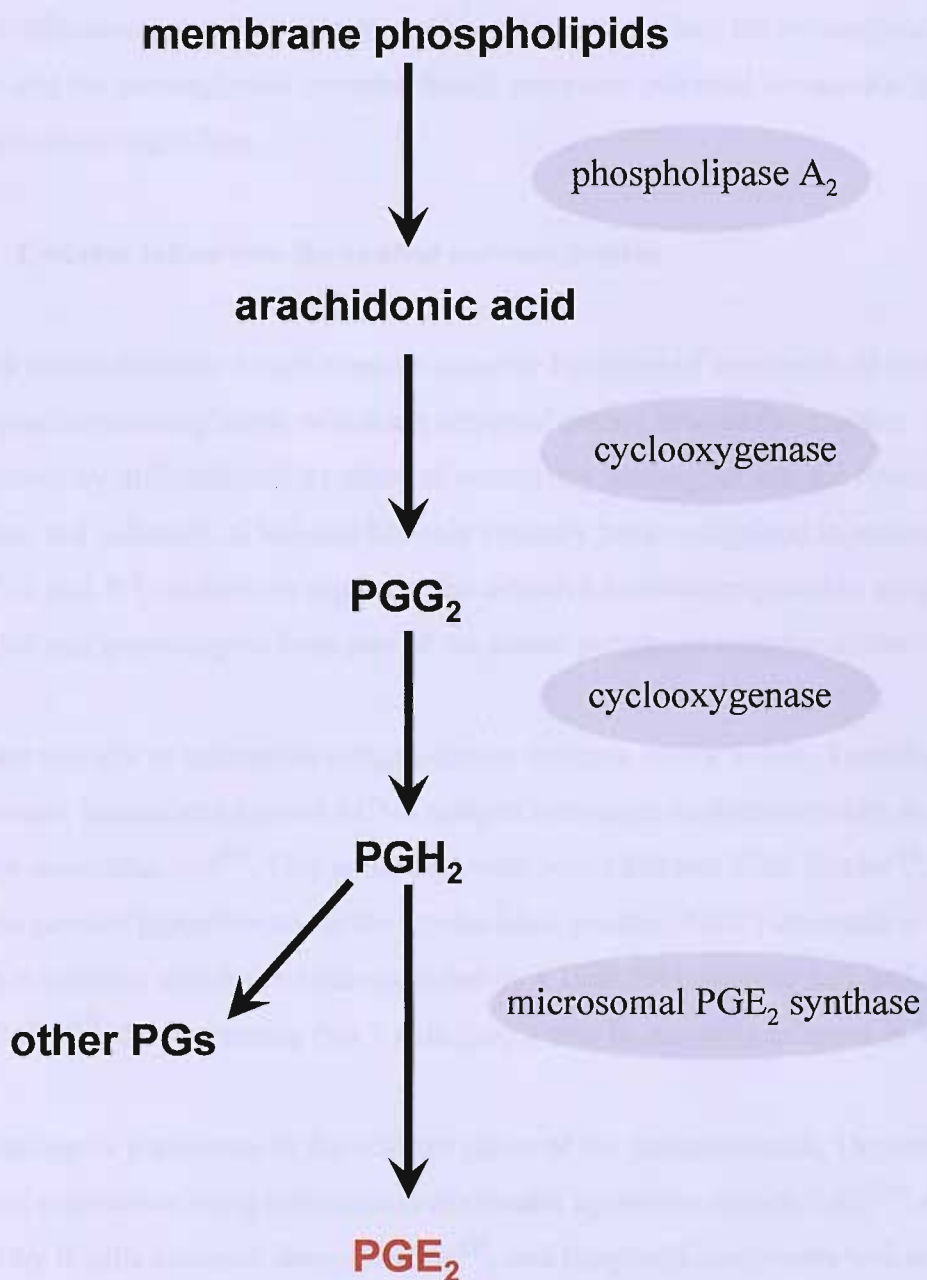


**Figure 1.4. The prostaglandin synthetic pathway**

randomized controlled crossover trial demonstrated a significant effect of aspirin on fatigue in MS patients<sup>98</sup>.

Whether PGE<sub>2</sub> also mediates the *de novo* transcription of cytokines seen in the brain after systemic inflammation is still unknown. This is important since the prostaglandin synthetic pathway and the prostaglandin receptor family represent potential therapeutic targets in immune-to-brain signalling.

### **1.6.2 Cellular influx into the central nervous system**

The CNS has an intrinsic innate immune capacity by virtue of a network of microglia and CD163-positive macrophages, which are activated during neuroinflammation. This may be accompanied by infiltration of a variety of circulating leucocytes into the brain. Such infiltration is a hallmark of MS and has only recently been recognized in animal models of AD<sup>99,100</sup>. T and B lymphocytes represent the adaptive immune response to an antigen while monocytes and granulocytes form part of the innate peripheral immune system.

T cells are thought to initiate the antigen-driven immune attack in MS. Transfer of T cells from animals immunized against a CNS antigen into naïve recipients results in EAE, which strikingly resembles MS<sup>101</sup>. This is the case with both CD4 and CD8 T cells<sup>102</sup>. A trial of an altered peptide ligand based on the myelin basic protein (MBP) sequence in MS patients resulted in relapses which were accompanied by a 1000 fold increase in T cell reactivity against MBP<sup>103</sup>, demonstrating that T cells play a role in initiating relapses in MS.

Other leucocytes participate in the effector phase of the immune attack. Depletion of peripheral monocytes using intravenous clodronate liposomes arrests EAE<sup>104</sup>. Antibodies secreted by B cells augment demyelination<sup>105</sup>, and lymphoid neogenesis within the CNS in established neuroinflammation is thought to play a role in disease maintenance<sup>106</sup>. Granulocytes are only seen in infiltrates in severe or hyperacute cases of EAE<sup>107</sup> but a recent study has suggested a role in the effector phase of EAE<sup>108</sup> possibly by regulating the recruitment of lymphocytes.

Systemic infection results in stimulation of circulating T cells as well as enhancing their transendothelial migration. Since T cells are thought to initiate neuroinflammation in MS, this represents a potential mechanism underlying relapse following a systemic infection.

### 1.6.2.1 T cell stimulation

Systemic infection may result in T cell stimulation in two ways: antigen-specific and bystander.

**Antigen-specific stimulation** occurs as a result of T cell receptor (TCR) ligation. The antigen is processed by antigen-presenting cells (APCs) into smaller peptides which are displayed on their surface in the context of major histocompatibility molecules (MHC). Interaction between the MHC-peptide complex and the TCR leads to T cell stimulation. CD8 and CD4 T cells recognize MHC Class I and MHC Class II-restricted peptides respectively. Molecular mimicry between microbial and neural antigens is thought to play a role in the initiation of encephalitogenic T cell responses in MS. Thus a viral infection might trigger activation of T cells bearing a TCR which cross-reacts with neural antigen. Although molecular mimicry was initially sought on the basis of amino-acid sequence similarities<sup>109</sup>, it is now thought to be much more degenerate. Thus single amino acid similarities at TCR and MHC anchor positions are enough<sup>110</sup>. Indeed, it was calculated that a single TCR might have the capacity to recognize one million different peptide-MHC combinations<sup>111</sup>. Extending the concept further, it now seems that there does not even need to be any amino acid similarity as long as the additive stimulatory potency of all amino acids exceeds a certain threshold<sup>112</sup>.

**Bystander stimulation** occurs via TCR-independent pathways, and is not well characterized. Several instances of bystander activation have been described:

(1) **Contact-dependent activation of CD4 T cells.** LPS administration induced relapse after monophasic EAE in mice previously immunized with MBP peptide. This was shown to occur as a result of TCR-independent activation of CD4 T cells which depended on contact with CD4-negative splenic cells. Half of this bystander stimulation was inhibited by the addition of a cocktail of antibodies directed against a variety of B7 family costimulatory molecules<sup>22</sup>.

**(2) IL15-dependent proliferation of memory CD8 T cells.** There is evidence that both viral and bacterial products induce a prominent burst of bystander memory CD8 T cell proliferation, for example after exposure to LPS<sup>113</sup>, polyIC<sup>114</sup> and CpG<sup>115</sup>. This phenomenon is a true bystander effect and is not secondary to degeneracy of MHC Class I – TCR interactions since it still occurred in a  $\beta_2$ -microglobulin<sup>-/-</sup> system<sup>115</sup>. IL15 has been shown to be the common final effector, downstream of Type I IFN, IFN $\gamma$ , IL12 or IL18<sup>116</sup>.

**(3) Dendritic cell activation by provision of danger signal.** The immune system's response to an antigenic challenge is sensitive to the context in which this occurs<sup>117</sup>. Danger signals may come from self (e.g. heat shock proteins, IFN $\alpha$ , hyaluron breakdown products, CpG, CD40L) or non-self (e.g. LPS, LTA, polyIC). Thus cytokines released during systemic infection or products from the infecting organism itself may act as natural adjuvants to stimulate an immune response against a CNS antigen, initiating a relapse. This has been shown to be mediated by dendritic cells expressing receptors for danger signals (e.g. toll-like receptors) which upregulate MHC and costimulatory molecules in response to these signals leading to proliferation of antigen-specific T cells<sup>118</sup>. Viral, bacterial or parasitic infections may also break down tolerance of circulating CD4 and CD8 T cells to autoantigens<sup>119,120</sup> as a result of provision of danger signals<sup>121</sup>. Thus although the T cell response is antigen-specific, the danger signal is not. It is relevant that costimulation is equally effective whether it is delivered by the same APC (cis-costimulation) or separately by two different APCs (trans-costimulation)<sup>122</sup>. In the latter case, it has been shown that the two signals need not be delivered simultaneously<sup>123</sup>. This means that the danger signal provided by the systemic infection may be spatially and temporally separated from encephalitogenic T cell activation.

**(4) Superantigen-induced activation of T cells.** Superantigens are bacterial or viral products which hyperstimulate T cells nonspecifically<sup>124</sup> and have been shown to induce relapse in EAE<sup>23</sup>. They bind to the V $\beta$  region of particular subsets of T cell receptors and non-polymorphic regions of class II MHC molecules, outside of the peptide binding groove. As a consequence, superantigen recognition is not classically MHC restricted, and both CD4 and CD8 T cells respond<sup>125</sup>.

T cell stimulation results in proliferation, cytokine secretion and cytotoxicity. CD4 T cells secrete a wide array of cytokines and direct the adaptive immune response by facilitating

antigen-specific activation of CD8 T cells and B cells. CD8 T cell activation leads to synthesis of cytokines (TNF $\alpha$ , TNF $\beta$  and IFN $\gamma$ ) and acquisition of cytotoxic function by expression of perforin, granzymes and fas ligand. T cell stimulation also results in upregulation of surface molecules which enhance their capacity for transendothelial migration, which places them in close proximity to their target within the brain.

### 1.6.2.2 Transendothelial migration of T cells

Systemic infections may result in enhanced transendothelial migration of T cells into the brain, setting the stage for a relapse. There is a wealth of *in vitro* evidence showing that transendothelial migration of T cells is markedly increased with cytokine or pathogen-induced activation of either T cells or endothelium or both<sup>126-133</sup>. T cells from EAE animals exhibited increased adhesion to cerebral endothelium *in vitro*, and this was increased further after LPS administration<sup>134</sup>. An intravital microscopy study showed that injected activated T cells only rolled and arrested when cerebral endothelium was pre-activated by LPS or TNF $\alpha$ <sup>135</sup>. Importantly, blockade of transendothelial migration of T cells in both EAE<sup>136</sup> and MS<sup>36</sup> ameliorated disease course, showing that changes in T cell traffic into the CNS correlate with disease activity.

Transendothelial migration of T cells is a 3 step process<sup>137</sup>:

(1) **Rolling.** Circulating T cells “roll” along the surface of endothelium via the interaction of endothelial E- and P-selectins with glycoconjugates on the T cell surface, alternately engaging and disengaging.

(2) **Adhesion.** Rolling is arrested when chemokines bound to glycosaminoglycans on the outer surface of endothelial cells interact with chemokine receptors on the surface of the rolling T cell. This results in a conformational change of integrins on the T cell surface increasing their avidity for Ig superfamily proteins on the endothelial cell surface.

Examples of such integrin/Ig superfamily pairs are LFA1/ICAM1 and VLA4/VCAM1. The firm adhesion which ensues is essential for diapedesis.

(3) **Diapedesis**, or transendothelial migration, then follows.

Brain-infiltrating T cells will only initiate disease if they recognize their cognate antigen within the CNS. Various studies have shown that T cell infiltration into the brain occurs

independently of antigen specificity<sup>138-143</sup>. Activated CD4 T cells reactive against neural or irrelevant antigens were transferred into animals and it was observed that they infiltrated the brain equally well. However, whether antigen specificity is a feature of CD8 T cell infiltration is unknown. In some experiments<sup>138,139</sup>, CD8 T cells were present amongst the transferred cells but no efforts were made to elucidate whether the antigen specificity of CD8 T cells was influencing their infiltration into the brain.

In support of CNS antigen-specific CD8 T cell traffic, several studies have reported oligoclonal dominance of CD8 T cells in the CNS. Mice immunized with a myelin oligodendrocyte protein peptide (MOG 35-55) develop EAE and on day 10, tetramer staining revealed that 56% of brain infiltrating CD8 T cells were specific for MOG 37-50<sup>144</sup>. Oligoclonal dominance of CD8 T cells was also seen in CSF<sup>145</sup> and plaques<sup>146</sup> from MS patients. This has been largely interpreted as oligoclonal expansion within the CNS compartment. Whether CNS antigen-specific CD8 T cell infiltration contributes to this oligoclonal dominance is unknown.

CNS antigen-specific CD8 T cell infiltration is important given the recent realization of the role of CD8 T cells in MS<sup>102,147</sup>. A role in disease initiation was shown when systemic transfer of MBP or MOG specific CD8 T cells into mice induced severe EAE<sup>148,149</sup>: initiation of a relapse can only occur if the infiltrating CD8 T cells are antigen-specific. Using intravital microscopy it has been shown that circulating memory CD8 T cells but not CD4 T cells from MS patients in the first 24 hours into a relapse exhibit increased migration across murine cerebral endothelium<sup>150</sup>, leading the authors to suggest that CD8 T cells might play a major role in disease initiation in humans.

CD8 T cells also play a significant role in disease maintenance. For instance, they outnumber CD4 T cells in the parenchyma of MS plaques<sup>151</sup> and a high prevalence of circulating neuroantigen-specific CD8 T cells, but not CD4 T cells, was seen in patients with MS<sup>152</sup>. In support of a pathogenic role, CD8 T cells correlated with axon injury in acute MS plaques<sup>153</sup> and MRI features of tissue damage<sup>154</sup>, and granzyme B-expressing CD8 T cells were seen contacting injured axons with polarization of cytotoxic granules towards the axon<sup>102</sup>. CD8 T cell-related neuropathology may be mediated directly by encephalitogenic CD8 T cells<sup>155</sup> or may occur indirectly as a result of bystander damage by co-infiltrating CD8 T cells with irrelevant antigen specificities<sup>156,157</sup>. However the overall

contribution of bystander damage has been shown to be small<sup>158,159</sup>. Therefore CNS antigen-specific CD8 T cell traffic is important during ongoing neuropathology.

## 1.7 Aims

The studies reported in this thesis aimed to investigate several events occurring at the immune-brain interface which may be implicated in the genesis of neuroinflammatory relapse:

(1) **Prostaglandins in immune-to-brain signalling.** PGs have been shown to mediate several brain responses to systemic inflammation: fever, hyperalgesia, activation of the HPA axis and sickness behaviour. All these responses can be inhibited by NSAIDs. It remains to be shown whether NSAIDs affect the expression of the major cytokines TNF $\alpha$ , IL1 $\beta$  and IL6 which occurs in the brain during systemic inflammation. Such cytokine expression is thought to underlie relapse genesis and/or accelerated neurodegeneration following a systemic infection. Therefore the effect of an archetypal NSAID, indomethacin, on the *de novo* transcription of cytokines within the rat brain during systemic endotoxin challenge was investigated (Chapter 3).

(2) **CD163-positive macrophages in immune-to-brain signalling.** Two cell types at the immune-brain interface are known to respond to systemic inflammation: cerebral endothelial cells and CD163-positive macrophages. It is thought this cellular activation at the immune-brain interface plays a crucial role in relaying the inflammatory message into the brain. However this is based on observational evidence namely the upregulation of COX2 by these cells. Functional studies of the relative contribution of cerebral endothelial cells and CD163-positive macrophages in immune-to-brain signalling are awaited. Therefore an intracerebroventricular (ICV) infusion of clodronate liposomes in rats was used to deplete CD163-positive macrophages, and dissect the roles of these two cell types. Since ICV infusion of clodronate liposomes resulted in leakage to the periphery and suppression of the cytokine response to systemic endotoxin challenge, it was first necessary to optimize the clodronate liposome technique (Chapter 4). Then, *de novo* transcription of cytokines within the brain during systemic endotoxin challenge was investigated in rats which had previously received an ICV infusion of clodronate or control liposomes using the optimized technique (Chapter 5).

**(3) Antigen-specific CD8 T cell traffic.** It has been shown that CD4 T cells cross the BBB to infiltrate the brain irrespective of their antigen specificity. Whether the same can be said for CD8 T cells is not known. Antigen-specific CD8 T cell traffic into the brain is important since it has been shown to be responsible for initiation of relapse and subsequent tissue damage. In order to investigate this, a MHC Class I restricted TCR transgenic mouse was utilized in which >95% of CD8 T cells recognize a haemagglutinin peptide<sup>160</sup>. Cerebral perivascular macrophages (PVMs) are considered to be the prime APC at the BBB and therefore are highly relevant to antigen-specific T cell traffic into the brain. However the technology to study PVMs in mice was not available. Therefore a new surface marker which specifically reveals murine PVMs was identified and the clodronate liposome technique was adapted for use in mice (Chapter 6). Antigen-specific CD8 T cell traffic into the brain was then investigated using intrastriatal injections of cognate (haemagglutinin peptide) or irrelevant antigen (Chapter 7). The tools developed in Chapter 6 were used in order to further study CD8 T cell traffic into the brain.

## **Chapter 2**

### **Materials and methods**

## Materials and methods

### 2.1 Animals

Adult male Wistar or Lewis rats weighing *circa* 200g and BALB/c mice weighing *circa* 20g were purchased from Harlan (Bicester, UK). Animals were housed in a conventional animal facility under a 12h light:12h dark schedule and controlled environmental conditions with pelleted food and water *ad libitum*.

CL4 transgenic mice were a gift from Professor Roland Liblau at INSERM U563, Purpan University Hospital, Toulouse. CL4 transgenic mice express the V $\alpha$ 10 V $\beta$ 8.2 T cell receptor (TCR) from clone 4 (CL4), a CD8 T cell clone from a B10.D2 mouse previously immunized with influenza virus (strain A/PR/8/34 Mt Sinai), specific for the peptide IYSTVASSL restricted by the K $^d$  major histocompatibility complex Class I molecule<sup>160</sup>. Heterozygous CL4 mice had been fully backcrossed (>8 generations) onto the BALB/c genetic background. They had also been backcrossed with Thy1.1<sup>+/+</sup> BALB/c mice for 2 generations to achieve homozygosity for Thy1.1. The CL4 mice were heterozygous for the transgene and they were maintained by breeding with Thy1.1<sup>+/+</sup> BALB/c mice: transgenic offspring was obtained at roughly Mendelian rates. Offspring were screened for transgenicity one or two weeks after weaning. Their tail tips were clipped (1mm) and a drop of blood collected in heparin coated plastic capillary tubes. This blood was analyzed by fluorescence-assisted cell sorting (FACS) as described below. Transgenic and non-transgenic mice were clearly and unequivocably distinguishable (Figure 2.1). The transgenic colony was bred and maintained in individually ventilated cages in a separate room in the same conventional facility.

Rats and mice typically weighed 250g and 25g respectively when used. The experiments were carried out under Home Office Licence and in accordance with the Animals (Scientific Procedures) Act, 1986.

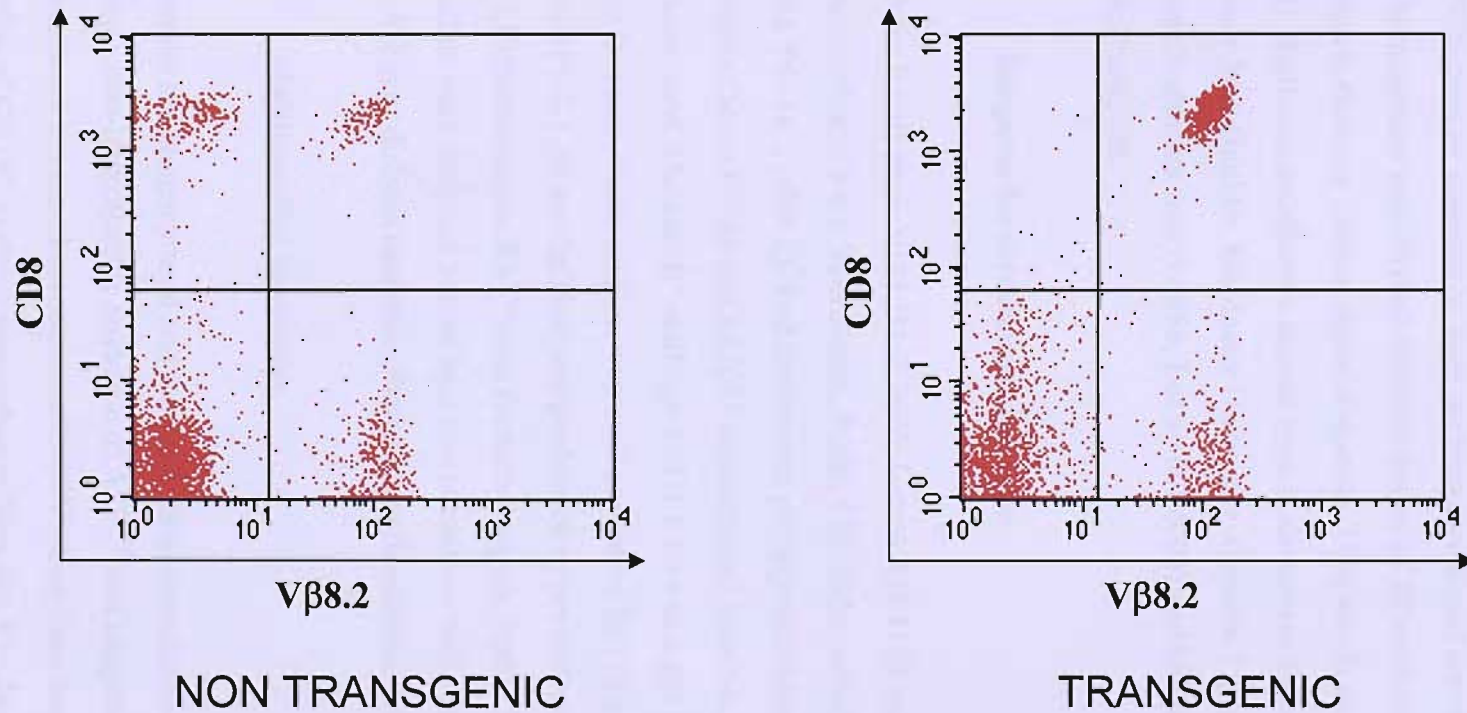


**Figure 2.1. The CL4 transgenic mouse**

>95% of CD8 T cells in the CL4 transgenic mouse express the cloned V $\alpha$ 10 V $\beta$ 8.2 TCR (HA 512-520 H-2K $^d$  restricted)

## 2.2 Reagents for intracranial injection

The haemagglutinin peptide (IYSTVASSL) and control K<sup>d</sup>-binding peptide (Cw3 peptide, RYLKNGKETL) were bought from Alta Bioscience, Birmingham, UK and were certified to be 95% pure as assessed by high performance liquid chromatography. The ME7 prion brain homogenate was derived from the brains of 22 week old C57BL/6J mice post-inoculation showing clinical signs of disease (10% w/v in sterile phosphate-buffered saline (PBS)). Replication-defective human type 5 adenovirus vector (Ad70-3) was a gift from Professor Jack Gauldie, McMaster University, Ontario. Lipopolysaccharide (LPS) from *Salmonella abortus equi* (L5886, Lot no 69F4003) and kainic acid were purchased from Sigma, Poole, UK.

## 2.3 Reagents for intravenous injection

LPS from *E coli* strain 0111:B4 (L2630, Lot no 42K4120 and L4391, Lot no 092K4019) and indomethacin were from Sigma, Poole, UK. Indomethacin was dissolved by sonication in 0.2M Tris HCl (pH8.2). Red fluorescent polystyrene fluospheres of 0.02 and 1µm diameters (Cat no F8786 and F13083 respectively) from Molecular Probes (Cambridge, UK) were used. The anti-K<sup>d</sup> antibody SF1-1.1.10 was a gift from Philippe Kourilsky, Pasteur Institute, Paris. IgG2ak was used as control IgG (Sigma, Poole, UK). Biotinylation of both SF1-1.1.10 and IgG2ak was performed as per instructions using the EZ-Link Sulfo-NHS-LC-Biotinylation Kit (Pierce Biotechnologies, Perbio Science UK Ltd, UK). All antibodies were dialyzed before injection to remove NaN<sub>3</sub> or Tris using 10kDa MW cut-off Slide-A-Lyzer dialysis cassettes (Pierce Biotechnologies, Perbio Science UK Ltd, UK).

## 2.4 Multilamellar liposomes

Liposomes are phagocytosed and intracellular accumulation of clodronate is toxic by forming a non-hydrolyzable analogue of ATP<sup>161</sup> and triggering apoptosis<sup>162</sup> (**Figure 2.2**). When infused intracerebroventricularly (ICV), they have been shown to result in complete depletion of CD163-positive macrophages from day 4 to day 10 after the procedure<sup>163</sup>.

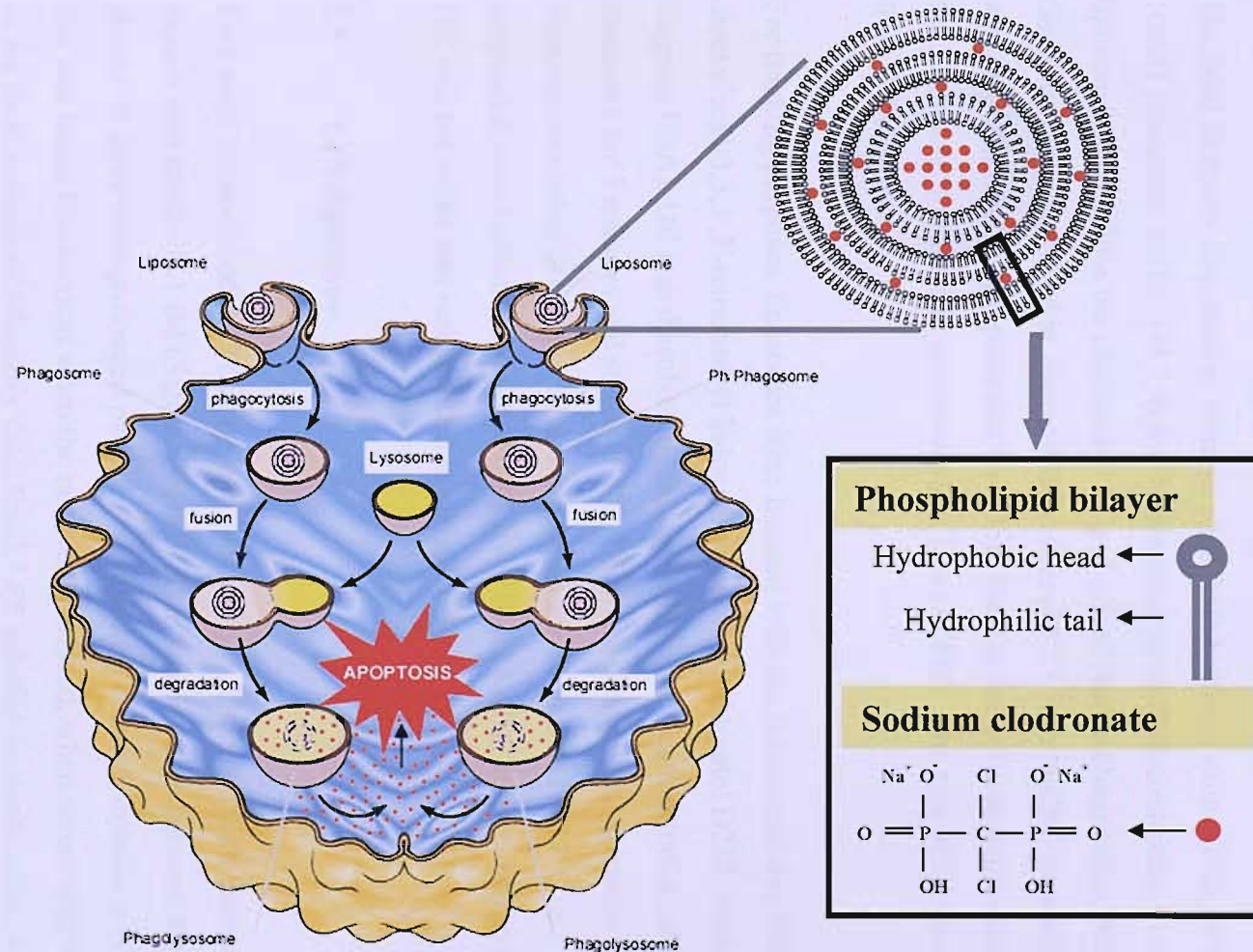


**Figure 2.2. Clodronate-loaded multilamellar liposomes**

Multilamellar mannosylated liposomes were prepared as described before<sup>164</sup>. Briefly, 178mg phosphatidylcholine (Lipoid GmbH, Ludwigshafen, Germany) and 27mg cholesterol (Sigma Chemicals) were dissolved in 8ml chloroform which was added to 9.25mg *p*-amino-phenyl- $\alpha$ -D-mannopyranoside (Sigma Chemicals) dissolved in 5ml methanol in a 500ml round-bottom flask. This was dried *in vacuo* on a rotary evaporator to form a film. The molar ratio of phosphatidylcholine / cholesterol / mannoside was 7:2:1. The lipid film was dispersed in 10ml of phosphate buffered saline (PBS, 0.15M NaCl in 10mM phosphate buffer, pH 7.4) for the preparation of PBS-containing mannosylated liposomes. To enclose the clodronate, 2.5g (a gift of Roche Diagnostics, Mannheim, Germany) was dissolved in 10ml milliQ (set at pH 7.3 with NaOH) in which the lipid film was dispersed and the preparations were kept for 2 hours at room temperature, sonicated for 3 minutes, washed and resuspended in 10ml of PBS. The size of the liposomes ranged from 0.2 to 3  $\mu$ m.

For tracking purposes, liposomes were labelled with the fluorescent dye DiI (1,1'-dioctadecyl-3,3,3',3'-tetramethyl indocarbocyanine perchlorate; D282; Molecular Probes, Eugene, USA). DiI was dissolved in absolute ethanol at a concentration of 2.5mg/ml, sonicated for 5 minutes and stored at 4°C. DiI was added to 1ml liposome suspension in a final concentration of 62.5  $\mu$ g/ml and incubated for 30 minutes at 37°C in a waterbath. The suspension was washed three times with 2ml PBS (24000g, 15 minutes) to remove free DiI, and the pellet was resuspended in 400  $\mu$ l PBS.

## 2.5 LPS injections

Rats were intraperitoneally (i.p.) or intravenously (i.v.) injected with a solution of LPS from *E coli* strain 0111:B4 (Sigma, Poole, UK) in sterile saline between 9 and 10AM (light phase). If there were prolonged periods (> 5 minutes) between injections of individual rats, this was taken into account when the rats were perfused, when serum was withdrawn and in the final analysis of telemetry data. Fresh LPS solution in sterile saline was made on the day for each experiment. Since LPS is not very soluble, the preparation was vortexed for 5 minutes when first prepared and then re-vortexed before each injection to ensure homogeneity. Initially LPS L2630 Lot no 42K4120 was used; this was changed to L4391 Lot no 092K4019 when stocks ran out. Bioequivalence was ensured by correcting for

endotoxin activity on LAL assay as certified by the manufacturer. The LAL assay is based on detection of the Lipid A component of LPS, which is the moiety responsible for its endotoxic activity. The validity of this approach was confirmed by observing that the area-under-the-curve for the febrile responses after both doses of LPS did not differ significantly.

## **2.6 Immunization**

Antigen was emulsified in complete Freund's adjuvant (Sigma, Poole, UK) using a homogenizer. Immunizations were done by intradermal injection of 100 $\mu$ l of active or control emulsion in the left thigh under isoflurane/O<sub>2</sub> anaesthesia.

## **2.7 Surgery**

Homeostatic blankets were used during prolonged surgery. Aseptic technique was used. Skin and muscle were sutured using Ethicon Vicryl and Mersilk sutures respectively (Johnson & Johnson International, Brussels, Belgium). Animals were allowed to recover in a temperature-controlled box following surgery before being returned to their cages.

### **2.7.1 Telemetry capsule implantation**

This surgery was performed under isoflurane/O<sub>2</sub> anaesthesia. Rats were fed blackcurrant jelly for a few days before surgery. This was done in order to encourage ingestion of analgesic-containing jelly post-operatively. TA10TAF20 telemetry capsules (Data Sciences International, Minnesota, USA) were implanted intraperitoneally under aseptic conditions through a right paramedian laparotomy. The skin over the abdomen was prepared by shaving and swabbing with chlorhexidine-alcohol. A right paramedian skin incision was made followed by blunt dissection of the fascial plane between the skin and abdominal muscle medially till the rectus sheath was identified. The muscle layer was then opened slightly medial to the overlying skin incision by blunt dissection. When the parietal peritoneum was reached, it was slit open and the capsule inserted into the peritoneal cavity. Muscle and skin layers were sutured separately using absorbable and non-absorbable material respectively (see above). The rats were administered subcutaneous buprenorphine

(Temgesic, Schering-Plough, Hertfordshire, UK) (0.05mg/kg) post-operatively and then fed buprenorphine-containing blackcurrant jelly (0.5mg/kg) the day afterwards.

### **2.7.2 Intracerebroventricular liposome infusion**

This surgery was performed under isoflurane/O<sub>2</sub> anaesthesia. An operating microscope was used. Anaesthetized rats had the skin overlying the skull prepared by shaving and swabbing with chlorhexidine-alcohol. They were then fixed in a stereotaxic frame. A midline incision was made. Lateral and rostro-caudal coordinates were taken and a burr hole was drilled. The dura was slit open. A Hamilton syringe fitted with a 27G needle was loaded with liposome suspension: this suspension was gently vortexed before each injection to ensure homogeneity. The syringe was fixed in a holder on the stereotaxic arm, which was positioned to the same lateral and rostro-caudal coordinates. The needle tip was gently lowered through the burr hole to the required depth in the brain. The required volume of liposome suspension was infused slowly ICV (3<sup>rd</sup> or 4<sup>th</sup> ventricle) at a rate of 2µl/minute. In order to minimize reflux into the subarachnoid space overlying the injection site, the needle was left in place for 2.5 minutes before being slowly withdrawn over another 2.5 minutes. The following coordinates were used: 4<sup>th</sup> ventricle: bregma -11.6mm, lateral 0mm, depth 8.2mm (**Figure 2.3**); lateral ventricle: bregma -0.8mm, lateral 1.4mm, depth 4.4mm (**Figure 2.4**) (*The Rat Brain in Stereotaxic Coordinates*, by Paxinos & Watson, 4th edition, 1998, Academic Press, California, USA).

A modification of the technique was developed for mice (see Chapter 6). Eight µl of mannosylated liposomes were infused into each lateral ventricle slowly over 12.5 minutes using a pulled glass capillary (co-ordinates: -0.22mm, lateral 1mm and depth 2mm). On each side, the capillary was left *in situ* for 2.5 minutes, withdrawn partially and left for a further 2.5 minutes before being removed completely to avoid reflux of liposomes along the injection tract.

### **2.7.3 Intracranial injections**

Stereotaxic intracranial injections were performed in mice anaesthetized with intraperitoneal Avertin (1.25% 2,2,2-tribromoethanol in tertiary amyl alcohol) at a dose of 0.1ml/5g body weight. Mice had the skin overlying the skull prepared by shaving and

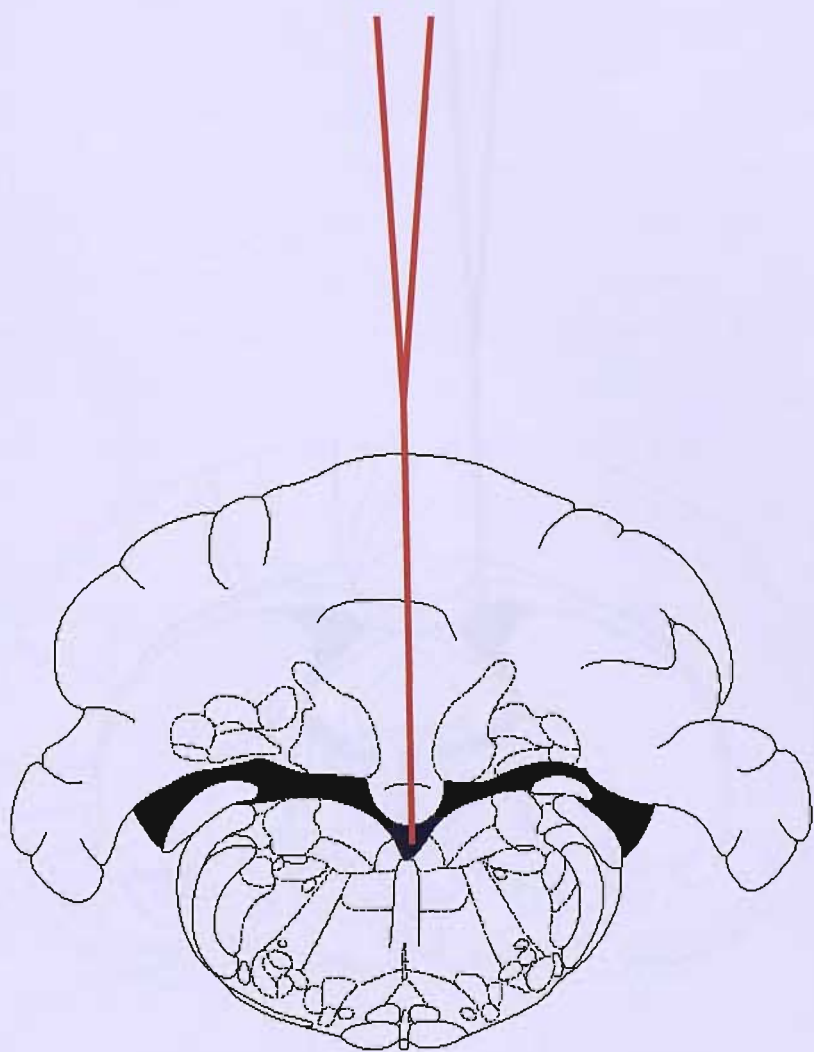


**Figure 2.3**

**Fourth ventricular infusion**

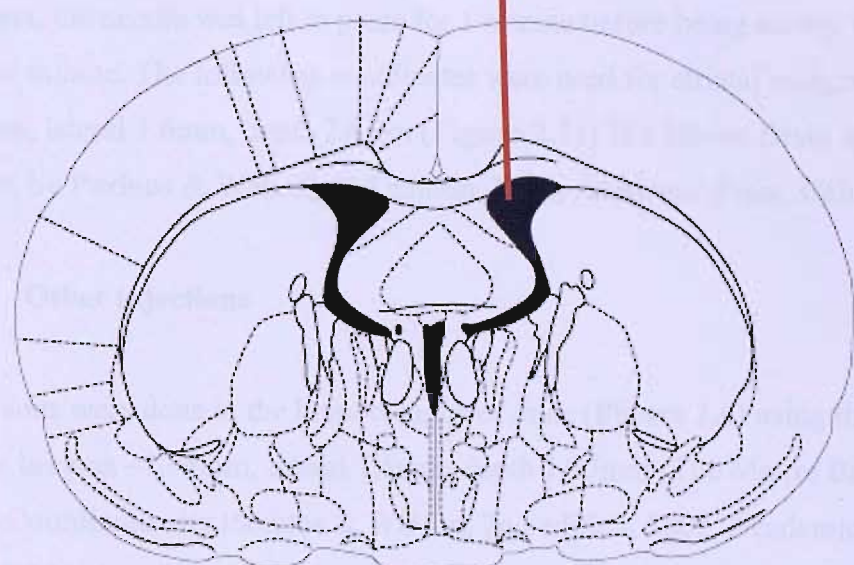


**Figure 2.4**

### **Lateral ventricular infusion**

swabbing with chlorhexidine-alcohol. They were then fixed in a stereotaxic frame. A midline incision was made. Lateral and rostro-caudal co-ordinates were taken and a burr hole was drilled. The dura was slit open.

#### **2.7.3.1 Antigen injections**

A pulled glass micropipette was used to deliver the antigen slowly into the striatum in a volume of 0.5 $\mu$ l of vehicle over a period of 1 minute. The tip of such a pulled glass micropipette is sterile and ultrafine, measuring a few micrometers in diameter. Injections invariably contained a trace of Colanyl Blue to help with localization of the lesion during subsequent tissue processing. This dye has been previously shown to be immunologically inert (Tracey A Newman, personal communication). In order to minimize reflux along the injection tract, the needle was left in place for 1 minute before being slowly withdrawn over another minute. The following coordinates were used for striatal antigen injections: bregma 1mm, lateral 1.6mm, depth 2.6mm (**Figure 2.5**) (*The Mouse Brain in Stereotaxic Coordinates*, by Paxinos & Watson, 2nd edition, 2002, Academic Press, California, USA).

#### **2.7.3.2 Other injections**

Other injections were done in the hippocampus of mice (**Figure 2.6**) using the following coordinates: bregma -1.94mm, lateral 1.5mm, depth 1.37mm (*The Mouse Brain in Stereotaxic Coordinates*, by Paxinos & Watson, 2nd edition, 2002, Academic Press, California, USA). A pulled glass micropipette was also used for LPS and kainic acid injection. For prion disease, mice were bilaterally injected in the dorsal hippocampus with 1 $\mu$ l of ME7 prion brain homogenate using a Hamilton syringe fitted with a blunt 26S needle.

#### **2.7.4 Optic nerve crush**

The mouse right optic nerve was crushed intraorbitally under an operating microscope with jeweller forceps for 10 seconds as described before<sup>165</sup>.

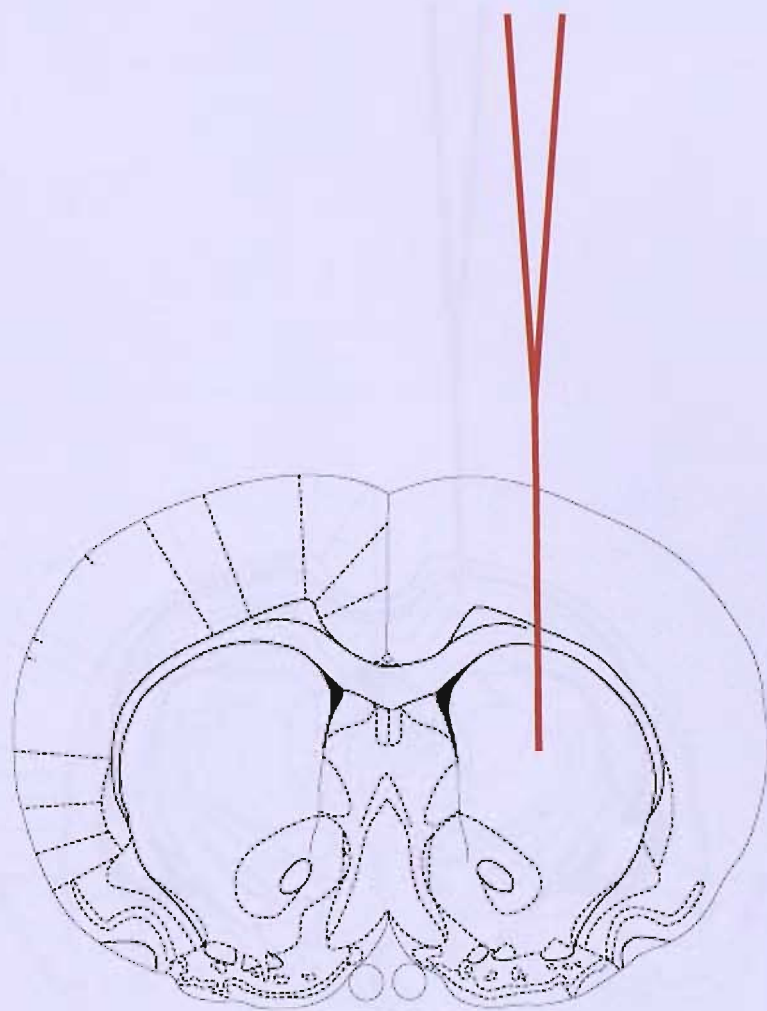


**Figure 2.5**  
**Intrastriatal injection**

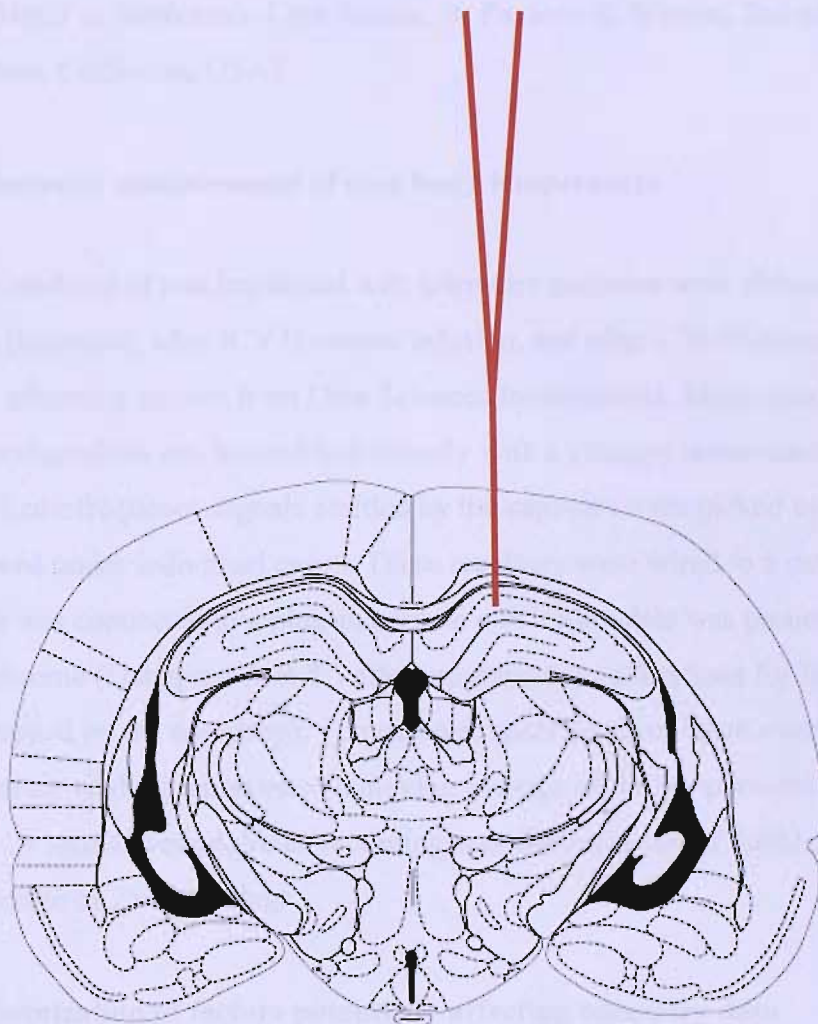


**Figure 2.6**

### **Intrahippocampal injection**

## **2.7.5 Stab lesions**

Striatal stab lesions were performed by lowering a sterile pointed scalpel blade into the right striatum using the following coordinates: bregma 1mm, lateral 1.6mm, depth 2.6mm (The Mouse Brain in Stereotaxic Coordinates, by Paxinos & Watson, 2nd edition, 2002, Academic Press, California, USA).

## **2.8 Telemetric measurement of core body temperature**

Temperature readouts of rats implanted with telemetry capsules were obtained after implantation (baseline), after ICV liposome infusion, and after LPS challenge. This was done using a telemetry system from Data Sciences International, Minnesota, USA (Figure 2.7). Each implanted rat was housed individually with a younger unoperated male conspecific. Radiofrequency signals emitted by the capsules were picked up by RPC-1 receivers placed under individual cages. These receivers were wired to a data exchange matrix which was connected to a plug-in card on a PC. Raw data was processed by a custom programme (Dataquest A.R.T.) after inputting the calibrations for individual capsules (supplied by the company). Temperature readings were taken every 5 minutes. Each temperature reading represented a moving average of the temperature recordings taken over a 10 second period. Since recording was done at a rate of 250Hz, this represents a moving average of 2500 readings.

### **2.8.1 Minimization of factors potentially affecting telemetry data**

Since the read-out was core body temperature which is sensitive to a variety of factors such as surgery, environmental temperature, light/dark cycle and stress, efforts were made to minimize these effects. During the intraperitoneal implantation of telemetry capsules, care was taken to avoid infection such as disinfection of instruments between each case and of the skin before incision. The rats were then left to convalesce for at least 10 days before being used in experiments to ensure that any peritoneal inflammation had subsided. A week before inclusion in the experiments they were transferred to the telemetry room in order to ensure adaptation to their new environment. Each operated rat was housed with an age-matched same-sex (male) rat in separate cages: this pairing was maintained throughout the experiment. Environmental enrichment in the cages was identical and did not vary.

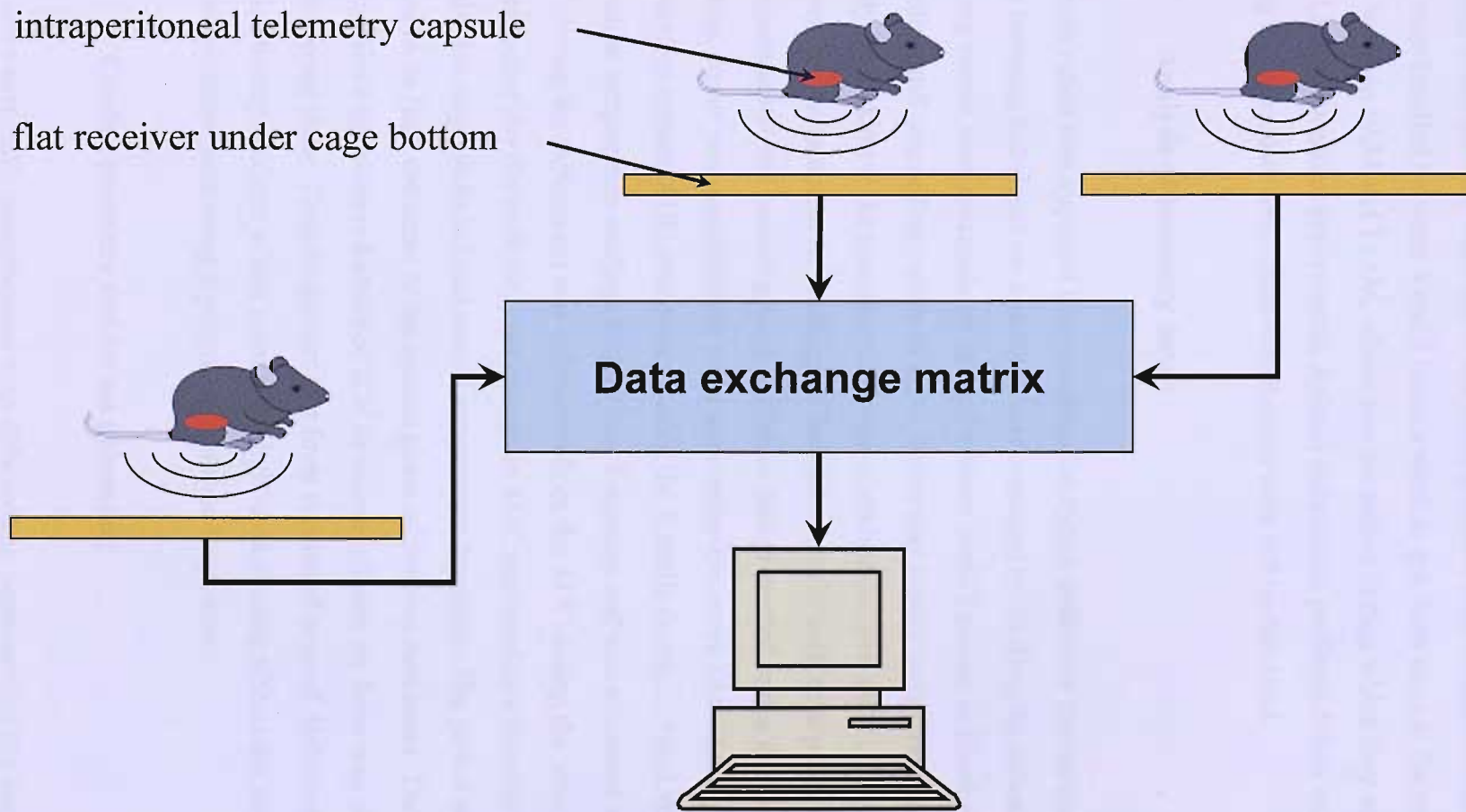


Figure 2.7. Telemetric measurement of core body temperature of rats

Cages were changed once every 5 days; some bedding from the dirty cages was transferred to the respective new cages to help the animals settle in quicker. The schedule of cage-cleaning was organized such that it was done at least 4 days before LPS administration. Rats were handled between 3 and 5 times a week to get them used to the operator: this was done between 9AM and 11AM, which was the period during which they were injected with LPS in the actual experiments. Animal technicians performed their maintenance tasks during this period as well. Otherwise the rats were left undisturbed.

### **2.8.2 Analysis of telemetry data**

Telemetry data was imported into Excel and analyzed uniformly throughout the study. Any delay between individual rat injections was corrected by shifting the datasets appropriately. Missing values were extrapolated using the linear trend function in Excel with the preceding and succeeding values as input. Fever was plotted over time. Data was examined closely by looking at the temperature charts of each individual rat. To observe group differences, the temperature readings of individual rats at each time point were averaged for experimental and control groups. All chart data presented in this thesis was derived in this way. Fever was quantified by using area-under-the-curve (AUC) analysis of temperature curves. AUC was derived using the formula  $(x_1+x_2+\dots+x_n)/5$  where  $x$  were the individual temperature readings taken every 5 minutes and was measured in  $^{\circ}\text{C}\text{min}$ . The AUC during the experiment was subtracted from the AUC during the same time frame on the preceding day for each rat. This change in AUC was used as a measure of temperature change that respects individual animal temperature baselines. The period analyzed was chosen to be from the onset of the second phase of fever to dark onset. The first phase was ignored since the observed effect of ICV liposome infusion on fever was always restricted to the second phase. Despite the fact that fever continued beyond dark onset, it was decided to stop analysis at that point since light-dark cycling affects the animals' activity and temperature, thus being a potentially confounding factor.

### **2.9 Cardiac puncture and serum processing**

Rats were terminally anaesthetized with 20% sodium pentobarbital 2½ hours after i.p. LPS injection. The heart was accessed via a midline sternotomy, the pericardium was excised and blood was drawn slowly through a left ventricular puncture. It was slowly transferred

into a polypropylene eppendorf and allowed to clot at room temperature for 2 hours. All subsequent processing was done at 4°C. It was centrifuged at high speed for 10 minutes, the serum was drawn off and re-centrifuged for 10 minutes, before being divided into smaller aliquots and frozen at -70°C until use.

## **2.10 Perfusion and tissue processing**

All animals were terminally anaesthetized with 20% sodium pentobarbital (Sagatal, Rhone Merieux Ltd., Harlow, Essex, UK) and transcardially perfused with 0.9% w/v heparinized saline. This was followed by perfusion with 4% paraformaldehyde or 10% neutral buffered formalin (NBF) in some cases. Tissue (brain, liver, spleen and cervical lymph nodes) was rapidly dissected. For fresh frozen tissue, samples were quickly embedded in Tissue-Tek OCT compound (Sakura Finetek Europe B.V, Zoeterwoude, NL) and frozen in isopentane on dry ice. For fixed frozen tissue, they were post-fixed in 4% paraformaldehyde for 4-6 hours. They were then transferred to a cryoprotectant solution (30% sucrose in 0.1M phosphate buffer) at 4°C for *circa* 48 hours, till the tissue sunk. Tissue was then cut into the required blocks, embedded in OCT and frozen in isopentane on dry ice. Blocks were stored at -20°C until use. For formalin-fixed tissue, samples were allowed to post-fix in 10% NBF for about 7 days before being dehydrated through serial concentrations of alcohol followed by Histoclear, and embedded in wax.

Tissue harvesting for RT-PCR was done very quickly. An appropriate 3mm slice of the brain containing the region of interest (frontoparietal cortex) was cut. The tissue was punched out and transferred immediately into RNAlater reagent (Qiagen, West Sussex, UK). Samples were incubated overnight in the reagent at 2–8°C and then transferred, still in the reagent, to -20°C for storage.

## **2.11 Immunohistochemistry**

Coronal sections of 10µm thickness were cut on a cryostat or microtome, dried at 37°C for 30 minutes (frozen sections) or at 59°C for 10 minutes (wax-embedded sections) and processed for indirect immunohistochemistry. Wax-embedded sections were first dewaxed in xylene and rehydrated through serial concentrations of alcohol. All incubations were

carried out at room temperature. If quenching was needed, this was done using 0.3% H<sub>2</sub>O<sub>2</sub> in methanol for 20 minutes, followed by a wash in 0.1M PBS. If antigen retrieval was required for formalin-fixed sections, this was done using microwave (3 minutes in citrate buffer, cooling for 5 minutes, re-microwave for 3 minutes in citrate buffer). After being washed in 0.1M PBS, sections were pre-adsorbed with 10% normal serum of the appropriate animal species for 30 minutes and then incubated for 1½ hours with the primary antibody. **Table 2.1** lists all the primary antibodies used in these studies. After washing, sections were incubated with biotinylated secondary antibody of the appropriate specificity for 30 minutes, washed again and then incubated with avidin-biotin-peroxidase complex (Vectastain Elite ABC) for 30 minutes. After another wash, the peroxidase was visualized using 0.05% 3,3'-diaminobenzidine (DAB) as chromogen and 0.05% hydrogen peroxide as substrate. All the sections were counterstained with Cresyl Violet or haematoxylin and dehydrated before mounting in DePeX (BDH Laboratory supplies, Poole, UK). Negative control sections were incubated in the absence of the primary antibody. Normal sera, biotinylated secondary antibodies, and avidin-biotin-peroxidase complex were purchased from Vector Laboratories, Burlingame, California. For antibodies raised in mouse, the MOM kit was used (Vector Laboratories). For Luxol Fast Blue (LFB) histochemistry, sections were dehydrated in 95% alcohol and then incubated in a 0.1% LFB solution at 60°C for 90 minutes, washed in 70% alcohol and distilled water, and differentiated in 0.01% lithium carbonate solution, followed by dehydration and mounting in DePeX. For Oil red O (ORO) histochemistry, sections were incubated in a 0.3% ORO/dextrin solution at room temperature for 20 minutes, rinsed in water, and mounted in an aqueous medium. Images were captured on a PC using LeicaQwin software (Cambridge, UK).

For double immunofluorescence, the same protocol was used but incubations were carried out in a dark box. The biotinylated secondary antibody step was substituted by an appropriate AlexaFluor-conjugated secondary; otherwise streptavidin-conjugated AlexaFluors were used (Molecular Probes, Cambridge Bioscience, Cambridge, UK). Sections were mounted in Mowiol (Harlow Chemical, Harlow, UK) and visualized with a LSM 510 Meta confocal laser scanning microscope (Carl Zeiss, Germany). Images were examined with the Zeiss LSM 5 Image Examiner software.

|      | Clone     | Antigen              | Species                        | Dilution                          | Source              |
|------|-----------|----------------------|--------------------------------|-----------------------------------|---------------------|
| IHC  |           | APP                  | rabbit anti-peptide polyclonal | 1:200                             | Zymed               |
|      | ED2       | CD163                | mouse anti-rat monoclonal      | 1:200                             | Serotec             |
|      | KT3       | CD3                  | mouse anti-rat monoclonal      | 1:200                             | Serotec             |
|      | YTS191.1  | CD4                  | mouse anti-rat monoclonal      | 1:200                             | Serotec             |
|      | ED1       | CD68                 | mouse anti-rat monoclonal      | 1:200                             | Serotec             |
|      | FA11      | CD68                 | rat anti-mouse monoclonal      | 1:100                             | Serotec             |
|      | YTS105.18 | CD8                  | mouse anti-rat monoclonal      | 1:200                             | Serotec             |
|      | 11-5B     | CNPase               | mouse anti-human monoclonal    | 1:200                             | Sigma               |
|      |           | GFAP                 | rabbit anti-cow polyclonal     | 1:5000                            | DAKO                |
|      |           | glut1                | rabbit polyclonal              | 1:2500                            | gift (JL Mankowski) |
|      |           | granzyme B           | rabbit anti-peptide polyclonal | 1:20                              | Abcam               |
|      | 5D3       | mannose receptor     | rat anti-mouse monoclonal      | 1:200                             | Serotec             |
|      | HM-2      | MAP2                 | mouse anti-rat monoclonal      | 1:200                             | Sigma               |
|      | anti-MBP  | MBP                  | mouse anti-cow monoclonal      | 1:50                              | Chemicon            |
|      | 2G5       | MHC Class I          | mouse anti-mouse monoclonal    | 1:200/800                         | Serotec             |
|      | ER-HR52   | MHC Class I          | rat anti-mouse monoclonal      | 1:200                             | Abcam               |
|      | OX6       | MHC Class II         | mouse anti-rat monoclonal      | 1:200/3000                        | Serotec             |
|      | A60       | NeuN                 | mouse anti-mouse monoclonal    | 1:5000                            | Chemicon            |
|      |           | pERK1/2              | rabbit anti-peptide polyclonal | 1:200                             | Cell Signaling      |
|      | OX7       | Thy1.1               | mouse anti-rat monoclonal      | 1:200                             | Serotec             |
|      | A5        | $\gamma$ 1-laminin   | rat anti-mouse monoclonal      | 1:250                             | Labvision           |
| FACS | CT-CD8a   | CD8 (R-PE)           | rat anti-mouse monoclonal      | 0.1 $\mu$ g/10 <sup>6</sup> cells | Caltag              |
|      | PC61.5.3  | CD25                 | rat anti-mouse monoclonal      | 0.2 $\mu$ g/10 <sup>6</sup> cells | Serotec             |
|      | F23.1     | V $\beta$ 8.2 (FITC) | mouse anti-mouse monoclonal    | 0.1 $\mu$ g/10 <sup>6</sup> cells | Pharmingen          |

**Table 2.1. Antibodies used for immunohistochemistry (IHC) and FACS**

## 2.12 Enzyme-linked immunosorbent assay

Serum cytokines TNF $\alpha$ , IL1 $\beta$  and IL6 were assayed using commercial ELISA kits as per manufacturer's instructions (R&D Systems, Abingdon, UK). Briefly, serum was incubated in wells coated with primary antibody for 2 hours. After washing, the wells were incubated with horseradish peroxidase-conjugated secondary antibody for 2 hours, washed again and then loaded with substrate solution (tetramethylbenzidine and H<sub>2</sub>O<sub>2</sub>). The chromogenic reaction was stopped with dilute hydrochloric acid and optical density read at 450nm with correction at 570nm. A standard curve as well as positive and negative controls were run within each ELISA run. The standard curve was run using serial dilution of recombinant cytokine in buffer: this was supplied with the kit as was the positive control. Naïve rat serum was used as negative control. During the initial run with each cytokine ELISA, a spike-and-recovery curve was done i.e. a standard curve was also run in naïve rat serum to exclude significant effects from serum inhibitors. Recovery of >90% was deemed satisfactory. All incubations were carried out in duplicate. Data was entered into an Excel spreadsheet. Data from duplicate wells was averaged and the average zero standard optical density subtracted. A standard curve was obtained by plotting OD values on the y-axis and cytokine concentration on the x-axis and the line of best fit determined using linear regression. Concentrations read from the standard curve were multiplied by the appropriate dilution factor used during the ELISA. Values below the lowest point on the standard curve were considered to be below the detection threshold of the kit and were assumed to be equal to the lowest value for statistical purposes. This is because sample values of zero interfere with logarithmic transformation which was necessary when serum cytokine levels did not follow a normal distribution.

Brain samples were homogenized in 0.1M PBS containing a protease inhibitor cocktail (10nM disodium EDTA, 5mM benzamidine HCL.H<sub>2</sub>O, 100mM E-amino-N-caproic acid and 0.02mM AEBSF.HCl) using a rotor and centrifuged at 4°C. Total protein and IL1 $\beta$  in supernatant were assayed using Biorad DC protein (Biorad, UK) and ELISA kits (R&D Systems, Abingdon, UK) respectively, as per manufacturers' instructions.

## **2.13 Semi-quantitative real time reverse transcriptase PCR (RT-PCR)**

All experimental procedures involving the extraction of messenger RNA (mRNA) from tissue and its subsequent reverse transcription into complimentary DNA (cDNA) were done under strict RNase-free conditions.

### **2.13.1 mRNA extraction**

Tissue samples were taken out of RNAlater solution and weighed quickly: samples were typically 30µg in weight. After rapid homogenization using a rotor and Qiashredder columns (Qiagen, West Sussex, UK), total RNA was extracted from tissue using RNeasy mini columns (Qiagen). These columns contain a silica gel based membrane which selectively binds RNA molecules >200 nucleotides long in the presence of a special high salt buffer and ethanol. This results in enrichment for mRNA since tRNA and rRNA are usually smaller. Contaminating DNA was removed by on-column digestion with RNase-free DNase I (Qiagen) according to the manufacturer's instructions. RNA yields were determined by spectrophotometry at 260nm. Isolated RNA was stored at -80°C till cDNA synthesis.

### **2.13.2 cDNA synthesis**

cDNA was synthesised from mRNA using RT-Gold reagents (Applied Biosystems, UK) according to the manufacturer's instructions.

### **2.13.3 RT-PCR**

Taqman technology was used. All equipment and reagents were supplied by Applied Biosystems (UK) unless otherwise stated. All primers and probes were synthesized using sequences which had been published or used by colleagues in the laboratory (**Table 2.2**). These sequences were double-checked using Primer Express software to ensure that they spanned an intron-exon boundary thereby increasing their specificity for cDNA and excluding genomic DNA. Probes were labelled at the 5' end with FAM or VIC as a reporter dye and at the 3' end with TAMRA as a quencher dye. Primers and probes for

| Cytokine     | Primer / probe | Sequence 5'-3'             |
|--------------|----------------|----------------------------|
| TNF $\alpha$ | forward        | CCAGGAGAAAGTCAGCCTCCT      |
| TNF $\alpha$ | reverse        | TCATACCAGGGCTTGAGCTCA      |
| TNF $\alpha$ | probe          | AGAGCCCTTGCCCTAAGGACACCCCT |
| IL1 $\beta$  | forward        | CACCTCTCAAGCAGAGCACAG      |
| IL1 $\beta$  | reverse        | GGGTTCCATGGTGAAGTCAAC      |
| IL1 $\beta$  | probe          | TGTCCCGACCATTGCTGTTCTAGG   |
| IL6          | forward        | CGAAAGTCAACTCCATCTGCC      |
| IL6          | reverse        | GGCAACTGGCTGGAAGTCTCT      |
| IL6          | probe          | TCAGGAACAGCTATGAAGTTCTCCG  |

**Table 2.2. Quantitative real time polymerase chain reaction (RT-PCR) primer and probe sequences**

glyderaldehyde-3-phosphate dehydrogenase (GAPDH), which was used as a housekeeping gene, were purchased in kit form.

All reactions were carried out using an Opticon Monitor RT-PCR machine (MJ Research Inc, USA). Reactions were performed in volumes of 25 $\mu$ L containing 1 $\mu$ L cDNA (equivalent to 20ng RNA), reverse and forward primers, probe, and Taqman universal Mastermix as per manufacturer's instructions. Cycling conditions were as follows: 50°C x 2 min, 95° x 10 min and 40 cycles of [95° x 15 sec, 60° x 1 min, plate read]. Samples were assayed in duplicate and quantified using a standard curve, as described below.

#### **2.13.4 Standard curve**

In order to prepare mRNA that could be used to generate a relative standard curve for RT-PCR, 3 male Wistar rats were injected intrastriatally with 1 $\mu$ g LPS dissolved in sterile saline. These treatments are known to induce robust expression of cytokines including TNF $\alpha$ , IL1 $\beta$  and IL6 (Leigh M Felton, personal communication). The striatum was harvested and frozen immediately. RNA was extracted and cDNA synthesized as described above. This cDNA was then diluted serially in DNase-free water (1:1, 1:5, 1:25, 1:125, 1:625, 1:3125) and used during each RT-PCR run as a relative standard curve of target gene expression (in arbitrary units). All results were normalized to the measurement of the housekeeping gene GAPDH in the same samples.

#### **2.14 T cell culture**

Single cell suspensions were prepared from spleen and lymph nodes of CL4 mice and non-transgenic littermates, and depleted of red blood cells by incubation with 0.83% NH<sub>4</sub>Cl (Sigma, Poole, UK) for 10 minutes at room temperature. CL4 CD8 T cells were purified by positive selection. Briefly, the CL4 cell suspension was incubated with anti-CD8a monoclonal antibody (CT-CD8a; Caltag, USA) for 45 minutes at 4°C, washed and then microbeads coupled to goat anti-rat IgG (Miltenyi Biotech, UK) were added for 15 minutes at 4°C, followed by another wash. Magnetic separation was performed on columns (MS columns; Miltenyi Biotech, UK). The purified population consisted of >98.5% CD8 cells, as revealed by FACS analysis. CL4 CD8 T cells were stimulated with irradiated syngeneic splenocytes (2500 rads) in a ratio of 1:10 in complete DMEM (Invitrogen, UK)

supplemented with 10% FCS (Invitrogen, UK) and containing 1 mM HA peptide, 1 ng/ml IL2 (R&D, UK), and 20 ng/ml IL12 (R&D, UK). On day 3, the cultures were fed with fresh medium containing 1ng/ml IL-2. On day 6, cells were harvested and living cells were collected by Ficoll density separation (Amersham Biosciences, UK) and washed in DMEM three times. FACS analysis of these cells consistently showed that they were CD8, V $\beta$ 8.2 and CD25-positive (**Figure 2.8**).

## 2.15 FACS

A few  $\mu$ L of blood or  $10^6$  resuspended cells were incubated with primary antibody for 10 minutes at RT or 30 minutes on ice respectively. Primary antibodies used are listed in **Table 2.1**. They were either directly conjugated with fluorochromes or else followed by a second incubation with the appropriate fluorochrome-conjugated secondary antibody. For blood, red cells were lysed by adding 2ml of proprietary lysis buffer (BD FACS Lysis Buffer, BD Biosciences) for 15 minutes at RT. Multiple staining was done by sequential steps involving not more than one secondary antibody. The appropriate control isotypes were used. Washing steps were done using Cellwash (BD Biosciences) and centrifugation at 200g for 5 minutes. FACS analysis was performed using a FACSCalibur flow cytometer (BD Biosciences) and the data was analysed using CellQuest software (BD Biosciences). T cells were gated according to their forward and side scatter characteristics.

## 2.16 Quantification of cells

This was done manually under light microscopy. The operator was blinded to the identity of the slides counted. Cells were counted using a graticule under a high power objective (x40 or x25) and density of cells converted to a value per  $\text{mm}^2$ . CD163-positive macrophages, Kupffer cells, splenic red pulp macrophages and endothelial cells were counted in several regions within the same section. In the case of CD8 T cells, these were counted in one area in the central most densely infiltrated region of the lesion. In all cases several sections from the same animal, and several animals from each experimental group (as denoted by number  $n$ ) were analyzed and counts averaged.

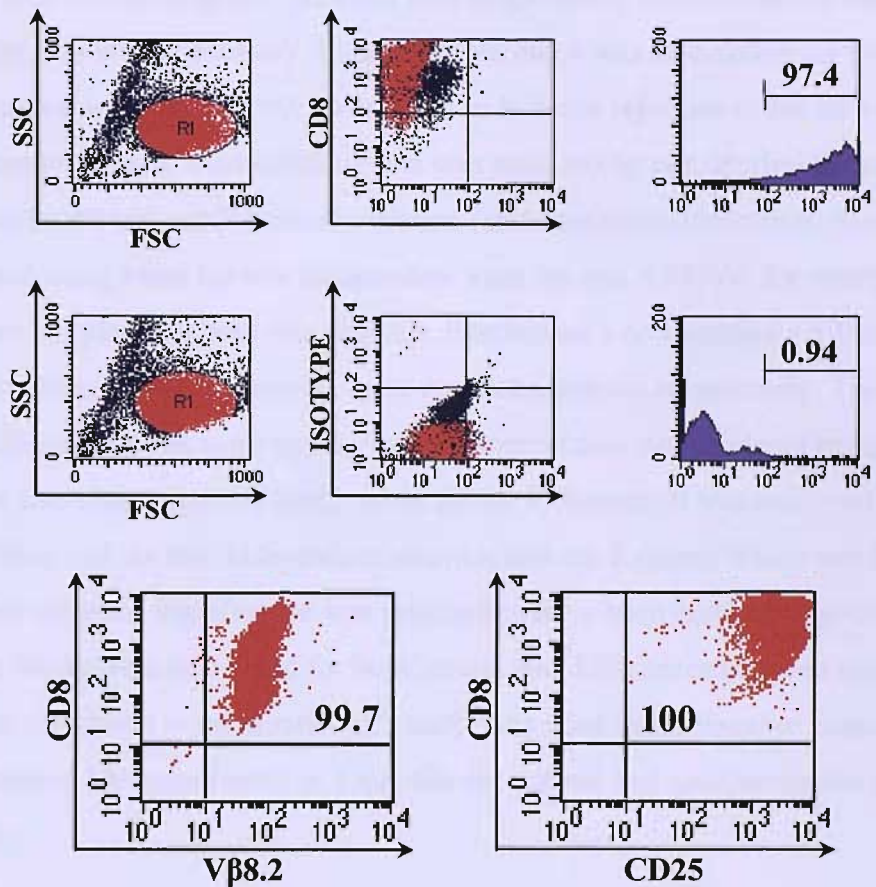


**Figure 2.8. CL4 CD8 T cells after culture protocol**  
(percentage of cells shown)

## 2.17 Statistics

Advice was sought from a professional statistician (Prof Prescott, Department of Mathematics, University of Southampton). Sample size calculations were done using EpiCalc 2000 version 1.02 (freeware). The alpha level was set at 0.05 and the power at 80%. Analysis was performed using Excel, SPSS and SigmaStat. Data was assessed for normality with the Kolmogorov-Smirnov test. Logarithmic transformation was carried out to normalize data when necessary. Equality of variance was assessed using Levene's test (significance value of statistic  $>0.1$  was taken to indicate rejection of the null hypothesis i.e. variances are equal). Variability of data was assessed by considering the mean, standard deviation and coefficient of variation (standard deviation/mean). Parametric data was analyzed using t-test for two independent samples and ANOVA for multiple independent samples. For post-hoc analysis, Bonferroni's or Tamhane's T2 methods were used when variances were homogenous or non-homogenous respectively. The latter was only done if sample sizes were equal. Non-parametric data was rendered parametric by logarithmic transformation and analyzed as above. Otherwise it was analyzed using the Mann-Whitney test for two independent samples and the Kruskal-Wallis test for multiple independent samples. Significance was assumed to have been reached at  $p<0.05$ . 95% confidence limits were calculated for both means and differences between means where appropriate. Graphical representation of results was done using Excel or SigmaPlot. Error bars represented 1 standard error or 1 quartile for normal and non-parametric data respectively.

## Chapter 3

# **Inhibition of prostaglandin synthesis does not prevent *de novo* cytokine transcription in the brain parenchyma during systemic inflammation**

## **Inhibition of prostaglandin synthesis does not prevent *de novo* cytokine transcription in the brain parenchyma during systemic inflammation**

### **3.1 Introduction**

Non-steroidal anti-inflammatory drugs (NSAIDs) have proved to be very effective in the management of systemic inflammatory diseases such as rheumatoid arthritis. It is therefore a widely held belief that NSAIDs similarly exert a direct anti-inflammatory effect in the central nervous system (CNS). However several lines of evidence argue against this.

In multiple sclerosis (MS), an archetypal inflammatory disease of the CNS, a small open-label study in which 8 patients were scanned by magnetic resonance (MR) imaging before and after a 7 day course of ibuprofen (1.6mg/day) found that there was no statistically significant difference observed in the number or volume of active lesions<sup>166</sup>. In addition NSAIDs are commonly prescribed drugs in MS for a variety of indications such as back pain or headache, yet no effect of NSAIDs on relapse frequency has been reported.

In Alzheimer's disease (AD) epidemiological studies have shown that NSAIDs are moderately effective in primary prevention<sup>167-169</sup> but this protective effect disappears 2 years prior to the onset of clinical dementia<sup>170-172</sup>. The early pathology in AD is characterized by high cerebrospinal (CSF) prostaglandin E<sub>2</sub> (PGE<sub>2</sub>) levels which correlate positively with survival<sup>173</sup>. This suggests that traditional anti-inflammatory properties of NSAIDs, including cyclooxygenase inhibition, cannot account for their protective effects in AD. Since low fibrillar A<sub>β</sub> deposits precede microglial inflammation<sup>174</sup>, their newly recognized anti-amyloidogenic effects<sup>175</sup> may be responsible.

Whether NSAIDs modify neuroinflammation directly therefore remains a question. Cytokines are the major orchestrators of inflammation in the CNS. The clinical course of neuroinflammatory diseases is frequently punctuated by exacerbations which are characterized by upregulation in proinflammatory cytokine expression and microglial activation; such exacerbation in ongoing neuroinflammation is thought to underlie relapses in MS and delirium in AD<sup>54</sup>. It is now known that a significant number of these exacerbations are triggered by systemic infection<sup>15,25</sup>. Circulating cytokines do not readily

cross the blood-brain barrier (BBB) during a systemic infection but *de novo* transcription of cytokines is seen within the brain parenchyma<sup>176</sup>. The cerebral vasculature has the synthetic machinery enabling it to respond to blood-borne cytokines by synthesizing lipophilic prostaglandins which can diffuse across the BBB<sup>72</sup>. These prostaglandins have the potential to modulate inflammation within the brain parenchyma. Whether prostaglandins diffusing across the BBB are responsible for triggering the *de novo* transcription of cytokines within the brain is unknown.

For these reasons, NSAIDs and their effect on cytokine-mediated neuroinflammation *in vivo* is a fundamental clinical issue which does not deserve ambiguity. In order to address this question, it was decided to study the effect of an archetypal NSAID, indomethacin, on the *de novo* transcription of cytokines that occurs within the brain after a peripheral infection. Peripheral inflammation was modelled using an intravenous injection of lipopolysaccharide (LPS) in indomethacin pre-treated or control rats. Transcription of the cytokines TNF $\alpha$ , IL1 $\beta$ , and IL6 in the cortex was studied using semi-quantitative real-time reverse transcriptase polymerase chain reaction (RT-PCR). It is shown that indomethacin does not prevent *de novo* cytokine transcription in the brain parenchyma.

### 3.2 Results

#### 3.2.1 *De novo cytokine transcription within the brain after systemic LPS challenge*

An established experimental model of systemic infection using LPS was employed. Rats (n=5) receiving 500 $\mu$ g/kg LPS intravenously showed signs of a peripheral infection: they developed a fever, adopted a hunched posture, exhibited piloerection and their cage activity decreased. Control rats (n=5) receiving saline intravenously did not demonstrate any of these signs. Three hours after intravenous injection, the rats were terminally anaesthetized and briefly perfused with saline. Brains were quickly dissected and the right frontoparietal cortex was harvested for RT-PCR analysis of the cytokines TNF $\alpha$ , IL1 $\beta$  and IL6. There was a significant upregulation of all three cytokine transcripts after LPS (p<0.01 by two-tailed Student's t test, **Figure 3.1**).

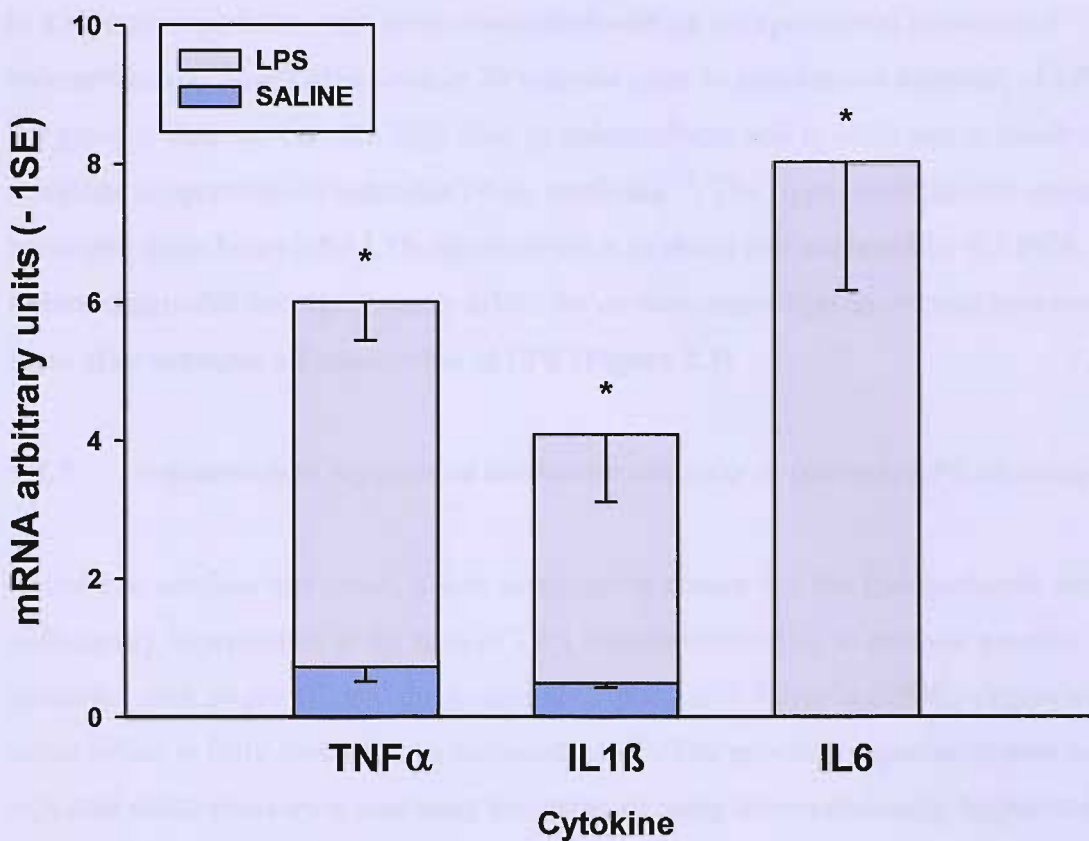


**Figure 3.1. *De novo* cytokine transcription in the rat brain during systemic inflammation.** Rats were challenged with 200 $\mu$ g/kg LPS or saline i.v. (n=5 per group) and right frontoparietal cortex was harvested 3 hours later for cytokine mRNA analysis by RT-PCR. A significant upregulation (\*) of TNF $\alpha$  ( $p<0.001$ , 95% CI = 4.7 – 7.8), IL1 $\beta$  ( $p=0.008$ , 95% CI = 1.6 – 7.7) and IL6 ( $p=0.003$ , 95% CI = 2.6 – 8.5) was seen (2-tailed Student's t-test).

### **3.2.2 *De novo cytokine transcription within the brain after systemic LPS challenge occurred despite indomethacin treatment***

In a second experiment, rats were pre-treated with an intraperitoneal injection of indomethacin (15mg/kg) or vehicle 30 minutes prior to intravenous injection of LPS (n=6 per group). This represents a high dose of indomethacin and is sufficient to result in complete suppression of inducible PGE<sub>2</sub> synthesis<sup>177</sup>. The right frontoparietal cortex was harvested three hours after LPS administration as above and analyzed by RT-PCR. Indomethacin did not significantly affect the *de novo* transcription of cytokines seen in the brain after systemic administration of LPS (**Figure 3.2**).

### **3.2.3 *Indomethacin suppressed the febrile response to systemic LPS challenge***

In order to confirm this result, it was necessary to ensure that the indomethacin was sufficiently bioavailable at the time of LPS administration (i.e. to rule out possible scenarios such as insufficient dose, poor absorption etc). Fever is a PGE<sub>2</sub>-dependent CNS event which is fully reversible by indomethacin<sup>61</sup>. The previous experiment was therefore repeated while measuring core body temperature using intraperitoneally-implanted telemetric thermistors (n=5 per group). Hyperthermia was seen in saline pre-treated animals 2½ hours after LPS injection. Indomethacin pre-treatment resulted in complete suppression of this fever (**Figure 3.3**).

## **3.3 Discussion**

In this proof-of-principle study, a simple experimental design was used to show that indomethacin does not prevent cytokine transcription in the brain parenchyma during systemic inflammation. In these experiments mRNA rather than protein was assayed in order to study *de novo* cytokine transcription as opposed to blood-to-brain transport of serum cytokines. Additionally, by perfusing animals prior to tissue collection it was ensured that all cytokine transcripts measured originated from CNS tissue.

NSAIDs inhibit cyclooxygenase (COX) and therefore prostaglandin synthesis. The role of prostaglandin E<sub>2</sub> (PGE<sub>2</sub>) in inflammation is complex since it depends on its biological context. There is no doubt that PGE<sub>2</sub> is predominantly pro-inflammatory in the systemic

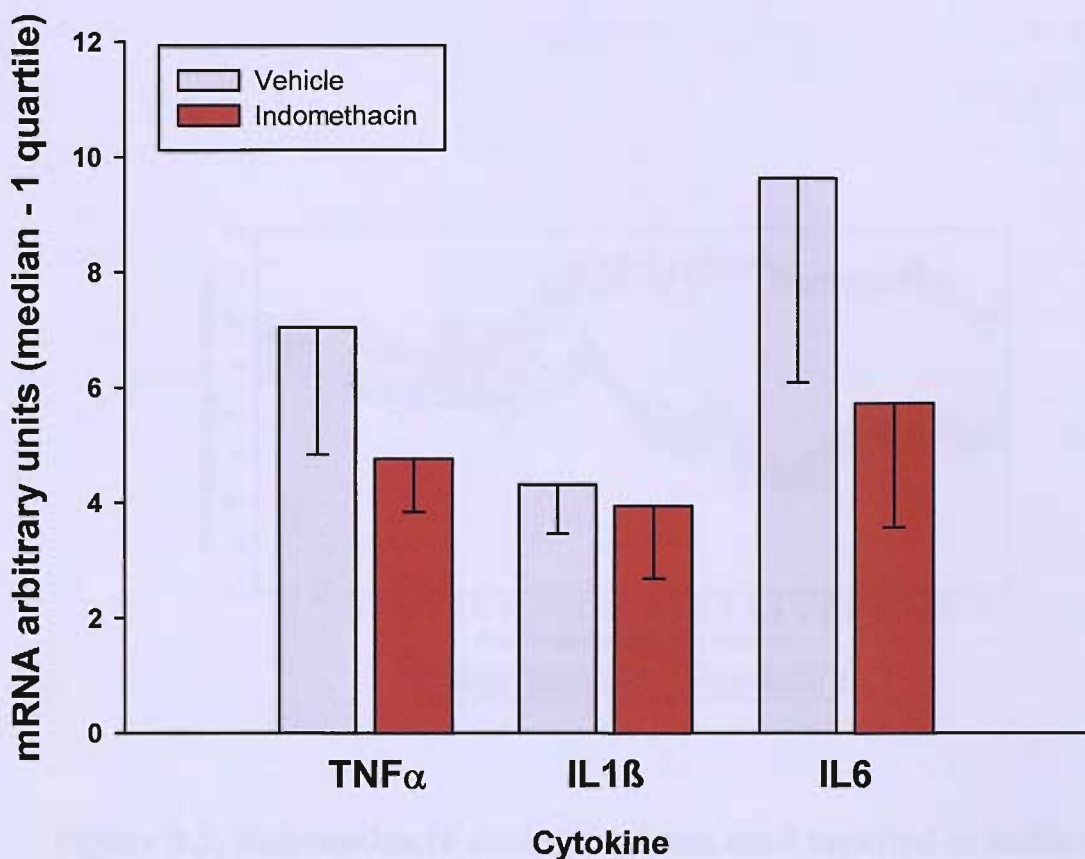


**Figure 3.2. Indomethacin did not significantly affect cytokine mRNA upregulation in frontoparietal cortex after systemic endotoxin challenge.** Two groups of rats (n=6 each) were pre-treated with an i.p. dose of indomethacin (15mg/kg) or vehicle respectively, 30 minutes before receiving 500 $\mu$ g/kg LPS i.v. Cortical samples were harvested 3 hours later and analyzed by RT-PCR for TNF $\alpha$ , IL1 $\beta$ , and IL6 mRNA. No significant differences in cytokine mRNA levels were seen (p>0.05 by Mann-Whitney test).

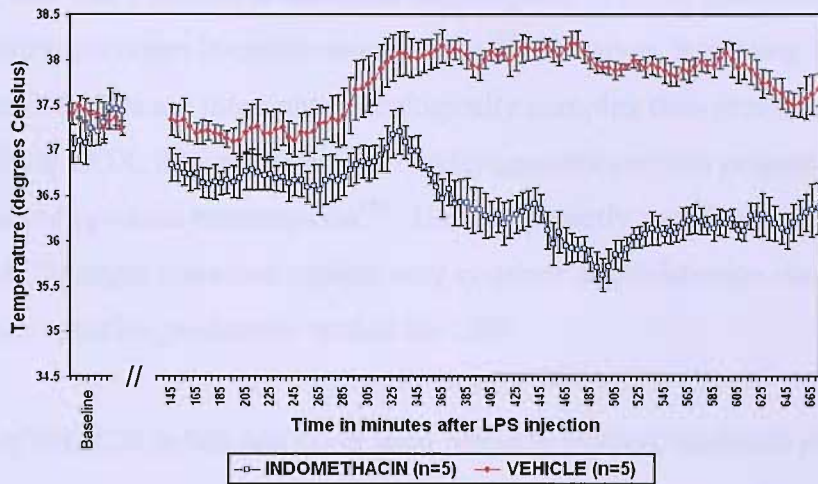


**Figure 3.3. Indomethacin dosing regimen used resulted in sufficient bioavailability in the CNS.** Core body temperature was measured telemetrically in two groups of rats ( $n=5$  each) which were pre-treated with an i.p. dose of indomethacin (15mg/kg) or vehicle respectively, 30 minutes before receiving 500 $\mu$ g/kg LPS i.v. Indomethacin abolished the hyperthermia seen in rats pre-treated with vehicle. AUC during the experiment was subtracted from the AUC during the same time on the preceding day. This change in AUC was used as a measure of temperature change that respects individual animal temperature baselines. Comparison of change in AUC between the two groups of rats revealed that indomethacin significantly lowered core body temperature ( $p=0.009$  by 2-tailed Student t-test, 95% CI = 62-321°Cmin).

compartment given the vast clinical experience with cyclo-oxygenase-2-specific antagonists in conditions like rheumatoid arthritis. Indeed, indomethacin reduced production of LPS-induced PGE<sub>2</sub> and cytokine production in whole blood<sup>178</sup>. On the other hand, most studies point towards an anti-inflammatory effect of PGE<sub>2</sub> within the CNS compartment: it downregulates microglial activation *in vitro*<sup>179</sup>, intracerebral injection of PGE<sub>2</sub> in endotoxaemic rats downregulates microglial activation and transcription of IL-1 $\beta$  and TNF $\alpha$ <sup>180</sup>, and PGE<sub>2</sub> inhibition enhances transcription of genes associated with the CNS innate immune system in endotoxaemic mice<sup>181</sup>. However, it is being increasingly recognized that NSAIDs are more pharmacologically complex than previously thought. Besides inhibiting COX, they are effective PPAR $\gamma$  agonists and this property results in downregulation of cytokine transcription<sup>182</sup>. These apparently conflicting inflammatory effects of NSAIDs might therefore explain why systemic administration does not *overall* prevent *de novo* cytokine production within the CNS.

The efficacy of NSAIDs in MS has never been properly studied. Barkhoff *et al* used MRI to follow 8 patients receiving ibuprofen for a week<sup>166</sup>, which therefore represents a short study with a small number of patients. However the results from this study would support the hypothesis that NSAIDs do not modify the inflammatory course of MS. In contrast, there is early evidence that NSAIDs might be beneficial in the treatment of complex behavioural aspects of multiple sclerosis. Indomethacin inhibited EAE-associated sickness behaviour in mice<sup>97</sup> and a randomized controlled crossover trial demonstrated a significant effect of aspirin on fatigue in MS patients<sup>98</sup>. These observations are most likely to be related to the inhibition of PGE<sub>2</sub>-mediated immune-to-brain signalling, a pathway which is known to mediate complex behavioural changes in the context of inflammation<sup>96</sup>. In the light of the current findings, it is therefore proposed that inflammation contributes to disease manifestation in MS by two distinct pathways: (1) a prostaglandin-dependent pathway that underlies some of the behavioural symptoms of MS, including fatigue, and (2) a prostaglandin-independent pathway leading to cytokine induction within the CNS which drives the tissue damage characteristic of MS pathology. Thus although NSAIDs may alleviate some behavioural symptoms in MS including fatigue, it is unlikely that they will affect disease progression. This needs further clinical investigation, and it would therefore be useful for future clinical studies of NSAIDs in MS fatigue to incorporate MR lesional activity as a secondary outcome measure.

Long-term use of NSAIDs lowers the risk of developing AD as concluded by all meta-analyses to date<sup>167-169</sup>. There is evidence to suggest that NSAIDs lose their protective effect about 2 years before the onset of clinical dementia<sup>170-172</sup>. It is thus no surprise that randomized controlled trials of treatment of AD with NSAIDs have failed<sup>183,184</sup>. The early pathological phase of Alzheimer's disease offers the initial clues as to the mechanism of NSAID-mediated protection. Compared with controls, CSF PGE<sub>2</sub> levels are higher in patients with mild memory impairment, but lower in those with more advanced Alzheimer's disease, and initial PGE<sub>2</sub> levels are associated with prolonged survival<sup>173</sup>. Early pathology is characterized by upregulation in neuronal COX2 expression and low amounts of low-fibrillar A $\beta$  deposits but no microglial activation<sup>174</sup>. This suggests that the preventive effect of NSAIDs in the preclinical years is not related to cyclo-oxygenase inhibition or other direct anti-inflammatory activity. Moreover the study here shows that NSAIDs, specifically indomethacin, do not prevent cytokine-mediated inflammation in the brain *in vivo*. It is therefore more likely that an alternative mechanism underlies NSAID-mediated protection and indeed, evidence is accumulating that NSAIDs such as indomethacin exert anti-amyloidogenic effects via several pathways<sup>175</sup>.

NSAIDs have been shown to reduce both glial inflammation and amyloid burden in animal models of AD<sup>185-187</sup>, but the relationship between these two processes is not clear. Since inflammation is amyloidogenic<sup>188,189</sup> and amyloid is pro-inflammatory<sup>190</sup>, the observed effects of NSAIDs could be secondary to their anti-amyloidogenic or anti-inflammatory properties or both. The data presented here indicates that the decrease in inflammation occurring after administration of NSAIDs *in vivo* is more likely to result from a reduction in amyloid burden rather than from a direct anti-inflammatory effect of these drugs. Future pharmacological research should therefore concentrate on the anti-amyloidogenic rather than anti-inflammatory properties of NSAIDs.

Systemic infections trigger relapses in MS<sup>15</sup> and delirium in AD<sup>25</sup>. The brain responds to a systemic infection by mounting a febrile response and initiating *de novo* cytokine transcription behind the BBB<sup>176</sup>. The seminal observation that cerebral vasculature can respond to circulating cytokines by synthesizing PGE<sub>2</sub> provided a plausible mechanism<sup>72</sup>. Fever is prostaglandin-dependent<sup>61</sup> but whether the same applies to cytokine synthesis is unknown. The results above, whereby indomethacin inhibited hyperthermia but not *de novo* cytokine transcription, suggest that exacerbation in neuroinflammation following a

systemic infection occurs via a prostaglandin-independent route. Identifying the mechanism underlying such relapses is important for the rational development of drugs in AD and MS.

### 3.4 Materials and methods

Male Wistar rats weighing *circa* 200g were obtained from Harlan (Bicester, UK). The animals were housed under standard conditions and all procedures were carried out under the Home Office Animals Act 1986 (UK). LPS (*E. coli* 0111:B4) and indomethacin were purchased from Sigma (Poole, UK). In telemetry experiments, rats were implanted intraperitoneally with temperature sensors (Data Sciences International, Minnesota, USA) 10 days prior to the experiment. Temperature data was acquired continually every 5 minutes and processed using Dataquest and Excel. Area-under-curve (AUC) analysis was performed using the following formula  $(x_1+x_2+\dots+x_n)/5$  where  $x$  were the individual temperature readings taken every 5 minutes. The AUC during the experiment was then subtracted from the AUC during the same time frame on the preceding day to obtain a measure of change in temperature for each rat. In a separate experiment, 3 hours after receiving LPS, the rats were terminally anaesthetized with sodium pentobarbital and transcardially perfused with heparinized 0.9% saline. Brains were rapidly removed and the right frontoparietal cortex was punched out and snap-frozen in liquid nitrogen. Total RNA was extracted using RNeasy mini columns (Qiagen, UK). Taqman semi-quantitative RT-PCR was performed using Applied Biosystems reagents as previously described<sup>191</sup>. Primers and probes were designed using Primer Express software and crossed an intron-exon boundary. Data was assessed for normality using the Kolmogorov-Smirnov test and analysed by Student's t-test if normal or by Mann-Whitney U test if non-parametric. For more details, please refer to Chapter 2.

## **Chapter 4**

### **Characterization and optimization of the clodronate liposome technique to deplete CD163-positive macrophages in rats**

## Characterization and optimization of the clodronate liposome technique to deplete CD163-positive macrophages in rats

### 4.1 Introduction

CD163 expression distinguishes a subset of macrophages in the brain which are located in the brain regions acting as an immune-brain interface i.e. the perivascular space of cerebral blood vessels (perivascular macrophages) in brain parenchyma including circumventricular organs (CVOs), the meninges (meningeal macrophages) and the choroid plexus (choroid plexus macrophages) (see Chapter 1). CD163 is a member of the scavenger superfamily<sup>192</sup>, has been identified as the haemoglobin scavenger receptor<sup>193</sup>, and plays a role in cell adhesion<sup>194</sup>, including adhesion to endothelial cells<sup>195</sup>. In the rat, monocytes express CD163 only after entering the tissue and differentiating into macrophages<sup>196</sup>. In keeping with this, chimeric experiments have shown that cerebral CD163 macrophages are bone marrow derived<sup>197</sup> and undergo a steady turnover, this being faster for meningeal macrophages (70% versus 30% for perivascular macrophages in 3 months)<sup>198</sup>. In the rat, CD163 is the antigen recognized by the mouse monoclonal antibody ED2.

A method to selectively deplete cerebral CD163-positive macrophages in the rat was described in 2001<sup>163</sup>. It employed an infusion of 50µl of a concentrated suspension of mannosylated clodronate liposomes in the 4<sup>th</sup> ventricle over 25 minutes. Since CD163-positive macrophages are the only constitutively phagocytic cells in the healthy central nervous system (CNS), they selectively take up the liposomes. Mannosylation of the liposomes would be expected to favour their uptake since these macrophages express the mannose receptor (see Chapter 6<sup>199</sup>). Once ingested, the phospholipid bilayers of the liposomes are disrupted under the influence of lysosomal phospholipases and the clodronate is released. Intracellular accumulation of clodronate is toxic by forming a non-hydrolyzable analogue of ATP<sup>161</sup> and triggering apoptosis<sup>162</sup>.

In the above study, depletion was assessed at 8 time points after infusion up to 36 days. Complete depletion of cerebral CD163-positive macrophages was achieved from day 4 to day 10 post intracerebroventricular (ICV) liposome infusion, with a slow repopulation starting at day 14. Systemic effects were studied by quantification of hepatic Kupffer cell

density and blood monocyte counts at each time point. Although there was evidence of temporary depletion of these cell populations, normal counts were restored by a week post ICV infusion.

The ultimate intention was to employ this technique to investigate the role of CD163-positive macrophages in the CNS cytokine response to systemic infection (see Chapter 5). In order to do this, it was planned to measure fever and CNS cytokine mRNA after systemic endotoxin challenge of rats which had previously received clodronate or control liposomes ICV. Since Kupffer cell numbers were shown to normalize between 7 and 10 days while cerebral CD163-positive repopulation was evident between 10 and 14 days<sup>163</sup>, the window of opportunity for systemic endotoxin challenge was considered to be between 8 and 12 days.

Before proceeding with the actual experiment, it was important to verify the depletion of CD163-positive macrophages using the clodronate liposome technique, especially in the specific brain regions constituting the immune-brain interface. It was also necessary to ensure that the peripheral immune system of animals receiving clodronate liposomes ICV had recovered sufficiently to be able to mount a circulating cytokine response to endotoxin challenge identical to that of animals receiving control liposomes. It is shown that complete depletion was observed all over the brain except for the CVOs. However serum levels of TNF $\alpha$ , IL1 $\beta$  and IL6 after endotoxin challenge were lower in clodronate-treated rats. The technique was therefore optimized.

## 4.2 Results

### 4.2.1 *ICV infusion of 50 $\mu$ l of clodronate liposomes completely depletes meningeal and perivascular macrophages but not CVO macrophages*

In order to confirm the effectiveness of the published protocol, depletion was checked at several relevant time points post-procedure: three, ten and eleven days after infusion of 50 $\mu$ l of a concentrated suspension of mannosylated clodronate liposomes into the 4<sup>th</sup> ventricle (minimum of n=3 per group). There was complete depletion of CD163-positive perivascular macrophages (PVMs) (Figure 4.1) and meningeal macrophages (MMs)

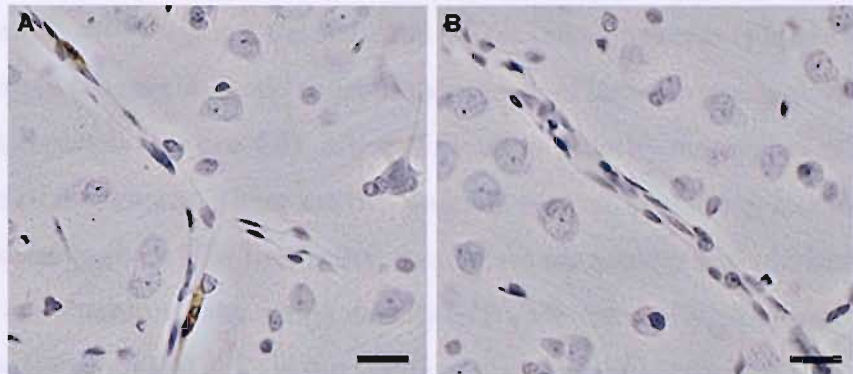


**Figure 4.1. Complete depletion of perivascular macrophages in brain parenchyma after ICV infusion of 50 $\mu$ l clodronate liposomes in the 4th ventricle.** Brain sections were processed for ED2 immunohistochemistry (brown). Representative images of brain parenchyma are shown. A: PBS liposomes; B: clodronate liposomes. Scale bar = 0.02mm.

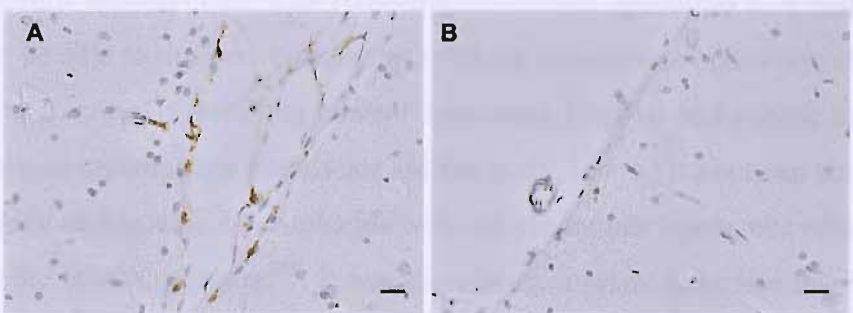


**Figure 4.2. Complete depletion of meningeal macrophages after ICV infusion of 50 $\mu$ l clodronate liposomes in the 4th ventricle.** Brain sections were processed for ED2 immunohistochemistry (brown). Representative images of meninges in the hippocampal fissure are shown. A: PBS liposomes; B: clodronate liposomes. Scale bar = 0.02mm.

(Figure 4.2) throughout the brain at days 3 and 10. Small numbers of round immature meningeal macrophages were seen on day 11.

Careful examination of sections from throughout the brain revealed that PVMs were still present in the following regions: the sensorial CVOs (area postrema (Figure 4.3), subfornical organ (Figure 4.4) and organum vasculosum laminae terminalis (Figure 4.5) and the choroid plexus (Figure 4.6). It was difficult to quantify macrophages because of the small size of these areas. There are two possible reasons explaining incomplete depletion in these regions. The first is that these areas are heavily vascularized (personal observation) and therefore have a high density of PVMs. Secondly, tight junctions are present between ependymal cells at the ventricular surface of sensorial CVOs and between the cuboidal epithelial cells of the choroid plexus, thus providing a formidable obstruction to the passage of liposomes from the ventricles to the interstitium<sup>50</sup>.

#### **4.2.2 *Kupffer cell and splenic red pulp macrophage numbers recover ten days after ICV infusion of 50µl of clodronate liposomes***

For future application of the liposome technique, it was necessary to ensure that the peripheral immune system of animals receiving clodronate liposomes ICV had recovered sufficiently to be able to mount a circulating cytokine response to endotoxin challenge identical to that of animals receiving control liposomes. Hepatic and splenic macrophages are the two largest macrophage populations in the body. Indeed it has been shown that depleting hepatic and splenic macrophages with i.v. clodronate liposomes results in abrogation of the febrile response<sup>200</sup>. It was therefore important to ensure that hepatic and splenic macrophage populations in rats which had received clodronate and control liposomes ICV were identical within the window of opportunity of endotoxin challenge. Thus Kupffer cells (n=5 per group) and splenic red pulp macrophages (n=3 per group) were counted 10 days after ICV infusion of 50µl of clodronate or control liposomes. There were no significant differences in the density of these macrophages in the liver and spleen of rats which had previously received clodronate or control liposomes ICV (Figures 4.7 & 4.8). It was noted however that in clodronate-treated animals, some Kupffer cells had a different morphology, being smaller, more rounded and with finer and shorter processes.

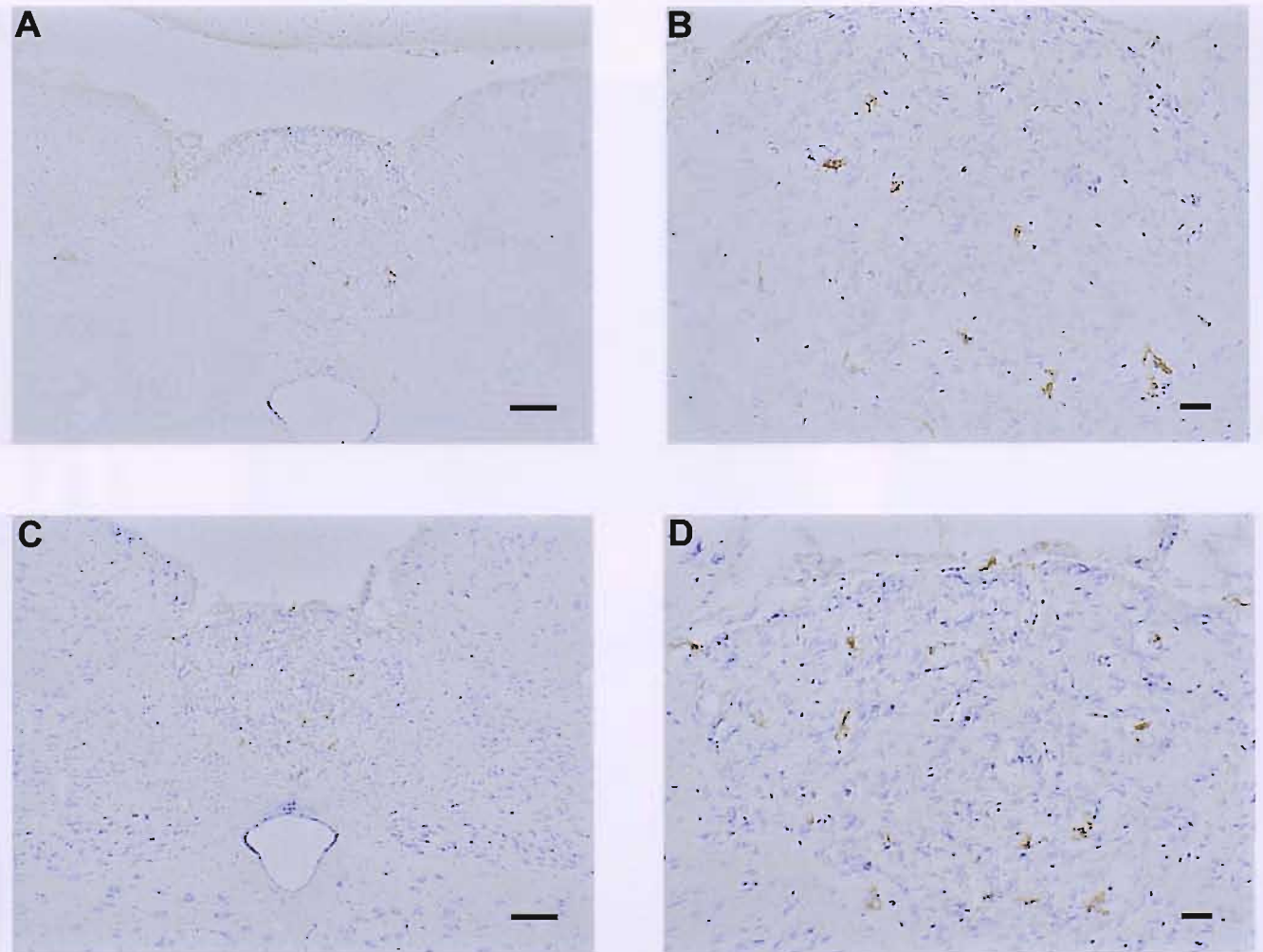


**Figure 4.3. No depletion of CD163-positive macrophages (brown) in the area postrema after infusion of 50 $\mu$ l clodronate liposomes in the fourth ventricle. A,B: PBS liposomes; C,D: clodronate liposomes. Scale bars: A,C = 0.1mm; B,D = 0.01mm.**

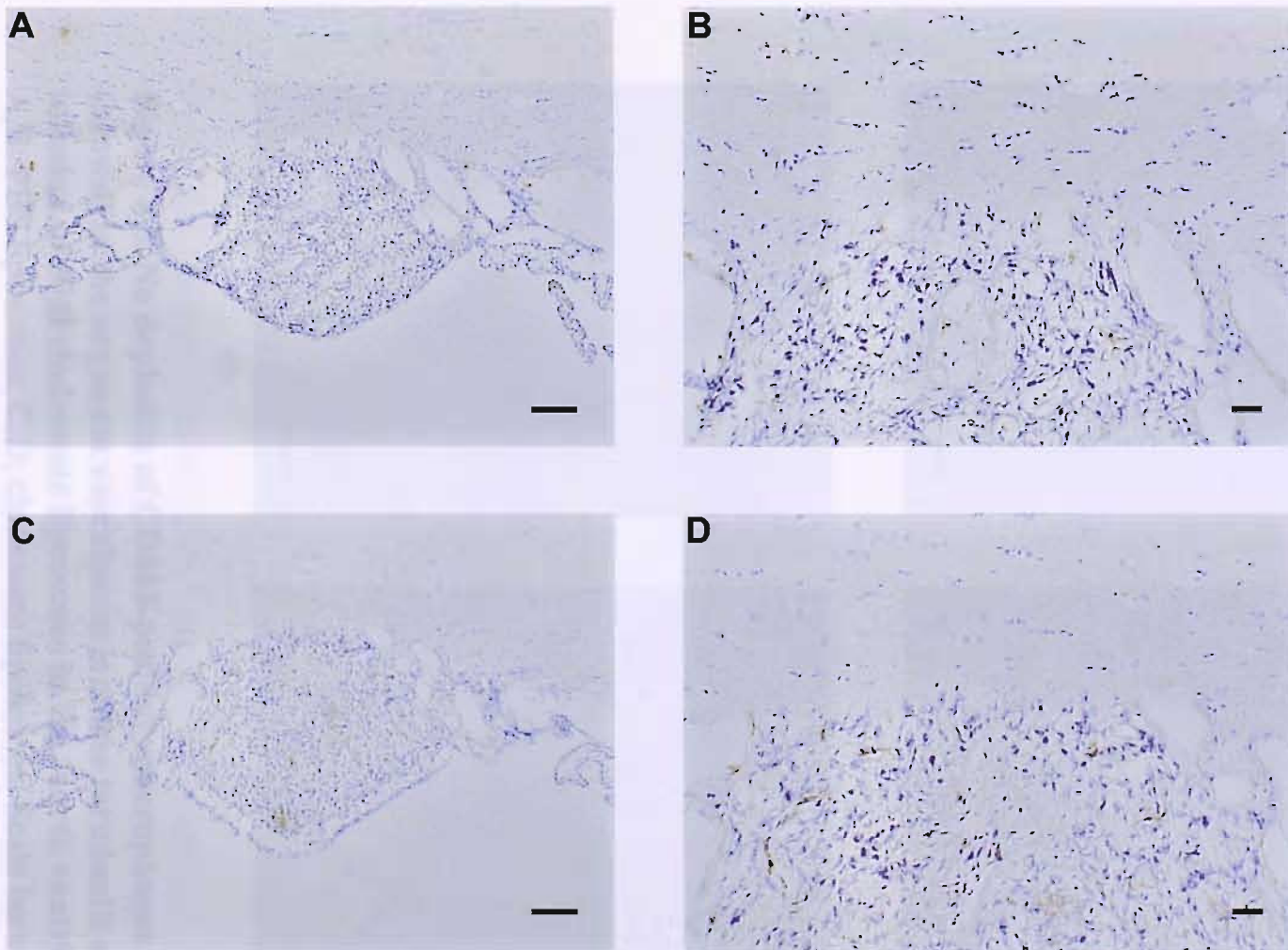


**Figure 4.4. No depletion of CD163-positive macrophages (brown) in the subfornical organ after infusion of 50 $\mu$ l clodronate liposomes in the fourth ventricle. A,B: PBS liposomes; C,D: clodronate liposomes. Scale bars: A,C = 0.1mm; B,D = 0.01mm.**

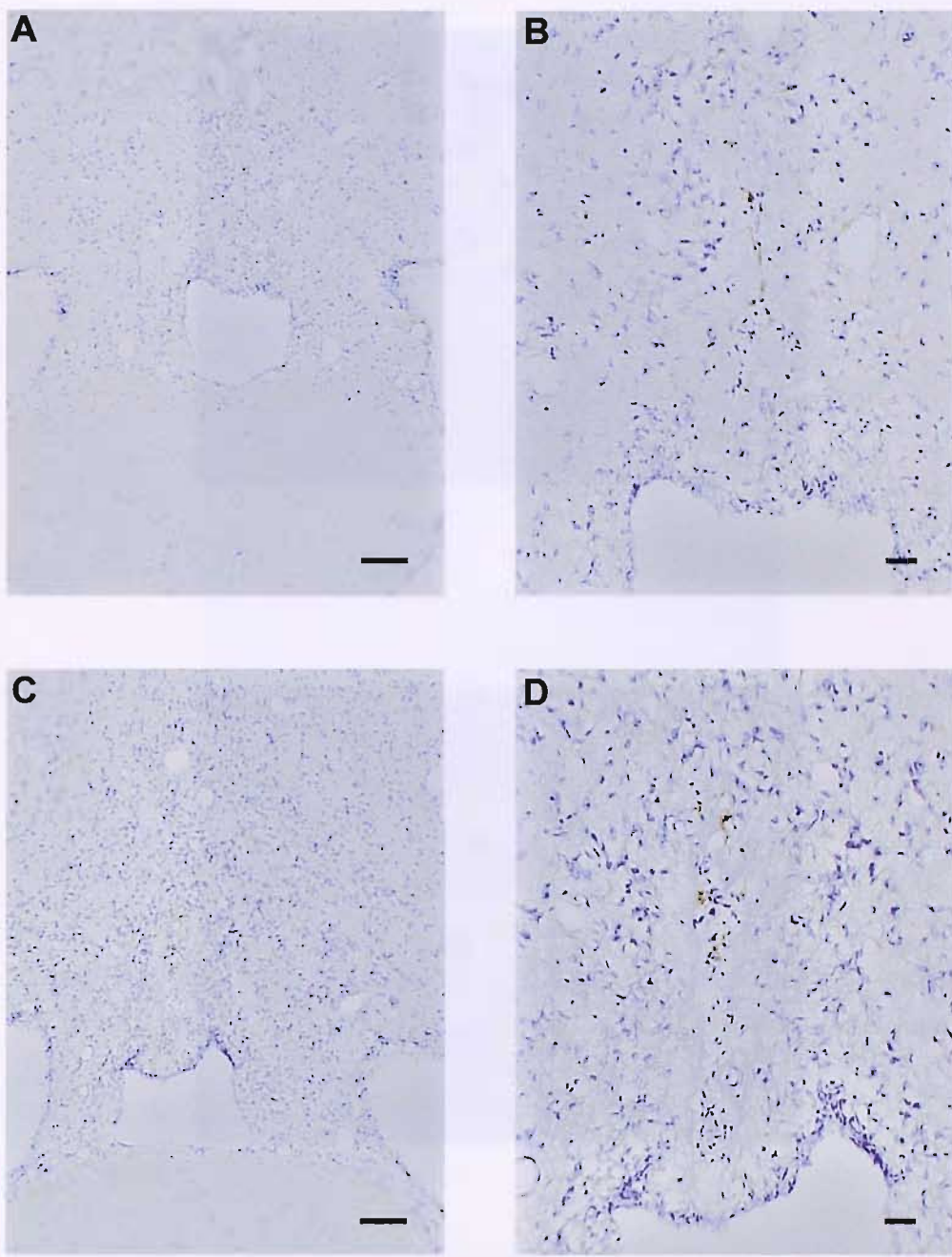


**Figure 4.5. No depletion of CD163-positive macrophages (brown) in the organum vasculosum laminae terminalis after infusion of 50 $\mu$ l clodronate liposomes in the fourth ventricle.**  
A,B: PBS liposomes; C,D: clodronate liposomes. Scale bars: A,C = 0.1 mm; B,D = 0.01 mm.

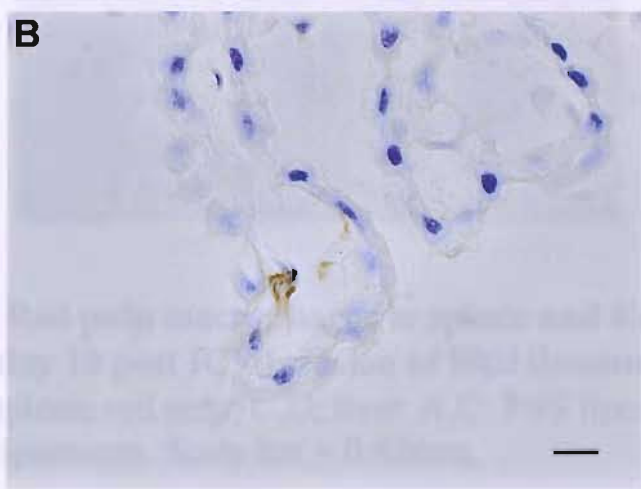
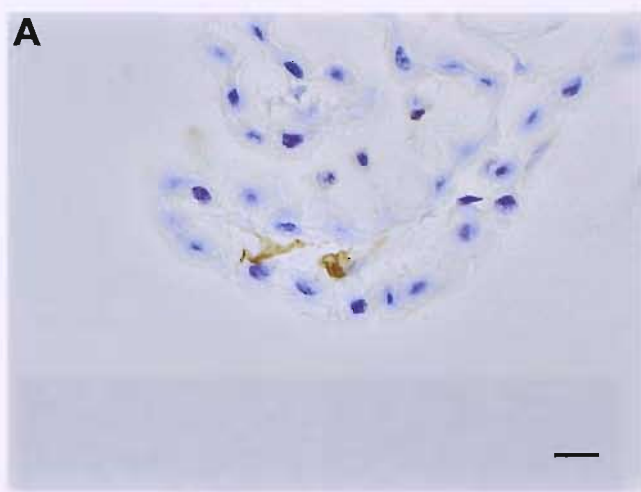


**Figure 4.6. No depletion of CD163-positive macrophages (brown) in the choroid plexus after infusion of 50 $\mu$ l clodronate liposomes in the fourth ventricle. A: PBS liposomes; B: clodronate liposomes.**  
Scale bar = 0.01mm.

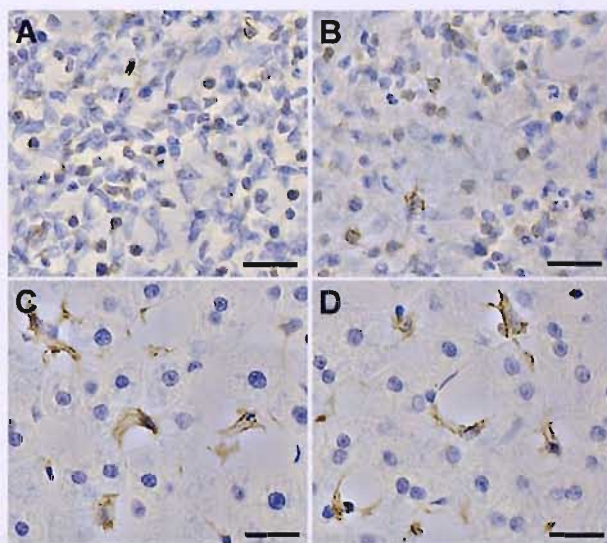


**Figure 4.7. Red pulp macrophages in spleen and Kupffer cells in liver on day 10 post ICV infusion of 50 $\mu$ l liposomes. ED2 IHC. A,B: splenic red pulp; C,D: liver. A,C: PBS liposomes; B,D: clodronate liposomes. Scale bar = 0.02mm.**

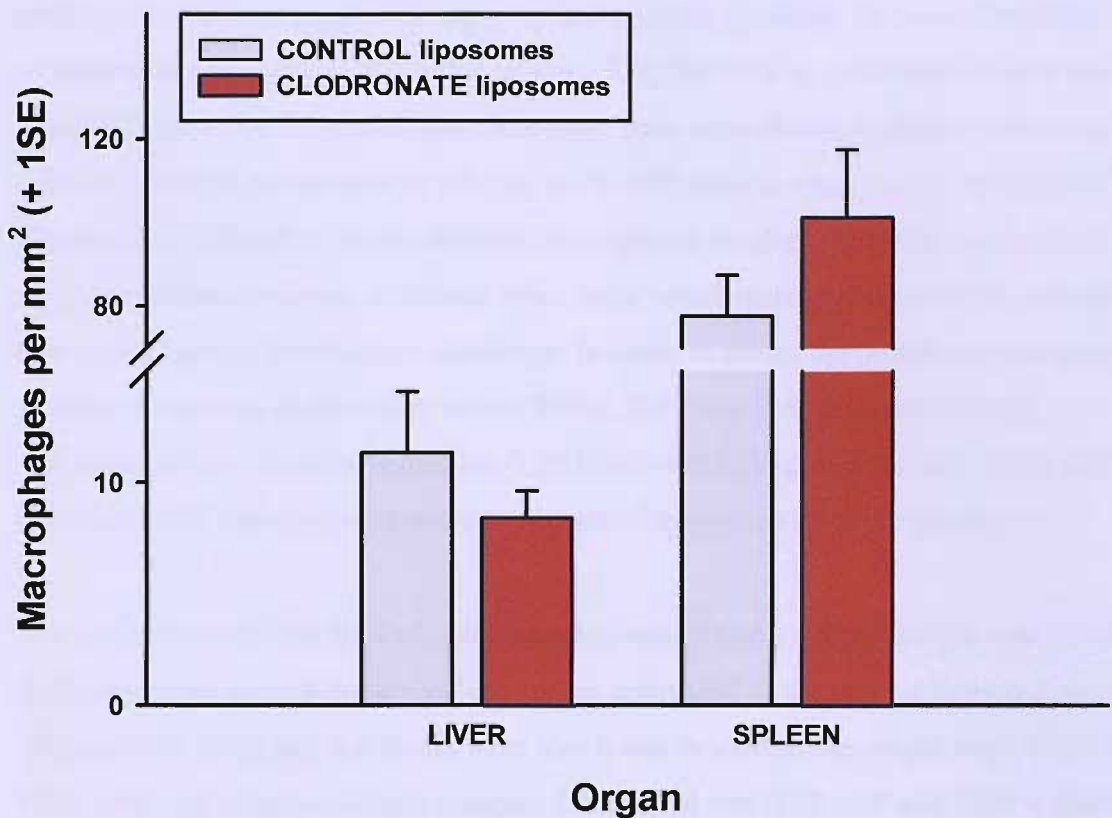


**Figure 4.8. Hepatic and splenic macrophages after ICV liposome infusion.** ED2-positive Kupffer cells in liver (n=3 per group) and red pulp macrophages in spleen (n=5 per group) were quantified on day 9 after ICV infusion of 50 $\mu\text{l}$  clodronate or control liposomes: no statistically significant difference was seen (2-tailed Student's t-test: p=0.384 for liver and p=0.248 for spleen).

#### **4.2.3 *ICV infusion of 50µl of clodronate liposomes attenuates the circulating cytokine response to systemic endotoxin challenge***

Although there was no difference in the numbers of hepatic and splenic macrophages on day 10 after ICV infusion of clodronate and control liposomes, this was not considered sufficient to indicate equivalent capacity for cytokine synthesis for several reasons. Firstly, an abnormal morphology was noted in some Kupffer cells in clodronate-treated rats. Secondly, both free and liposomal clodronate have been shown to inhibit endotoxin-induced cytokine production *in vitro* by RAW 264 cells in sub-cytotoxic conditions<sup>201</sup>. Thirdly, it is difficult to assess absolute macrophage numbers elsewhere in the body such as lymph nodes or tissues, or indeed other cells, which also contribute to the circulating cytokine response to endotoxin challenge. In order to assess the peripheral immune system directly, it was decided to assay serum TNF $\alpha$ , IL1 $\beta$  and IL6 2½ hours after i.p. administration of lipopolysaccharide (LPS) (300 000 EU/kg of E coli 0111:B4) to rats 9 days after ICV infusion of clodronate or control liposomes (n=4 per group).

The group treated with 50µl of clodronate liposomes had a significantly lower serum TNF $\alpha$  response to endotoxin challenge when compared to the control liposome group (**Figure 4.9**). IL1 $\beta$  and IL6 levels were also lower in clodronate-treated rats (145 ± 51 and 1820 ± 571 pg/ml respectively) compared to control rats (227 ± 58 and 6579 ± 1884 pg/ml respectively) although these differences failed to reach statistical significance (p=0.328 and p=0.052 on Student's t test). It thus became clear that the ICV clodronate liposome infusion was affecting the peripheral immune system.

#### **4.2.4 *ICV infusion of clodronate liposomes affects the circulating cytokine response to systemic endotoxin challenge and depletes cerebral CD163-positive perivascular macrophages in a dose-dependent fashion***

In order to investigate whether the peripheral immune system's blunted cytokine response was related to the amount of clodronate liposomes infused ICV, a dose-response study was performed. Rats were infused ICV with 50µl of control liposomes (n=12) or 10, 20 and 50µl of clodronate liposomes (n=3, 6 & 4 respectively). Volumes refer to the original concentrated suspensions. The 10 and 20µl doses were made up to 25µl with sterile PBS.

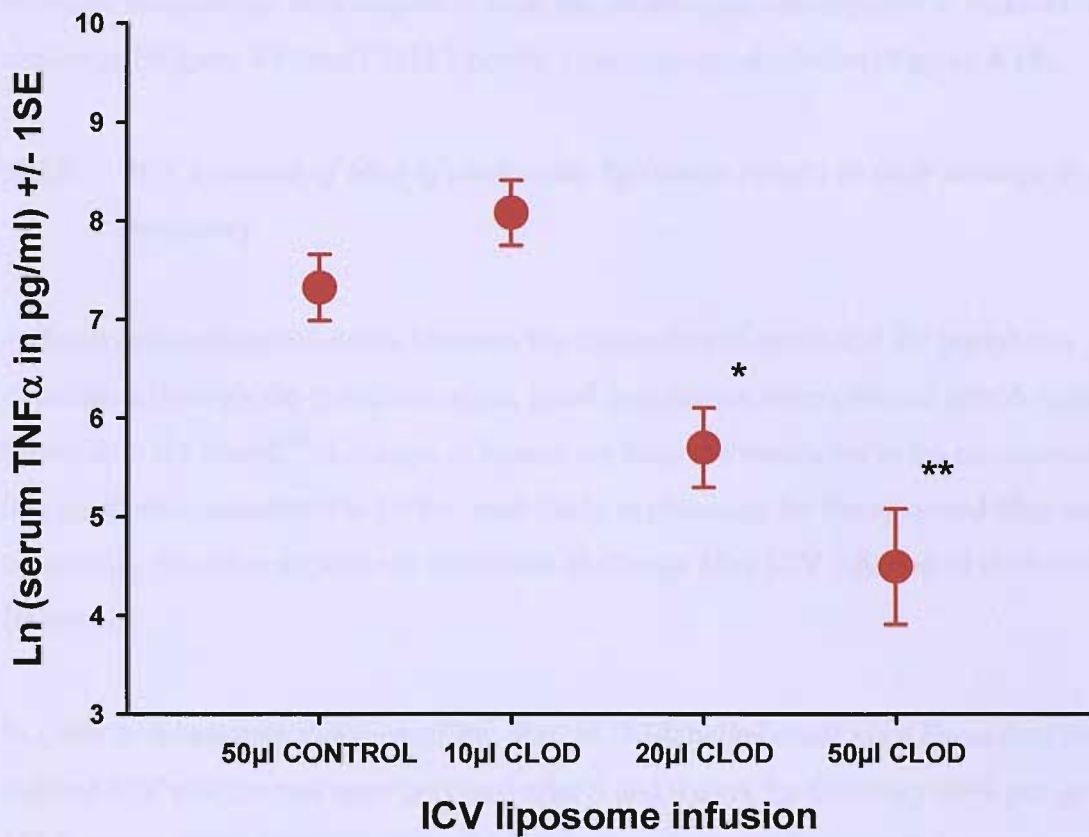


**Figure 4.9. ICV clodronate liposome infusion attenuated the circulating cytokine response to systemic endotoxin challenge in a dose-dependent manner.** Rats received ICV infusions of several doses of clodronate (n=13 total) or control liposomes (n=12 total) followed by an i.p. injection of 200 $\mu$ g/kg LPS. Serum was collected 2½ hours later for TNF $\alpha$  assay by ELISA. A dose-response was seen (one-way ANOVA: p<0.001; Bonferroni post hoc comparison: p<0.05 for 20 $\mu$ L [\*] and p<0.01 for 50 $\mu$ L [\*\*]). Data was normalized by logarithmic transformation.

After 9 days, rats were challenged with i.p. LPS (300 000 EU/kg of E coli 0111:B4). They were terminally anaesthetized 2½ hours later, and blood was collected by cardiac puncture. They were then perfused and the brains harvested for histology. There was a clear dose-response relationship with respect to both the serum cytokine response to endotoxin challenge (**Figure 4.9**) and CD163-positive macrophage depletion (**Figure 4.10**).

#### **4.2.5 *ICV infusion of 50µl of clodronate liposomes results in their leakage to the periphery***

A direct communication exists between the subarachnoid space and the peripheral circulation through the cribriform plate, nasal lymphatics, deep cervical lymph nodes and thence into the blood<sup>202</sup>. Leakage of liposomes from the ventricles to the circulation along this route was considered to be the most likely explanation for the observed blunting of the circulating cytokine response to endotoxin challenge after ICV infusion of clodronate liposomes.

In order to investigate this possibility, 50µl of DiI-labelled clodronate liposomes were infused ICV and the rats were perfused after 3 and 9 days for histology (n=3 per group). DiI is a very stable lipophilic dye which is known to persist for at least 2 weeks *in vivo* after i.v. injection of DiI-labelled liposomes<sup>203</sup>. Brain, cervical lymph nodes, liver and spleen were harvested. Immunofluorescence microscopy revealed the presence of dye in all the organs, most marked on day 9. In the brain, DiI was seen in the perivascular spaces and in the ependyma but was strongest in the meninges at both time points. DiI signal was picked up in the cervical lymph nodes, liver and spleen (**Figures 4.11, 4.12 & 4.13**), confirming the leakage of liposomes. In the cervical lymph nodes they preferentially accumulated in the subcapsular sinus, which is the first port of entry into lymph nodes in general (**Figure 4.11**). In the liver they were found in the hepatic sinusoids and spaces of Disse (**Figure 4.12**). Their localization in the spleen was widespread but greater in the red pulp and marginal zones as compared to the white pulp (**Figure 4.13**). Confocal microscopy was used in order to study the cellular localization of dye. In the cervical lymph nodes (**Figure 4.11**) and spleen (**Figure 4.13**), DiI colocalized with ED1-positive macrophages while in the liver it was present within ED2-positive Kupffer cells (**Figure 4.12**). All macrophage populations in the spleen had ingested DiI including macrophages

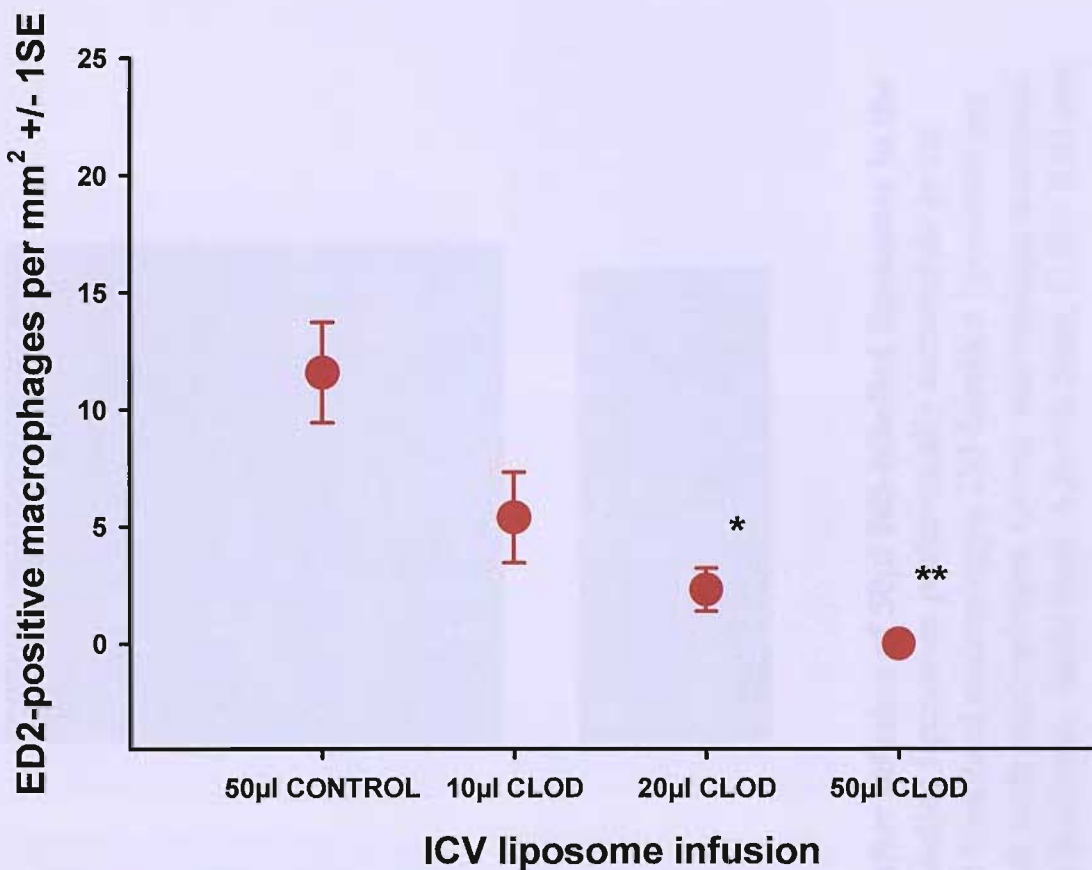


**Figure 4.10. ICV clodronate liposome infusion depleted CD163-positive macrophages in a dose-dependent manner.** Rats received ICV infusions of several doses of clodronate (n=13 total) or control liposomes (n=12 total) followed by an i.p. injection of 200µg/kg LPS. Rats were perfused 2½ hours later. Brains were harvested and processed for immunohistochemistry with ED2, which recognizes CD163. CD163-positive macrophages were quantified. A dose-response was seen (one-way ANOVA: p<0.001; Bonferroni post hoc comparison: p<0.05 for 20µL [\*] and p<0.01 for 50µL [\*\*]).

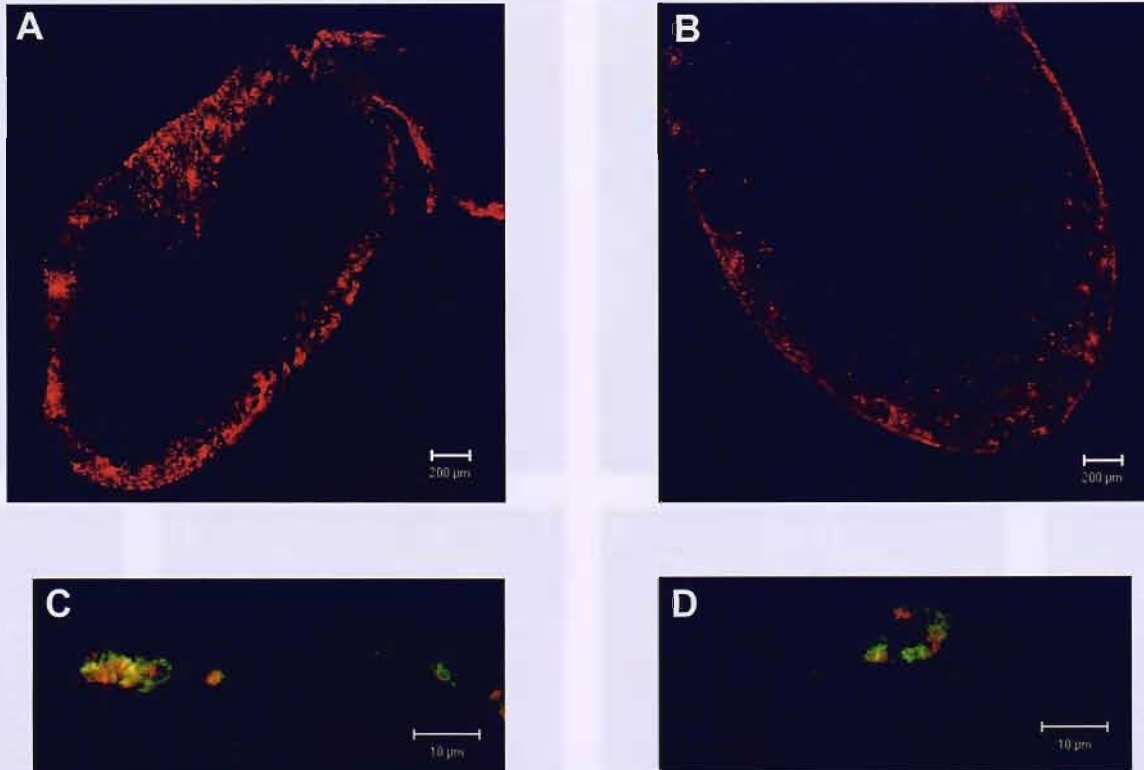


**Figure 4.11. Cervical lymph nodes on day 9 after infusion of 50 $\mu$ l Dil-labelled liposomes in the fourth ventricle.** A-B (epifluorescence): Dil-labelled liposomes preferentially accumulate in the subcapsular sinus of cervical lymph nodes. C-D (confocal microscopy): Dil-labelled liposomes are present in the cytoplasm and lysosomes of lymph node macrophages. Green: macrophage lysosomal marker ED1. Confocal sections were 0.43 $\mu$ m in thickness. Scale bars: A,B = 0.2mm; C,D = 0.01mm.

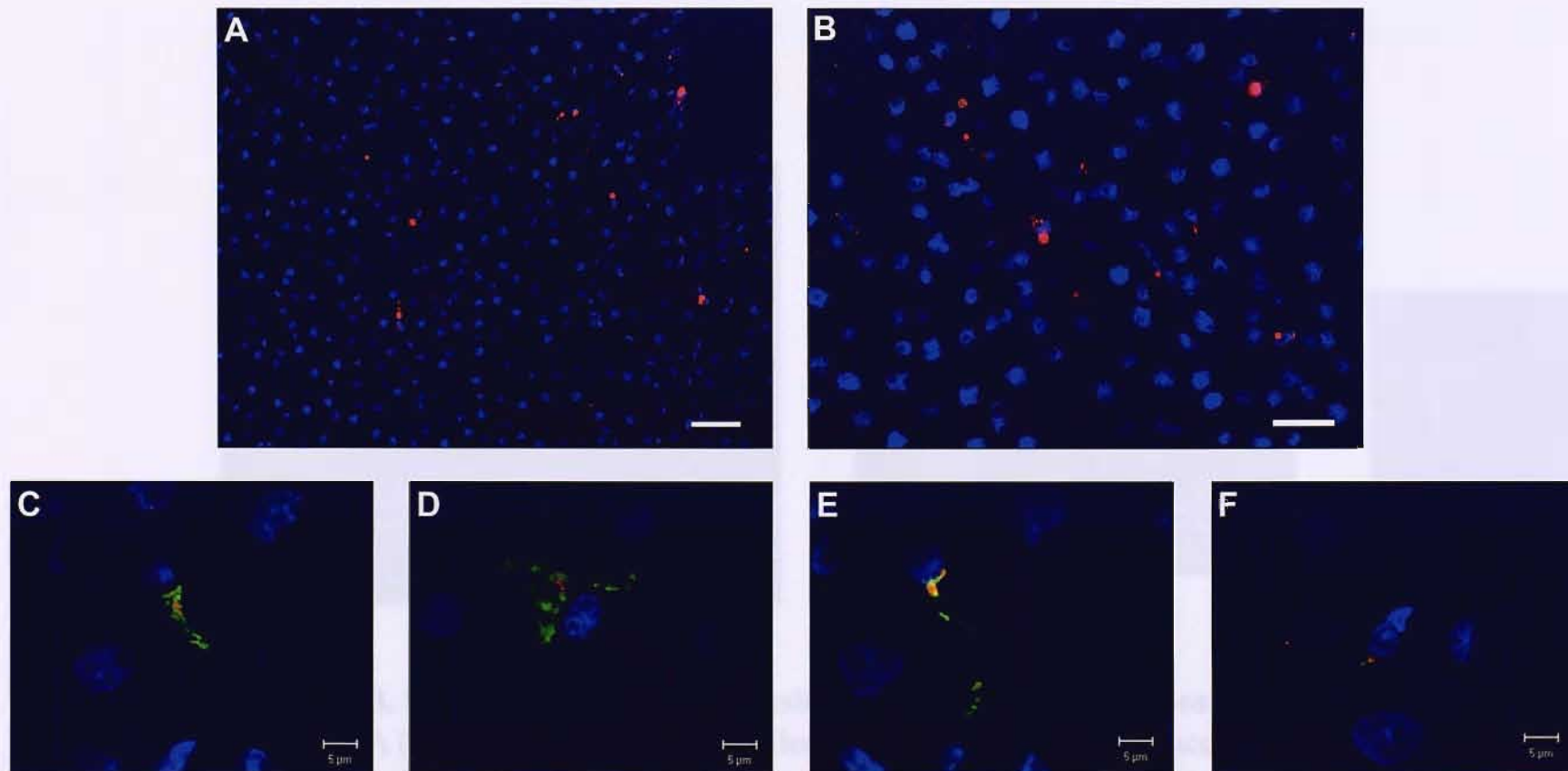


**Figure 4.12. Liver on day 9 after infusion of 50 $\mu$ l DiI-labelled liposomes in the fourth ventricle.** A-B (epi-fluorescence): DiI-labelled liposomes preferentially accumulate in the hepatic sinusoids and spaces of Disse. C-F (confocal microscopy): DiI-labelled liposomes are present within Kupffer cell processes. Green: Kupffer cell surface marker ED2. DAPI (blue) was used as a nuclear counterstain. All confocal sections are 0.43 $\mu$ m thick except D (0.99 $\mu$ m). Scale bars: A = 0.1mm; B = 0.04mm; C-F = 0.005mm.

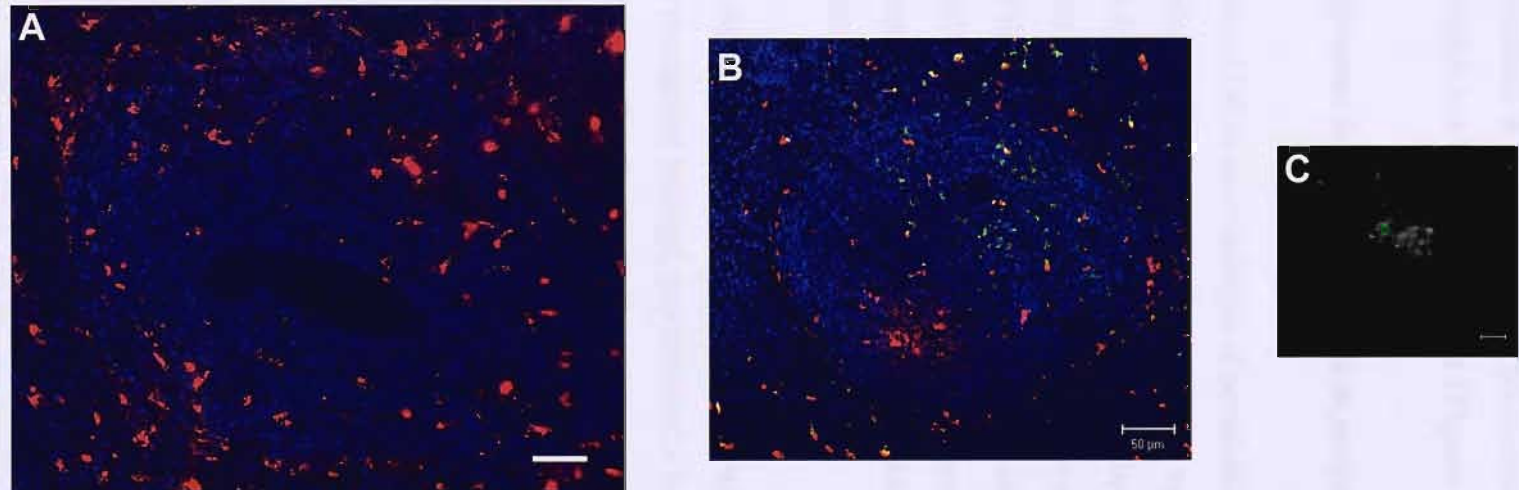


**Figure 4.13. Spleen on day 9 after infusion of 50 $\mu$ l DiI-labelled liposomes in the fourth ventricle.** A (epifluorescence): DiI-labelled liposomes preferentially accumulate in the splenic red pulp and marginal zones. B-C (confocal microscopy): DiI-labelled liposomes are present within splenic macrophages. Green: macrophage marker ED1. Confocal sections B&C are 1.7 $\mu$ m and 0.54 $\mu$ m in thickness respectively. Scale bars: A = 0.04mm; B = 0.05mm; C = 0.005mm.

in the red pulp, marginal zones and white pulp (**Figure 4.13**). The subcellular localization of DiI was studied: it colocalized with lysosomes as shown by double immunofluorescence with ED1, which is a lysosomal marker (**Figure 4.11**).

#### **4.2.6 *Liposome leakage from brain to periphery is a protracted process***

The presence of DiI in macrophages of peripheral organs on days 3 and 9 after ICV liposome infusion confirmed leakage from the ventricles to the circulation. However DiI is a lipophilic dye and its presence might persist beyond the effects of the liposomes which carried it. For this reason, it was not possible to study the kinetics of this leakage with DiI labelling of liposomes. In particular it was not clear whether the leakage occurred only during the ICV infusion or was an ongoing process. This was important information needed for optimization of the technique to reduce the effects of leakage on the peripheral immune system.

In order to reproduce the systemic effects of predominant leakage during the ICV infusion, as opposed to ongoing leakage, rats received a bolus i.v. injection of 50 $\mu$ l of clodronate or control liposomes (i.e. the same dose as that was initially administered ICV). On day 9, their serum TNF $\alpha$  response was assayed 2½ hours after i.p. administration of LPS (300 000 EU/kg of *E coli* 0111:B4). There was no significant difference between groups ( $4128 \pm 3311$  pg/ml in clodronate liposome group and  $4323 \pm 1796$  pg/ml in control liposome group,  $p=0.958$  on two-tailed Student's t test). Thus the systemic immune effects of the leakage occurring after ICV administration of 50 $\mu$ l of clodronate liposomes could not be simulated by intravenous infusion of the same dose of clodronate liposomes. This suggested that, even if leakage of liposomes from the CNS to the circulation occurred during the ICV infusion, there was a substantial ongoing leakage which continued to affect the peripheral immune system up to at least day 9 after the infusion. One possible mechanism is a depot effect of clodronate-loaded cell debris from effete CD163-positive macrophages within the CNS causing gradual leakage to the periphery.

#### **4.2.7 *Optimization of the clodronate liposome technique***

Optimization of the technique was necessary for its application to study the interaction between the CNS and the periphery. The target was reasonable depletion of cerebral

CD163-positive macrophages while maintaining the circulating cytokine response to systemic endotoxin challenge. Two approaches were possible:

- (1) **delaying** the i.p. LPS injection further to allow the peripheral immune system to recover. The major disadvantage of this approach was the repopulation of cerebral CD163-positive macrophages which was observed to start on day 11 post ICV infusion.
- (2) **optimizing** the infusion technique in order to minimize leakage to the periphery from the outset.

Since the previous experiment suggested that leakage was a slow and gradual process, it was decided to pursue the second approach. The ICV clodronate liposome infusion was optimized by varying the following factors: dose of original liposome suspension, volume infused, duration of infusion and site of injection. In order to minimize leakage into the subarachnoid space, infusions were performed considerably more rostrally than the 4<sup>th</sup> ventricle. The right lateral ventricle was finally chosen, rostral to the interventricular foramen of Munro. The optimum dose was found to be 15 $\mu$ l of the original suspension made up to 25 $\mu$ l with PBS, and infused in the right lateral ventricle over 12.5 minutes. This optimized technique did not affect the circulating TNF $\alpha$  response to endotoxin challenge (Figure 4.14) while achieving 65% depletion of CD163-positive macrophages in the septum and a more focal depletion in the right frontoparietal cortex and striatum (98% and 95% respectively). All meningeal CD163-positive macrophages were depleted.

### 4.3 Discussion

ICV infusion of clodronate liposomes results in depletion of cerebral CD163-positive macrophages and is therefore a useful tool to investigate the role of these macrophages in immune-to-brain signalling. Before employing this technique in further experiments, it was first characterized. The published protocol completely depleted CD163-positive macrophages throughout most of the CNS though incomplete depletion was observed in the CVOs and choroid plexus. This was thought to be secondary to the presence of tight junctions between cells lining the ventricular surface of these organs. Repopulation of CD163-positive macrophages was first seen in the meninges on day 11 and is consistent with their bone marrow origin<sup>197</sup>.

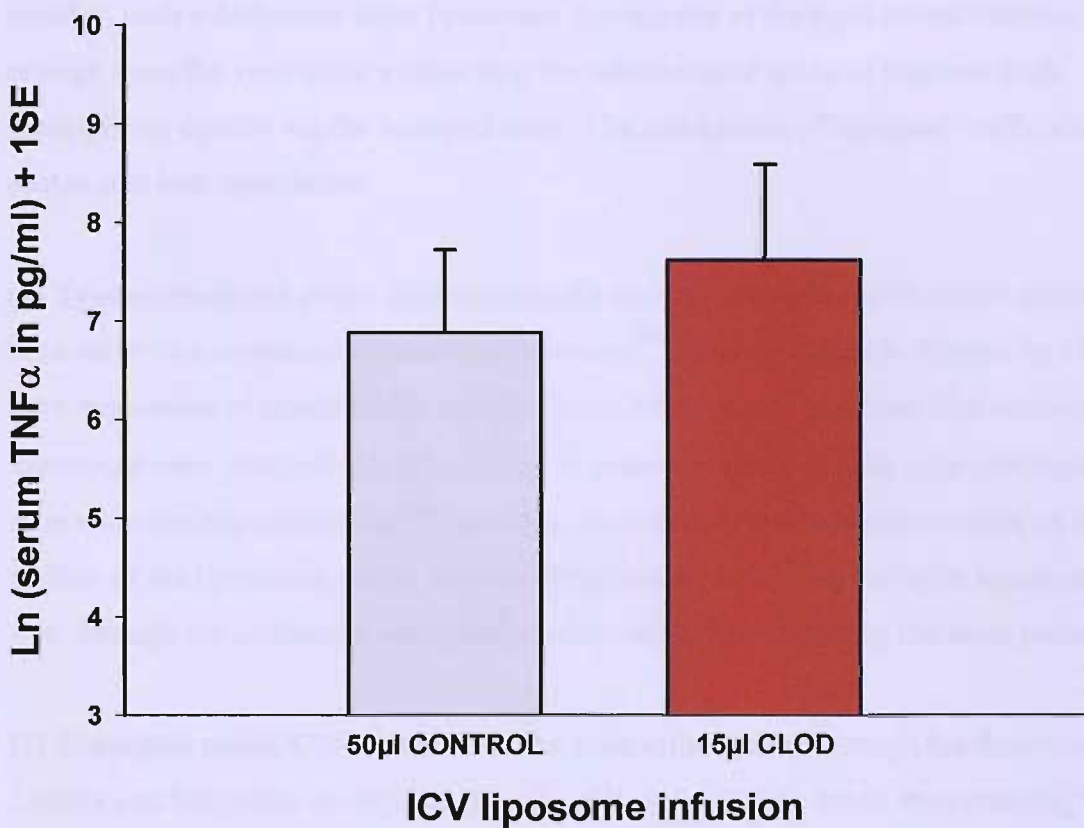


**Figure 4.14. The optimized technique did not affect the circulating cytokine response to systemic endotoxin challenge.** Serum TNF $\alpha$  levels 2½ hours after 200 $\mu$ g/kg LPS i.p. in animals treated with clodronate or control liposomes (n=5 per group) using the optimized method (see text) 9 days previously. No statistically significant difference was seen (2-tailed Student's t-test: p=0.582). Data was normalized by logarithmic transformation. CLOD = clodronate.

There are two routes by which the ICV-infused liposomes (measuring 0.2-3 $\mu$ m in diameter) may reach CD163-positive macrophages throughout the CNS: the transependymal and transpial routes (**Figure 4.15**). The asymmetry in depletion of CD163-positive macrophages observed with unilateral intraventricular infusions of clodronate liposomes shows that the transependymal route is dominant. The transpial route would not result in such a difference since liposomes flowing out of the right lateral ventricle would emerge from the ventricular system into the subarachnoid space to infiltrate both hemispheres equally via the transpial route. The mechanism of liposome traffic along these routes is at best speculative:

**(1) Transependymal route.** Ependymal cells do not have tight junctions but adhere to each other by a mannose-dependent mechanism<sup>204</sup>. This is thought to happen by virtue of their expression of carbohydrate specific lectin, which binds mannose. Physical opening of interependymal channels 0.5-2.5 $\mu$ m wide to mannosylated synthetic glycoconjugates was seen with electron microscopy<sup>204</sup>. It is thus possible that the mannose residues on the surface of the liposomes enable them to disaggregate the ependymal tight junctions and pass through the so formed interependymal channels thus accessing the brain parenchyma.

**(2) Transpial route.** CSF flows out of the ventricular system through the foramina of Lushka and Magendie to circulate over the pial surface of the brain, thus reaching the meningeal macrophages. Penetration into the outer layers of the cortex can occur through openings in the pia mater which have been described in the rat and tend to occur around vessels in the subarachnoid space, especially at their point of entry into the brain<sup>205</sup>. They are *circa* 0.2 $\mu$ m in diameter and therefore large enough to allow passage of smaller liposomes.

Given the fact that it was ultimately intended to use the clodronate liposome technique to study the role of CD163-positive macrophages in immune-to-brain signalling, an intact circulating cytokine response to systemic inflammatory challenge was essential. Although Kupffer cell and splenic red pulp macrophage numbers had recovered by day 9 when the rats were systemically challenged with endotoxin, the circulating cytokine response was attenuated in a dose-dependent fashion. It was found that liposomes leaked slowly from the CNS to peripheral immune organs such as cervical lymph nodes, liver and spleen. The ICV infusion technique was optimized to preserve the circulating cytokine response to

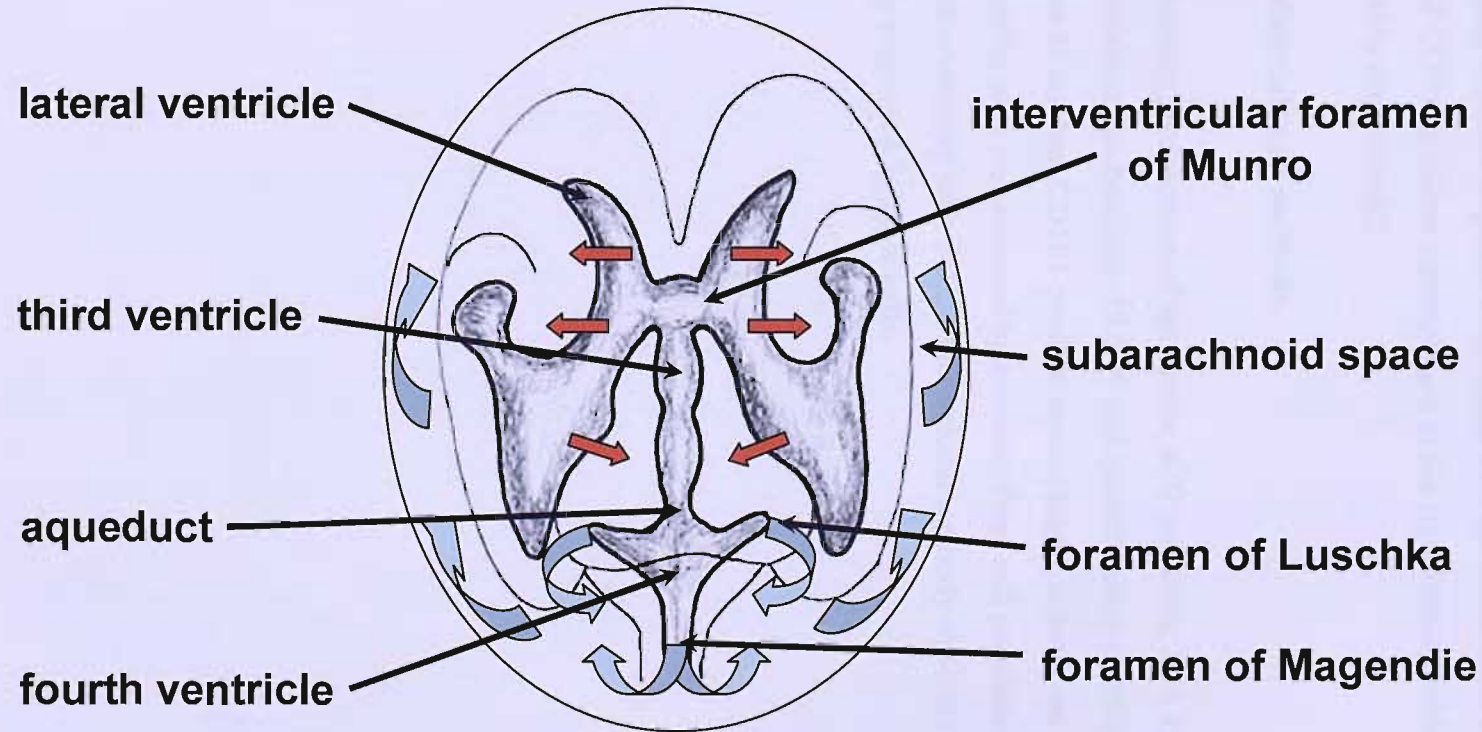


Figure 4.15. Transependymal (red) and transpial (blue) routes for ICV liposomes

endotoxin challenge, which was essential for future studies of immune-to-brain signalling. The optimum protocol was 15 $\mu$ l of the original suspension made up to 25 $\mu$ l and infused into the right lateral ventricle over 12.5 minutes. This optimized technique did not affect the circulating cytokine response to systemic LPS administration while achieving a focal depletion of CD163-positive macrophages in the right frontoparietal cortex and striatum (98% and 95% respectively).

#### **4.4 Materials and methods**

Animals, housing, preparation of liposomes, ICV infusions, LPS injections, perfusion of animals, immunohistochemistry, ELISA and quantification of cells are detailed in Chapter 2. Depletion of cerebral CD163-positive macrophages, splenic red pulp macrophages and hepatic Kupffer cells was assessed by counting these cell populations after immunohistochemistry with ED2, a monoclonal antibody against CD163, which is specifically expressed by these cells.

## **Chapter 5**

### **Cerebral CD163-positive macrophages in immune-to-brain signalling**

CD163 is a marker for macrophages in the brain. It is expressed on microglia and on a subset of CD45<sup>+</sup> CD11b<sup>+</sup> CD163<sup>+</sup> cells that are recruited from the periphery. CD163<sup>+</sup> cells are found in the perivascular space and in the parenchyma. They are involved in the removal of cellular debris and in the production of cytokines. CD163<sup>+</sup> cells are also involved in the regulation of the blood-brain barrier. CD163<sup>+</sup> cells are found in the brain in various diseases, including multiple sclerosis, Alzheimer's disease, and stroke. CD163<sup>+</sup> cells are also found in the brain in normal conditions, such as during pregnancy and after exercise. CD163<sup>+</sup> cells are found in the brain in various diseases, including multiple sclerosis, Alzheimer's disease, and stroke. CD163<sup>+</sup> cells are also found in the brain in normal conditions, such as during pregnancy and after exercise.

### 5.1 Introduction

Neuroinflammatory diseases are characterized by exacerbations which occur in association with systemic infections. One third of relapses in multiple sclerosis (MS) are infection-related and lead to more sustained clinical deficit than non-infection related relapses<sup>15</sup>. In Alzheimer's disease (AD) patients, delirium is frequently precipitated by systemic infections<sup>206</sup>, which are associated with accelerated cognitive decline<sup>41,207</sup>. The pathway for inflammatory signals across the blood-brain barrier (BBB) is therefore an appropriate therapeutic target.

The brain parenchyma is shielded from the circulation by the presence of blood-brain and blood-cerebrospinal fluid barriers. Yet, a delayed and distinct inflammatory response is observed within the brain during systemic inflammation<sup>176</sup>. The brain's contact with its external environment is limited to three anatomical areas which represent the immune-brain interface: cerebral blood vessels, meninges and circumventricular organs. Circulating inflammatory molecules can theoretically access the brain parenchyma constituting a direct humoral route<sup>60,63</sup>. However the brain's inflammatory response during systemic inflammation occurs in a biphasic manner<sup>64,69,78,79</sup>. The first to respond are cells at the immune-brain interface, followed by a second delayed and prolonged phase of cellular activation within the brain parenchyma. This biphasic response argues against a predominant role for direct entry of circulating humoral mediators and suggests the existence of a relay mechanism whereby cells at the immune-brain interface respond first and then relay the inflammatory message into the brain.

The two main cells at the blood-brain barrier, endothelial cells and CD163-positive perivascular macrophages, have both been implicated in immune-to-brain signalling. This has been inferred on the basis of observational studies which used immunohistochemistry or *in situ* hybridization to look at the response of these cells to systemic inflammation<sup>72,74,82,83</sup>. However there are no studies interrogating the individual role of these two cell types in immune-to-brain signalling and their relative functional contribution

remains unknown. This is clearly important for therapeutic manipulation of immune-to-brain signalling.

CD163-positive macrophages are found at each of the three immune-brain interfaces: the perivascular space of cerebral blood vessels, meninges and choroid plexus<sup>199</sup>. Their location between the glial and endothelial basement membranes might be considered to make them inaccessible to therapeutic intervention. Cerebral CD163-positive macrophages are constitutively phagocytic<sup>45</sup> and undergo steady turnover by virtue of their bone marrow origin<sup>197,198</sup>. Transfer of genetically-modified haematopoietic cells which give rise to this population of macrophages is a form of gene therapy that has been shown to be technically feasible<sup>208,209</sup>. However engraftment was not specific, with replacement of all macrophage populations in the body, including microglia. By virtue of their location, cerebral endothelial cells are more accessible than CD163-positive macrophages. Moreover, endothelial cells at the BBB are sufficiently specialized to be able to offer several possibilities for targeted drug delivery<sup>210</sup>.

In order to dissect the contribution of cerebral CD163-positive macrophages and endothelial cells to immune-to-brain signalling, the former population was depleted using the optimized clodronate liposome technique described in Chapter 4. Immune-to-brain signalling after a systemic endotoxin challenge was assessed by looking at several events which are considered to reflect the brain's response to systemic inflammation. The first was fever, which is a complex prostaglandin-dependent phenomenon involving the interplay of several brain regions<sup>211</sup>, but ultimately mediated by the diencephalon<sup>61</sup>. Secondly, as cytokine expression within the brain is thought to underlie exacerbations in human neuroinflammatory diseases<sup>54</sup>, *de novo* cytokine transcription within the brain was studied using real-time reverse-transcriptase polymerase chain reaction (RT-PCR). In order to confirm translation of message, IL1 $\beta$  protein was then assayed. Finally phosphorylation of ERK1/2, an event downstream of cytokine expression, was investigated. It is shown that cerebral CD163-positive macrophages are not essential for immune-to-brain signalling. Cerebral endothelial cells are able to fully execute this process in the absence of CD163-positive macrophages.

## 5.2 Results

### 5.2.1 *An intact cerebral CD163-positive macrophage population is not essential for the febrile response to systemic inflammation*

Since fever is initiated by the CNS, its occurrence in the context of systemic inflammation is a sign that an inflammatory message has crossed the BBB and induced a transcriptional programme within key areas in the brain<sup>61</sup>. The meninges are responsible for  $\frac{2}{3}$  of IL1 $\beta$  produced within the CNS during systemic endotoxin challenge<sup>212</sup> and its neutralization by ICV administration of IL1 receptor antagonist (ILIRA) attenuated fever<sup>213</sup>. The optimized clodronate liposome technique achieved complete depletion of meningeal CD163-positive macrophages, which are responsible for IL1 $\beta$  production in the meninges<sup>212</sup>. In order to investigate the role of CD163-positive macrophages in fever generation, telemetry was used to measure the hyperthermic response to systemic endotoxin challenge 9 days after ICV liposome infusion. Both clodronate and control liposome treated animals reacted identically, with typical signs of sickness behaviour including a hunched posture, piloerection, and decreased cage activity. No significant difference in febrile response was observed between the two groups (Figure 5.1, fever index was  $158.6 \pm 66.1$  °Cmin and  $253.6 \pm 69.9$  °Cmin in control and clodronate liposome treated animals respectively,  $p=0.353$ ). This indicated that an intact cerebral CD163-positive macrophage population was not essential for immune-to-brain signalling in the context of fever and sickness behaviour. However, it was possible that more crucial thermoregulatory areas such as the hypothalamus and circumventricular organs, which were not depleted of CD163-positive macrophages (see Chapter 4), were responding directly to systemic inflammation thereby maintaining fever in this experiment. These brain regions also receive neural input from the periphery during systemic inflammation resulting in their activation independent of any immune-to-brain signalling mediated by cerebral CD163-positive macrophages or endothelial cells<sup>61</sup>.

### 5.2.2 *Systemic endotoxin challenge induces gene transcription of the cytokines TNF $\alpha$ , IL1 $\beta$ and IL6 in the frontoparietal cortex*

Fever was used as a readout in the above experiment. Since there was no significant difference between experimental groups, it was possible that brain regions incompletely

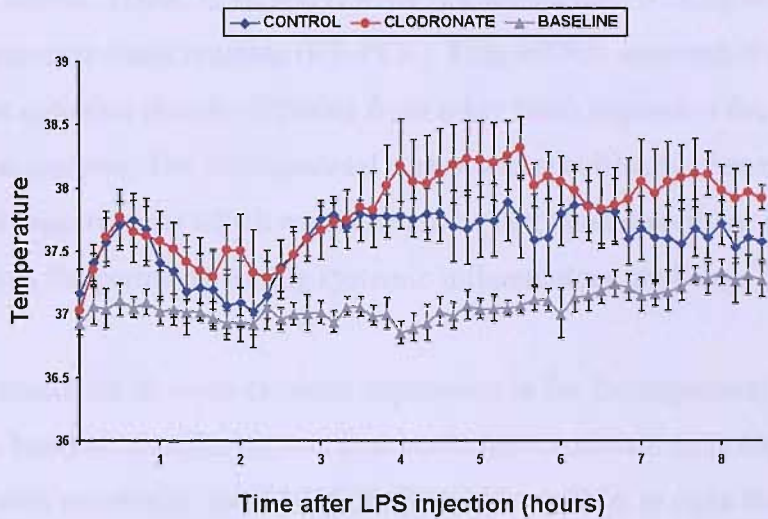


**Figure 5.1. An intact cerebral CD163-positive macrophage population is not essential for the febrile response to systemic inflammation.** Rats were implanted with sensor capsules intraperitoneally and core body temperature was measured continuously using telemetry. A fortnight later, they received an ICV infusion of 15 $\mu$ l clodronate or control liposomes (n=5 per group). After 9 days, they were challenged with an i.p. injection of 200 $\mu$ g/kg LPS. No statistically significant difference in febrile response was seen using area-under-curve analysis (see text).

depleted of CD163-positive macrophages were compensating to sustain fever generation. A different approach was therefore utilized, taking advantage of the focal near total depletion of CD163-positive macrophages in the right frontoparietal cortex.

Systemic inflammation is accompanied by a delayed *de novo* expression of cytokines behind the BBB<sup>176</sup>. In order to study *de novo* cytokine expression within the right frontoparietal cortex, TNF $\alpha$ , IL1 $\beta$  and IL6 mRNA were assayed using semi-quantitative real-time polymerase chain reaction (RT-PCR). This mRNA approach does away with the possibility that cytokine protein diffusing from other brain regions or the circulation is included in the analysis. The frontoparietal cortex was specifically chosen for analysis in order to avoid brain regions which are known to be activated directly or indirectly by vagal projections from the periphery during systemic inflammatory challenge<sup>61</sup>.

In order to characterize *de novo* cytokine expression in the frontoparietal cortex in the model used, a baseline experiment was first performed. Animals were challenged systemically with endotoxin, and TNF $\alpha$ , IL1 $\beta$  and IL6 mRNA in right frontoparietal cortex were assayed 3 hours later using RT-PCR. Significant transcription of these cytokine genes occurred in endotoxin treated animals; none occurred in animals receiving vehicle (**Figure 5.2**). *De novo* transcription of cytokines within the brain during systemic inflammation is therefore another sign that an inflammatory message has crossed the BBB.

### **5.2.3 *Cerebral CD163-positive macrophage depletion does not affect de novo cytokine expression in the brain occurring during systemic inflammation***

The focal depletion achieved in the right frontoparietal cortex by the optimized technique made it possible to study the role of cerebral CD163-positive macrophages in immune-to-brain signalling by assaying *de novo* transcription of cytokines in this brain region after systemic endotoxin challenge. It was first established that ICV infusion of control liposomes *per se* did not affect the central cytokine response to systemic endotoxin challenge (**Figure 5.3**). Then, animals received a clodronate or control liposome ICV infusion, and 9 days later were challenged with endotoxin systemically. No significant differences in TNF $\alpha$ , IL1 $\beta$  and IL6 mRNA levels in the frontoparietal cortex were detected between clodronate and control liposome treated animals (**Figure 5.4**). This shows that

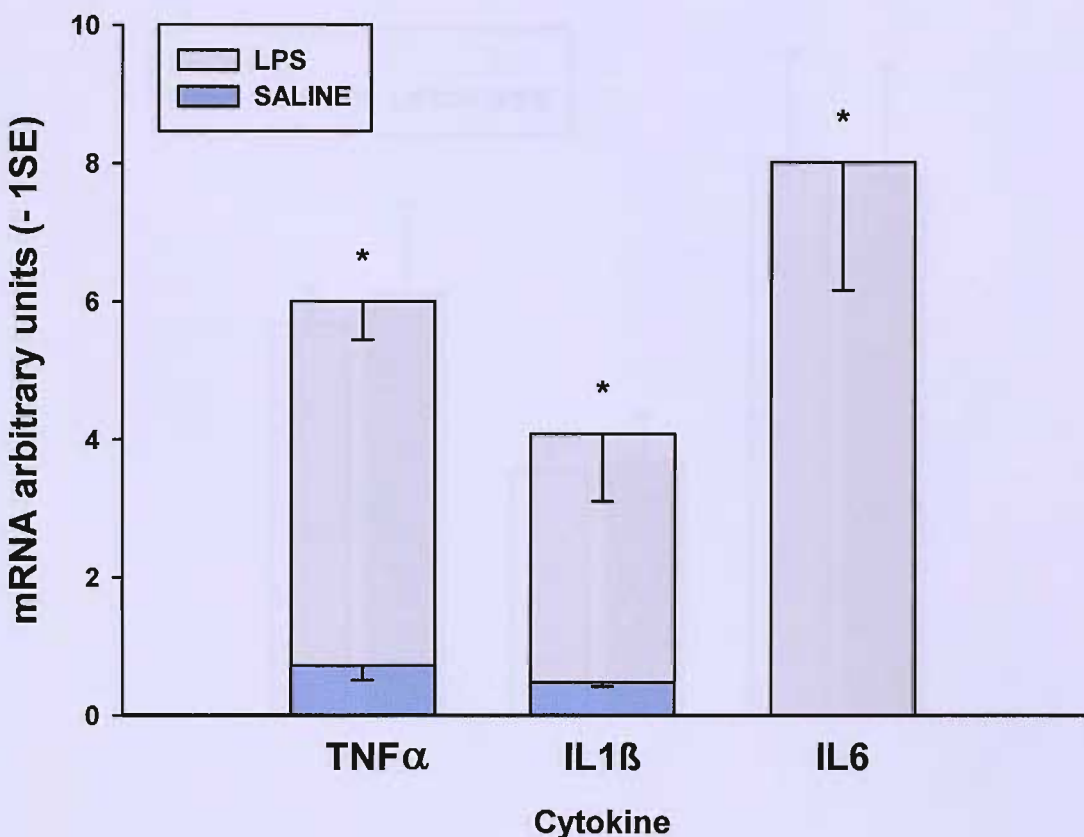


**Figure 5.2. *De novo* cytokine transcription in the rat brain during systemic inflammation.** Rats were challenged with 200 $\mu$ g/kg LPS or saline i.v. (n=5 per group) and right frontoparietal cortex was harvested 3 hours later for cytokine mRNA analysis by RT-PCR. A significant upregulation (\*) of TNF $\alpha$  ( $p<0.001$ , 95% CI = 4.7 – 7.8), IL1 $\beta$  ( $p=0.008$ , 95% CI = 1.6 – 7.7) and IL6 ( $p=0.003$ , 95% CI = 2.6 – 8.5) was seen (2-tailed Student's t-test).

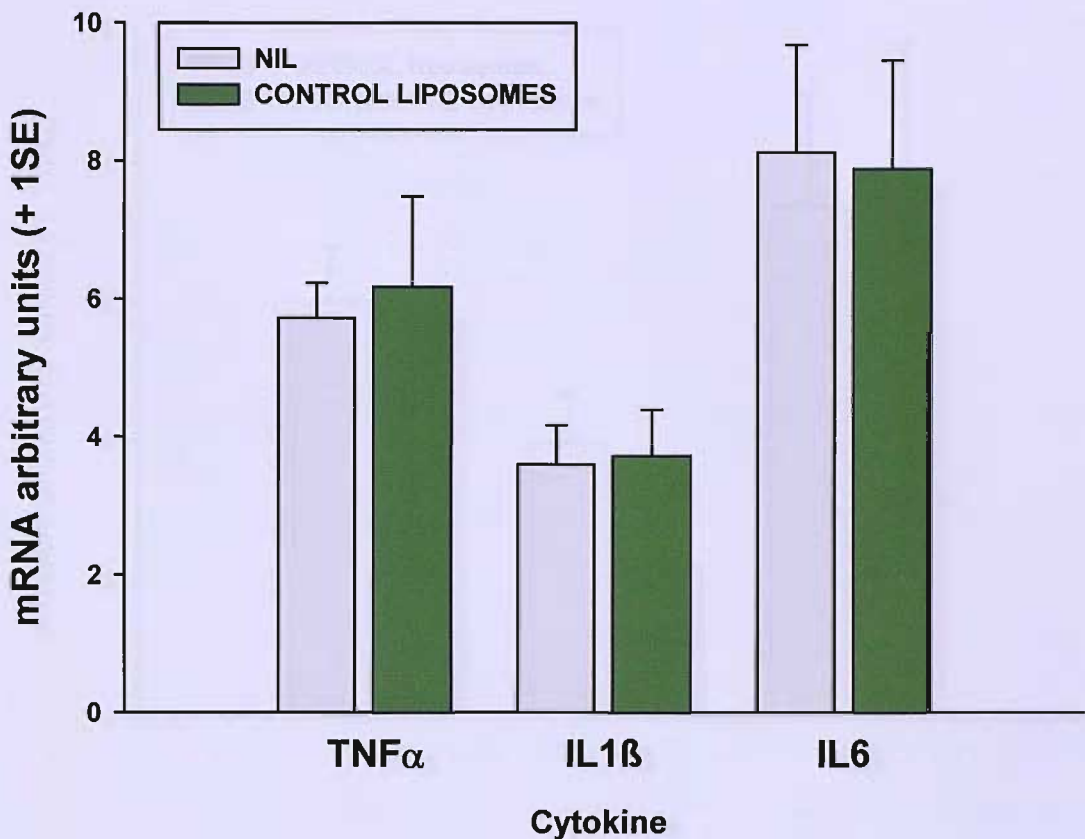


**Figure 5.3. Liposome infusion does not affect *de novo* cytokine expression in the brain occurring during systemic inflammation.**  
 Cytokine mRNA upregulation in right frontoparietal cortex after an i.v. challenge of 200 $\mu$ g/kg LPS was not affected by ICV infusion of control liposomes 9 days previously compared to naïve rats (n=5 per group). No statistically significant difference was observed in TNF $\alpha$  ( $p=0.751$ ), IL1 $\beta$  ( $p=0.895$ ) and IL6 ( $p=0.918$ ) mRNA between groups (2-tailed Student's t-test).

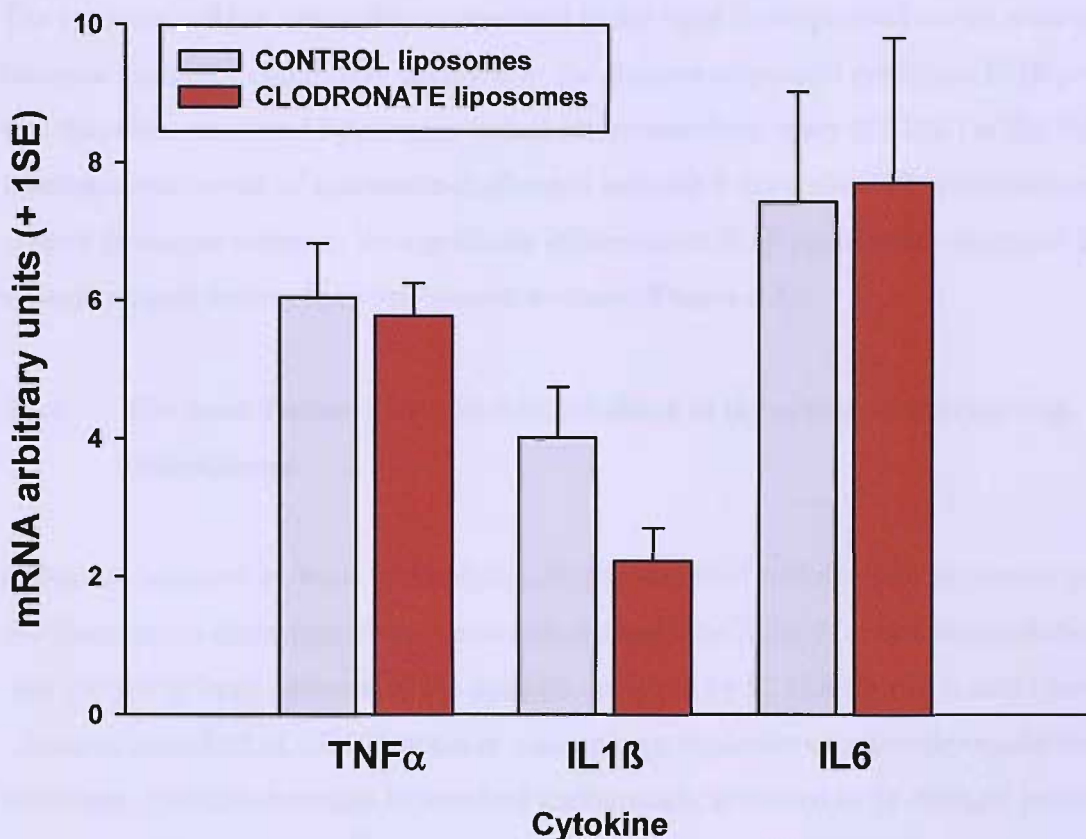


**Figure 5.4. Cerebral CD163-positive macrophage depletion does not affect *de novo* cytokine expression in the brain occurring during systemic inflammation.** Right frontoparietal cortex cytokine mRNA levels (by RT-PCR) 3 hours after 500 $\mu$ g/kg LPS i.v. in animals pre-treated with clodronate or control liposomes (n=4 per group) using the optimized method (see text) 9 days previously. No statistically significant difference was observed in TNF $\alpha$  (p=0.782), IL1 $\beta$  (p=0.084) and IL6 (p=0.920) mRNA between groups (2-tailed Student's t-test).

cerebral CD163-positive macrophages are not necessary for the elaboration of cytokine synthesis within the CNS during systemic inflammation.

The cytokine mRNA upregulation observed in the right frontoparietal cortex after systemic immune challenge could have occurred in the absence of protein synthesis. IL1 $\beta$  protein was therefore measured by enzyme-linked immunosorbent assay (ELISA) in the right frontoparietal cortex of endotoxin-challenged animals 9 days after ICV clodronate or control liposome infusion. No significant difference in IL1 $\beta$  protein was observed between clodronate and control liposome treated animals (**Figure 5.5**).

#### **5.2.4 *The contribution of cerebral endothelium to the cytokines assayed was insignificant***

Cytokines secreted by brain parenchyma, but not cerebral endothelium, represent evidence that immune-to-brain signalling has occurred across the BBB. If endothelium-derived IL1 $\beta$  was present in large amounts in the samples analyzed by ELISA above, it could have obscured the effect of CD163-positive macrophage depletion on parenchyma-derived IL1 $\beta$ . However, cytokine secretion by cerebral endothelium is known to be strongly polarized favouring luminal release<sup>214</sup>. Therefore most IL1 $\beta$  secreted by the cerebral endothelium would not have been included in the brain samples, as they were harvested after thorough perfusion. Nevertheless, it was important to determine whether the cerebral endothelium was responsible for secretion of significant amounts of IL1 $\beta$  in the model employed. The expression of phosphorylated ERK1/2 (pERK1/2) was therefore studied using immunohistochemistry. IL1 $\beta$  results in phosphorylation of ERK1/2<sup>215</sup> and rat cerebral endothelium is known to express pERK1/2 in response to IL1 $\beta$ <sup>216</sup>. Therefore cerebral endothelial cells would be expected to express pERK1/2 if they were responsible for significant synthesis of IL1 $\beta$ , which would act in an autocrine and/or paracrine manner. In naïve brains or after injection of sterile saline as a control, pERK1/2 was only detectable in some neurons (**Figure 5.6a**). After systemic endotoxin challenge, neurones and microglia boldly upregulated pERK1/2 expression in both control and clodronate liposome pre-treated animals (**Figure 5.6b**). Endothelial cells did not express pERK1/2 (**Figure 5.6b,c**), showing that endothelium-derived IL1 $\beta$  secretion was negligible and that it was unlikely to have contributed significantly to total IL1 $\beta$  measured in the brain samples above. The persistence of pERK1/2 upregulation in neurones and microglia after systemic endotoxin

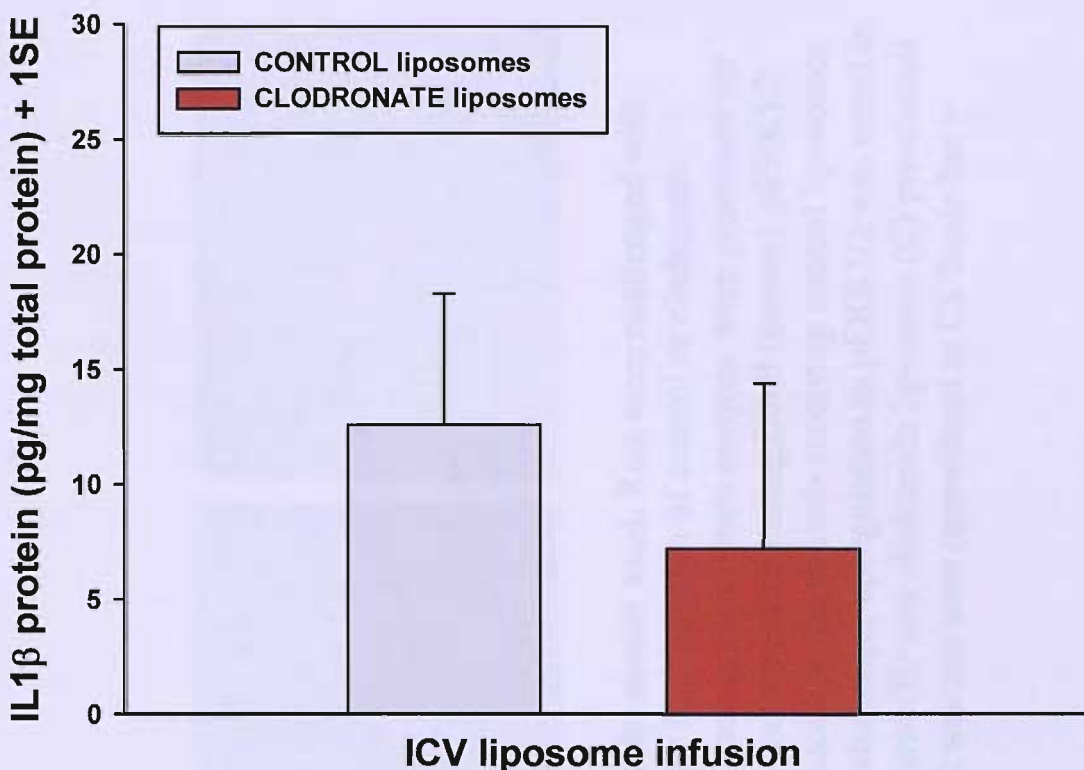


**Figure 5.5. IL1 $\beta$  protein in the right frontoparietal cortex.** IL $\beta$  protein levels were measured by ELISA in right frontoparietal cortex 3 hours after 500 $\mu$ g/kg LPS i.v. in animals pre-treated with clodronate (n=6) or control liposomes (n=7) using the optimized method (see text) 9 days previously. No statistically significant difference was seen (2-tailed Student's t-test: p=0.564). No IL1 $\beta$  was detected after i.p. saline injection of rats receiving control liposomes ICV 9 days previously.

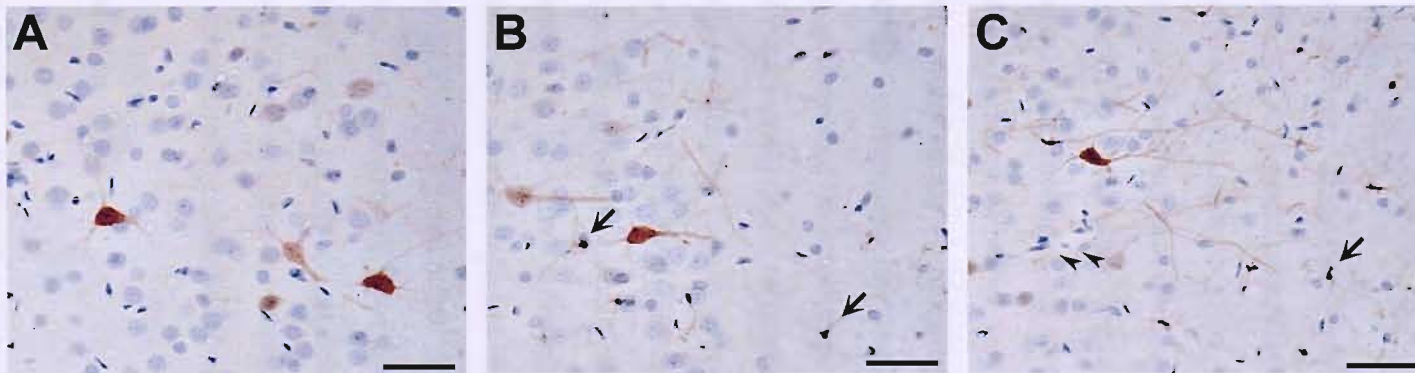


**Figure 5.6. Phosphorylation of ERK1/2 in the model used.** Rats were challenged with sterile saline or 500 $\mu$ g/kg LPS i.v. 9 days after ICV infusion of control or clodronate liposomes using the optimized method (n=4 each group). Brain sections were processed for immunohistochemistry for pERK1/2, which was visualized using DAB (brown). pERK1/2 immunoreactivity was restricted to some neurons in the animals receiving control liposomes ICV and saline i.v. (A). After systemic LPS challenge, upregulation in pERK1/2 was noted in neurones and microglia (arrows) in both control (B) and clodronate liposome (C) pre-treated animals. Endothelial expression of pERK1/2 was not seen (arrowhead in C). Scale bar = 0.05mm.

challenge despite depletion of cerebral CD163-positive macrophages also corroborates the finding that these macrophages are not essential for immune-to-brain signalling.

### **5.2.5 *CD163-positive macrophages are excluded at the blood-brain interface***

In the above experiments, clodronate liposomes were used to dissect the immune-to-brain signalling roles of CD163-positive macrophages and endothelial cells at the BBB. It was found that despite their strategic location, CD163-positive macrophages do not contribute significantly to this signalling process. One possible reason is that endothelium is the component of the BBB which is in direct contact with the circulation. Cerebral CD163-positive perivascular macrophages are situated between the endothelial basement membrane and glia limitans. Whether they are in direct contact with circulating blood has not been entirely excluded. Cerebral CD163-positive perivascular macrophages have been reported to take up intravenously injected substances such as fluorescently labelled acetyl-low density lipoprotein and horseradish peroxidase<sup>87</sup>, but whether this occurs as a result of direct uptake by the macrophages or transendothelial transport is unclear. Electron microscopy failed to identify cellular processes of these macrophages extending to the vascular space (William F Hickey, personal communication). In order to resolve this issue, intravenous injection of red fluorescent polystyrene microspheres was used to investigate whether cerebral CD163-positive macrophages are capable of direct uptake of material from the circulation. Rats were injected intravenously with red fluospheres of either 1 $\mu$ m or 0.1 $\mu$ m diameter ( $5 \times 10^8$ /kg and  $5 \times 10^{11}$ /kg respectively) followed by perfusion at 3, 6 and 24 hours (at least n=2 per group). Uptake was seen by macrophages in lung, liver, spleen and lymph nodes but not by CD163-positive macrophages in the brain at any time point. This shows that CD163-positive macrophages are excluded from the blood-brain interface, which is fully constituted by endothelial cells.

## **5.3 Discussion**

Both endothelial cells and CD163-positive macrophages lying at the immune-brain interface have been implicated in immune-to-brain signalling<sup>72,74,82,83</sup>. However this is based on the observation of cyclooxygenase 2 (COX2) upregulation by both cell types after systemic immune challenge and the precise identity of the vascular cell or cells functionally responsible for immune-to-brain signalling has not been resolved. Such

information is essential for the rational design of therapies to antagonize the inflammatory pathway across the BBB. In order to differentiate between the functional contributions of cerebral endothelial cells and CD163-positive macrophages, the latter population was depleted using an ICV infusion of clodronate liposomes. It is shown that several aspects of immune-to-brain signalling, ranging from behavioural to molecular, remained intact after this intervention. Therefore, cerebral CD163-positive macrophages do not contribute significantly and, by exclusion, endothelial cells are the prime mediators of immune-to-brain signalling.

It is interesting that cerebral CD163-positive macrophages have been reported to upregulate COX2 expression during systemic inflammatory challenges in the absence of an endothelial cell response<sup>73,83</sup>. This might be a result of a lower threshold of activation expected of a myeloid cell compared to an endothelial cell in certain situations and might be seen to contradict the findings here. However the physiological relevance of COX2 expression is uncertain since its mere observation does not necessarily translate into effective immune-to-brain signalling function. Moreover recent data suggests that COX2 expression is irrelevant to some aspects of immune-to-brain signalling. For instance, NSAIDs did not prevent *de novo* transcription of cytokines (see Chapter 3) and other pro-inflammatory genes within the CNS<sup>181</sup>, and ibuprofen was not observed to suppress active MS lesions on gadolinium-enhanced magnetic resonance imaging (MRI)<sup>166</sup>.

The expression of CD163 is associated with the alternatively activated phenotype of macrophages which do not secrete the pro-inflammatory cytokines TNF $\alpha$ , IL1 $\beta$  and IL6 but synthesize the anti-inflammatory cytokines IL10 and TGF $\beta$  instead<sup>217</sup>. CD163 is the haptoglobin-haemoglobin receptor<sup>193</sup> and the consequent delivery of haemoglobin to these macrophages is thought to further downregulate classical pro-inflammatory activity by virtue of heme metabolites which have potent anti-inflammatory effects<sup>218</sup>. Moreover exposure to endotoxin results in shedding of soluble CD163<sup>219</sup> which is anti-inflammatory<sup>220</sup>. It is therefore possible that CD163-positive macrophages have an anti-inflammatory role at the BBB which is not detectable by the experimental approaches used here and which is overridden by the endothelial pro-inflammatory response to systemic endotoxin challenge.

There are several reasons why endothelial cells are the prime players of immune-to-brain signalling. It is demonstrated here that endothelial cells are solely responsible for the physical interface of the brain with the circulation. In addition the density of endothelial cells in rat brain is up to 25 fold higher than that of CD163-positive macrophages (personal observation). Therefore any role of these macrophages to immune-to-brain signalling is likely to be dwarfed by the endothelial contribution. It is still possible that cerebral CD163-positive macrophages play a minor role in immune-to-brain signalling which may be compensated for by endothelial cells. However depletion of these macrophages shows that they are not *essential* for immune-to-brain signalling. Therefore manipulation of CD163-positive macrophages at the BBB, as suggested by some<sup>209,221</sup>, loses its attraction as a therapeutic option. Cerebral endothelial cells are also more accessible and various strategies have been developed to target drugs to these cells by making use of their expression of specific molecules, such as peptide and transferrin receptors, involved in receptor-mediated endocytosis<sup>210</sup>.

Activation of cells lying at the immune-brain interface is complemented by other immune-to-brain signalling pathways which can be classified as either humoral or neural<sup>222</sup>. In the humoral route, direct entry of circulating cytokines occurs via a saturable active transport mechanism at the BBB<sup>60</sup>. However it has been suggested that insufficient quantities of cytokines enter the brain following acute intravenous administration to account for CNS responses to acute infection<sup>61,62</sup>. In any case *de novo* transcription of cytokine genes was used to complement other readouts in the experiments described here. The neural route is another potentially important route of immune-to-brain signalling which is mediated by neural connections between individual systemic compartments and the CNS. Areas of the neural axis exposed to peripheral organs or the circulation (e.g. circumventricular organs, vagal and somatic afferents) project to specific areas of the brain (e.g. brainstem, hypothalamus and hippocampus) to induce neuronal and glial activation and behavioural changes<sup>61</sup>. By studying frontoparietal cortex and striatum, these brain regions were avoided in the analysis of cytokine mRNA after systemic endotoxin challenge. Therefore the neural route is unlikely to account for the preservation of immune-to-brain signalling seen after depletion of cerebral CD163-positive macrophages.

The transfer of an inflammatory message across the BBB is important in a range of biological responses to ongoing systemic infection or inflammation in both health and

disease. In otherwise healthy individuals with a systemic infection, immune-to-brain signalling results in a co-ordinated set of responses referred to collectively as “sickness behaviour”. This includes lethargy, anhedonia, anorexia, fever and social withdrawal. It is geared towards protecting the host. However in chronic disease, immune-to-brain signalling becomes disadvantageous. People with chronic systemic inflammatory diseases such as cancer suffer from continuous fatigue, cognitive dysfunction and affective symptoms<sup>223</sup>. When chronic inflammation affects the brain directly, as in MS and AD, systemic infections result in exacerbation of ongoing neuroinflammation<sup>54</sup>. This can occur in the absence of any breakdown in the BBB as detected by gadolinium enhancement on T1-weighted MRI in MS<sup>15,16</sup>. AD is not usually associated with BBB breakdown unless cerebrovascular pathology is present<sup>224,225</sup>.

Therapeutic intervention in these pathological situations necessitates a solid understanding of the key players involved. The inflammatory response of the CNS during systemic infection is delayed, occurs first at the immune-brain interface and is followed by a second inflammatory wave which progressively penetrates the brain parenchyma. This suggests the involvement of a relay mechanism at the immune-brain interface. Several observational studies have identified cerebral CD163-positive macrophages and endothelial cells as being responsible for this signal transduction. In this chapter, interventional evidence was presented showing that the role of cerebral CD163-positive macrophages in immune-to-brain signalling is not essential. By exclusion, the cerebral endothelium is mostly responsible for the inflammatory pathway across the BBB. Further research efforts in modulating immune-to-brain signalling should therefore target this cell.

## 5.4 Materials and methods

### 5.4.1 *Animals*

Adult male Wistar rats, from Harlan (Bicester, UK), weighing 200-300g were used in all experiments. They were housed in cages under a 12h light:12h dark schedule and controlled environmental conditions with pelleted food and water *ad libitum*. The experiments were carried out under Home Office Licence and in accordance with the Animals (Scientific Procedures) Act 1986, UK.

#### **5.4.2 *Reagents***

LPS from *E. coli* 0111:B4 was purchased from Sigma (Poole, UK). The manufacturer's quoted endotoxin activity was 30,000,000 EU/mg (catalogue no L2630 Lot no 110K4060). Red fluorescent polystyrene fluospheres of 0.02 and 1  $\mu$ m diameters (Cat no F8786 and F13083 respectively) from Molecular Probes (Cambridge, UK) were used.

#### **5.4.3 *Telemetry***

A radio-telemetry system (Data Sciences International, Minnesota, USA) was used to remotely monitor core body temperature of rats. Briefly, rats were implanted with sensor capsules intraperitoneally under isoflurane anaesthesia. Oral buprenorphine (0.5mg/kg) was used for postoperative analgesia. Rats were allowed to recover for at least 10 days. Continuous temperature was collected before and during experiments by means of receivers placed under the animals' cages. Fever was quantified by using area-under-the-curve (AUC) analysis of temperature curves. AUC was derived using the formula  $(x_1+x_2+\dots+x_n)/5$  where x were the individual temperature readings taken every 5 minutes and was measured in  $^{\circ}\text{Cmin}$ . The AUC during the experiment was subtracted from the AUC during the same time frame on the preceding day for each rat. This change in AUC was used as a measure of temperature change that respects individual animal temperature baselines.

#### **5.4.4 *Liposomes***

Multilamellar mannosylated liposomes were prepared as described in Chapter 2. The size of the liposomes ranged from 0.2 to 3  $\mu$ m.

#### **5.4.5 *ICV infusions***

Rats were deeply anaesthetized with isoflurane in  $\text{O}_2$  and mounted on a stereotaxic frame. Clodronate or PBS-containing mannosylated liposomes were infused using a Hamilton syringe fitted with a 27G needle. Two protocols were used: 50  $\mu$ l into the 4th ventricle over 25 minutes and 15  $\mu$ l (diluted up to 25  $\mu$ l with PBS) into the right lateral ventricle over 12.5 minutes. The latter protocol was developed after several attempts at alternative protocols.

#### **5.4.6 *Blood and tissue processing***

Rats were subjected to terminal anaesthesia with 20% sodium pentobarbital. Blood was obtained immediately by cardiac puncture, allowed to clot at room temperature for 2 hours, and centrifuged at 4°C for 2 x 10 minutes. Serum was frozen at -70°C till further use. Animals were thoroughly transcardially perfused with 0.9% w/v heparinized saline. For RT-PCR and ELISA, right frontoparietal cortex and striatum (avoiding injection site) were harvested quickly and frozen. Samples for RT-PCR were transferred immediately into RNAlater reagent (Qiagen, West Sussex, UK) before -20°C storage. For immunohistochemistry, rats were perfused with 4% paraformaldehyde or 10% neutral buffered formalin. Brain, liver, spleen, lung and/or cervical lymph nodes were rapidly dissected. For fixed frozen tissue, samples were post-fixed in 4% paraformaldehyde for 4-6 hours and then cryoprotected by immersion in 30% sucrose in 0.1M phosphate buffer at 4°C for *circa* 48 hours. Tissue blocks were embedded in Tissue-Tek OCT compound (Sakura Finetek Europe B.V, Zoeterwoude, NL) and frozen in isopentane on dry ice. Blocks were stored at -20°C until use. For formalin-fixed tissue, samples post-fixed in 10% NBF for about 7 days before dehydration through serial concentrations of alcohol, clearing in Histoclear, and wax-embedding. For histology, coronal sections of 10µm thickness were cut on a cryostat or microtome.

#### **5.4.7 *Immunohistochemistry***

Wax-embedded sections were first dewaxed in xylene and rehydrated through serial concentrations of alcohol. All incubations were carried out at room temperature. If quenching was required, this was done using 0.3% H<sub>2</sub>O<sub>2</sub> in methanol for 20 minutes, followed by a wash in 0.1M phosphate-buffered saline. If antigen retrieval was required for formalin-fixed sections, this was done using a microwave (3 minutes in citrate buffer, cooling for 5 minutes, re-microwave for 3 minutes in citrate buffer). After being washed in 0.1M phosphate-buffered saline, sections were pre-adsorbed with 10% normal serum of the appropriate animal species for 30 minutes and then incubated for 1½h with the primary antibody. Primary antibodies used are listed in Chapter 2. After washing, sections were incubated with biotinylated secondary antibody of the appropriate specificity for 30 minutes, washed again and then incubated with avidin-biotin-peroxidase complex (Vectastain Elite ABC from Vector Laboratories, Burlingame, California) for 30 minutes.

After another wash, the peroxidase was visualized using 0.05% 3,3'-diaminobenzidine as chromogen and 0.05% hydrogen peroxide as substrate. All the sections were counterstained with Cresyl Violet or haematoxylin and dehydrated before mounting in DePeX (BDH Laboratory supplies, Poole, UK). Negative control sections were incubated in the absence of the primary antibody. Normal sera, biotinylated secondary antibodies, and avidin-biotin-peroxidase complex were purchased from Vector Laboratories (Peterborough, UK). Images were captured on a PC using LeicaQwin software (Cambridge, UK).

#### **5.4.8 *Quantification of cells***

This was done manually under light microscopy. The operator was blinded to the identity of the slides counted. Cells were counted using a graticule under a high power objective (x25 or x40) and the density of cells was converted to a value per mm<sup>2</sup>. In all cases, at least 4 sections from the same animal, and several animals from each experimental group (as denoted by number *n*) were analyzed and counts averaged.

#### **5.4.9 *Semi-quantitative RT-PCR***

This was performed as detailed in Chapter 2. Briefly, samples were homogenized using a rotor and Qiashredder columns (Qiagen, Crawley, UK). Total RNA was extracted using RNeasy mini columns (Qiagen) and contaminating DNA degraded with RNase-free DNase 1 (Qiagen), all according to the manufacturer's instructions. RNA yields were determined by spectrophotometry at 260 nm. Taqman semi-quantitative RT-PCR was performed using Applied Biosystems reagents (Warrington, UK) as previously described<sup>191</sup>. Primers and probes were designed using Primer Express software (Applied Biosystems) and crossed an intron-exon boundary. Their sequences are listed in Chapter 2.

#### **5.4.10 *Protein assay and ELISA***

These were performed as detailed in Chapter 2.

#### **5.4.11 *Statistics***

Data was analyzed using SPSS version 14. Normality was assessed by the Kolmogorov-Smirnov test. Non-parametric data was normalized by log transformation. Analysis was done using Student's t-test for two independent samples and one way ANOVA for multiple independent samples. For post-hoc analysis, Bonferroni's method was used since variance was homogenous. The confidence level was 95%. Significant evidence against the null hypothesis was accepted at  $p \leq 0.05$

## **Chapter 6**

### **Mannose receptor expression specifically reveals murine cerebral perivascular macrophages**

John D. Haskins, <sup>1</sup> Daniel J. Gitter, <sup>1</sup> and Michael J. Henklein <sup>2</sup>  
Departments of <sup>1</sup>Neurology and <sup>2</sup>Pathology, University of Michigan Medical School, Ann Arbor, Michigan 48104-0033  
Received June 1, 1993; accepted July 1, 1993  
Address reprint requests to Dr. Michael J. Henklein, Department of Pathology, University of Michigan Medical School, 1500 E. Medical Center Drive, Ann Arbor, MI 48104-0033.  
Copyright © 1994 by the International Society for Experimental Pathology, Inc.  
0885-5716/94/0101-0001\$04.00/0

## **Mannose receptor expression specifically reveals murine cerebral perivascular macrophages**

### **6.1 Introduction**

Cerebral perivascular macrophages (PVMs) are interesting cells by virtue of their location at the blood-brain barrier (BBB). They are situated between the endothelial basement membrane and the glia limitans<sup>226</sup>. They are the only cells in the brain parenchyma which display constitutive phagocytic potential<sup>45</sup> and immunophenotypical markers of activation such as MHC class II, B7, CD40 and FcR<sup>227</sup>. They are the first cells to respond to inflammation within the brain in various experimental settings such as EAE<sup>228</sup>, neuronal damage<sup>229</sup> and intracerebroventricular injection of IFN- $\gamma$  or TNF- $\alpha$ <sup>230</sup>. They also readily respond to peripheral immune activation after systemic lipopolysaccharide administration<sup>69,73,79,83</sup>. Moreover, they have been shown to be capable of effective antigen presentation<sup>197,231</sup>. Thus they are ideally situated to respond to pro-inflammatory stimuli arising from both within the brain and from the periphery.

Cerebral PVMs have mostly been studied in the rat because of the availability of the monoclonal antibody ED2, which recognizes CD163. CD163 is a member of the scavenger receptor Type B family and has several functions: haemoglobin scavenging<sup>193</sup>, cell adhesion<sup>194,195</sup>, and perhaps an anti-inflammatory role<sup>220</sup>. In the rat central nervous system (CNS), ED2 selectively labels perivascular, meningeal and choroid plexus macrophages in both normal and inflamed CNS<sup>196</sup>. Recently a monoclonal antibody (EDHu-1) recognizing human CD163 and thus perivascular macrophages, has become available<sup>193</sup>. Studying cerebral PVM biology in the mouse has been hampered by the lack of availability of such a selective marker. This was essential for further studies on the role of cerebral PVMs in T cell traffic into the brain, which used TCR transgenic mice (see Chapter 7). Although murine CD163 has been cloned<sup>232</sup>, an anti-mouse CD163 antibody is still lacking. The monoclonal antibody 2F8 recognizes the murine scavenger receptor A which is limited to PVMs in the normal brain<sup>87</sup>. However this receptor is expressed by microglia during different forms of injury<sup>233</sup>, making it hard to study cerebral PVMs selectively in pathological conditions.

In order to further characterize the murine cerebral PVMs' expression profile, a number of monoclonal antibodies to mouse macrophage antigens were systematically studied. This was also expected to help in gaining more insight into the function of cerebral PVMs. One of the antibodies studied was the monoclonal antibody 5D3 which recognizes the mannose receptor (MR). The MR is a Type I transmembrane C-type lectin which best recognizes branched mannose-containing carbohydrate structures on both microbial and host proteins<sup>234</sup>. Its extracellular portion includes 8 carbohydrate recognition domains (CRDs) and an N-terminal cysteine-rich domain (CR), which display separate lectin activities. It is expressed by tissue macrophages, hepatic and lymphatic endothelium, glomerular mesangial cells and "perivascular microglia" in the normal brain<sup>235</sup>. Its functions include receptor-mediated endocytosis and phagocytosis, modulation of microbicidal potential, cell adhesion, stimulation of cytokine secretion, targeting of antigen to MHC Class II pathway and antigen trafficking in lymphoid organs<sup>236</sup>.

MR expression was investigated in the normal CNS as well as in several models of pathology. In particular, it was interesting to determine whether the MR was still selectively expressed on cerebral PVMs in these models. The data presented here clearly shows that the MR is exclusively expressed by perivascular macrophages (PVMs), meningeal macrophages (MMs) and choroid plexus macrophages (CPMs) in the normal CNS, as is the case with ED2 in the rat. Moreover its expression remains limited to these macrophages even under conditions of acute and chronic neurodegeneration and following an inflammatory challenge. Mannose receptor expression by macrophages situated at blood-brain (perivascular), brain-CSF (meningeal) and CSF-blood (choroid plexus) interfaces supports a functional role of these cells in responding to external stimuli such as infection.

## 6.2 Results

### 6.2.1 *Control animals*

Sections from the brains of three naïve C57BL/6J mice and from the intact contralateral optic nerves of mice with a right ONC were incubated with the anti-MR antibody. Three populations of macrophages were clearly stained: PVMs, meningeal macrophages (MMs) and choroid plexus macrophages (CPMs), reminiscent of ED2 staining in the rat (**Figure**

**6.1a,c).** PVMs were seen exclusively around vessels and located abluminal to endothelial cells and separate from the surrounding brain parenchyma. Double immunofluorescence showed MR-positive cells sandwiched between the  $\gamma$ 1-laminin-chain-positive endothelial and glial basement membranes (**Figure 6.2**). The cells had stout cell bodies and bore elongated flattened processes which both encircled and ran longitudinally along the vessels. They were particularly noticeable at bifurcations/trifurcations. Few cells in the white matter tracts such as the corpus callosum and the normal optic nerve were revealed by the anti-MR antibody.

Perivascular and meningeal macrophages, which were considered to express the MR in the above experiment, are known to be the only constitutively phagocytic cells in the normal CNS<sup>45</sup>. Indeed, this is in keeping with MR expression since one of the MR's described functions is receptor-mediated endocytosis<sup>236</sup>. Moreover, the MR-positive cells were located at sites (perivascular spaces and meninges) which are readily accessible to intracerebroventricularly injected substances. This is reminiscent of ED2-positive macrophages in the rat brain, which have been shown to be selectively depleted after intracerebroventricular injection of clodronate-loaded liposomes<sup>163</sup>. Liposomes are phagocytosed and intracellular accumulation of clodronate is toxic by forming a non-hydrolyzable analogue of ATP<sup>161</sup> and triggering apoptosis<sup>162</sup>. Clodronate-loaded liposomes were therefore injected intracerebroventricularly in control mice to interrogate the function of MR-positive cells and verify their identity as PVMs. In these mice, no mannose receptor could be detected in perivascular spaces after immunohistochemistry with the 5D3 monoclonal antibody (**Figure 6.1**). Sections of brains from naïve or PBS-containing liposome injected mice revealed MR positivity during the same immunohistochemistry experiment. This showed that the MR expressing cells were constitutively phagocytic, which confirms their identity as PVMs.

Meningeal macrophages were also depleted (**Figure 6.1**), though not completely. This is in sharp contrast with the rat, where complete depletion of meningeal macrophages is achievable with 5-fold lower doses (on a per brain weight basis) of intracerebroventricular clodronate-loaded liposomes<sup>163</sup>. This might be due to a smaller subarachnoid space in the mouse and thus a more restricted flow of CSF over the brain surface, effecting liposomal delivery to the meninges. Alternatively it could mean that the mannose receptor is expressed by other cells in the meninges besides macrophages.

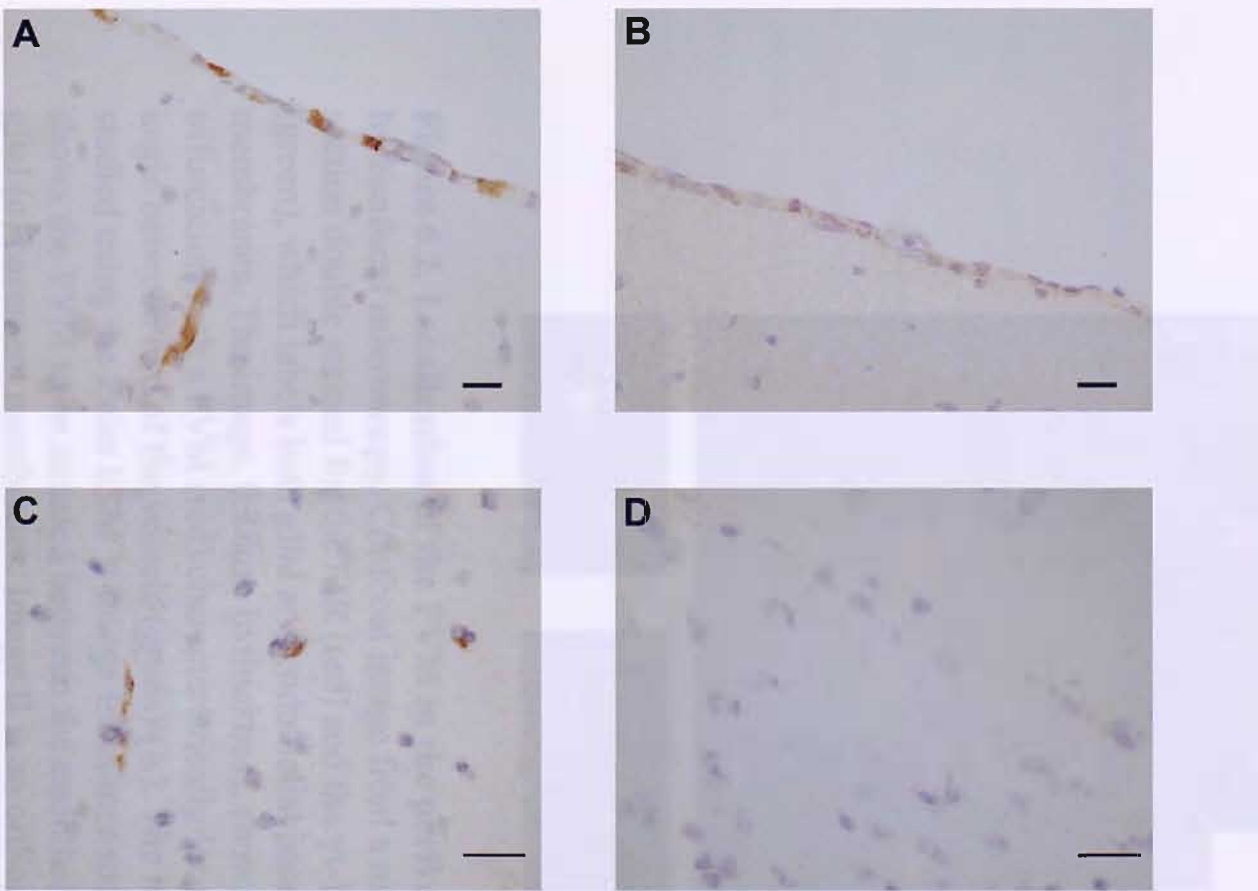


**Figure 6.1. Mannose receptor expression in naïve brain.** Representative brain sections from mice injected intracerebroventricularly with PBS-loaded (A,C) or clodronate-loaded liposomes (B,D), showing complete depletion of meningeal (B) and perivascular (D) macrophages. The sections were stained with the anti-mannose receptor antibody 5D3 and counterstained with haematoxylin. (A) and (B) show the meninges overlying the cortex; (C) and (D) show the cerebral parenchyma. Scale bar = 0.02mm.

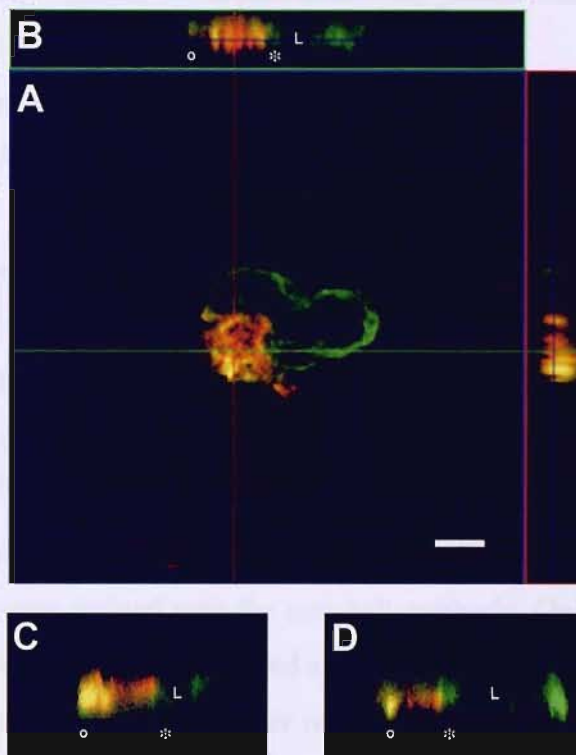


**Figure 6.2. Localization of the PVM in the perivascular space by confocal microscopy.** Confocal image from a naïve brain section double stained for the MR (red) and the  $\gamma 1$ -laminin chain (green), which labels both glial and endothelial basement membranes. The image, 0.28 $\mu$ m in thickness, shows a vessel trifurcation with a PVM (red) characteristically located in the angle between two of the vessels (green) (A). The image was studied using the Zeiss LSM V Image Examiner software, which shows the PVM to be situated between the endothelial (\*) and glial (o) basement membranes. Image B is an orthogonal view of the PVM in image A, taken at the level of the green line. Images C-D are two other examples. Yellow colour represents areas of adhesion between the PVM and adjacent basement membrane. L = lumen. Scale bar = 0.05mm.

Choroid plexus macrophages were the least affected by the intracerebroventricular injection, similar to the rat (see Chapter 4). This is because tight junctions are expressed in the cuboidal epithelium of the choroid plexus<sup>50</sup>. This impedes the access of intracerebroventricularly injected liposomes to choroid plexus macrophages.

The immunohistochemistry protocol used in this study revealed the MR equally well in C57BL/6J and BALB/c mice.

### **6.2.2 *Acute inflammatory model***

To model an acute inflammatory injury without cell death, an intracerebral injection of 2 $\mu$ g of lipopolysaccharide (LPS) was made into the right dorsal hippocampus of 3 mice, as described previously<sup>237</sup>. The animals were sacrificed 24 hours later. At this time point, neutrophil margination to cerebral endothelium and microglial activation is observed in the brain<sup>237</sup>. The sections were stained with the anti-MR antibody. Only the PVMs were revealed by the antibody, in both the injected and uninjected hemispheres (**Figure 6.3a**). While widespread upregulation of scavenger receptor, CD68, CR3 and MHC Class II on microglia occurs in this model<sup>233</sup>, MR expression was confined to PVMs, MMs and CPMs; it was not upregulated on microglia or other cells.

### **6.2.3 *Excitotoxic model***

Acute cerebral inflammation associated with neuronal death was modelled by intracerebral injection of the excitotoxin kainic acid (1nM) in the right dorsal hippocampus. Mice were sacrificed 3 days later. Little or no neutrophil recruitment is usually observed in these pathological conditions whereas microglia are activated<sup>238</sup>. The MR antibody still selectively and exclusively labelled PVMs around the blood vessels (**Figure 6.3b**), MMs and CPMs, with more PVMs in the ipsilateral side compared to the contralateral one. There was no detectable microglial expression of the MR, although it is known that microglia express scavenger receptor, CD68, CR3, and MHC Class II in this model<sup>233,238</sup>.

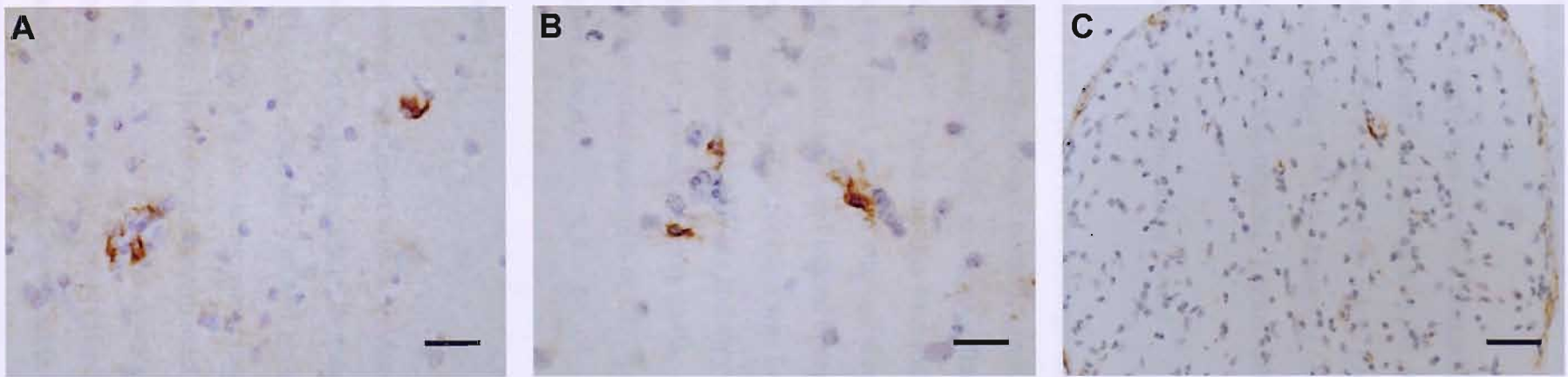


**Figure 6.3. Perivascular macrophages in different pathologies.** Mice received intrahippocampal injections of LPS (A) or kainic acid (B) or an optic nerve crush (C), and were perfused after 1, 3 and 7 days respectively. Representative sections stained with the anti-mannose receptor antibody 5D3 and counterstained with haematoxylin are shown. MR expression remains restricted to the perivascular and meningeal compartments in these different pathologies. Scale bars: A,B = 0.02mm; C = 0.04mm.

#### 6.2.4 *Wallerian degeneration model*

The mouse right optic nerve was crushed intraorbitally. The animals were killed at 7 and 28 days. It has been shown that microglia in the degenerating distal optic nerve segment in this model are activated as evidenced by F4/80 glycoprotein and CD68 expression, reaching a maximum at day 7<sup>165</sup>. However the MR antibody still only revealed PVMs and MMs; the former were few in number (**Figure 6.3c**).

#### 6.2.5 *Chronic neurodegeneration model*

Bilateral injection of ME7 prion brain homogenate was performed in the mouse dorsal hippocampus. This induces chronic neurodegeneration accompanied by an atypical inflammation which contrasts with the acute inflammation accompanying the above-mentioned two models<sup>239</sup>. Three animals were killed during the late stage of the disease, at 21 weeks. At this time point, marked microglial and astrocytic activation as well as T cell infiltration has been described<sup>240</sup> and indeed upregulation of CR3 and CD68 was seen (**Figure 6.4c**). Once again, MR expression was limited to PVMs (**Figure 6.4a,b**), MMs and CPMs: it was upregulated on PVMs and they appeared to be more numerous compared to naïve mice. The strict perivascular distribution of the MR was incompatible with expression by CD68-positive microglia or CD3-positive T cells which were found in the parenchyma (**Figure 6.4c,d**).

### 6.3 Discussion

The results above are in agreement with a previous study showing restricted perivascular expression of the MR in the healthy adult CNS using immunohistochemistry and *in situ* hybridization<sup>235</sup>. The only other study of MR expression in the brain<sup>241</sup> found a more diverse expression of the MR including astrocytes and neurons using immunohistochemistry. However this group used a different antibody (a rabbit polyclonal antibody raised against a 22-mer from the cytoplasmic domain of MR) while 5D3, used in this study, is a mouse monoclonal antibody raised against a much larger fragment of the MR, spanning carbohydrate recognition domains 4-7<sup>242</sup>. The antibody 5D3 has been thoroughly characterized using immunocytochemistry, immunoprecipitation, Western blot, enzyme-linked immunosorbent assay and fluorescence-activated cell sorting<sup>242,243</sup>.

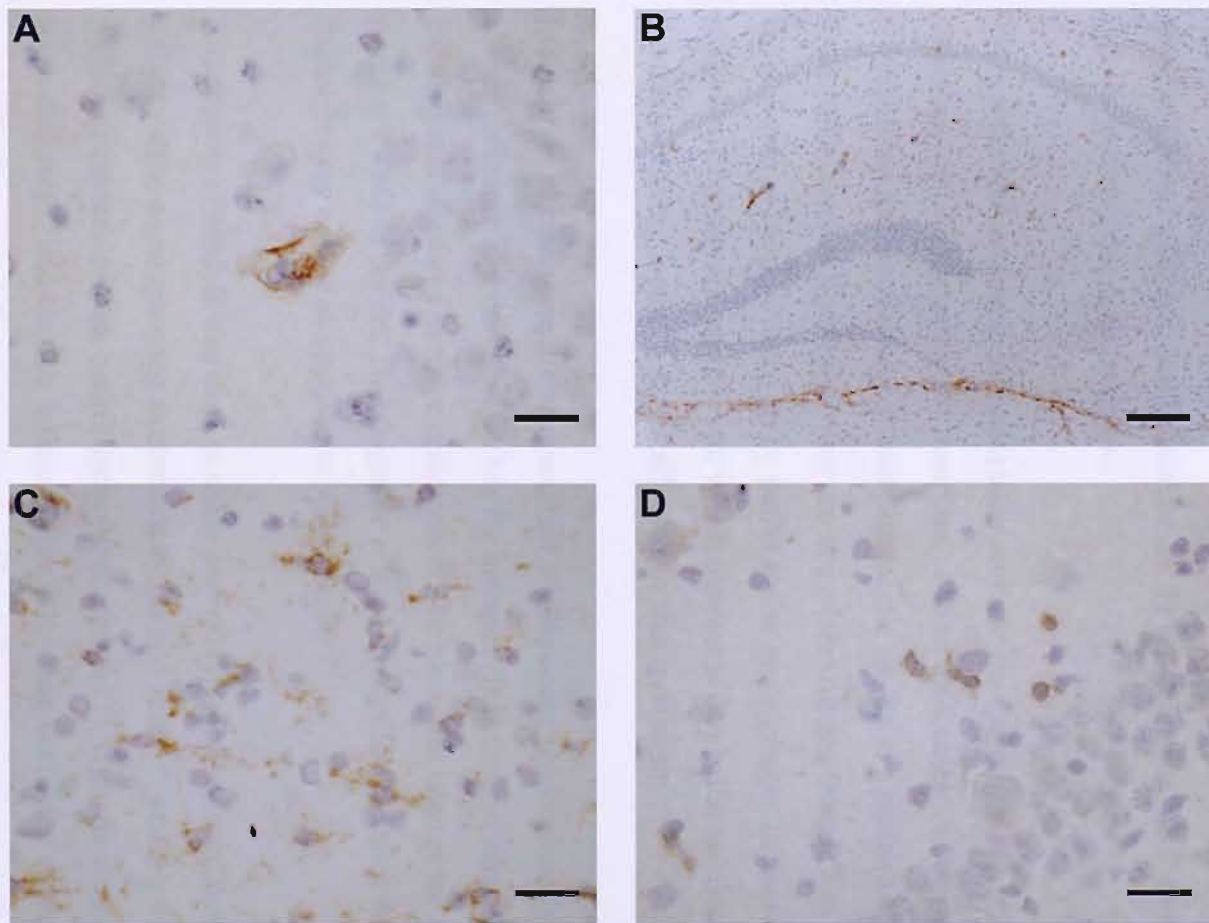


**Figure 6.4. Perivascular macrophages in chronic neurodegenerative disease.** Representative brain sections at the level of the dorsal hippocampus from mice injected with ME7 prion. They were stained with the anti-mannose receptor antibody 5D3 (A,B), the anti-CD68 antibody FA11 (C) and the anti-CD3 antibody KT3 (D). The slides were counter-stained with haematoxylin. MR expression has a strict perivascular distribution (A,B) incompatible with expression by microglia (C) and T cells (D) which are situated in the parenchyma proper. Scale bars: A, C, D = 0.02mm; B = 0.1mm.

The phagocytic capacity of MR-positive cells in the brain was explored by injecting clodronate-loaded liposomes intracerebroventricularly – these are lethal to cells which ingest them. It is shown that MR-positive cells possess constitutive phagocytic potential since they were depleted. This also confirms their perivascular location since the intraventricularly injected liposomes could reach these cells. Their precise location within the perivascular space was established using confocal microscopy – they lie between the endothelial and glial basement membranes. This establishes the identity of the MR-positive cells as perivascular macrophages.

The liposomes used were mannosylated and one may argue that they would therefore target any cell which expresses mannose-binding molecules, including the MR. However it is quite clear that constitutive robust phagocytic ability is a prerequisite for ingestion of these multilamellar liposomes: they are large (size ranges from 0.2 to 3 $\mu$ m), they have been shown to be only taken up by perivascular macrophages in the rat<sup>163</sup>, and the non-phagocytic ependymal epithelium, which expresses cerebellar soluble lectin (CSL), a mannose-binding lectin<sup>204</sup>, is not affected by this treatment.

In the brain parenchyma it was noted that PVMs occur predominantly in grey matter: the corpus callosum had very few PVMs for instance. It is thus no surprise that little MR staining was observed in naïve optic nerve. The same has been noted with regard to ED2-positive PVMs in the rat. This might be related to capillary density which is *circa* 4-fold higher in grey matter as opposed to white matter<sup>244</sup>.

A spectrum of models was used to study several types of brain inflammation: acute inflammation accompanying excitotoxicity (kainic acid)<sup>238</sup>, acute inflammation associated with the presence of endotoxin (lipopolysaccharide)<sup>237</sup>, chronic neurodegeneration (ME7 prion disease)<sup>240</sup> and chronic inflammation following Wallerian degeneration (optic nerve crush)<sup>165</sup>. These models are characterized by different cytokine profiles<sup>59,245,246</sup> yet this was not reflected in the distribution of MR expression. In all models, MR expression was restricted to PVMs (as well as meningeal and choroid plexus macrophages), with no staining of either microglia or infiltrating haematogenous leucocytes in the parenchyma. Thus the identification of the MR as a PVM marker supports the notion that PVMs do not migrate into the parenchyma during inflammation, an issue which has been brought into question previously<sup>247</sup>. The possibility still remains that they migrate but lose MR

expression. Also, the availability of such a marker in the mouse which retains its selectivity during brain pathology provides the opportunity to study this macrophage population in a species which is more amenable to genetic manipulation.

The mannose receptor has various functions which are of interest with regard to its expression by cerebral PVMs. The first is the recognition of various microbial ligands (from *Mycobacterium tuberculosis*, *Candida albicans*, *Pneumocystis carinii*, *Klebsiella pneumoniae*, *Streptococcus pneumoniae*) resulting in their receptor-mediated phagocytosis and enhanced microbicidal activity<sup>234</sup>. Interestingly most of these pathogens are known to infect the CNS. Perivascular and meningeal macrophages, with the MR as a member of their broad armamentarium, are ideally situated to prevent infectious organisms from gaining access to the brain parenchyma. Indeed their depletion using liposomes resulted in a worsening of disease in a *Streptococcus pneumoniae* model of meningitis in the rat<sup>49</sup>.

The second identified function of the MR is recognition and clearance of endogenous ligands, of which several have been identified<sup>248</sup>. One of these is tissue plasminogen activator (tPA): the MR serves in its clearance by receptor-mediated endocytosis<sup>249</sup>. This function would be expected to be protective in acute inflammation accompanying excitotoxicity or focal ischaemia, since tPA is a key player in tissue destruction in this setting via activation of plasmin<sup>250,251</sup>.

The third role of the MR is adhesion. Binding between the MR on lymphatic endothelium and L-selectin on T cells was found to be important in the adherence of T cells to the endothelium<sup>252</sup>. The MR is not expressed on circulating rodent monocytes, so it must be expressed once the monocyte enters the perivascular space. It is tempting to suggest that it is important in tethering cerebral PVMs in the perivascular space. Interestingly brain microvessels display binding sites for the carbohydrate recognition domains 4-7 on the extracellular portion of the MR<sup>253</sup>. The MR knockout mouse should help in identifying any such role in adhesion<sup>254</sup>.

A fourth hypothesized role of the MR is antigen transport. Ligand binding sites for the cysteine-rich domain of the MR have been detected in developing germinal centres in spleen and have been followed on dendritic-like cells migrating from the subcapsular area of lymph nodes into follicular areas<sup>255</sup>. It has thus been suggested that the MR directs

antigen (bound by the carbohydrate recognition domains) towards sites of developing clonal immune responses (by the cysteine-rich domain). It would be interesting to see whether such migration is seen in cervical lymph nodes following brain inflammation. A fully functional soluble form of MR is generated by shedding of cellular MR by metalloprotease activity<sup>256</sup> and a similar antigen transport potential has been suggested for soluble MR. Such a scenario is possible during CNS inflammation since interstitial fluid from the perivascular space is known to drain directly into nasal lymphatics and thus cervical lymph nodes through channels in the cribriform plate<sup>257</sup>.

CD163, a member of the scavenger receptor Type B superfamily, is a selective PVM marker in rat<sup>196</sup> and human CNS<sup>258</sup>. Several similarities in function between CD163 and the MR are thus apparent. CD163 is similarly restricted to the perivascular macrophage in both normal and diseased brain parenchyma, plays a role in cell adhesion<sup>194,195</sup> and is shed from the cell surface in a soluble form by metalloprotease activity<sup>219</sup>.

In summary, the experiments described in this chapter show that murine cerebral PVMs express the mannose receptor, which is involved in receptor-mediated phagocytosis, and that they are constitutively phagocytic. The mannose receptor is also expressed by MMs and CPMs, but not by microglia. Mannose receptor expression by macrophages located at the immune-brain interface supports a functional role of these cells in immunosurveillance of the brain's external environment. Moreover, mannose receptor expression remains restricted to these subsets of macrophages in various models of brain pathology. The identification of the mannose receptor as a specific marker of murine cerebral PVMs, as well as the optimization of the clodronate liposome technique for depletion of PVMs in mice, were essential for further studies of the role of these macrophages in T cell traffic into the brain, which is the topic of the next Chapter.

## 6.4 Materials and methods

### 6.4.1 *Animals*

Female C57BL/6J mice, obtained from Harlan (Bicester, UK), were 4-6 weeks old on arrival and were group-housed under a 12h light:12h dark schedule. Mice were maintained under controlled environmental conditions with pelleted food and water *ad libitum*. The

experiments were carried out under Home Office Licence and in accordance with the Animals (Scientific Procedures) Act, 1986.

#### **6.4.2 *Preparation of multilamellar liposomes***

Multilamellar mannosylated liposomes were prepared as described in Chapter 2. The size of the liposomes ranged from 0.2 to 3 $\mu$ m.

#### **6.4.3 *Intraventricular liposome infusion***

Mice were deeply anaesthetized with isoflurane in O<sub>2</sub> and mounted on a stereotaxic frame. In a first experiment the published protocol for cerebral PVM depletion in the rat<sup>163</sup> was adapted to the mouse on a per brain weight basis. Thus 8 $\mu$ l of clodronate or PBS-containing mannosylated liposomes were infused into the 4<sup>th</sup> ventricle of 4 mice over 25 minutes using a Hamilton syringe fitted with a 27G needle. This preliminary study resulted in suboptimal depletion despite correct localization of the injection being confirmed by serial sectioning of the brain around the injection site. The protocol was therefore modified. The liposome dose was doubled and injections were made rostrally in the lateral ventricles in order to facilitate access of the liposomes to the whole brain parenchyma. Thus, in a second experiment, 8 $\mu$ l of clodronate or PBS-containing mannosylated liposomes were infused into *each* lateral ventricle of 3 mice slowly over 12.5 minutes using a pulled glass capillary (co-ordinates: -0.22mm, lateral 1mm and depth 2mm). On each side, the capillary was left *in situ* for 2.5 minutes, withdrawn partially and left for a further 2.5 minutes before being removed completely, to avoid reflux of liposomes along the injection tract. The operated mice were sacrificed 5 days later.

#### **6.4.4 *Controls***

Three naïve mice were used as controls for the brain pathology models, except in the case of the Wallerian degeneration model, where the contralateral left unoperated optic nerve was used as control.

#### 6.4.5 *Brain pathology models*

Experiments were carried out as described previously<sup>165,237,238,240</sup>. All surgery was performed on animals anaesthetized with Avertin (2,2,2-tribromoethanol in tertiary amyl alcohol) at a dose of 0.1ml/5g body weight. With the exception of the Wallerian degeneration model, all the mice were injected stereotactically in the dorsal hippocampus (co-ordinates: bregma -1.94mm, lateral 1.5mm and depth -1.37mm). A pulled glass micropipette was used for LPS and kainic acid injection, and a Hamilton syringe with a blunt 26S needle for the ME7 prion brain homogenate injection. For all animal models, the mice were allowed to recover under a warm lamp and then housed in IVC racks (Techniplast UK, Kettering, UK) following surgery. All the mice were sacrificed by deep anaesthesia with 20% sodium pentobarbital (Sagatal, Rhone Merieux Ltd., Harlow, Essex, UK).

**Acute inflammatory model.** Three animals were injected with 1µl of LPS (2µg/µl) (*Salmonella abortus equi*, Lot No 69F4003, Sigma Chemicals, Poole, UK) in the right dorsal hippocampus and sacrificed 24h later<sup>237</sup>.

**Acute neurodegeneration model.** Three mice were injected with 1µl of KA (1nM) (Sigma Chemicals, Poole, UK) in the right dorsal hippocampus and sacrificed three days later<sup>238</sup>.

**Chronic neurodegeneration model.** Mice were bilaterally injected in the dorsal hippocampus with 1µl of ME7 prion brain homogenate using a Hamilton syringe fitted with a blunt 26S needle<sup>240</sup>. The syringe was left *in situ* for an additional 1 minute to prevent reflux along the injection tract. The ME7 prion brain homogenate was derived from the brains of C57BL/6J mice at 22 weeks old post-inoculation showing clinical signs of disease (10% w/v in sterile PBS). Mice were sacrificed at the terminal stage of the disease (21 weeks, n=3).

**Wallerian degeneration model.** The mouse right optic nerve was crushed intraorbitally under an operating microscope with jeweller forceps for 10 seconds (ONC)<sup>165</sup>. Mice were killed at 7 and 28 days after the injury (n=3 at each time point).

#### **6.4.6 *Tissue processing and immunohistochemistry***

Animals were transcardially perfused with 0.9% w/v heparinized saline under terminal anaesthesia with 20% sodium pentobarbital. Brain tissue was rapidly dissected, frozen in Tissue-Tek OCT embedding compound (Sakura Finetek Europe B.V, Zoeterwoude, NL) and stored at -20°C until use. Coronal sections of 10µm thickness were cut on a cryostat, dried, fixed in absolute alcohol for 10 minutes at 4°C and processed for indirect immunohistochemistry. All incubations were carried out at room temperature. The sections were first pre-adsorbed with 10% normal rabbit serum for 30 minutes and then incubated for 2 hours with rat monoclonal anti-mouse antibodies against the following antigens: mannose receptor (clone 5D3), CD68 (clone FA11), CD11b (clone 5C6), CD204 (clone 2F8), CD3 (clone KT3) or MHC Class II (clone TIB120). After washing in 0.1M phosphate-buffered saline, sections were incubated with biotinylated rabbit anti-rat IgG secondary antibody for 30 minutes, washed again and then incubated with avidin-biotin-peroxidase complex (Vectastain Elite ABC) for 30 minutes. After another wash, the peroxidase was visualized using 0.05% 3,3'-diaminobenzidine (DAB) as chromogen and 0.05% hydrogen peroxide as substrate. All the sections were counterstained with haematoxylin and dehydrated before mounting in DePeX (BDH Laboratory supplies, Poole, UK). Negative control sections were incubated in the absence of the primary antibody. Normal rabbit serum, biotinylated secondary antibody, and avidin-biotin-peroxidase complex were purchased from Vector Laboratories (Peterborough, UK). The antibodies from clones 5D3, 2F8, 5C6 and TIB120 were kindly provided by Professor S Gordon (Sir William Dunn School of Pathology, Oxford, UK); FA11 and KT3 was purchased from Serotec Ltd (Kidlington, UK). The immunohistochemistry protocol for the anti-MR antibody (5D3) was also investigated on brains fixed in 10% neutral buffered formalin, Bouin's solution, 4% paraformaldehyde and periodate-lysine-paraformaldehyde (PLP). Positive staining was achieved on formalin-fixed sections only if pepsin (pepsin 0.04% in 0.1M HCl, 10 minutes) or microwave (3 minutes in citrate buffer, cooling for 5 minutes, re-microwave for 3 minutes in citrate buffer) antigen retrieval steps were included, the former giving the better results. No positive staining was seen in Bouin's solution, 4% paraformaldehyde or PLP-fixed tissue.

For double immunofluorescence, brain sections were first blocked with 10% rabbit serum and then incubated overnight with mannose receptor antibody (1:50) followed by

biotinylated rabbit anti-rat IgG for 45 minute and streptavidin-conjugated AF546 (Molecular Probes, Cambridge Bioscience, Cambridge, UK) for 30 minutes. During the second round, sections were blocked with 10% goat serum, incubated with a rat monoclonal antibody against the  $\gamma 1$  chain of mouse laminin (Neomarkers, Freemont, CA, USA) (1:250) for 90 minutes, followed by AF488-conjugated goat anti-rat IgG (Molecular Probes) for 30 minutes. Sections were mounted in Mowiol (Harlow Chemical, Harlow, UK) and visualized with a LSM 510 Meta confocal laser scanning microscope (Carl Zeiss Ltd, Germany). Images were examined with the Zeiss LSM 5 Image Examiner software.

## **Chapter 7**

# **The role of cerebral endothelial cells and perivascular macrophages in antigen-specific CD8 T cell traffic into the brain**

CD8 T cells are a major component of the adaptive immune response to viral infections of the central nervous system (CNS). In the mouse, CD8 T cells are recruited to the CNS in response to viral infection via the blood-brain barrier (BBB). The BBB is formed by a layer of endothelial cells that line the blood vessels in the CNS. These endothelial cells express a variety of molecules that regulate the entry of immune cells into the CNS. One of these molecules is the chemokine receptor CX3CR1, which is expressed on the surface of CD8 T cells. CX3CR1 is a receptor for the chemokine CX3CL1, which is produced by perivascular macrophages in the CNS. Perivascular macrophages are a type of immune cell that is found in the perivascular space, which is the area around blood vessels in the CNS. They are a source of CX3CL1, which can bind to CX3CR1 on CD8 T cells and promote their entry into the CNS. This process is known as "chemotaxis".

## **The role of cerebral endothelial cells and perivascular macrophages in antigen-specific CD8 T cell traffic into the brain**

### **7.1 Introduction**

The traffic of leucocytes into the central nervous system (CNS) is a highly regulated process. This protects the brain against the full ravages of the systemic inflammatory response which would otherwise compromise the delicate homeostasis required for neural activity. T cells, which initiate the adaptive immune response, traffic into the brain at a relatively low level compared to other organs<sup>259</sup>. This is partly due to the functional characteristics of the blood-brain barrier (BBB) which call for more stringent requirements for T cell entry into the brain. For instance the vast majority of brain-infiltrating T cells are of the memory or activated phenotype<sup>260</sup>. The question of whether antigen specificity is a prerequisite for T cell traffic into the brain has been previously addressed. Several investigators have transferred activated T cells reactive against neural and irrelevant antigens into naïve animals and observed that both infiltrated the brain equally well<sup>138-143</sup>. However all these studies concentrated on CD4 T cells; although CD8 T cells were present amongst the transferred cells in some experiments<sup>138,139</sup>, no attempt was made to elucidate whether the antigen specificity of the CD8 T cells was influencing their infiltration into the brain.

There is reason to suspect that traffic of CD8 T cells recognizing antigens within the brain is favoured over that of irrelevant CD8 T cells. In mice immunized with the myelin oligodendrocyte glycoprotein peptide MOG 35-55, which develop experimental autoimmune encephalomyelitis (EAE), 56% of brain-infiltrating CD8 T cells on day 10 were MOG-specific<sup>144</sup>. In humans with multiple sclerosis, oligoclonal dominance of T cells in CSF<sup>145</sup> and brain parenchyma<sup>146</sup> are seen more commonly with CD8 than CD4 T cells. Although this has been interpreted as oligoclonal expansion within the CNS compartment, antigen-specific CD8 T cell infiltration could also contribute since the CD8 T cell clones were present in blood.

CD8 T cells are instrumental in the body's response to viral encephalitides and brain tumours. However they are also responsible for various inflammatory neurological

conditions such as multiple sclerosis, HTLV-associated myelopathy and a number of neurological paraneoplastic syndromes<sup>102</sup>. The crucial role of CD8 T cells in multiple sclerosis has only recently been recognized<sup>147</sup>. That CD8 T cells initiate disease was shown when adoptive transfer of CD8 T cells specific for neural antigens (myelin associated glycoprotein and myelin oligodendrocyte glycoprotein) resulted in severe EAE<sup>148,149</sup>. However CD8 T cells are also important in disease maintenance since they correlated with axon injury in MS plaques<sup>153</sup> and MRI features of tissue destruction<sup>154</sup>. CD8 T cell-mediated neuropathology may be mediated directly by encephalitogenic CD8 T cells<sup>155</sup> or may occur indirectly as a result of bystander damage by co-infiltrating CD8 T cells with irrelevant antigen specificities<sup>156,157</sup>. However the overall contribution of bystander damage has been shown to be small<sup>158,159</sup>. The factors governing antigen-specific infiltration of CD8 T cells into the brain are therefore important in both disease induction and maintenance.

In order to study antigen-specific CD8 T cell traffic into the brain, antigen was injected into the striatum of CL4 transgenic mice in which more than 95% of CD8 T cells express the V $\alpha$ 10 V $\beta$ 8.2 T cell receptor (TCR)<sup>160</sup>. It is shown that CD8 T cell infiltration only occurred when the cognate antigen was present within the brain parenchyma. This shows that a mechanism capable of favouring antigen-specific CD8 T cell infiltration exists. In order to elucidate the origin of this antigen specificity, the brain was depleted of perivascular macrophages (PVMs) which are considered to be the foremost antigen-presenting cells at the BBB, but this had no significant effect on CD8 T cell infiltration. It was found that MHC Class I expression by cerebral endothelium was luminal and when blocked, resulted in a marked reduction of CD8 T cell infiltration.

## 7.2 Results

### 7.2.1 *Antigen-specific CD8 T cell traffic into the brain*

In CL4 mice, CD8 T cells exhibit high avidity for the HA512-520 peptide (HA), which is K<sub>d</sub>-restricted<sup>261</sup>. To investigate CD8 T cell traffic, antigen was injected in the right striatum of CL4 mice. A small injectate volume (0.5 $\mu$ l) was delivered with a sterile finely drawn glass micropipette, the tip of which measures 2-10 $\mu$ m in diameter, in order to minimize tissue trauma and reflux into the periphery. Mice were sacrificed on days 1, 3, 5 and 7

post-injection (p.i.) (minimum n=3 per time point). Since virtually all CD8 T cells in this mouse express the transgenic TCR, CD8 immunohistochemistry was used to track infiltration of antigen-specific CD8 T cells into the brain parenchyma. Serial section immunohistochemistry had shown that all CD8-positive cells were CD3-positive.

Intrastratal injection of HA resulted in a focal CD8 T cell infiltrate, which was strictly limited to the area of antigen deposition (*circa* 7.5mm<sup>2</sup>) as shown by a co-injected inert blue dye (**Figure 7.1a**). This T cell infiltrate peaked at day 3, reaching a density of 88 cells/mm<sup>2</sup>, and had nearly disappeared by day 7 (**Figure 7.1b**). No CD8 T cells were seen in the contralateral hemisphere. Moreover, CD8 T cell infiltration did not occur at any time point after control intrastratal injections of a K<sup>d</sup>-restricted non-cognate antigen, Cw3 peptide (**Figure 7.1c**). This showed that CD8 T cells were accumulating at the site of injection as a result of the presence of antigen.

The CD8 T cell infiltrate observed was not a peculiarity of the CL4 transgenic mouse. Using a different approach in a non-transgenic animal, 3 million *in vitro* activated CL4 Thy1.1-positive CD8 T cells were transferred into Thy1.2-positive wild-type BALB/c recipients at the time of intrastratal HA injection (n=3). These mice were perfused after 1 or 3 days. As expected, CD8 T cells were observed in the right striatum of HA-injected animals. The vast majority of infiltrating CD8 T cells (>95%) were Thy1.1-positive (**Figure 7.2a-c**), indicating that they were donor HA-specific CD8 T cells. No T cells were seen infiltrating the brains of wild-type BALB/c mice at either 1 or 3 days after receiving Cw3 in the right striatum and 3 or 30 million *in vitro* activated CL4 CD8 T cells intravenously (n=3 each dose) (**Figure 7.2d,e**).

The marked difference in CD8 T cell infiltration between the HA and Cw3 injections in CL4 mice suggested that CD8 T cells were sensitive to the local presence of their cognate antigen in the CNS. HA is a soluble peptide and is likely to “leak” to the periphery<sup>262</sup>. One possibility was that CD8 T cells were migrating into the striatum in a non-antigen specific way at the site of intracerebral injection after being activated in the periphery by the leaking HA. In order to investigate this possibility HA was injected into one hemisphere and Cw3 into the contralateral hemisphere of CL4 mice and they were sacrificed on day 3 p.i. (n=3). If peripherally activated transgenic T cells were migrating non-specifically to the site of injection, CD8 T cells would have been expected to infiltrate the Cw3-injected

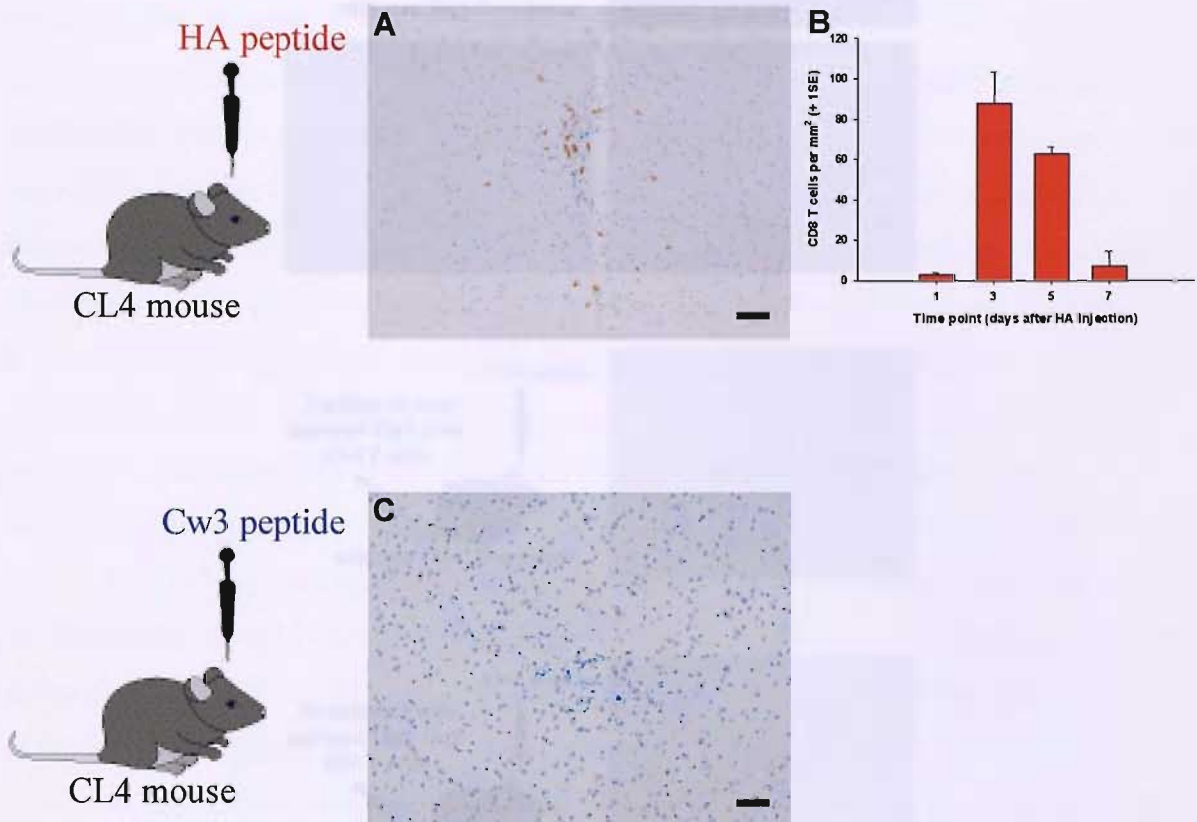


**Figure 7.1. An antigen-specific model of CD8 T cell infiltration into the brain.** HA peptide (cognate antigen) (A,B) or Cw3 peptide (irrelevant antigen) (C) were injected in the right striatum of CL4 transgenic mice. A blue inert tracer was used to localize the injection site. They were perfused on days 1, 3, 5 and 7 (day 3 shown). Brains were processed for CD8 immunohistochemistry using DAB (brown) as chromogen. The kinetics of CD8 T cell recruitment after HA injection are shown in B (n=3 per time point). No CD8 T cells were seen after Cw3 injection. Scale bar = 0.05mm.

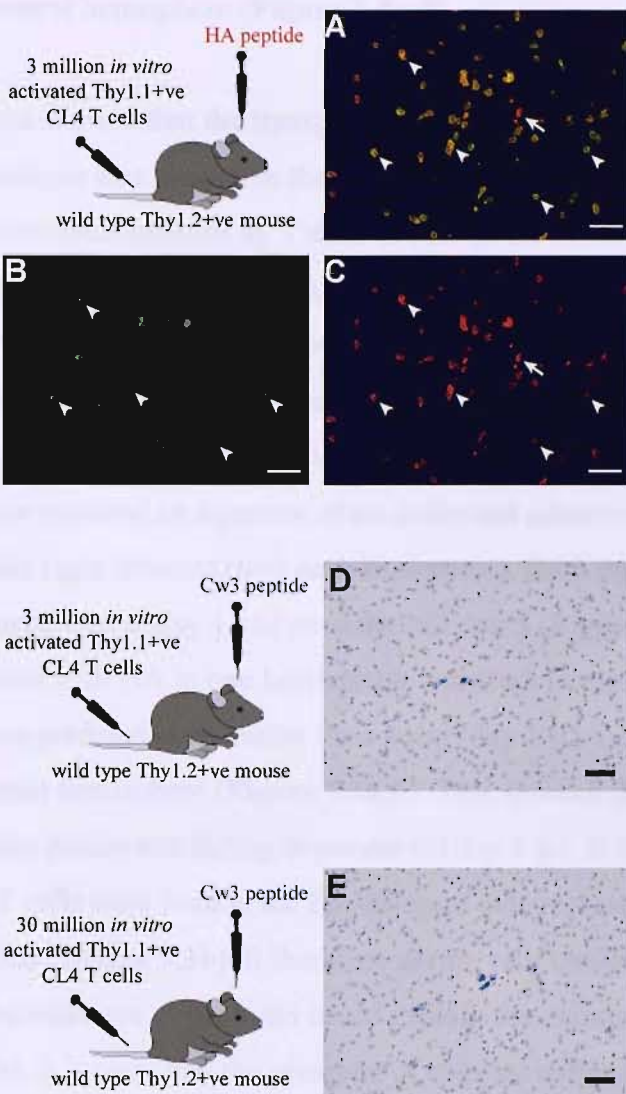


**Figure 7.2. Antigen-specific CD8 T cell infiltration in non-transgenic mice** was studied using double immunofluorescence. Three million *in vitro* activated CL4 Thy1.1-positive CD8 T cells were injected i.v. in Thy1.2+ve wild-type BALB/c mice at the time of right intrastriatal HA peptide injection. The vast majority (>95%) of infiltrating CD8 T cells (red) on day 3 were Thy1.1+ve (green) indicating that they were antigen-specific and of donor origin (white arrowheads in A-C). A few recipient CD8 T cells were seen coinfiltrating the striatum (white arrows in A-C). No CD8 T cells were seen infiltrating the brain when 3 million (D) or 30 million (E) *in vitro* activated CL4 CD8 T cells were injected i.v. in wild-type BALB/c mice at the time of right intrastriatal Cw3 peptide injection (day 3 shown). A blue inert tracer was used to localize the injection site. Scale bar = 0.05mm.

hemisphere. However CD8 T cells only infiltrated the HA-injected hemisphere; none were present in the contralateral hemisphere (**Figure 7.3c,d**).

The above experiments showed that the transgenic CD8 T cells were recruited to the brain only where cognate antigen was present in the parenchyma. It is currently thought that a basal low level of immunosurveillance by T cells occurs in the brain<sup>263</sup>. Therefore, the CD8 T cells could, as part of normal surveillance, have infiltrated the parenchyma in a non-antigen specific fashion only to be retained if their cognate antigen was present. It was therefore asked whether CD8 T cells recruited into the brain in a non-antigen specific fashion persist for any length of time in the absence of their cognate antigen. In separate experiments, CL4 mice received an injection of an irrelevant adenovirus (Ad70-3) or a sterile stab lesion in the right striatum (n=3 each time point). Both manipulations recruited CD8 T cells, which were seen at day 1 and persisted till day 3 (**Figure 7.4**). In addition, when CL4 mice injected with HA in one hemisphere and Cw3 in the contralateral hemisphere (n=3) were perfused at an earlier time point (day 1 p.i.), no CD8 T cells were seen in the Cw3-injected hemisphere (**Figure 7.3a,b**). This showed that CD8 T cells were not infiltrating the brain earlier and failing to persist till day 3 p.i. in the absence of cognate antigen. A few CD8 T cells were seen in the HA-injected side representing the initial phase of CD8 T cell migration (**Figure 7.3b**). It therefore seems very unlikely that background CD8 T cell immunosurveillance of the brain could explain the exquisite antigen specificity observed in this model. It is clear that the presence of cognate antigen behind the blood-brain barrier was instrumental in directing circulating naive CD8 T cells into the brain.

### **7.2.2     *The role of cerebral perivascular macrophages***

It was next addressed whether antigen presentation at the blood-brain barrier (BBB) is a potential mechanism whereby CD8 T cells specifically home in on their target behind the BBB. Cerebral perivascular macrophages (PVMs) are strategically located at the BBB between the endothelial basement membrane and the glia limitans, and are considered to be the brain's foremost antigen-presenting cells<sup>46</sup>. It is known that cerebral PVMs constitutively express major histocompatibility complex (MHC) Class I across species<sup>226,264,265</sup>. In Chapter 6, the development of tools to study cerebral PVMs in mice was described<sup>199</sup>. The mannose receptor was identified as a specific marker of murine cerebral PVMs and a clodronate liposome technique to selectively deplete these

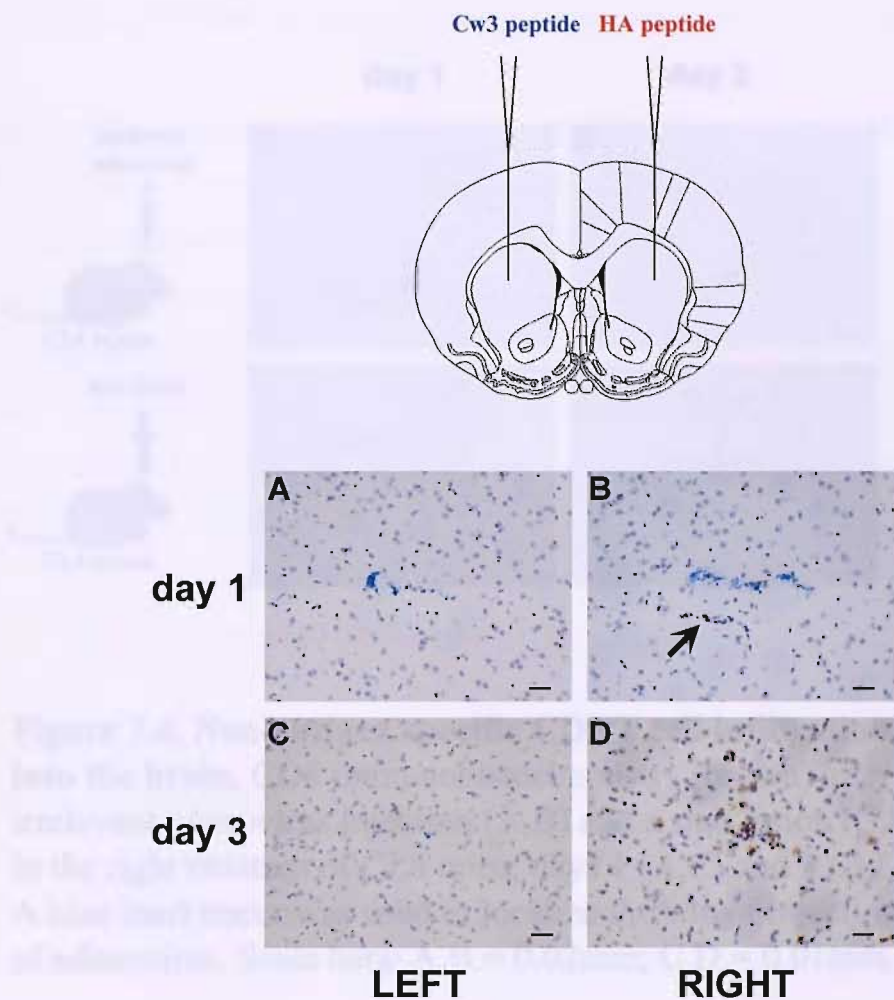


**Figure 7.3. Antigen-specific CD8 T cell infiltration into the brain.** HA and Cw3 peptides were simultaneously injected in the right (B,D) and left (A,C) striatum of CL4 transgenic mice, which were perfused on days 1 (A,B) and 3 (C,D). A blue inert tracer was used to localize the injection site. Brains were processed for CD8 immunohistochemistry using DAB (brown) as chromogen. No CD8 T cells infiltrated the Cw3-injected hemisphere at any time point. Scale bar = 0.03mm.

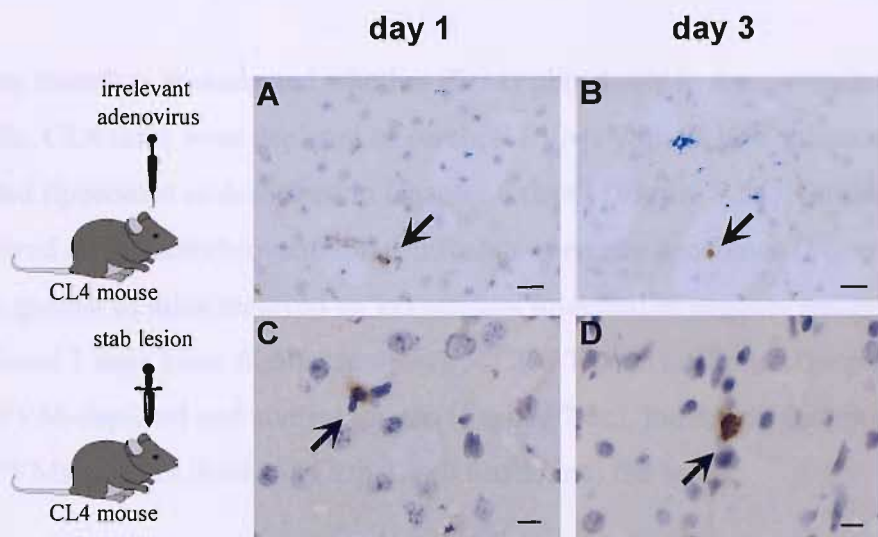


**Figure 7.4. Non-antigen specific CD8 T cell infiltration into the brain.** CD8 immunohistochemistry (brown) after irrelevant adenovirus injection (A,B) and a stab lesion (C,D) in the right striatum of CL4 mice, days 1 (A,C) and 3 (B,D). A blue inert tracer was used to localize the site of injection of adenovirus. Scale bars: A,B = 0.02mm; C,D = 0.01mm.

macrophages in rats was optimized for use in mice. Using this technique, intracerebroventricular (ICV) infusion of clodronate liposomes results in complete depletion of cerebral PVMs by day 5. The liposomes are selectively phagocytosed by cerebral PVMs leading to progressive intracellular accumulation of sodium clodronate which is lethal as a result of adenosine triphosphate depletion<sup>161</sup> and apoptosis<sup>162</sup>.

It was therefore investigated whether PVMs play a role in antigen-specific CD8 T cell traffic. CL4 mice were depleted of cerebral PVMs with an ICV infusion of clodronate-loaded liposomes as described in Chapter 6 (n=6) (**Figure 7.5a**). Control CL4 mice (n=4) received an intracerebroventricular infusion of empty liposomes (**Figure 7.5b**). On day 5 both groups of mice received an intrastriatal injection of cognate antigen, and they were perfused 3 days later. Similar numbers of CD8 T cells infiltrated the parenchyma in both the PVM-depleted and control groups (**Figure 7.5c**), indicating that antigen presentation by PVMs was not directing CD8 T cell traffic into the brain.

### **7.2.3 *The role of cerebral endothelium***

Since an antigen-presenting process was suspected to play an important role in CD8 T cell infiltration, the expression of MHC I was studied by immunohistochemistry on days 0, 0.5, 1, 1.5, 2, 2.5, 3, 5 and 7 after intrastriatal injection of HA in CL4 mice (at least n=3 each time point). In naïve or uninjected animals, a basal level of MHC I expression by endothelium was noted (**Figure 7.6a**). Constitutive MHC I expression was slightly upregulated upon injection of Cw3 (**Figure 7.6b**). After injection of HA, there was dramatic upregulation of MHC I by endothelial cells, peaking at day 3 (**Figure 7.6c**). This upregulation was largely limited to the site of antigen deposition (**Figure 7.6d**) and coinciding temporally and spatially with peak CD8 T cell infiltration. CD8 T cells were seen in association with MHC I-positive blood vessels at various stages of infiltration (**Figure 7.6e,f**). This raised the possibility that CD8 T cell traffic into the brain was facilitated by recognition of the cognate antigen presented by cerebral endothelial cells. For this to occur however, antigen presentation by cerebral endothelial MHC I would have to be luminal.

To investigate whether the upregulated endothelial MHC I was luminally expressed, CL4 mice received an intracerebral injection of HA followed 3 days later by an intravenous

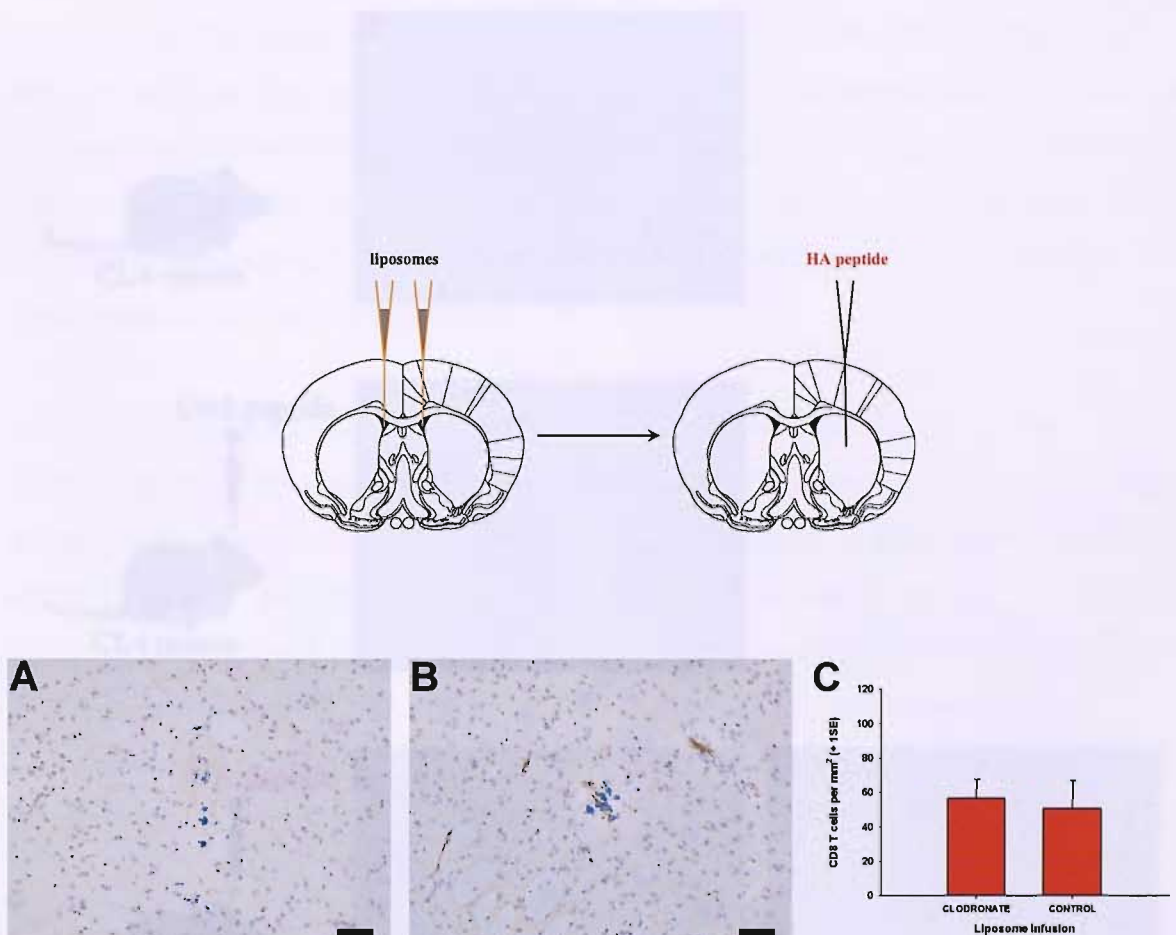


**Figure 7.5. Cerebral perivascular macrophage depletion did not affect antigen-specific CD8 T cell infiltration into the brain.** CL4 mice received an intracerebroventricular infusion of clodronate (A) ( $n=6$ ) and control (B) ( $n=4$ ) liposomes. Five days later, HA peptide was injected in the right striatum and mice were perfused after 3 days. A blue inert tracer was used to localize the injection site. Brains were processed for mannose receptor (A,B) and CD8 (C) immunohistochemistry using DAB (brown) as chromogen. Complete PVM depletion is seen in A. This depletion did not affect CD8 T cell infiltration into the brain (C: 2-tailed Student's t test,  $p = 0.767$ ). Scale bar = 0.05mm.

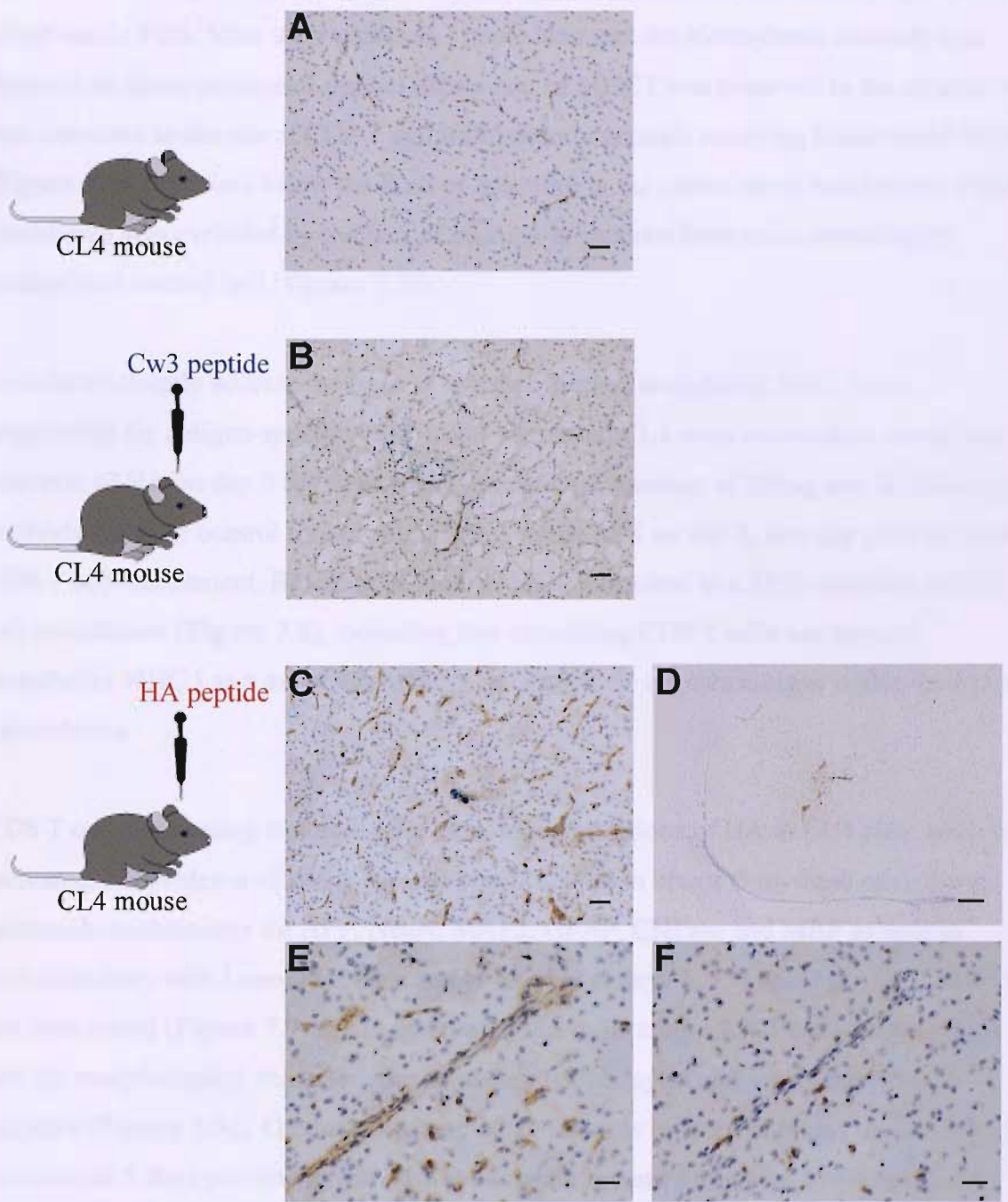


**Figure 7.6. Endothelial MHC Class I in antigen-specific CD8 T cell infiltration into the brain.** Immunohistochemistry for MHC Class I (A-E) and CD8 (F) using DAB (brown) as chromogen in naive CL4 mice (A) and 3 days after right intrastriatal injection of Cw3 peptide (B) or HA peptide (C-F). Blue inert tracer was used to localize the injection site. E and F are serial sections. Scale bars: A-C = 0.05mm; D = 0.2mm; E,F = 0.03mm.

injection of 200 $\mu$ g biotinylated anti-K<sup>d</sup> antibody (n=3) or biotinylated control IgG (n=3) in 200 $\mu$ l sterile PBS. Mice were perfused 3 hours later and the biotinylated antibody was detected on tissue sections. Luminal expression of MHC I was observed in the striatum and was restricted to the site of CD8 T cell infiltration in animals receiving biotinylated anti-K<sup>d</sup> (**Figure 7.7a,b**); it was below the limit of detection in the contralateral hemisphere. BBB breakdown was excluded by the lack of staining in sections from mice receiving the biotinylated control IgG (**Figure 7.7c**).

In order to directly address the issue of whether luminal endothelial MHC I was responsible for antigen-specific CD8 T cell migration, CL4 mice received an intrastriatal injection of HA on day 0 followed by an intravenous injection of 200 $\mu$ g anti-K<sup>d</sup> blocking antibody (n=6) or control IgG (n=6) in 200 $\mu$ l sterile PBS on day 2, one day prior to peak CD8 T cell recruitment. Blocking of luminal MHC I resulted in a 76% reduction in CD8 T cell recruitment (**Figure 7.8**), indicating that circulating CD8 T cells use luminal endothelial MHC I as a molecular address to target their cognate antigen within the brain parenchyma.

CD8 T cells infiltrating the brain after intrastriatal injections of HA in CL4 mice were not activated. No evidence of tissue damage was observed in brains from these mice using immunohistochemistry for APP, NeuN, MAP2, GFAP, CNPase and MBP as well as histochemistry with Luxol Fast Blue and Oil Red O at days 1, 3, 5 and 7 p.i. (at least n=3 per time point) (**Figure 7.9a,b**). In addition, brain-infiltrating CD8 T cells in these mice had the morphological characteristics of resting lymphocytes and were Granzyme B negative (**Figure 7.9c**). On the other hand when HA was injected in brains of (1) CL4 mice immunized 5 days previously with HA in complete Freund's adjuvant (n=9) or (2) wild-type mice injected intravenously with 3 million *in vitro* activated CL4 CD8 T cells (n=8), extensive axon dysfunction and demyelination were seen (**Figure 7.9d,e,g,h**) and brain-infiltrating CD8 T cells had a blastic morphology and were immunoreactive for Granzyme B (**Figure 7.9f,i**). Thus CD8 T cells in CL4 mice receiving intrastriatal HA alone were not activated in either circulating or CNS compartments, most likely because these mice were naïve to the antigen. Given the fact that activation facilitates CD8 T cell traffic into the CNS<sup>266</sup>, the model used in this study, in which CD8 T cells remained antigen-naïve, excluded the possibility that the anti-K<sup>d</sup> blocking antibody could have affected the migratory potential of circulating CD8 T cells through changes in their activation status.

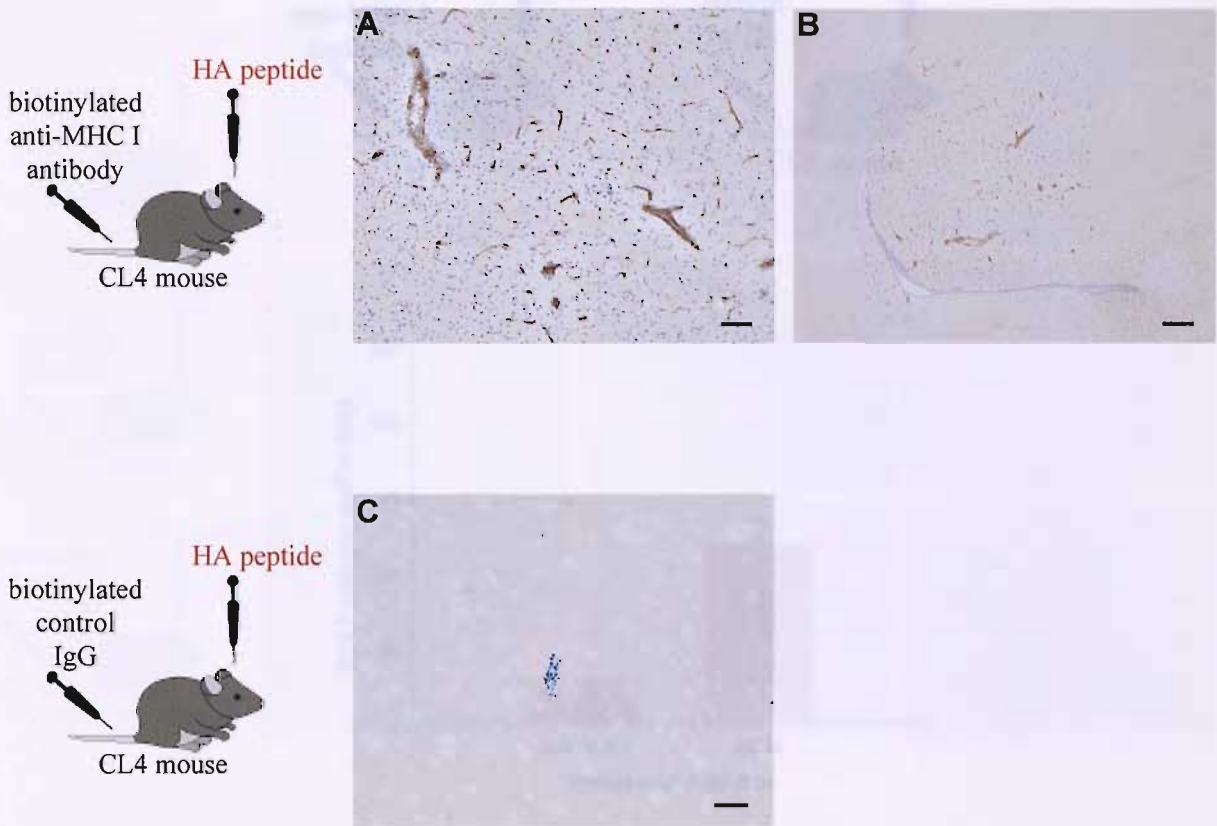


**Figure 7.7. Luminal endothelial MHC Class I upregulation.** CL4 mice received HA peptide injection in the right striatum. Blue inert tracer was used to localize the injection site. After 3 days, the mice were injected i.v. with 200 $\mu$ g biotinylated anti-MHC Class I antibody (A,B) or biotinylated control IgG (C) and perfused 3 hours later. Focal upregulation of luminal MHC Class I expression was seen after intrastriatal HA injection (A,B). Control IgG did not penetrate the endothelium (C). Scale bars: A,C = 0.1mm; B = 0.2mm.

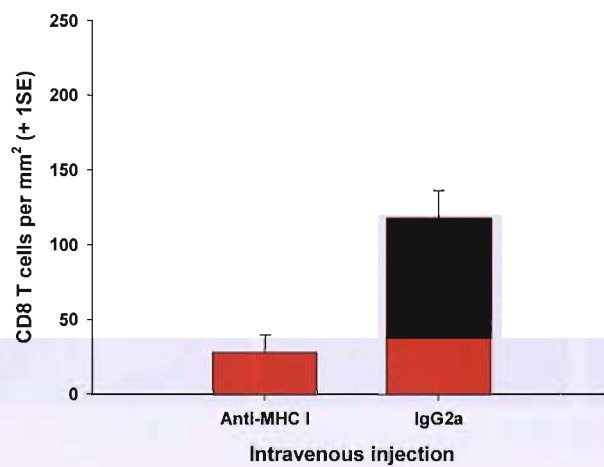
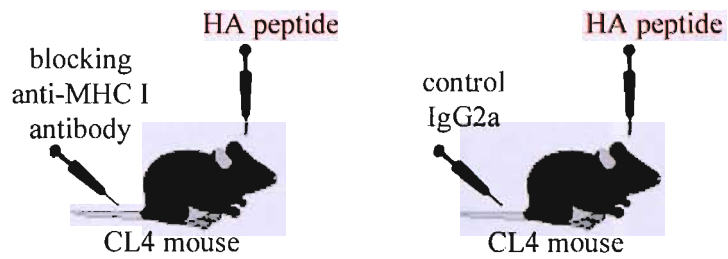


**Figure 7.8. Luminal endothelial MHC Class I plays a role in antigen-specific CD8 T cell traffic into the brain.** Mice injected with HA peptide in the right striatum received an i.v. bolus of blocking anti-MHC Class I antibody (n=6) or control IgG (n=6) on day 2, and were perfused on day 3. There was a 76% reduction (95% CI = -139.5 to -40.0) in CD8 T cell infiltration (2-tailed Student's t test, p = 0.002).

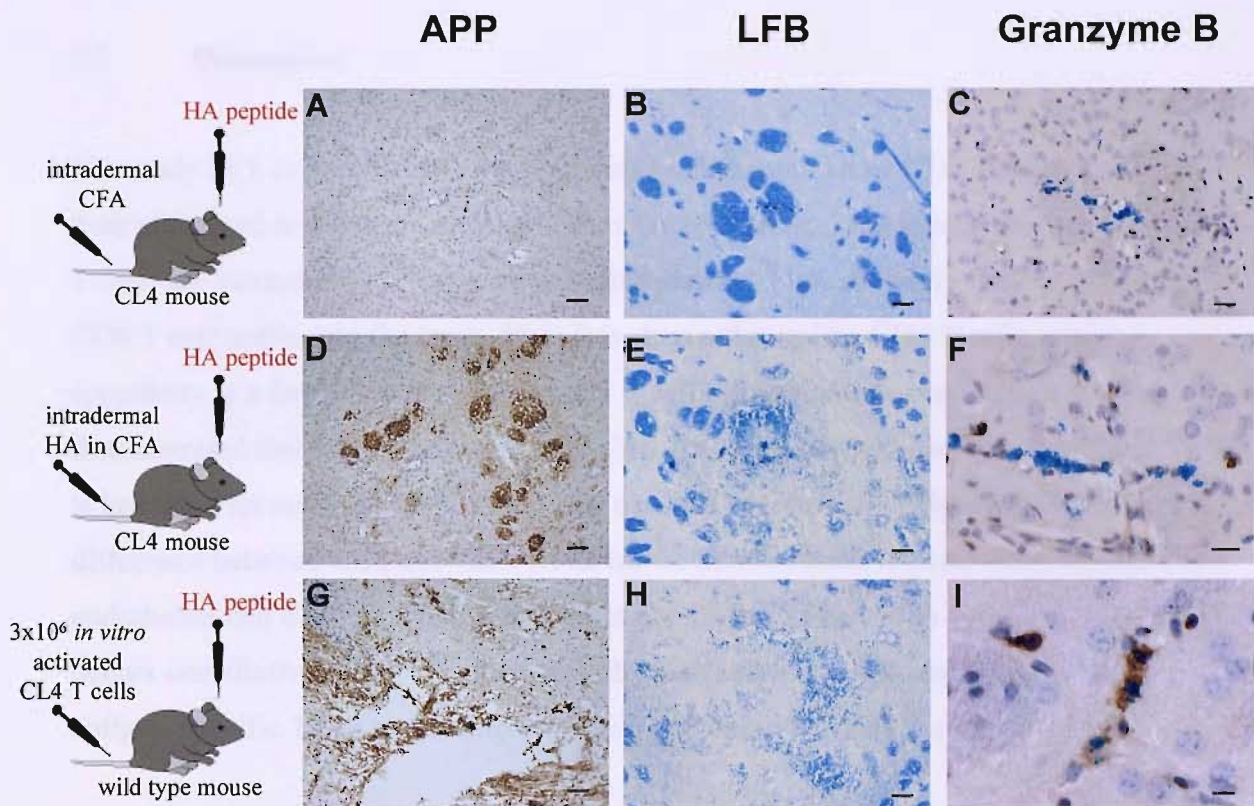


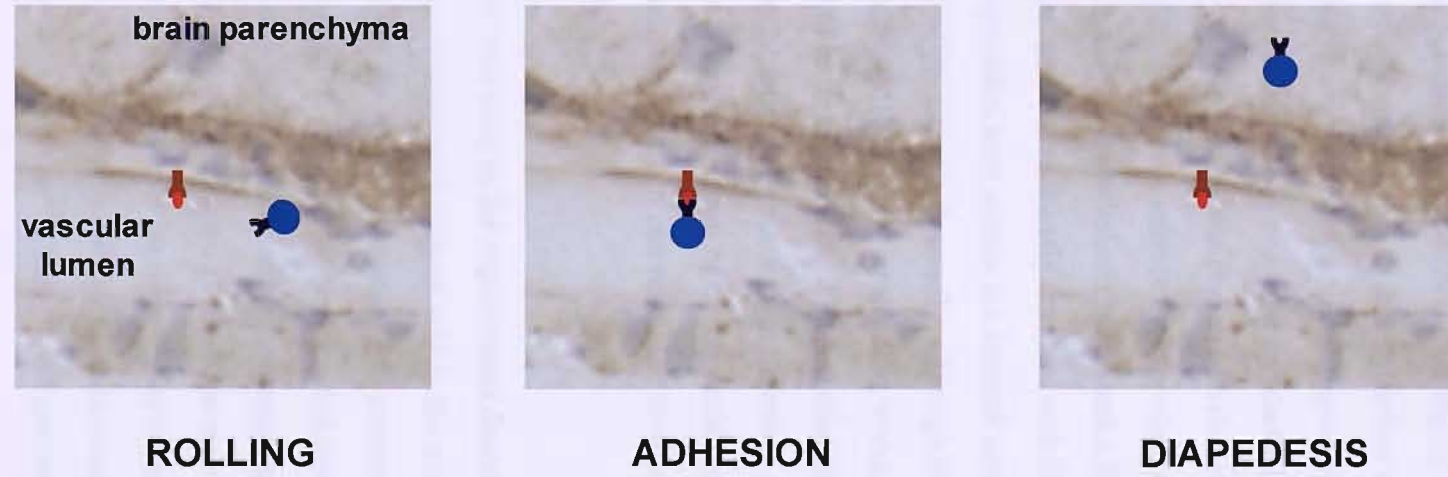
**Figure 7.9. Brain-infiltrating CD8 T cells were not activated in the model of antigen-specific CD8 T cell traffic used.** Representative sections 5 days after right intrastriatal injection of HA peptide in CL4 mice immunized intra-dermally with CFA alone (A,B,C) or HA in CFA (D,E,F) 5 days previously, and in wild-type littermates receiving 3 million *in vitro* activated CL4 CD8 T cells i.v. at the time of intrastriatal injection (G,H,I). Blue inert tracer was used to localize the injection site. Brain sections were processed for amyloid precursor protein (A,D,G) and granzyme B (C,F,I) immunohistochemistry using DAB (brown) as chromogen and Luxol Fast Blue histochemistry (B,E,H). Extensive axon damage and demyelination were observed when CD8 T cells were primed against the antigen. Scale bars: 0.06mm except: C = 0.03mm; F = 0.02mm; I = 0.01mm.

The lack of activation of brain-infiltrating CD8 T cells also excludes the possibility that proliferation within the brain after encounter with cognate antigen contributed to the size of the CD8 T cell infiltrate observed.

### 7.3 Discussion

The study of T cell traffic into the brain has been dominated by CD4 T cells in view of their perceived importance in neuroinflammatory disease. This is now changing, and CD8 T cells are increasingly recognized as major players<sup>102</sup> but relatively little is known about CD8 T cell traffic into the brain. Here it is shown that unlike CD4 T cells, antigen specificity is a factor which governs CD8 T cell infiltration into the brain. It is also demonstrated that the underlying mechanism favouring antigen-specific CD8 T cell traffic is luminal expression of MHC Class I by cerebral endothelium (**Figure 7.10**). This crucial difference between CD4 and CD8 T cell traffic into the brain is a reflection of cerebral endothelial cell biology. MHC Class I, but not Class II, expression by cerebral endothelium occurs constitutively<sup>265,267,268</sup>. Therefore the mechanism for initiating transendothelial antigen-specific T cell traffic into the brain only exists for CD8 T cells.

The molecular requirements for the MHC-dependent transendothelial T cell migration described here exist. As elsewhere in the body, T cell infiltration into the brain is a 3 step process: rolling, adhesion and diapedesis<sup>260</sup>. Strong adhesion is a requirement for subsequent diapedesis and this is classically thought to be mediated by interaction between integrins on the T cell surface and cellular adhesion molecules on the endothelium. An example of such a pair is LFA1 and ICAM, and the strength of this interaction is potentiated by chemokine receptor signalling. Arrest of T cell rolling suggesting adhesion, similar to that seen with chemokine ligand to chemokine receptor binding<sup>269</sup> has been observed after cognate MHCII-TCR interaction<sup>270</sup>. Also, MHCII-peptide-TCR interaction gives rise to a similar increase in avidity of LFA1 to ICAM1<sup>271</sup> as happens after chemokine receptor ligation<sup>272</sup>. Similar mechanisms might be expected to occur with MHC Class I. The affinity of a typical MHCI-peptide-TCR interaction is less than that of LFA1-ICAM ( $K_D$  of  $10\mu\text{M}^{273}$  and  $500\text{nM}^{274}$ , respectively) but the former would be strengthened by the accompanying MHCI-CD8 interaction. Moreover, cognate MHCI-peptide-TCR interaction results in the formation of a supramolecular activation cluster<sup>275</sup> which recruits LFA1, thereby strengthening overall adhesion.



► MHC I presenting antigen      ● CD8 T cell bearing antigen-specific TCR

**Figure 7.10. MHC-dependent transendothelial CD8 T cell migration into the brain**  
Immunohistochemistry of mouse striatum (MHC Class I is brown)

An integral requirement of MHC-dependent CD8 T cell traffic into the brain is the presentation of processed exogenous antigen by MHC Class I on the luminal surface of cerebral endothelium. Interestingly, presentation of endogenous antigen by endothelial cells in peritoneum and cremasteric venules facilitates diapedesis of T cells<sup>276</sup>. Here, evidence is presented that cerebral endothelial cells are able to take up *exogenous* antigen and present it luminally in amounts sufficient to attract CD8 T cells into the underlying tissue. A similar role for exogenous antigen presentation by systemic endothelium remains to be shown. It is likely to occur since labelled insulin-specific CD8 T cells did not infiltrate pancreatic islets well when transferred into mutant mice in which insulin-producing  $\beta$  cells cannot secrete their product extracellularly<sup>277</sup>. Luminal presentation of antigen by cerebral endothelium represents a formidable challenge compared to endothelium elsewhere. Firstly cerebral endothelium lacks fenestrations through which processed peptides may access the luminal surface of endothelial cells for extracellular loading of MHC Class I. Secondly, although it is conceivable that lateral diffusion of antigen-loaded MHC Class I molecules, which is well described<sup>278</sup>, can occur from abluminal to luminal surfaces of endothelial cells in peripheral vessels, this is impossible in cerebral endothelial cells since tight junctions encircle their whole perimeter and represent a barrier to lateral migration of transmembrane molecules<sup>279</sup>. Therefore the only way that intraparenchymal antigen can reach the luminal aspect of cerebral endothelium is by transcytosis.

HA peptide was used in the experiments described in this chapter to simulate the availability of processed antigen within the extracellular milieu of brain parenchyma under inflammatory conditions. Various CNS proteins are released into the CSF in the course of neuropathology<sup>280</sup> which may be degraded into smaller proteins or peptides by interstitial enzymes. Such extracellular antigen processing may result in peptides appropriate for MHC I loading straightaway, as has been reported on many occasions previously<sup>281-286</sup>. Alternatively antigen may be taken up by endothelial cells, processed intracellularly and cross-presented luminally. Although such cross-presentation by endothelial cells has been reported to occur in liver<sup>287</sup>, skin<sup>288</sup> and pancreas<sup>277</sup>, it remains to be shown to occur in the brain.

Classical antigen presentation to CD8 T cells results in death of the antigen-presenting cell (APC). However endothelial cells are known to be resistant to lysis by cytotoxic T cells

and a number of mechanisms have been put forward to account for this observation. These include reduced antigen presentation compared to professional APCs<sup>289</sup>, a lower costimulatory molecule to MHC Class I expression ratio<sup>290</sup> and expression of granzyme B inhibitors<sup>291</sup>. In severe cases, these mechanisms are over-ridden and a T cell mediated vasculitis ensues as happens in graft-versus-host disease<sup>292</sup>. A haemorrhagic vasculitis with accompanying hypoxic tissue injury was sometimes seen in the brains of wild-type mice injected with *in vitro* activated CL4 CD8 T cells (personal observation). This probably happened because the CD8 T cells were sufficiently activated *in vitro* to over-ride the mechanisms which usually protect the cerebral endothelium during CD8 T cell diapedesis. It is possible that such CD8 T cell mediated endothelial cell damage may underlie the hypoxic-like tissue injury seen in EAE induced by adoptive transfer of MBP-specific CD8 T cells<sup>148</sup> as well as the Type III lesions described in MS<sup>293</sup>.

In this study, an antigen-naïve system was used. CL4 mice were housed in individually filtered cages throughout and were not allowed to come into contact with sources of influenza infection. HA was injected in the striatum using a minimally invasive technique developed in a laboratory with many years of experience with stereotaxic intracranial injections in animals. Great care was taken to avoid reflux to the periphery and minimize trauma to surrounding tissue. Indeed brain-infiltrating CD8 T cells were not activated after such injections in CL4 mice and there was no detectable tissue damage. Cells within the non-inflamed CNS are incapable of priming naïve CD8 T cells<sup>294,295</sup>. In contrast, when CL4 mice were immunized with HA in complete Freund's adjuvant (CFA) prior to the intrastriatal HA injection, the infiltrating CD8 T cells were activated and extensive axon and myelin damage occurred. In agreement with a recent study<sup>296</sup>, these results suggest that activation is not an absolute prerequisite for CNS infiltration by CD8 T cells, as previously thought<sup>138,143</sup>. However, activation results in enhanced CD8 T cell traffic into the brain, as observed by others<sup>266</sup> and during the course of these experiments. More importantly, such an antigen-naïve system allowed: (1) the exclusion of the possibility that proliferation of CD8 T cells behind the BBB on encounter with cognate antigen was contributing to the size of the infiltrate observed; and (2) the study of CD8 T cell traffic into the brain after blocking MHC Class I without conflict with the effects of this treatment on CD8 T cell activation.

It is likely that the novel pathway described here for antigen-specific CD8 T cell traffic into the mouse brain also occurs in humans. Human cerebral endothelial cells constitutively express MHC Class I<sup>268</sup>, supporting a role in disease initiation by CD8 T cells reactive against antigens present behind the BBB. Also, oligoclonal dominance of CD8 T cells was observed within CSF<sup>145</sup> and brain parenchyma<sup>146</sup> from patients with MS. This has profound therapeutic consequences for neurological diseases mediated by CD8 T cell entry into the brain such as MS, HTLV-associated myelopathy and various paraneoplastic CNS syndromes as well as encephalitis and brain tumours. It might be possible to design treatments which block or augment MHC-dependent antigen-specific CD8 T cell traffic into the brain. This requires prior knowledge about the MHCI-peptide-TCR interaction involved in specific conditions, and recent work is starting to make such information available. For example, HLA A2 was reported to be responsible for presenting a cdr2 peptide in American patients with paraneoplastic cerebellar degeneration<sup>297</sup>, while HLA A24 was present in Japanese patients<sup>298</sup>. In seven Japanese patients with anti-Hu syndrome, which can manifest itself as a paraneoplastic encephalomyelitis, HLA B7 was involved in presenting Hu-derived peptides<sup>299</sup>. Also, it is now known that the A3 and B7 HLA haplotypes are associated with MS<sup>300</sup>.

In summary, it has been previously unclear how antigen-specific CD8 T cells are targeted to their cognate antigen within the brain. This study provides evidence that luminal cerebral endothelial MHC I expression is the mechanism which acts as a molecular address for antigen-specific CD8 T cell migration into the brain *in vivo* (Figure 7.10). This antigen-specific pathway for CD8 T cells across the BBB means that antigen-specific therapies aimed at blocking the migration of encephalitogenic CD8 T cells, as opposed to the whole T cell repertoire, are possible.

## 7.4 Materials and methods

### 7.4.1 *Mice*

CL4 mice are transgenic for a single TCR: *circa* 95% of its CD8 T cells bear the V $\alpha$ 10 V $\beta$ 8.2 TCR and recognize the peptide IYSTVASSL (HA) from haemagglutinin of influenza virus strain A/PR/8/34 Mt Sinai in a K $^d$ -restricted context<sup>160</sup>. The mice were backcrossed onto a Thy1.1 BALB/c genetic background as described in Chapter 2. Wild-

type Thy1.2 BALB/c mice were purchased from Harlan (Bicester, UK). CL4 transgenic mice, their non-transgenic littermates and wild-type BALB/c mice were included in experiments at 4–8 weeks of age. The mice were housed in individually ventilated cages under a 12h light:12h dark schedule and controlled environmental conditions with pelleted food and water *ad libitum*. The experiments were carried out under Home Office Licence and in accordance with the Animals (Scientific Procedures) Act, 1986, UK.

#### **7.4.2 *Liposomes***

Multilamellar mannosylated liposomes were prepared as described in Chapter 2.

#### **7.4.3 *Reagents***

Haemagglutinin peptide HA512-520 (IYSTVASSL) and control K<sup>d</sup>-binding peptide (Cw3 peptide, RYLKNGKETL) were purchased from Alta Bioscience, UK. They were certified to be 95% pure by high performance liquid chromatography (HPLC). Replication-defective human type 5 adenovirus vector (Ad70-3) was a gift from Prof Jack Gauldie (McMaster University, Ontario). The anti-K<sup>d</sup> antibody SF1-1.1.10 was a gift of Philippe Kourilsky (Pasteur Institute, Paris). IgG2ak was used as control IgG (Sigma, UK). Biotinylation of both SF1-1.1.10 and IgG2ak was performed as per instructions using the EZ-Link Sulfo-NHS-LC-Biotinylation Kit (Pierce Biotechnologies, Perbio Science UK Ltd, UK). All antibodies were dialyzed before injection to remove NaN<sub>3</sub> or Tris using 10kDa MW cut-off Slide-A-Lyzer dialysis cassettes (Pierce Biotechnologies, Perbio Science UK Ltd, UK).

#### **7.4.4 *Surgery***

Intracerebral injections of antigen were performed stereotactically using a minimally invasive technique, taking great care to minimize tissue trauma and reflux to the periphery. Mice were anaesthetized with intraperitoneal Avertin (1.25% 2,2,2-tribromoethanol in tertiary amyl alcohol) at a dose of 0.1ml/5g body weight. The vertex was prepared by shaving and swabbing with chlorhexidine-alcohol. Animals were then fixed in a stereotaxic frame and a 1mm diameter burr hole was drilled through a small skin incision. A sterile finely drawn glass micropipette, the tip of which measures 2–10µm in diameter, was used

to deliver antigen (0.5µg HA or Cw3, or  $5 \times 10^4$  PFU Ad70-3) in a volume of 0.5µl phosphate-buffered saline (PBS) over a period of 1 minute. In order to minimize reflux along the injection tract, the needle was left in place for 1 minute before being slowly withdrawn over another minute. Injections contained a trace of autoclaved Colanyl Blue (Clariant, UK) to help with localization of the lesion during subsequent tissue processing and to track antigen deposition. This dye had been previously shown to be immunologically inert in the laboratory (Tracey A Newman, personal communication). The following coordinates were used: bregma 1mm, lateral 1.6mm and depth 2.6mm. Striatal stab lesions were performed by lowering a sterile pointed scalpel blade into the brain using the same coordinates. For intracerebroventricular infusions, 8µl of mannosylated liposomes were similarly infused into each lateral ventricle slowly over 12.5 minutes using the following co-ordinates: bregma -0.22mm, lateral 1mm and depth 2mm. On each side, the micropipette was left in place for 2.5 minutes, withdrawn partially and left for a further 2.5 minutes before being removed completely, again to avoid reflux of liposomes along the injection tract.

#### **7.4.5 *Perfusion and tissue processing***

Mice were terminally anaesthetized with 20% sodium pentobarbital (Sagatal, Rhone Merieux Ltd., Harlow, Essex, UK) and transcardially perfused with 0.9% w/v heparinized saline. This was followed by perfusion with 10% neutral buffered formalin (NBF) if necessary. Brains were rapidly dissected. For fresh frozen tissue, samples were quickly embedded in Tissue-Tek OCT compound (Sakura Finetek Europe B.V, Zoeterwoude, NL) and frozen in isopentane on dry ice. Blocks were stored at -20°C until use. For formalin-fixed tissue, samples were allowed to post-fix in 10% NBF for about 7 days before being dehydrated through serial concentrations of alcohol, cleared in Histoclear and embedded in wax.

#### **7.4.6 *Immunohistochemistry and histochemistry***

Coronal sections of 10µm thickness were cut on a cryostat or microtome, dried at 37°C for 30 minutes (frozen sections) or at 59°C for a few hours (wax-embedded sections) and processed for indirect immunohistochemistry. Wax-embedded sections were first dewaxed in xylene and rehydrated through serial concentrations of alcohol. All incubations were

carried out at room temperature. Endogenous peroxidase activity was quenched using 0.3% H<sub>2</sub>O<sub>2</sub> in methanol for 20 minutes, followed by a wash in 0.1M phosphate-buffered saline. For formalin-fixed sections, antigen retrieval was performed using microwave (3 minutes in citrate buffer, cooling for 5 minutes, re-microwave for 3 minutes in citrate buffer). After being washed in 0.1M phosphate-buffered saline, sections were pre-adsorbed with 10% normal serum of the appropriate animal species for 30 minutes and then incubated for 90 minutes with the primary antibody. Primary antibodies used are listed in Chapter 2. After washing, sections were incubated with biotinylated secondary antibody of the appropriate specificity for 30 minutes, washed again and then incubated with avidin-biotin-peroxidase complex (Vectastain Elite ABC) for 30 minutes. After another wash, the peroxidase was visualised using 0.05% 3,3'-diaminobenzidine (DAB) as chromogen and 0.05% hydrogen peroxide as substrate. All the sections were counterstained with Cresyl Violet or haematoxylin and dehydrated before mounting in DePeX (BDH Laboratory supplies, Poole, UK). Negative control sections were incubated in the absence of the primary antibody. Normal sera, biotinylated secondary antibodies, and avidin-biotin-peroxidase complex were purchased from Vector Laboratories (Peterborough, UK). For antibodies raised in mouse, the MOM kit was used (Vector Laboratories). For double immunofluorescence on frozen sections, the same protocol was used but incubations were carried out in a dark box. The biotinylated secondary antibody step was followed by incubation with streptavidin-conjugated AF488 for Thy1.1 and substituted by goat anti-rat AF546 for CD8 (AlexaFluor reagents from Molecular Probes, Cambridge Bioscience, Cambridge, UK). Sections were mounted in Mowiol (Harlow Chemical, Harlow, UK) and visualized with a LSM 510 Meta confocal laser scanning microscope (Carl Zeiss, Germany). For Luxol Fast Blue (LFB) histochemistry, wax sections were dehydrated to 95% alcohol and then incubated in a 0.1% LFB solution at 60°C for 90 minutes, washed in 70% alcohol and distilled water, and differentiated in 0.01% lithium carbonate solution, followed by dehydration and mounting in DePeX. For Oil red O (ORO) histochemistry, sections were incubated in a 0.3% ORO/dextrin solution at room temperature for 20 minutes, rinsed in water, and mounted in an aqueous medium. Images were captured on a PC using LeicaQwin software (Cambridge, UK).

#### 7.4.7 *Cell culture*

Single cell suspensions were prepared from spleen and lymph nodes of CL4 mice and non-transgenic littermates, and depleted of red blood cells by incubation with 0.83% NH<sub>4</sub>Cl (Sigma, UK) for 10 minutes at room temperature. CL4 CD8 T cells were purified by positive selection. Briefly, the CL4 cell suspension was incubated with anti-CD8a monoclonal antibody (CT-CD8a; Caltag, USA) for 45 minutes at 4°C, washed and then microbeads coupled to goat anti-rat IgG (Miltenyi Biotech, UK) were added for 15 minutes at 4°C, followed by another wash. Magnetic separation was performed on columns (MS columns; Miltenyi Biotech, UK). The purified population consisted of >98.5% CD8 splenocytes, as revealed by FACS analysis. CL4 CD8 T cells were stimulated with irradiated syngeneic splenocytes (2500 rads) in a ratio of 1:10 in complete DMEM (Invitrogen, UK) supplemented with 10% FCS (Invitrogen, UK) and containing 1 mM HA peptide, 1 ng/ml IL2 (R&D, UK), and 20 ng/ml IL12 (R&D, UK). On day 3, the cultures were fed with fresh medium containing 1ng/ml IL-2. On day 6, cells were harvested and living cells were collected by Ficoll density separation (Amersham Biosciences, UK) and washed with DMEM at least three times. FACS analysis of these cells consistently showed that they were CD8, V $\beta$ 8.2 and CD25-positive (see Figure 2.8, Chapter 2).

#### **7.4.8 Immunization**

On day 0, CL4 mice were immunized with an intradermal injection of 100 $\mu$ l of PBS/CFA (1:1) with or without 5 $\mu$ g HA. On day 5 the animals received an intrastriatal injection of HA as described previously and they were perfused 5 days later.

#### **7.4.9 Adoptive transfer**

CL4 mice received an intrastriatal injection of HA or Cw3 as described previously followed by intravenous injection of 3 million *in vitro* activated CL4 CD8 T cells in 200 $\mu$ l DMEM. They were perfused 3 days later.

#### **7.4.10 Quantification**

This was done manually under light microscopy. The operator was blinded to the identity of the slides counted. Cells were counted using a graticule under a high power objective (x25) and the density of cells was converted to a value per mm<sup>2</sup>. In all cases, at least 4

lesion-centre sections (as shown by the co-injected blue dye) from the same animal, and several animals from each experimental group (as denoted by number  $n$ ) were analyzed and counts averaged.

#### **7.4.11 *Statistics***

Sample size calculations were done using Epicalc 2000 version 1.02 (freeware). The alpha level was set at 0.05 and the power at 80%. Data was analyzed using SPSS version 14. Normality was assessed by the Kolmogorov-Smirnov test. Equality of variance was assessed using Levene's test. All the data was parametric and therefore two-tailed Student's t-test for two independent samples was used throughout. The confidence level was 95%. Graphical representation of results was done using SigmaPlot version 9.

## **Chapter 8**

### **Summary & Discussion**

Chapter 8 is a summary and discussion of the results of the study. It begins with a brief summary of the methodology used in the study. This is followed by a discussion of the results, which are presented in three main sections: (1) the results of the survey of the general public, (2) the results of the survey of the media, and (3) the results of the survey of the government. The discussion then moves on to a discussion of the implications of the results for the future of the country. The chapter concludes with a summary of the main findings of the study and a discussion of the limitations of the study.

Inflammation in the central nervous system (CNS) underlies a variety of neurological conditions characterized by permanent disability. Multiple sclerosis (MS) is the archetypal example of CNS inflammatory disease. Although Alzheimer's disease (AD) is mainly a neurodegenerative disorder, it is accompanied by atypical neuroinflammation<sup>54</sup>. These conditions result in a markedly diminished quality of life, accumulation of irreversible neurological and/or cognitive deficit, and consequently carry a substantial health economic cost. The neuroinflammatory process in these conditions is punctuated by exacerbations which may manifest clinically as relapses in MS. Fluctuations in the behavioural and psychiatric symptoms of AD, including delirium, are commonly seen<sup>4</sup>. There is evidence that exacerbations in ongoing neuroinflammation results in neuronal and axonal death<sup>42,52</sup>, the substrate of permanent disability. Systemic infections are associated with clinical exacerbations in these diseases<sup>15,25</sup> and it is increasingly being recognized that such an association is causal<sup>27,54</sup>. It therefore follows that systemic infections may contribute to neurodegeneration and hence accumulation of permanent disability.

For a systemic infection to impact on the brain, cross-talk between the peripheral immune system and the CNS is necessary. Such immune-to-brain signalling occurs across the blood-brain barrier (BBB). Although it was formerly thought that the BBB is absolute, conferring "immune privilege" to the CNS, it is now increasingly accepted that this is not the case. Instead, the BBB allows the peripheral immune system access to the CNS, but this occurs in a highly regulated manner. Such immune-to-brain signalling may occur via humoral and cellular routes which involve the entry of circulating humoral mediators and immune cells into the CNS during a systemic infection. The consequence is triggering or worsening of neuroinflammation. It is clearly important to understand the cellular and molecular mechanisms underlying these routes of immune-to-brain signalling. This information is necessary in order to facilitate the rational design of therapies to prevent clinical exacerbations and arrest disability progression.

In the introduction to this thesis, the potential routes mediating immune-to-brain signalling were reviewed. This is an evolving field and it is likely that future discoveries will unearth

new mechanisms. Three components believed to be important in immune-to-brain signalling were studied:

**(1) Prostaglandin E<sub>2</sub> (PGE<sub>2</sub>) signalling across the BBB.** PGE<sub>2</sub> is synthesized by cerebral endothelial cells and CD163-positive macrophages<sup>72,74,82,83</sup> during systemic inflammation. It is thought to act as an inflammatory mediator which diffuses across the BBB by virtue of its small size and lipophilicity<sup>301</sup>. Although PGE<sub>2</sub> has been shown to play a role in mediating fever<sup>61</sup>, sickness behaviour<sup>96</sup> and HPA axis activation<sup>95</sup>, it was unknown whether it is essential for inducing cytokine expression within the brain during systemic inflammation. *De novo* cytokine transcription within the brain occurs during systemic inflammation<sup>176</sup> and is thought to be one of the mechanisms underlying exacerbation of neuroinflammatory disease<sup>54</sup>. Data presented here shows that administration of the non-steroidal anti-inflammatory drug (NSAID), indomethacin, during a systemic endotoxin challenge did not prevent the *de novo* transcription of the cytokines TNF $\alpha$ , IL1 $\beta$  and IL6 in the brain. This might explain why NSAIDs have not been effective in AD<sup>183,184</sup>. Further study is needed to look at the effect of NSAIDs on other cytokines, especially anti-inflammatory ones such as TGF $\beta$ , IL10 and IL13. The results presented here suggest that cytokine induction within the brain during systemic inflammation is prostaglandin-independent. This is an unexpected finding which has prompted efforts in the CNS Inflammation Group (University of Southampton) to look for other potential candidates mediating humoral immune-to-brain signalling. A promising candidate is Substance P, which is a neuropeptide whose constitutive synthesis by cerebral endothelium is upregulated after cytokine exposure<sup>302</sup>. Astrocytes within the brain parenchyma are able to respond to endothelial substance P since they express functional receptors for this peptide; ligation results in cytokine production<sup>303</sup>. Another interesting candidate is endothelin-1 (ET1), which is produced by cerebral endothelial cells after cytokine stimulation<sup>304</sup>. It is known that ET1 secretion is heavily polarized abluminally, which is relevant for immune-to-brain signalling<sup>305</sup>. ET1 has been shown to stimulate cytokine production by astrocytes through their expression of ET-B receptors<sup>306</sup>. Other endothelial cell products which are potential candidates for immune-to-brain signalling include nitric oxide<sup>307</sup>, bradykinin<sup>308</sup>, complement proteins<sup>309</sup> and purines<sup>310</sup>.

**(2) The role of cerebral CD163-positive macrophages and endothelial cells in signalling across the BBB.** These cells occupy a strategic location at the BBB and have

been observed to respond to systemic inflammation<sup>72,74,82,83</sup>. It has therefore been suggested that they play a role in immune-to-brain signalling during systemic inflammation<sup>221</sup>. However the relative contribution of these two cell types was unknown. In experiments described here, an intracerebroventricular (ICV) infusion of clodronate liposomes was used to selectively deplete cerebral CD163-positive macrophages. Immune-to-brain signalling after a systemic endotoxin challenge was then assessed by looking at several events which are considered to reflect the brain's response to systemic inflammation: fever, *de novo* cytokine transcription, IL1 $\beta$  protein expression and upregulation of microglial phosphorylated ERK1/2. It is shown that cerebral CD163-positive macrophages are not essential for immune-to-brain signalling. Therefore, cerebral endothelial cells are mainly responsible for this process. These results will direct future research efforts on the cerebral endothelium, which is accessible to systemically administered drugs and sufficiently specialized to enable brain-targeted therapy<sup>210</sup>.

CD163-positive macrophages are the main scavengers of the cerebral perivascular spaces<sup>45,87</sup> and this has been confirmed in the studies described here by their selective phagocytosis of liposomes. This is important in maintaining homeostasis and protecting the brain from potential microbial threats. It is shown here that perivascular and meningeal macrophages express the mannose receptor in the mouse, which is able to recognize pathogen-associated molecular patterns on various bacteria causing meningitis<sup>234</sup>. Indeed their depletion resulted in a significantly poorer outcome in a rat model of pneumococcal meningitis<sup>49</sup>. Expression of the mannose receptor by CD163-positive macrophages has subsequently been confirmed in human brain in a collaboration with Babs O Fabriek (VU Medical Centre, Amsterdam)<sup>258</sup>.

As discussed in Chapter 5, the expression of CD163 and the mannose receptor are associated with the alternatively activated phenotype of macrophages which do not secrete the pro-inflammatory cytokines TNF $\alpha$ , IL1 $\beta$  and IL6 but synthesize the anti-inflammatory cytokines IL10 and TGF $\beta$  instead<sup>217</sup>. It is therefore possible that these macrophages have an anti-inflammatory role at the BBB which has not been detected by the experimental approaches used in this thesis. It would therefore be interesting to study the effect of their depletion in other models of inflammation such as systemic challenges with lower doses of endotoxin and intracerebral endotoxin injections.

**(3) Traffic of antigen-specific CD8 T cells across the BBB.** Infiltration of the brain by T cells underlies various neuroinflammatory diseases and CD8 T cells have been recently recognized to play an important role in this respect<sup>147</sup>. In order to initiate inflammation, neuroantigen-specific CD8 T cells need to infiltrate the brain. However studies in T cell traffic into the brain have concentrated on CD4 T cells<sup>138-143</sup>. They established that CD4 T cell traffic occurs irrespective of antigen specificity. CD8 T cell traffic into the brain was therefore studied using a transgenic system whereby cognate peptide antigen was injected into the striatum of CD8 TCR transgenic mice. It was found that antigen-specific CD8 T cell infiltration occurs. Further experiments were performed in order to elucidate the mechanism underlying the antigen specificity of the CD8 T cell infiltration observed in this model. The results showed that luminal expression of major histocompatibility complex (MHC) Class I by cerebral endothelium was important in directing CD8 T cells to their cognate antigen behind the BBB. This is an interesting result with implications for CD8 T cell-mediated neuroinflammatory diseases. For example, it opens the possibility of using rationally designed peptides in order to block the specific MHC-peptide-TCR interaction at the cerebral endothelium mediating traffic of encephalitogenic CD8 T cells into the brain in these diseases. The existence of an MHC-dependent CD8 T cell pathway across the BBB also raises a lot of questions. Is cerebral endothelium capable of cross-presentation as has been described with other endothelia<sup>277,287,288</sup>? Is the antigen-specific CD8 T cell traffic mechanism described here relevant in disease models and in humans? Does it play a role in disease initiation or maintenance or both? Finally, the role of cerebral endothelial MHC Class I expression in antigen-specific CD8 T cell traffic raises an interesting potential scenario during systemic inflammation. It is known that cerebral endothelium upregulates MHC Class I expression during inflammatory challenge<sup>311</sup>. Also, systemic infection may result in bystander proliferation of antigen-specific CD8 T cells<sup>116</sup>. It is therefore possible to hypothesize that encephalitogenic CD8 T cell traffic into the CNS is favoured during a systemic infection. This needs further study.

The existence of a potential mechanism for immune-to-brain signalling does not mean that it is an adequate target for therapeutic intervention. This is because its contribution to overall signalling may be minor or else because its contribution may be fully compensated for by other mechanisms in its absence. This philosophy has guided the direction of work described in this thesis. Therefore emphasis was put on functional interrogation of the mechanism involved by inhibition, depletion or blocking strategies. PGE<sub>2</sub> synthesis was

inhibited by systemic administration of indomethacin. Cerebral CD163-positive macrophages were depleted using ICV infusion of clodronate liposomes. Antibodies against MHC Class I were used to block CD8 T cell traffic into the CNS.

In the course of these experiments, various models and methodologies were optimized or developed in order to investigate hypotheses: the optimization of the clodronate liposome technique to deplete cerebral CD163-positive macrophages in rats while preserving the peripheral immune response to systemic inflammatory challenge, the optimization of the same technique for use in mice, the description of the mannose receptor as a specific marker of murine cerebral perivascular macrophages and the development of a model of antigen-specific CD8 T cell traffic into the brain using the CL4 transgenic mouse. These tools will be of use during future research in the field.

A unifying theme which emerges from the work described in this thesis is the predominant role of the cerebral endothelial cell in immune-to-brain signalling. Dissemination of these findings will underline this fact and help direct future research towards this crucial and highly specialized cell. It is hoped that in the long term, data presented here will help to alleviate the burden of disease in patients with inflammatory neurological conditions.

## References

## Reference List

1. Smith, K.J. & Hall, S.M. Factors directly affecting impulse transmission in inflammatory demyelinating disease: recent advances in our understanding. *Curr. Opin. Neurol.* **14**, 289-298 (2001).
2. Akiyama, H. *et al.* Inflammation and Alzheimer's disease. *Neurobiol. Aging* **21**, 383-421 (2000).
3. Bjartmar, C. & Trapp, B.D. Axonal and neuronal degeneration in multiple sclerosis: mechanisms and functional consequences. *Curr. Opin. Neurol.* **14**, 271-278 (2001).
4. Hope, T., Keene, J., Fairburn, C.G., Jacoby, R. & McShane, R. Natural history of behavioural changes and psychiatric symptoms in Alzheimer's disease. A longitudinal study. *Br. J. Psychiatry* **174**, 39-44 (1999).
5. Wingerchuk, D.M. The clinical course of acute disseminated encephalomyelitis. *Neurol. Res.* **28**, 341-347 (2006).
6. Rehman, H.U. Primary angiitis of the central nervous system. *J. R. Soc. Med.* **93**, 586-588 (2000).
7. Serdaroglu, P. Behcet's disease and the nervous system. *J. Neurol.* **245**, 197-205 (1998).
8. Delalande, S. *et al.* Neurologic manifestations in primary Sjogren syndrome: a study of 82 patients. *Medicine (Baltimore)* **83**, 280-291 (2004).
9. Birnbaum, G. *et al.* Heat shock proteins and experimental autoimmune encephalomyelitis. II: environmental infection and extra-neuraxial inflammation alter the course of chronic relapsing encephalomyelitis. *J Neuroimmunol* **90**, 149-161 (1998).
10. Lehmann, P.V., Forsthuber, T., Miller, A. & Sercarz, E.E. Spreading of T-cell autoimmunity to cryptic determinants of an autoantigen. *Nature* **358**, 155-157 (1992).
11. McRae, B.L., Vanderlugt, C.L., Dal Canto, M.C. & Miller, S.D. Functional evidence for epitope spreading in the relapsing pathology of experimental autoimmune encephalomyelitis. *J. Exp. Med.* **182**, 75-85 (1995).
12. Phillips, M.J., Weller, R.O., Kida, S. & Iannotti, F. Focal brain damage enhances experimental allergic encephalomyelitis in brain and spinal cord. *Neuropathol Appl. Neurobiol.* **21**, 189-200 (1995).
13. Borghans, J.A., De Boer, R.J., Sercarz, E. & Kumar, V. T cell vaccination in experimental autoimmune encephalomyelitis: a mathematical model. *J. Immunol.* **161**, 1087-1093 (1998).

14. Thorpe, J.W. *et al.* Serial gadolinium-enhanced MRI of the brain and spinal cord in early relapsing-remitting multiple sclerosis. *Neurology* **46**, 373-378 (1996).
15. Buljevac, D. *et al.* Prospective study on the relationship between infections and multiple sclerosis exacerbations. *Brain* **125**, 952-960 (2002).
16. Edwards, S., Zvartau, M., Clarke, H., Irving, W. & Blumhardt, L.D. Clinical relapses and disease activity on magnetic resonance imaging associated with viral upper respiratory tract infections in multiple sclerosis. *J. Neurol. Neurosurg. Psychiatry* **64**, 736-741 (1998).
17. Sibley, W.A., Bamford, C.R. & Clark, K. Clinical viral infections and multiple sclerosis. *Lancet* **1**, 1313-1315 (1985).
18. Andersen, O., Lygner, P.E., Bergstrom, T., Andersson, M. & Vahlne, A. Viral infections trigger multiple sclerosis relapses: a prospective seroepidemiological study. *J. Neurol.* **240**, 417-422 (1993).
19. Panitch, H.S. Influence of infection on exacerbations of multiple sclerosis. *Ann. Neurol.* **36 Suppl**, S25-S28 (1994).
20. Goverman, J. *et al.* Transgenic mice that express a myelin basic protein-specific T cell receptor develop spontaneous autoimmunity. *Cell* **72**, 551-560 (1993).
21. Peacock, J.W., Elsawa, S.F., Petty, C.C., Hickey, W.F. & Bost, K.L. Exacerbation of experimental autoimmune encephalomyelitis in rodents infected with murine gammaherpesvirus-68. *Eur. J Immunol* **33**, 1849-1858 (2003).
22. Nogai, A. *et al.* Lipopolysaccharide injection induces relapses of experimental autoimmune encephalomyelitis in nontransgenic mice via bystander activation of autoreactive CD4+ cells. *J. Immunol.* **175**, 959-966 (2005).
23. Brocke, S. *et al.* Induction of relapsing paralysis in experimental autoimmune encephalomyelitis by bacterial superantigen. *Nature* **365**, 642-644 (1993).
24. Smith, T., Hewson, A.K., Kingsley, C.I., Leonard, J.P. & Cuzner, M.L. Interleukin-12 induces relapse in experimental allergic encephalomyelitis in the Lewis rat. *Am J Pathol* **150**, 1909-1917 (1997).
25. Elie, M., Cole, M.G., Primeau, F.J. & Bellavance, F. Delirium risk factors in elderly hospitalized patients. *J. Gen. Intern. Med.* **13**, 204-212 (1998).
26. Rockwood, K. *et al.* The risk of dementia and death after delirium. *Age Ageing* **28**, 551-556 (1999).
27. Combrinck, M.I., Perry, V.H. & Cunningham, C. Peripheral infection evokes exaggerated sickness behaviour in pre-clinical murine prion disease. *Neuroscience* **112**, 7-11 (2002).
28. O'Brien, J.A., Ward, A.J., Patrick, A.R. & Caro, J. Cost of managing an episode of relapse in multiple sclerosis in the United States. *BMC. Health Serv. Res.* **3**, 17 (2003).

29. Fick, D.M., Kolanowski, A.M., Waller, J.L. & Inouye, S.K. Delirium superimposed on dementia in a community-dwelling managed care population: a 3-year retrospective study of occurrence, costs, and utilization. *J. Gerontol. A Biol. Sci. Med. Sci.* **60**, 748-753 (2005).
30. Foong, J. *et al.* Neuropsychological deficits in multiple sclerosis after acute relapse. *J. Neurol. Neurosurg. Psychiatry* **64**, 529-532 (1998).
31. Kroencke, D.C., Denney, D.R. & Lynch, S.G. Depression during exacerbations in multiple sclerosis: the importance of uncertainty. *Mult. Scler.* **7**, 237-242 (2001).
32. Confavreux, C., Vukusic, S., Moreau, T. & Adeleine, P. Relapses and progression of disability in multiple sclerosis. *N. Engl. J. Med.* **343**, 1430-1438 (2000).
33. Chard, D.T. *et al.* The longitudinal relation between brain lesion load and atrophy in multiple sclerosis: a 14 year follow up study. *J. Neurol. Neurosurg. Psychiatry* **74**, 1551-1554 (2003).
34. Coles, A.J. *et al.* The window of therapeutic opportunity in multiple sclerosis Evidence from monoclonal antibody therapy. *J. Neurol.* **253**, 98-108 (2006).
35. Confavreux, C. & Vukusic, S. Non-specific immunosuppressants in the treatment of multiple sclerosis. *Clin. Neurol. Neurosurg.* **106**, 263-269 (2004).
36. Polman, C.H. *et al.* A randomized, placebo-controlled trial of natalizumab for relapsing multiple sclerosis. *N. Engl. J. Med.* **354**, 899-910 (2006).
37. Newman, T.A. *et al.* T-cell- and macrophage-mediated axon damage in the absence of a CNS-specific immune response: involvement of metalloproteinases. *Brain* **124**, 2203-2214 (2001).
38. Versijpt, J. *et al.* Microglial imaging with positron emission tomography and atrophy measurements with magnetic resonance imaging in multiple sclerosis: a correlative study. *Mult. Scler.* **11**, 127-134 (2005).
39. Murray, A.M. *et al.* Acute delirium and functional decline in the hospitalized elderly patient. *J. Gerontol.* **48**, M181-M186 (1993).
40. Pitkala, K.H., Laurila, J.V., Strandberg, T.E. & Tilvis, R.S. Prognostic significance of delirium in frail older people. *Dement. Geriatr. Cogn. Disord.* **19**, 158-163 (2005).
41. Holmes, C. *et al.* Systemic infection, interleukin 1beta, and cognitive decline in Alzheimer's disease. *J. Neurol. Neurosurg. Psychiatry* **74**, 788-789 (2003).
42. Cunningham, C., Wilcockson, D.C., Campion, S., Lunnon, K. & Perry, V.H. Central and systemic endotoxin challenges exacerbate the local inflammatory response and increase neuronal death during chronic neurodegeneration. *J. Neurosci.* **25**, 9275-9284 (2005).

43. Nguyen, M.D., D'Aigle, T., Gowing, G., Julien, J.P. & Rivest, S. Exacerbation of motor neuron disease by chronic stimulation of innate immunity in a mouse model of amyotrophic lateral sclerosis. *J. Neurosci.* **24**, 1340-1349 (2004).
44. Abbott, N.J., Ronnback, L. & Hansson, E. Astrocyte-endothelial interactions at the blood-brain barrier. *Nat. Rev. Neurosci.* **7**, 41-53 (2006).
45. Kida, S., Steart, P.V., Zhang, E.T. & Weller, R.O. Perivascular cells act as scavengers in the cerebral perivascular spaces and remain distinct from pericytes, microglia and macrophages. *Acta Neuropathol (Berl)* **85**, 646-652 (1993).
46. Fabriek, B.O., Galea, I., Perry, V.H. & Dijkstra, C.D. Cerebral perivascular macrophages and the blood brain barrier. In *The blood-brain barrier and its microenvironment: basic physiology to neurological disease* (ed. de Vries, H.E. & Prat, A.) 295-316 (Taylor and Francis, New York, 2005).
47. Weller, R.O. Fluid compartments and fluid balance in the central nervous system. In *Gray's Anatomy* (ed. Williams, P.L.) 1202-1223 (Churchill Livingstone, New York, 1995).
48. Allt, G. & Lawrenson, J.G. Is the pial microvessel a good model for blood-brain barrier studies? *Brain Res. Brain Res. Rev.* **24**, 67-76 (1997).
49. Polfliet, M.M. *et al.* Meningeal and perivascular macrophages of the central nervous system play a protective role during bacterial meningitis. *J. Immunol.* **167**, 4644-4650 (2001).
50. Abbott, N.J. Dynamics of CNS barriers: evolution, differentiation, and modulation. *Cell Mol. Neurobiol.* **25**, 5-23 (2005).
51. Pedersen, E.B. *et al.* Enriched immune-environment of blood-brain barrier deficient areas of normal adult rats. *J. Neuroimmunol.* **76**, 117-131 (1997).
52. Sun, D., Newman, T.A., Perry, V.H. & Weller, R.O. Cytokine-induced enhancement of autoimmune inflammation in the brain and spinal cord: implications for multiple sclerosis. *Neuropathol Appl Neurobiol* **30**, 374-384 (2004).
53. Stepanichev, M.Y. *et al.* Effects of tumor necrosis factor-alpha central administration on hippocampal damage in rat induced by amyloid beta-peptide (25-35). *J Neurosci Res* **71**, 110-120 (2003).
54. Perry, V.H., Newman, T.A. & Cunningham, C. The impact of systemic infection on the progression of neurodegenerative disease. *Nat Rev Neurosci* **4**, 103-112 (2003).
55. Parant, M.A. *et al.* Selective modulation of lipopolysaccharide-induced death and cytokine production by various muramyl peptides. *Infect. Immun.* **63**, 110-115 (1995).
56. Gifford, G.E. & Lohmann-Matthes, M.L. Gamma interferon priming of mouse and human macrophages for induction of tumor necrosis factor production by bacterial lipopolysaccharide. *J. Natl. Cancer Inst.* **78**, 121-124 (1987).

57. Lee, J., Chan, S.L. & Mattson, M.P. Adverse effect of a presenilin-1 mutation in microglia results in enhanced nitric oxide and inflammatory cytokine responses to immune challenge in the brain. *Neuromolecular Med.* **2**, 29-45 (2002).
58. Sly, L.M. *et al.* Endogenous brain cytokine mRNA and inflammatory responses to lipopolysaccharide are elevated in the Tg2576 transgenic mouse model of Alzheimer's disease. *Brain Res. Bull.* **56**, 581-588 (2001).
59. Palin, K., Cunningham, C. & Perry, V.H. Systemic inflammation alters the cytokine profile and phagocytosis associated with Wallerian degeneration. *Manuscript in preparation.* (2006).
60. Banks, W.A., Kastin, A.J. & Broadwell, R.D. Passage of cytokines across the blood-brain barrier. *Neuroimmunomodulation.* **2**, 241-248 (1995).
61. Elmquist, J.K., Scammell, T.E. & Saper, C.B. Mechanisms of CNS response to systemic immune challenge: the febrile response. *Trends Neurosci.* **20**, 565-570 (1997).
62. Rothwell, N.J., Luheshi, G. & Toulmond, S. Cytokines and their receptors in the central nervous system: physiology, pharmacology, and pathology. *Pharmacol Ther* **69**, 85-95 (1996).
63. Davidson, J., Abul, H.T., Milton, A.S. & Rotondo, D. Cytokines and cytokine inducers stimulate prostaglandin E2 entry into the brain. *Pflugers Arch* **442**, 526-533 (2001).
64. Quan, N., Whiteside, M., Kim, L. & Herkenham, M. Induction of inhibitory factor kappaBalpha mRNA in the central nervous system after peripheral lipopolysaccharide administration: an in situ hybridization histochemistry study in the rat. *Proc. Natl. Acad. Sci. U. S. A* **94**, 10985-10990 (1997).
65. Laflamme, N. & Rivest, S. Effects of systemic immunogenic insults and circulating proinflammatory cytokines on the transcription of the inhibitory factor kappaB alpha within specific cellular populations of the rat brain. *J Neurochem* **73**, 309-321 (1999).
66. Nakamori, T., Morimoto, A., Yamaguchi, K., Watanabe, T. & Murakami, N. Interleukin-1 beta production in the rabbit brain during endotoxin-induced fever. *J Physiol* **476**, 177-186 (1994).
67. Quan, N., Whiteside, M. & Herkenham, M. Time course and localization patterns of interleukin-1beta messenger RNA expression in brain and pituitary after peripheral administration of lipopolysaccharide. *Neuroscience* **83**, 281-293 (1998).
68. Van, D., Bauer, J., Tilders, F.J. & Berkenbosch, F. Endotoxin-induced appearance of immunoreactive interleukin-1 beta in ramified microglia in rat brain: a light and electron microscopic study. *Neuroscience* **65**, 815-826 (1995).
69. Breder, C.D. *et al.* Regional induction of tumor necrosis factor alpha expression in the mouse brain after systemic lipopolysaccharide administration. *Proc Natl Acad Sci U S A* **91**, 11393-11397 (1994).

70. Cunningham, E.T. *et al.* In situ histochemical localization of type I interleukin-1 receptor messenger RNA in the central nervous system, pituitary, and adrenal gland of the mouse. *J Neurosci* **12**, 1101-1114 (1992).
71. Vallier, L. & Rivest, S. Regulation of the genes encoding interleukin-6, its receptor, and gp130 in the rat brain in response to the immune activator lipopolysaccharide and the proinflammatory cytokine interleukin-1beta. *J Neurochem* **69**, 1668-1683 (1997).
72. Ek, M. *et al.* Inflammatory response: pathway across the blood-brain barrier. *Nature* **410**, 430-431 (2001).
73. Elmquist, J.K. *et al.* Intravenous lipopolysaccharide induces cyclooxygenase 2-like immunoreactivity in rat brain perivascular microglia and meningeal macrophages. *J Comp Neurol* **381**, 119-129 (1997).
74. Quan, N., Whiteside, M. & Herkenham, M. Cyclooxygenase 2 mRNA expression in rat brain after peripheral injection of lipopolysaccharide. *Brain Res* **802**, 189-197 (1998).
75. Cao, C., Matsumura, K., Yamagata, K. & Watanabe, Y. Endothelial cells of the rat brain vasculature express cyclooxygenase-2 mRNA in response to systemic interleukin-1 beta: a possible site of prostaglandin synthesis responsible for fever. *Brain Res* **733**, 263-272 (1996).
76. Lacroix, S. & Rivest, S. Effect of acute systemic inflammatory response and cytokines on the transcription of the genes encoding cyclooxygenase enzymes (COX-1 and COX-2) in the rat brain. *J Neurochem* **70**, 452-466 (1998).
77. Matsumura, K. *et al.* Brain endothelial cells express cyclooxygenase-2 during lipopolysaccharide-induced fever: light and electron microscopic immunocytochemical studies. *J Neurosci* **18**, 6279-6289 (1998).
78. Lacroix, S., Feinstein, D. & Rivest, S. The bacterial endotoxin lipopolysaccharide has the ability to target the brain in upregulating its membrane CD14 receptor within specific cellular populations. *Brain Pathol.* **8**, 625-640 (1998).
79. Herkenham, M., Lee, H.Y. & Baker, R.A. Temporal and spatial patterns of c-fos mRNA induced by intravenous interleukin-1: a cascade of non-neuronal cellular activation at the blood-brain barrier. *J Comp Neurol* **400**, 175-196 (1998).
80. Konsman, J.P., Kelley, K. & Dantzer, R. Temporal and spatial relationships between lipopolysaccharide-induced expression of Fos, interleukin-1beta and inducible nitric oxide synthase in rat brain. *Neuroscience* **89**, 535-548 (1999).
81. Nadeau, S. & Rivest, S. Regulation of the gene encoding tumor necrosis factor alpha (TNF-alpha) in the rat brain and pituitary in response in different models of systemic immune challenge. *J Neuropathol Exp Neurol* **58**, 61-77 (1999).
82. Rivest, S. What is the cellular source of prostaglandins in the brain in response to systemic inflammation? Facts and controversies. *Mol. Psychiatry* **4**, 500-507 (1999).

83. Schiltz, J.C. & Sawchenko, P.E. Distinct brain vascular cell types manifest inducible cyclooxygenase expression as a function of the strength and nature of immune insults. *J Neurosci* **22**, 5606-5618 (2002).
84. Van Dam, A.M. *et al.* Interleukin-1 receptors on rat brain endothelial cells: a role in neuroimmune interaction? *FASEB J.* **10**, 351-356 (1996).
85. Ericsson, A., Liu, C., Hart, R.P. & Sawchenko, P.E. Type 1 interleukin-1 receptor in the rat brain: distribution, regulation, and relationship to sites of IL-1-induced cellular activation. *J Comp Neurol* **361**, 681-698 (1995).
86. Bebo, B.F. & Linthicum, D.S. Expression of mRNA for 55-kDa and 75-kDa tumor necrosis factor (TNF) receptors in mouse cerebrovascular endothelium: effects of interleukin-1 beta, interferon-gamma and TNF-alpha on cultured cells. *J Neuroimmunol* **62**, 161-167 (1995).
87. Mato, M. *et al.* Involvement of specific macrophage-lineage cells surrounding arterioles in barrier and scavenger function in brain cortex. *Proc. Natl. Acad. Sci. U. S. A* **93**, 3269-3274 (1996).
88. Van Dam, A.M., Brouns, M., Louisse, S. & Berkenbosch, F. Appearance of interleukin-1 in macrophages and in ramified microglia in the brain of endotoxin-treated rats: a pathway for the induction of non-specific symptoms of sickness? *Brain Res.* **588**, 291-296 (1992).
89. Vane, J.R., Bakhle, Y.S. & Botting, R.M. Cyclooxygenases 1 and 2. *Annu. Rev. Pharmacol. Toxicol.* **38**, 97-120 (1998).
90. Moore, S.A., Spector, A.A. & Hart, M.N. Eicosanoid metabolism in cerebromicrovascular endothelium. *Am. J. Physiol* **254**, C37-C44 (1988).
91. Van Dam, A.M., Brouns, M., Man, A.H. & Berkenbosch, F. Immunocytochemical detection of prostaglandin E2 in microvasculature and in neurons of rat brain after administration of bacterial endotoxin. *Brain Res.* **613**, 331-336 (1993).
92. Ushikubi, F. *et al.* Impaired febrile response in mice lacking the prostaglandin E receptor subtype EP3. *Nature* **395**, 281-284 (1998).
93. Ek, M., Arias, C., Sawchenko, P. & Ericsson-Dahlstrand, A. Distribution of the EP3 prostaglandin E(2) receptor subtype in the rat brain: relationship to sites of interleukin-1-induced cellular responsiveness. *J. Comp Neurol.* **428**, 5-20 (2000).
94. Hori, T., Oka, T., Hosoi, M., Abe, M. & Oka, K. Hypothalamic mechanisms of pain modulatory actions of cytokines and prostaglandin E2. *Ann. N. Y. Acad. Sci.* **917**, 106-120 (2000).
95. Matsuoka, Y. *et al.* Impaired adrenocorticotropic hormone response to bacterial endotoxin in mice deficient in prostaglandin E receptor EP1 and EP3 subtypes. *Proc. Natl. Acad. Sci. U. S. A* **100**, 4132-4137 (2003).
96. Crestani, F., Seguy, F. & Dantzer, R. Behavioural effects of peripherally injected interleukin-1: role of prostaglandins. *Brain Res.* **542**, 330-335 (1991).

97. Pollak, Y., Ovadia, H., Orion, E. & Yirmiya, R. The EAE-associated behavioral syndrome: II. Modulation by anti-inflammatory treatments. *J Neuroimmunol* **137**, 100-108 (2003).
98. Wingerchuk, D.M. *et al.* A randomized controlled crossover trial of aspirin for fatigue in multiple sclerosis. *Neurology* **64**, 1267-1269 (2005).
99. Malm, T.M. *et al.* Bone-marrow-derived cells contribute to the recruitment of microglial cells in response to beta-amyloid deposition in APP/PS1 double transgenic Alzheimer mice. *Neurobiol. Dis.* **18**, 134-142 (2005).
100. Simard, A.R., Soulet, D., Gowing, G., Julien, J.P. & Rivest, S. Bone marrow-derived microglia play a critical role in restricting senile plaque formation in Alzheimer's disease. *Neuron* **49**, 489-502 (2006).
101. Wekerle, H., Kojima, K., Lannes-Vieira, J., Lassmann, H. & Linington, C. Animal models. *Ann. Neurol.* **36 Suppl**, S47-S53 (1994).
102. Neumann, H., Medana, I.M., Bauer, J. & Lassmann, H. Cytotoxic T lymphocytes in autoimmune and degenerative CNS diseases. *Trends Neurosci* **25**, 313-319 (2002).
103. Bielekova, B. *et al.* Encephalitogenic potential of the myelin basic protein peptide (amino acids 83-99) in multiple sclerosis: results of a phase II clinical trial with an altered peptide ligand. *Nat. Med.* **6**, 1167-1175 (2000).
104. Tran, E.H., Hoekstra, K., van, R., Dijkstra, C.D. & Owens, T. Immune invasion of the central nervous system parenchyma and experimental allergic encephalomyelitis, but not leukocyte extravasation from blood, are prevented in macrophage-depleted mice. *J Immunol* **161**, 3767-3775 (1998).
105. Linington, C., Bradl, M., Lassmann, H., Brunner, C. & Vass, K. Augmentation of demyelination in rat acute allergic encephalomyelitis by circulating mouse monoclonal antibodies directed against a myelin/oligodendrocyte glycoprotein. *Am. J. Pathol.* **130**, 443-454 (1988).
106. Aloisi, F. & Pujol-Borrell, R. Lymphoid neogenesis in chronic inflammatory diseases. *Nat. Rev. Immunol.* **6**, 205-217 (2006).
107. Levine, S. & Saltzman, A. The hyperacute form of allergic encephalomyelitis produced in rats without the aid of pertussis vaccine. *J. Neuropathol. Exp. Neurol.* **48**, 255-262 (1989).
108. McColl, S.R. *et al.* Treatment with anti-granulocyte antibodies inhibits the effector phase of experimental autoimmune encephalomyelitis. *J. Immunol.* **161**, 6421-6426 (1998).
109. Fujinami, R.S. & Oldstone, M.B. Amino acid homology between the encephalitogenic site of myelin basic protein and virus: mechanism for autoimmunity. *Science* **230**, 1043-1045 (1985).

110. Wucherpfennig, K.W. & Strominger, J.L. Molecular mimicry in T cell-mediated autoimmunity: viral peptides activate human T cell clones specific for myelin basic protein. *Cell* **80**, 695-705 (1995).
111. Mason, D. A very high level of crossreactivity is an essential feature of the T-cell receptor. *Immunol Today* **19**, 395-404 (1998).
112. Martin, R. *et al.* Molecular mimicry and antigen-specific T cell responses in multiple sclerosis and chronic CNS Lyme disease. *J. Autoimmun.* **16**, 187-192 (2001).
113. Tough, D.F., Sun, S. & Sprent, J. T cell stimulation in vivo by lipopolysaccharide (LPS). *J. Exp. Med.* **185**, 2089-2094 (1997).
114. Sprent, J., Zhang, X., Sun, S. & Tough, D. T-cell proliferation in vivo and the role of cytokines. *Philos. Trans. R. Soc. Lond B Biol. Sci.* **355**, 317-322 (2000).
115. Tough, D.F., Borrow, P. & Sprent, J. Induction of bystander T cell proliferation by viruses and type I interferon in vivo. *Science* **272**, 1947-1950 (1996).
116. Sprent, J. Turnover of memory-phenotype CD8+ T cells. *Microbes. Infect.* **5**, 227-231 (2003).
117. Matzinger, P. The danger model: a renewed sense of self. *Science* **296**, 301-305 (2002).
118. Gallucci, S., Lolkema, M. & Matzinger, P. Natural adjuvants: endogenous activators of dendritic cells. *Nat. Med.* **5**, 1249-1255 (1999).
119. Ehl, S. *et al.* Viral and bacterial infections interfere with peripheral tolerance induction and activate CD8+ T cells to cause immunopathology. *J. Exp. Med.* **187**, 763-774 (1998).
120. Rocken, M., Urban, J.F. & Shevach, E.M. Infection breaks T-cell tolerance. *Nature* **359**, 79-82 (1992).
121. Ichikawa, H.T., Williams, L.P. & Segal, B.M. Activation of APCs through CD40 or Toll-like receptor 9 overcomes tolerance and precipitates autoimmune disease. *J. Immunol.* **169**, 2781-2787 (2002).
122. Ding, L. & Shevach, E.M. Activation of CD4+ T cells by delivery of the B7 costimulatory signal on bystander antigen-presenting cells (trans-costimulation). *Eur. J. Immunol.* **24**, 859-866 (1994).
123. Pardigon, N. *et al.* Delayed and separate costimulation in vitro supports the evidence of a transient "excited" state of CD8+ T cells during activation. *J Immunol* **164**, 4493-4499 (2000).
124. Torres, B.A., Kominsky, S., Perrin, G.Q., Hobeika, A.C. & Johnson, H.M. Superantigens: the good, the bad, and the ugly. *Exp. Biol. Med. (Maywood.)* **226**, 164-176 (2001).

125. Herrmann, T., Baschieri, S., Lees, R.K. & MacDonald, H.R. In vivo responses of CD4+ and CD8+ cells to bacterial superantigens. *Eur. J. Immunol.* **22**, 1935-1938 (1992).
126. Pryce, G., Male, D., Campbell, I. & Greenwood, J. Factors controlling T-cell migration across rat cerebral endothelium in vitro. *J. Neuroimmunol.* **75**, 84-94 (1997).
127. Ding, Z., Xiong, K. & Issekutz, T.B. Regulation of chemokine-induced transendothelial migration of T lymphocytes by endothelial activation: differential effects on naive and memory T cells. *J. Leukoc. Biol.* **67**, 825-833 (2000).
128. Oppenheimer-Marks, N., Brezinschek, R.I., Mohamadzadeh, M., Vita, R. & Lipsky, P.E. Interleukin 15 is produced by endothelial cells and increases the transendothelial migration of T cells In vitro and in the SCID mouse-human rheumatoid arthritis model In vivo. *J. Clin. Invest.* **101**, 1261-1272 (1998).
129. Saukkonen, J.J. *et al.* In vitro transendothelial migration of blood T lymphocytes from HIV-infected individuals. *AIDS* **11**, 1595-1601 (1997).
130. Brezinschek, R.I., Lipsky, P.E., Galea, P., Vita, R. & Oppenheimer-Marks, N. Phenotypic characterization of CD4+ T cells that exhibit a transendothelial migratory capacity. *J. Immunol.* **154**, 3062-3077 (1995).
131. Borthwick, N.J. *et al.* Transendothelial migration confers a survival advantage to activated T lymphocytes: role of LFA-1/ICAM-1 interactions. *Clin. Exp. Immunol.* **134**, 246-252 (2003).
132. Gergel, E.I. & Furie, M.B. Activation of endothelium by Borrelia burgdorferi in vitro enhances transmigration of specific subsets of T lymphocytes. *Infect. Immun.* **69**, 2190-2197 (2001).
133. Borthwick, N.J. *et al.* Selective migration of highly differentiated primed T cells, defined by low expression of CD45RB, across human umbilical vein endothelial cells: effects of viral infection on transmigration. *Immunology* **90**, 272-280 (1997).
134. Matsuda, M., Tsukada, N., Miyagi, K. & Yanagisawa, N. Adhesion of lymphocytes to endothelial cells in experimental allergic encephalomyelitis before and after treatment with endotoxin lipopolysaccharide. *Int. Arch. Allergy Immunol.* **106**, 335-344 (1995).
135. Piccio, L. *et al.* Molecular mechanisms involved in lymphocyte recruitment in inflamed brain microvessels: critical roles for P-selectin glycoprotein ligand-1 and heterotrimeric G(i)-linked receptors. *J. Immunol.* **168**, 1940-1949 (2002).
136. Yednock, T.A. *et al.* Prevention of experimental autoimmune encephalomyelitis by antibodies against alpha 4 beta 1 integrin. *Nature* **356**, 63-66 (1992).
137. Thomsen, A.R., Nansen, A., Madsen, A.N., Bartholdy, C. & Christensen, J.P. Regulation of T cell migration during viral infection: role of adhesion molecules and chemokines. *Immunol. Lett.* **85**, 119-127 (2003).

138. Hickey, W.F., Hsu, B.L. & Kimura, H. T-lymphocyte entry into the central nervous system. *J Neurosci Res* **28**, 254-260 (1991).
139. Irani, D.N. & Griffin, D.E. Regulation of lymphocyte homing into the brain during viral encephalitis at various stages of infection. *J. Immunol.* **156**, 3850-3857 (1996).
140. Krakowski, M.L. & Owens, T. Naive T lymphocytes traffic to inflamed central nervous system, but require antigen recognition for activation. *Eur. J. Immunol.* **30**, 1002-1009 (2000).
141. Ludowyk, P.A., Willenborg, D.O. & Parish, C.R. Selective localisation of neuro-specific T lymphocytes in the central nervous system. *J. Neuroimmunol.* **37**, 237-250 (1992).
142. Carrithers, M.D., Visintin, I., Kang, S.J. & Janeway, C.A., Jr. Differential adhesion molecule requirements for immune surveillance and inflammatory recruitment. *Brain* **123 ( Pt 6)**, 1092-1101 (2000).
143. Wekerle, H., Linington, C., Lassmann, H. & Meyermann, R. Cellular immune reactivity within the CNS. *Trends Neurosci* **27** (1986).
144. Ford, M.L. & Evavold, B.D. Specificity, magnitude, and kinetics of MOG-specific CD8+ T cell responses during experimental autoimmune encephalomyelitis. *Eur. J. Immunol.* **35**, 76-85 (2005).
145. Jacobsen, M. *et al.* Oligoclonal expansion of memory CD8+ T cells in cerebrospinal fluid from multiple sclerosis patients. *Brain* **125**, 538-550 (2002).
146. Babbe, H. *et al.* Clonal expansions of CD8(+) T cells dominate the T cell infiltrate in active multiple sclerosis lesions as shown by micromanipulation and single cell polymerase chain reaction. *J. Exp. Med.* **192**, 393-404 (2000).
147. Friese, M.A. & Fugger, L. Autoreactive CD8+ T cells in multiple sclerosis: a new target for therapy? *Brain* **128**, 1747-1763 (2005).
148. Huseby, E.S. *et al.* A pathogenic role for myelin-specific CD8(+) T cells in a model for multiple sclerosis. *J Exp Med* **194**, 669-676 (2001).
149. Sun, D. *et al.* Myelin antigen-specific CD8+ T cells are encephalitogenic and produce severe disease in C57BL/6 mice. *J. Immunol.* **166**, 7579-7587 (2001).
150. Battistini, L. *et al.* CD8+ T cells from patients with acute multiple sclerosis display selective increase of adhesiveness in brain venules: a critical role for P-selectin glycoprotein ligand-1. *Blood* **101**, 4775-4782 (2003).
151. Gay, F.W., Drye, T.J., Dick, G.W. & Esiri, M.M. The application of multifactorial cluster analysis in the staging of plaques in early multiple sclerosis. Identification and characterization of the primary demyelinating lesion. *Brain* **120 ( Pt 8)**, 1461-1483 (1997).

152. Crawford, M.P. *et al.* High prevalence of autoreactive, neuroantigen-specific CD8+ T cells in multiple sclerosis revealed by novel flow cytometric assay. *Blood* **103**, 4222-4231 (2004).

153. Bitsch, A., Schuchardt, J., Bunkowski, S., Kuhlmann, T. & Bruck, W. Acute axonal injury in multiple sclerosis. Correlation with demyelination and inflammation. *Brain* **123 (Pt 6)**, 1174-1183 (2000).

154. Killestein, J. *et al.* Cytokine producing CD8+ T cells are correlated to MRI features of tissue destruction in MS. *J. Neuroimmunol.* **142**, 141-148 (2003).

155. Medana, I., Martinic, M.A., Wekerle, H. & Neumann, H. Transection of major histocompatibility complex class I-induced neurites by cytotoxic T lymphocytes. *Am. J. Pathol.* **159**, 809-815 (2001).

156. Haring, J.S., Pewe, L.L. & Perlman, S. Bystander CD8 T cell-mediated demyelination after viral infection of the central nervous system. *J Immunol* **169**, 1550-1555 (2002).

157. McPherson, S.W., Heuss, N.D., Roehrich, H. & Gregerson, D.S. Bystander killing of neurons by cytotoxic T cells specific for a glial antigen. *Glia* **53**, 457-466 (2006).

158. Chen, A.M., Khanna, N., Stohlman, S.A. & Bergmann, C.C. Virus-specific and bystander CD8 T cells recruited during virus-induced encephalomyelitis. *J. Virol.* **79**, 4700-4708 (2005).

159. McGavern, D.B. & Truong, P. Rebuilding an immune-mediated central nervous system disease: weighing the pathogenicity of antigen-specific versus bystander T cells. *J. Immunol.* **173**, 4779-4790 (2004).

160. Morgan, D.J. *et al.* CD8(+) T cell-mediated spontaneous diabetes in neonatal mice. *J Immunol* **157**, 978-983 (1996).

161. Russell, R.G. & Rogers, M.J. Bisphosphonates: from the laboratory to the clinic and back again. *Bone* **25**, 97-106 (1999).

162. van Rooijen, N., Sanders, A. & van den Berg, T.K. Apoptosis of macrophages induced by liposome-mediated intracellular delivery of clodronate and propamidine. *J. Immunol. Methods* **193**, 93-99 (1996).

163. Polfliet, M.M. *et al.* A method for the selective depletion of perivascular and meningeal macrophages in the central nervous system. *J. Neuroimmunol.* **116**, 188-195 (2001).

164. van Rooijen, N. & Sanders, A. Liposome mediated depletion of macrophages: mechanism of action, preparation of liposomes and applications. *J. Immunol. Methods* **174**, 83-93 (1994).

165. Lawson, L.J., Frost, L., Risbridger, J., Fearn, S. & Perry, V.H. Quantification of the mononuclear phagocyte response to Wallerian degeneration of the optic nerve. *J. Neurocytol.* **23**, 729-744 (1994).

166. Barkhof, F., van Waesberghe, J.H., Uitdehaag, B.M. & Polman, C.H. Ibuprofen does not suppress active multiple sclerosis lesions on gadolinium-enhanced MR images. *Ann Neurol* **42**, 982 (1997).

167. Etminan, M., Gill, S. & Samii, A. Effect of non-steroidal anti-inflammatory drugs on risk of Alzheimer's disease: systematic review and meta-analysis of observational studies. *BMJ* **327**, 128 (2003).

168. McGeer, P.L., Schulzer, M. & McGeer, E.G. Arthritis and anti-inflammatory agents as possible protective factors for Alzheimer's disease: a review of 17 epidemiologic studies. *Neurology* **47**, 425-432 (1996).

169. Szekely, C.A. *et al.* Nonsteroidal anti-inflammatory drugs for the prevention of Alzheimer's disease: a systematic review. *Neuroepidemiology* **23**, 159-169 (2004).

170. Zandi, P.P. *et al.* Reduced incidence of AD with NSAID but not H2 receptor antagonists: the Cache County Study. *Neurology* **59**, 880-886 (2002).

171. in 't Veld *et al.* Nonsteroidal antiinflammatory drugs and the risk of Alzheimer's disease. *N. Engl. J. Med.* **345**, 1515-1521 (2001).

172. Breitner, J.C. NSAIDs and Alzheimer's disease: how far to generalise from trials? *Lancet Neurol.* **2**, 527 (2003).

173. Combrinck, M. *et al.* Levels of CSF prostaglandin E2, cognitive decline, and survival in Alzheimer's disease. *J. Neurol. Neurosurg. Psychiatry* **77**, 85-88 (2006).

174. Hoozemans, J.J., Veerhuis, R., Rozemuller, J.M. & Eikelenboom, P. Neuroinflammation and regeneration in the early stages of Alzheimer's disease pathology. *Int. J. Dev. Neurosci.* **24**, 157-165 (2006).

175. Gasparini, L., Ongini, E. & Wenk, G. Non-steroidal anti-inflammatory drugs (NSAIDs) in Alzheimer's disease: old and new mechanisms of action. *J. Neurochem.* **91**, 521-536 (2004).

176. Laye, S., Parnet, P., Goujon, E. & Dantzer, R. Peripheral administration of lipopolysaccharide induces the expression of cytokine transcripts in the brain and pituitary of mice. *Brain Res Mol Brain Res* **27**, 157-162 (1994).

177. Fabricio, A.S., Veiga, F.H., Cristofoletti, R., Navarra, P. & Souza, G.E. The effects of selective and nonselective cyclooxygenase inhibitors on endothelin-1-induced fever in rats. *Am. J. Physiol Regul. Integr. Comp Physiol* **288**, R671-R677 (2005).

178. Bour, A.M., Westendorp, R.G., Laterveer, J.C., Bollen, E.L. & Remarque, E.J. Interaction of indomethacin with cytokine production in whole blood. Potential mechanism for a brain-protective effect. *Exp. Gerontol.* **35**, 1017-1024 (2000).

179. Levi, G., Minghetti, L. & Aloisi, F. Regulation of prostanoid synthesis in microglial cells and effects of prostaglandin E2 on microglial functions. *Biochimie* **80**, 899-904 (1998).

180. Zhang, J. & Rivest, S. Anti-inflammatory effects of prostaglandin E2 in the central nervous system in response to brain injury and circulating lipopolysaccharide. *J. Neurochem.* **76**, 855-864 (2001).
181. Blais, V., Turrin, N.P. & Rivest, S. Cyclooxygenase 2 (COX-2) inhibition increases the inflammatory response in the brain during systemic immune stimuli. *J. Neurochem.* **95**, 1563-1574 (2005).
182. Jiang, C., Ting, A.T. & Seed, B. PPAR-gamma agonists inhibit production of monocyte inflammatory cytokines. *Nature* **391**, 82-86 (1998).
183. Reines, S.A. *et al.* Rofecoxib: no effect on Alzheimer's disease in a 1-year, randomized, blinded, controlled study. *Neurology* **62**, 66-71 (2004).
184. Aisen, P.S. *et al.* Effects of rofecoxib or naproxen vs placebo on Alzheimer disease progression: a randomized controlled trial. *JAMA* **289**, 2819-2826 (2003).
185. Heneka, M.T. *et al.* Acute treatment with the PPARgamma agonist pioglitazone and ibuprofen reduces glial inflammation and Abeta1-42 levels in APPV717I transgenic mice. *Brain* **128**, 1442-1453 (2005).
186. Lim, G.P. *et al.* Ibuprofen suppresses plaque pathology and inflammation in a mouse model for Alzheimer's disease. *J. Neurosci.* **20**, 5709-5714 (2000).
187. Yan, Q. *et al.* Anti-inflammatory drug therapy alters beta-amyloid processing and deposition in an animal model of Alzheimer's disease. *J. Neurosci.* **23**, 7504-7509 (2003).
188. Blasko, I., Marx, F., Steiner, E., Hartmann, T. & Grubeck-Loebenstein, B. TNFalpha plus IFNgamma induce the production of Alzheimer beta-amyloid peptides and decrease the secretion of APPs. *FASEB J.* **13**, 63-68 (1999).
189. Sastre, M. *et al.* Nonsteroidal anti-inflammatory drugs and peroxisome proliferator-activated receptor-gamma agonists modulate immunostimulated processing of amyloid precursor protein through regulation of beta-secretase. *J. Neurosci.* **23**, 9796-9804 (2003).
190. Klegeris, A., Walker, D.G. & McGeer, P.L. Activation of macrophages by Alzheimer beta amyloid peptide. *Biochem. Biophys. Res. Commun.* **199**, 984-991 (1994).
191. Felton, L.M. *et al.* MCP-1 and murine prion disease: separation of early behavioural dysfunction from overt clinical disease. *Neurobiol. Dis.* **20**, 283-295 (2005).
192. Gordon, S. Homeostasis: a scavenger receptor for haemoglobin. *Curr Biol* **11**, R399-R401 (2001).
193. Kristiansen, M. *et al.* Identification of the haemoglobin scavenger receptor. *Nature* **409**, 198-201 (2001).

194. Barbe, E., Huitinga, I., Dopp, E.A., Bauer, J. & Dijkstra, C.D. A novel bone marrow frozen section assay for studying hematopoietic interactions in situ: the role of stromal bone marrow macrophages in erythroblast binding. *J. Cell Sci.* **109** (Pt 12), 2937-2945 (1996).
195. Wenzel, I., Roth, J. & Sorg, C. Identification of a novel surface molecule, RM3/1, that contributes to the adhesion of glucocorticoid-induced human monocytes to endothelial cells. *Eur. J. Immunol.* **26**, 2758-2763 (1996).
196. Dijkstra, C.D., Dopp, E.A., Joling, P. & Kraal, G. The heterogeneity of mononuclear phagocytes in lymphoid organs: distinct macrophage subpopulations in the rat recognized by monoclonal antibodies ED1, ED2 and ED3. *Immunology* **54**, 589-599 (1985).
197. Hickey, W.F. & Kimura, H. Perivascular microglial cells of the CNS are bone marrow-derived and present antigen in vivo. *Science* **239**, 290-292 (1988).
198. Hickey, W.F., Vass, K. & Lassmann, H. Bone marrow-derived elements in the central nervous system: an immunohistochemical and ultrastructural survey of rat chimeras. *J Neuropathol Exp Neurol* **51**, 246-256 (1992).
199. Galea, I. *et al.* Mannose receptor expression specifically reveals perivascular macrophages in normal, injured, and diseased mouse brain. *Glia* **49**, 375-384 (2005).
200. Derijk, R.H., Strijbos, P.J., van, R., Rothwell, N.J. & Berkenbosch, F. Fever and thermogenesis in response to bacterial endotoxin involve macrophage-dependent mechanisms in rats. *Am J Physiol* **265**, R1179-R1183 (1993).
201. Pennanen, N., Lapinjoki, S., Urtti, A. & Monkkonen, J. Effect of liposomal and free bisphosphonates on the IL-1 beta, IL-6 and TNF alpha secretion from RAW 264 cells in vitro. *Pharm Res* **12**, 916-922 (1995).
202. Weller, R.O., Kida, S. & Zhang, E.T. Pathways of fluid drainage from the brain--morphological aspects and immunological significance in rat and man. *Brain Pathol* **2**, 277-284 (1992).
203. Claassen, E. Post-formation fluorescent labelling of liposomal membranes. In vivo detection, localisation and kinetics. *J. Immunol. Methods* **147**, 231-240 (1992).
204. Kuchler, S. *et al.* Mannose dependent tightening of the rat ependymal cell barrier. In vivo and in vitro study using neoglycoproteins. *Neurochem. Int.* **24**, 43-55 (1994).
205. Frederickson, R.G. & Low, F.N. Blood vessels and tissue space associated with the brain of the rat. *Am J Anat* **125**, 123-145 (1969).
206. Elie, M., Cole, M.G., Primeau, F.J. & Bellavance, F. Delirium risk factors in elderly hospitalized patients. *J. Gen. Intern. Med.* **13**, 204-212 (1998).

207. Dunn, N., Mullee, M., Perry, V.H. & Holmes, C. Association between dementia and infectious disease: evidence from a case-control study. *Alzheimer Dis. Assoc. Disord.* **19**, 91-94 (2005).

208. Hahn, C.N., del Pilar, M.M., Zhou, X.Y., Mann, L.W. & d'Azzo, A. Correction of murine galactosialidosis by bone marrow-derived macrophages overexpressing human protective protein/cathepsin A under control of the colony-stimulating factor-1 receptor promoter. *Proc. Natl. Acad. Sci. U. S. A* **95**, 14880-14885 (1998).

209. Priller, J. *et al.* Targeting gene-modified hematopoietic cells to the central nervous system: use of green fluorescent protein uncovers microglial engraftment. *Nat Med* **7**, 1356-1361 (2001).

210. Cornford, E.M. & Cornford, M.E. New systems for delivery of drugs to the brain in neurological disease. *Lancet Neurol.* **1**, 306-315 (2002).

211. Cartmell, T., Luheshi, G.N. & Rothwell, N.J. Brain sites of action of endogenous interleukin-1 in the febrile response to localized inflammation in the rat. *J. Physiol* **518 ( Pt 2)**, 585-594 (1999).

212. Garabedian, B.V., Lemaigre, D. & Mariani, J. Central origin of IL-1beta produced during peripheral inflammation: role of meninges. *Brain Res Mol Brain Res* **75**, 259-263 (2000).

213. Luheshi, G. *et al.* Interleukin-1 receptor antagonist inhibits endotoxin fever and systemic interleukin-6 induction in the rat. *Am. J. Physiol* **270**, E91-E95 (1996).

214. Verma, S., Nakaoke, R., Dohgu, S. & Banks, W.A. Release of cytokines by brain endothelial cells: A polarized response to lipopolysaccharide. *Brain Behav. Immun.* (2005).

215. Molina-Holgado, E., Ortiz, S., Molina-Holgado, F. & Guaza, C. Induction of COX-2 and PGE(2) biosynthesis by IL-1beta is mediated by PKC and mitogen-activated protein kinases in murine astrocytes. *Br. J. Pharmacol.* **131**, 152-159 (2000).

216. Nadjar, A., Combe, C., Busquet, P., Dantzer, R. & Parnet, P. Signaling pathways of interleukin-1 actions in the brain: anatomical distribution of phospho-ERK1/2 in the brain of rat treated systemically with interleukin-1beta. *Neuroscience* **134**, 921-932 (2005).

217. Gordon, S. Alternative activation of macrophages. *Nat. Rev. Immunol* **3**, 23-35 (2003).

218. Moestrup, S.K. & Moller, H.J. CD163: a regulated hemoglobin scavenger receptor with a role in the anti-inflammatory response. *Ann. Med.* **36**, 347-354 (2004).

219. Hintz, K.A. *et al.* Endotoxin induces rapid metalloproteinase-mediated shedding followed by up-regulation of the monocyte hemoglobin scavenger receptor CD163. *J. Leukoc. Biol.* **72**, 711-717 (2002).

220. Hogger, P. & Sorg, C. Soluble CD163 inhibits phorbol ester-induced lymphocyte proliferation. *Biochem. Biophys. Res. Commun.* **288**, 841-843 (2001).

221. Schiltz, J.C. & Sawchenko, P.E. Signaling the brain in systemic inflammation: the role of perivascular cells. *Front Biosci.* **8**, s1321-s1329 (2003).
222. Eskandari, F., Webster, J.I. & Sternberg, E.M. Neural immune pathways and their connection to inflammatory diseases. *Arthritis Res. Ther.* **5**, 251-265 (2003).
223. Lee, B.N. *et al.* A cytokine-based neuroimmunologic mechanism of cancer-related symptoms. *Neuroimmunomodulation*. **11**, 279-292 (2004).
224. Blennow, K. *et al.* Blood-brain barrier disturbance in patients with Alzheimer's disease is related to vascular factors. *Acta Neurol. Scand.* **81**, 323-326 (1990).
225. Tomimoto, H. *et al.* Alterations of the blood-brain barrier and glial cells in white-matter lesions in cerebrovascular and Alzheimer's disease patients. *Stroke* **27**, 2069-2074 (1996).
226. Graeber, M.B., Streit, W.J., Buringer, D., Sparks, D.L. & Kreutzberg, G.W. Ultrastructural location of major histocompatibility complex (MHC) class II positive perivascular cells in histologically normal human brain. *J Neuropathol Exp Neurol* **51**, 303-311 (1992).
227. Williams, K., Alvarez, X. & Lackner, A.A. Central nervous system perivascular cells are immunoregulatory cells that connect the CNS with the peripheral immune system. *Glia* **36**, 156-164 (2001).
228. Hickey, W.F., Cohen, J.A. & Burns, J.B. A quantitative immunohistochemical comparison of actively versus adoptively induced experimental allergic encephalomyelitis in the Lewis rat. *Cell Immunol.* **109**, 272-281 (1987).
229. Streit, W.J., Graeber, M.B. & Kreutzberg, G.W. Expression of Ia antigen on perivascular and microglial cells after sublethal and lethal motor neuron injury. *Exp Neurol* **105**, 115-126 (1989).
230. Lassmann, H., Zimprich, F., Vass, K. & Hickey, W.F. Microglial cells are a component of the perivascular glia limitans. *J. Neurosci. Res.* **28**, 236-243 (1991).
231. Ford, A.L., Goodsall, A.L., Hickey, W.F. & Sedgwick, J.D. Normal adult ramified microglia separated from other central nervous system macrophages by flow cytometric sorting. Phenotypic differences defined and direct ex vivo antigen presentation to myelin basic protein-reactive CD4+ T cells compared. *J Immunol* **154**, 4309-4321 (1995).
232. Schaer, D.J. *et al.* Molecular cloning and characterization of the mouse CD163 homologue, a highly glucocorticoid-inducible member of the scavenger receptor cysteine-rich family. *Immunogenetics* **53**, 170-177 (2001).
233. Bell, M.D. *et al.* Upregulation of the macrophage scavenger receptor in response to different forms of injury in the CNS. *J. Neurocytol.* **23**, 605-613 (1994).
234. Linehan, S.A., Martinez-Pomares, L. & Gordon, S. Macrophage lectins in host defence. *Microbes. Infect.* **2**, 279-288 (2000).

235. Linehan, S.A., Martinez-Pomares, L., Stahl, P.D. & Gordon, S. Mannose receptor and its putative ligands in normal murine lymphoid and nonlymphoid organs: In situ expression of mannose receptor by selected macrophages, endothelial cells, perivascular microglia, and mesangial cells, but not dendritic cells. *J. Exp. Med.* **189**, 1961-1972 (1999).

236. Apostolopoulos, V. & McKenzie, I.F. Role of the mannose receptor in the immune response. *Curr. Mol. Med.* **1**, 469-474 (2001).

237. Andersson, P.B., Perry, V.H. & Gordon, S. The acute inflammatory response to lipopolysaccharide in CNS parenchyma differs from that in other body tissues. *Neuroscience* **48**, 169-186 (1992).

238. Andersson, P.B., Perry, V.H. & Gordon, S. The kinetics and morphological characteristics of the macrophage-microglial response to kainic acid-induced neuronal degeneration. *Neuroscience* **42**, 201-214 (1991).

239. Perry, V.H., Cunningham, C. & Boche, D. Atypical inflammation in the central nervous system in prion disease. *Curr. Opin. Neurol.* **15**, 349-354 (2002).

240. Betmouni, S., Perry, V.H. & Gordon, J.L. Evidence for an early inflammatory response in the central nervous system of mice with scrapie. *Neuroscience* **74**, 1-5 (1996).

241. Burudi, E.M. & Regnier-Vigouroux, A. Regional and cellular expression of the mannose receptor in the post-natal developing mouse brain. *Cell Tissue Res.* **303**, 307-317 (2001).

242. Zamze, S. *et al.* Recognition of bacterial capsular polysaccharides and lipopolysaccharides by the macrophage mannose receptor. *J. Biol. Chem.* **277**, 41613-41623 (2002).

243. Martinez-Pomares, L. *et al.* Analysis of mannose receptor regulation by IL-4, IL-10, and proteolytic processing using novel monoclonal antibodies. *J. Leukoc. Biol.* **73**, 604-613 (2003).

244. Cavaglia, M. *et al.* Regional variation in brain capillary density and vascular response to ischemia. *Brain Res.* **910**, 81-93 (2001).

245. Boche, D., Cunningham, C., Gauldie, J. & Perry, V.H. Transforming growth factor-beta 1-mediated neuroprotection against excitotoxic injury in vivo. *J. Cereb. Blood Flow Metab* **23**, 1174-1182 (2003).

246. Cunningham, C., Boche, D. & Perry, V.H. Transforming growth factor beta1, the dominant cytokine in murine prion disease: influence on inflammatory cytokine synthesis and alteration of vascular extracellular matrix. *Neuropathol. Appl. Neurobiol.* **28**, 107-119 (2002).

247. Angelov, D.N. *et al.* ED2-positive perivascular cells act as neuronophages during delayed neuronal loss in the facial nucleus of the rat. *Glia* **16**, 129-139 (1996).

248. Linehan, S.A., Martinez-Pomares, L. & Gordon, S. Mannose receptor and scavenger receptor: two macrophage pattern recognition receptors with diverse functions in tissue homeostasis and host defense. *Adv. Exp. Med. Biol.* **479**, 1-14 (2000).

249. Smedsrod, B., Einarsson, M. & Pertoft, H. Tissue plasminogen activator is endocytosed by mannose and galactose receptors of rat liver cells. *Thromb. Haemost.* **59**, 480-484 (1988).

250. Tsirka, S.E., Rogove, A.D., Bugge, T.H., Degen, J.L. & Strickland, S. An extracellular proteolytic cascade promotes neuronal degeneration in the mouse hippocampus. *J. Neurosci.* **17**, 543-552 (1997).

251. Wang, Y.F. *et al.* Tissue plasminogen activator (tPA) increases neuronal damage after focal cerebral ischemia in wild-type and tPA-deficient mice. *Nat. Med.* **4**, 228-231 (1998).

252. Irjala, H. *et al.* Mannose receptor is a novel ligand for L-selectin and mediates lymphocyte binding to lymphatic endothelium. *J. Exp. Med.* **194**, 1033-1042 (2001).

253. Linehan, S.A., Martinez-Pomares, L., da Silva, R.P. & Gordon, S. Endogenous ligands of carbohydrate recognition domains of the mannose receptor in murine macrophages, endothelial cells and secretory cells; potential relevance to inflammation and immunity. *Eur. J. Immunol.* **31**, 1857-1866 (2001).

254. Lee, S.J. *et al.* Mannose receptor-mediated regulation of serum glycoprotein homeostasis. *Science* **295**, 1898-1901 (2002).

255. Martinez-Pomares, L. *et al.* Fc chimeric protein containing the cysteine-rich domain of the murine mannose receptor binds to macrophages from splenic marginal zone and lymph node subcapsular sinus and to germinal centers. *J. Exp. Med.* **184**, 1927-1937 (1996).

256. Martinez-Pomares, L. *et al.* A functional soluble form of the murine mannose receptor is produced by macrophages in vitro and is present in mouse serum. *J. Biol. Chem.* **273**, 23376-23380 (1998).

257. Weller, R.O., Engelhardt, B. & Phillips, M.J. Lymphocyte targeting of the central nervous system: a review of afferent and efferent CNS-immune pathways. *Brain Pathol* **6**, 275-288 (1996).

258. Fabriek, B.O. *et al.* CD163-positive perivascular macrophages in the human CNS express molecules for antigen recognition and presentation. *Glia* **51**, 297-305 (2005).

259. Yeager, M.P. *et al.* Trauma and inflammation modulate lymphocyte localization in vivo: quantitation of tissue entry and retention using indium-111-labeled lymphocytes. *Crit Care Med.* **28**, 1477-1482 (2000).

260. Engelhardt, B. & Ransohoff, R.M. The ins and outs of T-lymphocyte trafficking to the CNS: anatomical sites and molecular mechanisms. *Trends Immunol.* **26**, 485-495 (2005).

261. Vizler, C. *et al.* Relative diabetogenic properties of islet-specific Tc1 and Tc2 cells in immunocompetent hosts. *J Immunol* **165**, 6314-6321 (2000).

262. Cserr, H.F., Harling, B. & Knopf, P.M. Drainage of brain extracellular fluid into blood and deep cervical lymph and its immunological significance. *Brain Pathol* **2**, 269-276 (1992).

263. Hickey, W.F. Basic principles of immunological surveillance of the normal central nervous system. *Glia* **36**, 118-124 (2001).

264. Schulz, M. & Engelhardt, B. The circumventricular organs participate in the immunopathogenesis of experimental autoimmune encephalomyelitis. *Cerebrospinal Fluid Res.* **2**, 8 (2005).

265. Vass, K. & Lassmann, H. Intrathecal application of interferon gamma. Progressive appearance of MHC antigens within the rat nervous system. *Am. J. Pathol.* **137**, 789-800 (1990).

266. Cabarrocas, J., Bauer, J., Piaggio, E., Liblau, R. & Lassmann, H. Effective and selective immune surveillance of the brain by MHC class I-restricted cytotoxic T lymphocytes. *Eur J Immunol* **33**, 1174-1182 (2003).

267. Girvin, A.M., Gordon, K.B., Welsh, C.J., Clipstone, N.A. & Miller, S.D. Differential abilities of central nervous system resident endothelial cells and astrocytes to serve as inducible antigen-presenting cells. *Blood* **99**, 3692-3701 (2002).

268. Sobel, R.A. & Ames, M.B. Major histocompatibility complex molecule expression in the human central nervous system: immunohistochemical analysis of 40 patients. *J. Neuropathol. Exp. Neurol.* **47**, 19-28 (1988).

269. Campbell, J.J. *et al.* Chemokines and the arrest of lymphocytes rolling under flow conditions. *Science* **279**, 381-384 (1998).

270. Dustin, M.L., Bromley, S.K., Kan, Z., Peterson, D.A. & Unanue, E.R. Antigen receptor engagement delivers a stop signal to migrating T lymphocytes. *Proc. Natl. Acad. Sci. U. S. A* **94**, 3909-3913 (1997).

271. Dustin, M.L. & Springer, T.A. T-cell receptor cross-linking transiently stimulates adhesiveness through LFA-1. *Nature* **341**, 619-624 (1989).

272. Weber, C., Lu, C.F., Casasnovas, J.M. & Springer, T.A. Role of alpha L beta 2 integrin avidity in transendothelial chemotaxis of mononuclear cells. *J. Immunol.* **159**, 3968-3975 (1997).

273. Hutchinson, S.L. *et al.* The CD8 T cell coreceptor exhibits disproportionate biological activity at extremely low binding affinities. *J. Biol. Chem.* **278**, 24285-24293 (2003).

274. Tominaga, Y. *et al.* Affinity and kinetic analysis of the molecular interaction of ICAM-1 and leukocyte function-associated antigen-1. *J. Immunol.* **161**, 4016-4022 (1998).

275. Lin, J., Miller, M.J. & Shaw, A.S. The c-SMAC: sorting it all out (or in). *J. Cell Biol.* **170**, 177-182 (2005).

276. Marelli-Berg, F.M. *et al.* Cognate recognition of the endothelium induces HY-specific CD8+ T-lymphocyte transendothelial migration (diapedesis) in vivo. *Blood* **103**, 3111-3116 (2004).

277. Savinov, A.Y., Wong, F.S., Stonebraker, A.C. & Chervonsky, A.V. Presentation of antigen by endothelial cells and chemoattraction are required for homing of insulin-specific CD8+ T cells. *J Exp Med* **197**, 643-656 (2003).

278. Stolpen, A.H., Pober, J.S., Brown, C.S. & Golan, D.E. Class I major histocompatibility complex proteins diffuse isotropically on immune interferon-activated endothelial cells despite anisotropic cell shape and cytoskeletal organization: application of fluorescence photobleaching recovery with an elliptical beam. *Proc. Natl. Acad. Sci. U. S. A* **85**, 1844-1848 (1988).

279. Gumbiner, B. Structure, biochemistry, and assembly of epithelial tight junctions. *Am. J. Physiol* **253**, C749-C758 (1987).

280. Lamers, K.J. *et al.* Protein S-100B, neuron-specific enolase (NSE), myelin basic protein (MBP) and glial fibrillary acidic protein (GFAP) in cerebrospinal fluid (CSF) and blood of neurological patients. *Brain Res. Bull.* **61**, 261-264 (2003).

281. Chen, L. & Jondal, M. Alternative processing for MHC class I presentation by immature and CpG-activated dendritic cells. *Eur. J. Immunol.* **34**, 952-960 (2004).

282. Diegel, M.L., Chen, F., Laus, R., Graddis, T.J. & Vidovic, D. Major histocompatibility complex class I-restricted presentation of protein antigens without prior intracellular processing. *Scand. J. Immunol.* **58**, 1-8 (2003).

283. Nakagawa, Y., Takeshita, T., Berzofsky, J.A. & Takahashi, H. Analysis of the mechanism for extracellular processing in the presentation of human immunodeficiency virus-1 envelope protein-derived peptide to epitope-specific cytotoxic T lymphocytes. *Immunology* **101**, 76-82 (2000).

284. Santambrogio, L. *et al.* Extracellular antigen processing and presentation by immature dendritic cells. *Proc. Natl. Acad. Sci. U. S. A* **96**, 15056-15061 (1999).

285. Eberl, G. *et al.* Extracellular processing and presentation of a 69-mer synthetic polypeptide to MHC class I-restricted T cells. *Mol. Immunol.* **36**, 103-112 (1999).

286. Accapezzato, D. *et al.* Generation of an MHC class II-restricted T cell epitope by extracellular processing of hepatitis delta antigen. *J. Immunol.* **160**, 5262-5266 (1998).

287. Limmer, A. *et al.* Efficient presentation of exogenous antigen by liver endothelial cells to CD8+ T cells results in antigen-specific T-cell tolerance. *Nat. Med.* **6**, 1348-1354 (2000).

288. Valujskikh, A., Lantz, O., Celli, S., Matzinger, P. & Heeger, P.S. Cross-primed CD8(+) T cells mediate graft rejection via a distinct effector pathway. *Nat. Immunol.* **3**, 844-851 (2002).

289. Kummer, M., Lev, A., Reiter, Y. & Biedermann, B.C. Vascular endothelial cells have impaired capacity to present immunodominant, antigenic peptides: a mechanism of cell type-specific immune escape. *J. Immunol.* **174**, 1947-1953 (2005).

290. Marelli-Berg, F.M. *et al.* Activated murine endothelial cells have reduced immunogenicity for CD8+ T cells: a mechanism of immunoregulation? *J. Immunol.* **165**, 4182-4189 (2000).

291. Bladergroen, B.A. *et al.* The granzyme B inhibitor, protease inhibitor 9, is mainly expressed by dendritic cells and at immune-privileged sites. *J. Immunol.* **166**, 3218-3225 (2001).

292. Biedermann, B.C. *et al.* Endothelial injury mediated by cytotoxic T lymphocytes and loss of microvessels in chronic graft versus host disease. *Lancet* **359**, 2078-2083 (2002).

293. Lassmann, H. Hypoxia-like tissue injury as a component of multiple sclerosis lesions. *J. Neurol. Sci.* **206**, 187-191 (2003).

294. Mendez-Fernandez, Y.V., Hansen, M.J., Rodriguez, M. & Pease, L.R. Anatomical and cellular requirements for the activation and migration of virus-specific CD8+ T cells to the brain during Theiler's virus infection. *J. Virol.* **79**, 3063-3070 (2005).

295. Stevenson, P.G., Hawke, S., Sloan, D.J. & Bangham, C.R. The immunogenicity of intracerebral virus infection depends on anatomical site. *J. Virol.* **71**, 145-151 (1997).

296. Brabb, T. *et al.* In situ tolerance within the central nervous system as a mechanism for preventing autoimmunity. *J. Exp. Med.* **192**, 871-880 (2000).

297. Albert, M.L. *et al.* Tumor-specific killer cells in paraneoplastic cerebellar degeneration. *Nat. Med.* **4**, 1321-1324 (1998).

298. Tanaka, M. & Tanaka, K. HLA A24 in paraneoplastic cerebellar degeneration with anti-Yo antibody. *Neurology* **47**, 606-607 (1996).

299. Tanaka, M. *et al.* Cytotoxic T cell activity against peptides of Hu protein in anti-Hu syndrome. *J. Neurol. Sci.* **201**, 9-12 (2002).

300. Dyment, D.A., Ebers, G.C. & Sadovnick, A.D. Genetics of multiple sclerosis. *Lancet Neurol.* **3**, 104-110 (2004).

301. Engblom, D. *et al.* Prostaglandins as inflammatory messengers across the blood-brain barrier. *J. Mol. Med.* **80**, 5-15 (2002).
302. Annunziata, P., Cioni, C., Santonini, R. & Paccagnini, E. Substance P antagonist blocks leakage and reduces activation of cytokine-stimulated rat brain endothelium. *J. Neuroimmunol.* **131**, 41-49 (2002).
303. Derocq, J.M. *et al.* Effect of substance P on cytokine production by human astrocytic cells and blood mononuclear cells: characterization of novel tachykinin receptor antagonists. *FEBS Lett.* **399**, 321-325 (1996).
304. Estrada, C., Gomez, C. & Martin, C. Effects of TNF-alpha on the production of vasoactive substances by cerebral endothelial and smooth muscle cells in culture. *J. Cereb. Blood Flow Metab* **15**, 920-928 (1995).
305. Dehouck, M.P. *et al.* Endothelin-1 as a mediator of endothelial cell-pericyte interactions in bovine brain capillaries. *J. Cereb. Blood Flow Metab* **17**, 464-469 (1997).
306. Morga, E., Faber, C. & Heuschling, P. Stimulation of endothelin B receptor modulates the inflammatory activation of rat astrocytes. *J. Neurochem.* **74**, 603-612 (2000).
307. Roth, J., Storr, B., Voigt, K. & Zeisberger, E. Inhibition of nitric oxide synthase attenuates lipopolysaccharide-induced fever without reduction of circulating cytokines in guinea-pigs. *Pflugers Arch.* **436**, 858-862 (1998).
308. Verderio, C. & Matteoli, M. ATP mediates calcium signaling between astrocytes and microglial cells: modulation by IFN-gamma. *J. Immunol.* **166**, 6383-6391 (2001).
309. Vastag, M. *et al.* Endothelial cells cultured from human brain microvessels produce complement proteins factor H, factor B, C1 inhibitor, and C4. *Immunobiology* **199**, 5-13 (1998).
310. Inoue, K. Microglial activation by purines and pyrimidines. *Glia* **40**, 156-163 (2002).
311. Male, D. & Pryce, G. Kinetics of MHC gene expression and mRNA synthesis in brain endothelium. *Immunology* **63**, 37-42 (1988).